THE EFFECTS OF CORNER RADII ON THE LOCAL BUCKLING OF COLD-FORMED SECTIONS

ARASH NASSIRIRAD

A Thesis

in

SCHOOL FOR BUILDING

Presented in partial fulfillment of the requirements

for the degree of Master of Applied Sciences (Building) at

Concordia University.

Montreal, Quebec, Canada

September 1998

0-612-39469-7

ABSTRACT

THE EFFECTS OF CORNER RADII ON THE LOCAL BUCKLING OF COLD-FORMED SECTIONS

ARASH NASSIRIRAD

In steel construction the methods to produce structural members include hot rolling, forming and welding hollow section (HSS) and welding plates to form I's (WWF). Another method, which is less widely known but is growing in acceptance, is cold-forming from steel sheet or strip using roll-forming machines, press and bending brakes, or folding operations. These cold-form steel sections have their own design codes.

The use of cold-formed structures in building constructions goes back to about the 1850s in both the United States and Great Britain but the formal design methods for these sections were developed only since 1940.

Cold-formed sections add aspects to the design procedure which are neglected in codes for hot-rolled shapes, namely local and torsional buckling. The elements of a box or channel section formed from thin sheet may buckle locally, leading to collapse. To calculate the buckling stress the

manufacturing process, makes the measurement of the width uncertain. Codes simply adopt the flat width. The objective of this study is to develop a more accurate method to predict the buckling stresses for two major kinds of cold-formed section, namely an open section (channel) and a closed section (box).

A theory has been developed to model the elastic local buckling mode for box and channel sections. This is extended to predict the behavior of the section after buckling and up to the collapse. Comparisons are made with the results of the numeric analysis carried out using the finite element program ABAQUS, and with the code requirements.

To **Dr. Shahin Izadian**

who supports this study by her life and spirit.

تقدیم به : خانم دکتر شهین ایزدیان

که زندگی‌اش بنیان این رساله است.

ACKNOWLEDGMENTS

The author wishes to express his gratitude to ProfessorCedric Marsh, for the initial encouragement in the project, and for his continuous guidance and suggestions, which have enriched the content of this work.

The author is also grateful to his colleagues, for their valuable criticism, helpful advice and solid support.

Financial support from NSERC is also acknowledged.

TABLE OF CONTENTS

	PAGE
LIST OF FIGURES	xi
LIST OF TABLES	xiv
LIST OF SYMBOLS	xv
DEFINITIONS	xix
CHAPTER 1	1
INTRODUCTION	1-1
1.1 General	1-1
1.2 Behavior of cold formed members	1-4
1.2.1 Rectangular box columns	1-6
1.2.2 Channel columns	1-7
CHAPTER 2	2
THEORETICAL MODEL	2-1
2.1 Overall buckling	2-1

2-2 Box section 2-2

2-2-1 Code procedures 2-2

2.2.2 Proposed analytical model 2-5

2.2.3 Theoretical post-buckling 2-6

2.3 Channel section 2-10

2.3.1 Code procedures 2-10

2.3.2 Proposed analytical model 2-12

2.3.4 Theoretical post-buckling 2-13

CHAPTER 3 3

FINITE ELEMENT STUDIES 3-1

3.1 Introduction 3-1

3.2 Eigenvalue method 3-2

3.3 Ultimate load 3-4

3.4 ABAQUS program 3-6

3.4.1 Introduction 3-6

3.4.2 Input of the program 3-7

3.4.3 Output of the program 3-8

CHAPTER 4 4

COMPARING THE RESULTS 4-1

4.1 Typical example 4-1

4.1.1 Theoretical calculation 4-2

4.1.2 Code predictions 4-3

4.1.3 Finite element results 4-4

4.1.3.1 Eigenvalue result 4-4

4.1.3.2 Postbuckling strength 4-4

4.2 Results for box sections 4-6

4.3 Results for channel sections 4-8

4.4 Conclusions 4-9

4.4.1 Box section 4-9

4.4.2 Channel section 4-9

4.4.3 Final comments 4-10

4.4.4 Future research 4-10

APPENDIX I I

ANALYSIS I-1

I.1 Introduction I-1

I.2 Box section I-1

I.3 Channel section I-9

I.3.1 Flange mode I-9

I.3.2 Web mode I-13

APPENDIX II II

WARPING CONSTANT II-1

II.1 Box section II-1

II.2 Channel section II-4

APPENDIX III III

List 1 III-1

List 2 III-4

FIGURES F1

TABLES T1

REFERENCES R1

LIST OF FIGURES

Figure D-1 Local buckling for a box section	FD-1
Figure D-2 Local buckling for a channel section	FD-2
Figure D-3 Flat, overall and effective widths	FD-3
Figure D-4 Collapse mode for a box section	FD-4
Figure D-5 Warping for I beam	FD-5
Figure 1-1 Cold-formed sections	F1-1
Figure 1-2 Cold-formed steel structure	F1-2
Figure 1-3 Cold-formed and hot-rolled steel structure	F1-3
Figure 1-4 Typical cold-formed panels	F1-4
Figure 1-5 Force-shortening relationship for column and plate	F1-5
Figure 1-6 Box and panel section dimensions	F1-6
Figure 1-7 Stress distribution on a simply supported plate	F1-7
Figure 2-1 Buckling and postbuckling strength	F2-1
Figure 2-2 Cold-formed and hot-rolled corners	F2-2
Figure 2-3 Simply Supported plate	F2-3
Figure 2-4 Postbuckling curve	F2-4
Figure 2-5 Buckling modes of a channel	F2-5
Figure 3-1 Sample plate for ABAQUS	F3-1

Figure 4-1 Typical box section F4-1

Figure 4-2 ABAQUS elastic buckling F4-2

Figure 4-3 Stress distribution across the wall of a box section F4-3

Figure 4-4 Mean stress and axial shorting for a box section F4-4

Figure 4-5 to 4-34 Critical and ultimate stress for box sections F4-5 to F4-34

Figure 4-35 to 4-37 m factor for box sections F4-35 to f4-37

Figure 4-38 to 4-40 Normalized m for box sections F4-38 to F4-40

Figure 4-41 Normalized mean postbuckling strength for box sections F4-41

Figure 4-42 to 4-56 Critical stress for channel sections F4-42 to F4-56

Figure 4-57 to 4-59 m factor for channel sections F4-57 to f4-59

Figure 4-60 to 4-62 Normalized m for channel sections F4-60 to F4-62

Figure 4-63 Normalized mean strength for channel sections F4-63

Figure I-1 Deflection of a box section FA-1

Figure I-2 Deflection of a channel section (flange mode) FA-2

Figure I-3 Deflection of a channel section (web mode) FA-3

Figure II-1 Corner of a box section FA-4

Figure II-2 Warping constant construction for the corner of a box section FA-5

Figure II-3 Warping constant for box sections FA-6

Figure II-4 Warping factor α for box sections FA-7

Figure II-5 Corner of a channel section FA-8

Figure II-6 Warping constant construction for the corner of a channel section FA-9

Figure II-7 Warping constant for channel sections FA-10

Figure II-8 Warping factor α for channel sections FA-11

LIST OF TABLES

Table 4-1 Summary of results for box sections T-1

Table 4-2 Summary of results for channel sections T-13

LIST OF SYMBOLS

A	Unreduced cross-sectional area of section
A_{eff}	Effective cross-sectional area of section
D	Plate rigidity
E	Elastic modulus
F_{cr}	Elastic buckling force
F_{ult}	Ultimate force
F_{ult}^{ABAQUS}	Ultimate load from ABAQUS
H	Warping constant
K	Factor
K_b	Elastic stiffness matrix
K_Q	Initial stiffness matrix
L	Length
M	Bending moment
N	Axial flux
Q	Loading pattern matrix
R	Bend radius to median line
U_B	Strain energy due to bending

U_H	Strain energy due to warping
U_w	Strain energy due to bending of web
T	External work
W	Work done by applied stresses
X	Axis
Y	Axis
Z	Axis

A	Shorter width of the box and width of the web of a channel
a1,a2,a3,a4	Deflection coefficients
b	Longer width of the box and width of the flange of a channel
b_{eff}	Effective width of the box and flange of a channel
c	Halfwave length of a buckled element
e	Distance to shear centre
m	Factor
$\bar{m}$	Normalized m factor
s	True length of section
t	Thickness
u	Displacement in X direction

Δu	Increment in displacement for load-displacement control
v	Displacement in Y direction
w	Flat width
w'	Flat width limit
x	Distance along X axis
y	Distance along Y axis
z	Distance along Z axis
α	Warping factor
θ	Angle of rotation
ρ	Factor
$[\delta]$	Deflection matrix for eigenvalue
ϕ	Angle of twist at the corner
$[\phi]$	Buckling mode matrix for eigenvalue
λ	Slenderness
$\bar{\lambda}$	Normalized slenderness
$[\lambda_I]$	Load multipliers for eigenvalue
ν	Poisson ratio (0.3 for steel)
σ	Stress

$\bar{\sigma}$	Normalized stress
σ_c	Actual buckling stress
σ_{cr}	Elastic buckling stress
σ_w	Actual buckling stress for web of channel section
σ_y	Yield strength
σ_{av}^{ABAQUS}	Average ultimate stress from ABAQUS
σ_{cr}^{ABAQUS}	Elastic critical stress from ABAQUS

DEFINITIONS

- LOCAL BUCKLING shown in Fig D-1 for box and Fig D-2 for a channel is a wavelike deflection form, with a wavelength independent of the overall length.
- CORNER RADIUS: is the radius of the median line at the corners of a formed section. It is usually a multiple of the thickness.
- CRITICAL FORCE (STRESS): is the force (stress) which causes initial elastic buckling of a member or element.
- EFFECTIVE DESIGN WIDTH (b_{eff}): is the width assumed to carry the yield strength, used to calculate the collapse load.
- FLAT WIDTH (w): is the width of the straight portion of the element, Fig D-3.
- LIMITING WIDTH/THICKNESS RATIO (w/t): is the width/thickness ratio below which local buckling need not be considered.
- OVERALL WIDTH (b): is the overall width of the element between points of intersections of the median lines, Fig D-3.

- ULTIMATE FORCE: is the load which causes the member to collapse, as shown in Fig D-4
- WIDTH/THICKNESS RATIO: is either the "flat width ratio" which is the ratio of the flat width (w) to the thickness (t) or "overall width ratio" which is the ratio of the overall width (b) to the thickness. (Fig D-3)
- WARPING: when twisting in open sections causes translation in the planes of elements of the section, the cross sections tend to warp from the original flat plane, as shown in Fig D-5. If this warping is resisted it contributes to the torsional stiffness.
- YIELD: is the stress at the limit of the elastic range, or at a 0.2% permanent offset strain.

CHAPTER 1

INTRODUCTION

1.1 GENERAL

Cold-formed steel sections represent an alternative to hot rolled sections in applications where the light weight sections can be used.

Although the use of cold-formed sections in construction has been known since the middle of the last century the use of cold formed members in buildings was formalized with the publication of "Specification for the Design of Cold-Formed Steel Structural Members" by the American Iron and Steel Institute (AISI 1946) which was the first to provide a formal design procedure base on the seminal work of Winter (1937). The most recent AISI code is "Specification for the design of cold-formed steel structural members" (1996). The first Canadian standard, "The Design of Light Gauge Steel Structural Members" appeared in 1963, while the latest CSA-S136-M94 "Cold formed steel structural members" was issued in 1994.

The America Society of Civil Engineers (ASCE) prepared a standard ANSI/ASCE 8-90 "Specification for the Design of Cold-Formed Stainless Steel Structural Members" in 1990.

By using cold forming it is possible to produce more efficient structural shapes, which have been used extensively in airplanes and car bodies, but in the construction industry the use was limited to roofing sheet and panels. Over the past 40 years, several studies for the design of thin walled sections have led to an increasing use of cold-formed steel in building structures. Open sections used as wall studs, floor and roof beams are found in institutional, commercial , residential and light factory buildings. Storage racks and latticed joists incorporate special cold formed shapes.

The major difference between cold-formed sections and hot-rolled sections is the relative thickness, or (b/t) ratio, which leads to the following advantages:

- Cold-formed members can be manufactured more easily.
- Unusual sectional configurations can be produced economically and consequently, more favorable strength-to-weight ratios can be obtained.

- Nesting sections can be produced, allowing for compact packaging for shipping.
- Great accuracy of the profile
- A wider variety of shapes
- A wider variety of steel tempers
- Coated and painted sheet
- Sections can be perforated

Cold-formed steel structural products can be classified into two major types:

- Individual structural framing members.
- Panels and decks.

Fig 1-1 shows some of the cold-formed sections generally used in structural framing. The more usual shapes are channels, Z-sections, angles, hat sections.

In general the thickness of cold-formed members ranges from 1 to 10 mm. In view of the fact that the major function of this type of individual framing member is to carry load, structural strength and stiffness are the main considerations in design. Such sections can be used as primary framing members in buildings. Fig 1-2 shows a two-story building framed using cold-formed steel sections. In tall multistory buildings the main framing is typically of heavy hot-rolled or welded sections, to support the primary loads, while the secondary elements such as studs and joists (Fig 1-3) may be of cold-formed steel to support secondary loads.

Typical cold-formed panels are shown in Fig 1-4. These products are generally used for such items as roofs, floor decks, wall panels, siding material, and concrete forms.

1.2 BEHAVIOUR OF COLD FORMED MEMBERS

The current approach to the design of structures is based on a limiting stress dictated by the proportions of the section. This limiting stress is related to the mode of failure which may be governed by any of a number of factors. Tension members under static loads can fail by general yielding of the cross section or rupture at the net section. Members in axial compression may reach their maximum strength by yielding, by local buckling of thin elements, or by overall buckling in flexure or torsion, or by a combination of modes. Members in bending may be controlled by yielding, rupture at a net section, local buckling or lateral buckling.

The study concentrates on two common cold-formed sections which belong to separate categories:

1. The behaviour of a box section is used to represent flat elements in formed panels, and channel webs, where the elements are supported along both long edges.
2. The channel section, in which the flange represents an element supported along one long edge only.

In all cases of buckling, the critical elastic stress, σ_{cr}, is given by:

$$\sigma_{cr} = \frac{\pi^2 E}{\lambda^2} \tag{1.1}$$

where

E : elastic modulus
λ: slenderness ratio
= KL/r for flexural buckling in columns
= mb/t for local buckling of plate elements
b: width
K: a factor related to flexural buckling
L : length
m: a factor related to local buckling
r: radius of gyration
t: thickness

For an axially loaded column failing in flexure or torsion, the critical load is the ultimate load and the theoretical force/shortening relationship is as shown in Fig 1-5 curve 1. In the case of flat elements supported along both long edges which posses postbuckling strength, the theoretical force/ shortening relationship is shown in Fig 1-5 curve 2.

1.2.1 RECTANGULAR BOX COLUMNS

The ultimate axial compressive strength of a rectangular box column is governed by either overall buckling or local buckling. Overall buckling leads to collapse, but after initial local buckling of the flat elements there is a reserve of strength.

The initial stress to cause elastic local buckling is given by:

$$\sigma_{cr} = \frac{\pi^2 E}{\left(m \frac{b}{t}\right)^2} \tag{1.2}$$

For a uniform axial stress, on a square box section, m=1.65 (CSA-S136-94)

The dimensions used are shown in Fig 1-6.

Up to initial local buckling, the force/shortening relationship is assumed to be linear and the stress is assumed to be uniformly distributed over the cross section. After buckling, the behaviour changes:

- The relation between force and shortening is nonlinear
- The distribution of stress over the section is not uniform but takes the form shown in Fig 1-7.
- The local deflection of a buckled element becomes large
- The applied force can be increased until the yield strength is reached at the corners of the section.

1.2.2 CHANNEL COLUMNS

Channels are open sections with only one axis of symmetry. In this case failure may be by local buckling of the flanges, overall flexure or torsion, or by a combination of these. Buckling in any of these modes precipitates collapse.

The flange of an open section, such as in a channel, is considered to be an unstiffened element, supported along only one longitudinal edge.

Local buckling of the flange is given by equation (1.2) with a value of m between 3 and 5 depending on the ratio of the flange width to the web depth.

If the flange buckles first, in a pin ended member, the section cannot carry more load and this critical buckling load can be assumed to be the ultimate load. However, if the web buckles first, the element can carry more load, as in a box section.

CHAPTER 2

THEORETICAL MODELS

In this chapter the current design methods, taken from CSA S136-94 "Cold formed steel structural members", which is typical of such Codes in general, are introduced, followed by a description of the analytical model used in this study for plates with one or both longitudinal edges supported, representing the flanges of channels and the walls of boxes.

2.1 OVERALL BUCKLING

For overall flexural buckling, CSAS136-94 uses a relationship between the elastic critical stress, σ_{cr}, and the actual buckling stress, σ_c, given by:

$$\begin{aligned} &for \quad \sigma_{cr} > \sigma_y/2 \;,\; \sigma_c = \sigma_y - \frac{\sigma_y^{2}}{4\;(\sigma_{cr}/1.2)} \\ &for \quad \sigma_{cr} < \sigma_y/2 \;,\; \sigma_c = \sigma_{cr}/1.2 \end{aligned} \tag{2.1}$$

When normalized this becomes:

$$\begin{aligned} &\bar{\sigma} = 1 - 0.3\bar{\lambda}^{2} \\ &\bar{\sigma} = \frac{1}{1.2\;\bar{\lambda}^{2}} \end{aligned} \tag{2.2}$$

where

$$\bar{\sigma} = \sigma_c / \sigma_y$$
$$\bar{\lambda} = \left(\sigma_y / \sigma_{cr} \right)^{1/2} \qquad \textbf{(2.3)}$$

The curve is shown in Fig 2-1. In this figure the CSA Code result for plate and column are compared with this thesis theory and von Karman's results.

2.2 BOX SECTION

2.2.1 CODE PROCEDURES

The manufacture of cold-formed section requires a radius at each corner. (The form of radius differs for that in hot-rolled sections as shown in Fig 2-2) In today's design codes the influence of this radius is to reduce the width to the "flat width", which is used in design.

In all the current codes for strength design in cold-formed steel the following procedure is adopted for walls with both long edges supported:

- For all proportions of the cross section, local buckling is treated by considering the flat elements to be joined together at the corners with simply supported edges.
- Only the flat width (w) is considered to buckle locally.

- Below a specified limit for the flat width (w') there is no buckling.
- For greater widths, after initial local buckling, zones at the edges of the flat width are assumed to carry the yield strength. (The sum of these two zones is called the "effective width", b_{eff})
- Radiused corners are assumed to carry the yield strength, but are otherwise disregarded

The critical buckling stress is given by (CSA S136-94) :

$$\sigma_{cr} = \frac{\pi^2 E t^2}{3(1-v^2)w^2} = \frac{\pi^2 E}{\lambda^2} \tag{2.4}$$

Using Poisson's ratio, v=0.3, this gives:

$$\lambda = 1.65(w/t) \tag{2.5}$$

The critical axial force for the flat width is then:

$$F_{cr} = \sigma_{cr} A \tag{2.6}$$

where

$$A = w\,t \tag{2.7}$$

To calculate the ultimate force, the Codes introduce an effective width which can carry the yield strength, based on a formula proposed by Winter (1967), given below in its normalized form (ASCE-8-90):

$$
\begin{aligned}
&for\ \ \bar{\lambda} \le 0.673, \ \ b_{eff} = w \\
&for\ \ \bar{\lambda} > 0.673, \ \ b_{eff} = \rho\, w
\end{aligned}
\tag{2.8}
$$

where:

$$\rho = \frac{1 - 0.22/\bar{\lambda}}{\bar{\lambda}} \tag{2.9}$$

and

$$\bar{\lambda} = \left(\frac{\sigma_y}{\sigma_{cr}}\right)^{1/2} = 0.53\, {}^{w}\!/_{t} \sqrt{\frac{\sigma_y}{E}} \tag{2.10}$$

The ultimate force on the "flat width" for a singular plate is then given by:

$$F_{ult} = \sigma_y b_{eff} t \tag{2.11}$$

The four walls of a square box will thus resist a total ultimate force:

$$F_{ult} = 4\ \sigma_y \left(b_{eff} + {}^{\pi\, R}\!/_{2}\right) t \tag{2.12}$$

That the "flat width" should be used was the result of a committee decision based on an intuitive feel for behavior but with no support from theoretical or experimental evidence.

This study undertakes to show the true influence of the radius, and, also, of the influence of adjoining elements.

2.2.2 PROPOSED ANALYTICAL MODEL

To obtain theoretically the critical stress, a rectangular box with the following dimensions is considered:

a: shorter width of box
b: longer width of box
c: halfwave length of buckled element
R: radius at the corner
t: thickness

The box is assumed to be subjected to a uniform axial stress. The energy method, (Timoshenko and Gere (1961)), in which the total strain energy of distortion of the plates is equated to the work done by the axial stress in the longitudinal direction as buckling occurs, is used to obtain the local initial elastic critical stress.

The strain energy has two components:

- That due to deflection of the plates
- That due to twisting at the corners

The strain energy due to bending of the plate of width b, supported on all edges, can be written in terms of the deflections as follow: (Fig 2-3)

$$U_B = \frac{D}{2}\iint\left(\frac{\partial^2 w}{\partial x^2}+\frac{\partial^2 w}{\partial y^2}\right)^2 dxdy \qquad \textbf{(2.13)}$$

(Timoshenko, The terms related to twisting is equal zero in box sections) where w is the deflection at the point (x,y) and D is the plate flexural rigidity given by:

$$D = \frac{Et^3}{12\left(1-\nu^2\right)} \qquad \textbf{(2.14)}$$

The strain energy due to twisting at the corners is calculated based on the resistance to warping of the radiused portion.

The general form of strain energy due to warping is (Timoshenko) :

$$U_w = \frac{EH}{2}\int\left(\frac{d^2\phi}{ds^2}\right)^2 ds \qquad \textbf{(2.15)}$$

where H is the warping constant and:

$$\phi = \frac{\partial w}{\partial y}_{y=0} \qquad \textbf{(2.16)}$$

The work done by the compressive external force as the elements shorten during buckling is given by:

$$T = \frac{N}{2}\iint\left(\frac{\partial w}{\partial x}\right)^2 dxdy \qquad \textbf{(2.17)}$$

in which N is the load per unit width of the section.

The change in strain energy in the member is equal to the work done, thus:

$$U_B + U_H - T = 0 \tag{2.18}$$

U_B ,U_H , and T are for the total section.

This is a minimum energy state. Differentiating equation (2.16) with respect to the coefficients a_1 and a_2 and equating the results to zero, gives two equations. The determinant of these two equations is then equated to zero and solved for N.

The deflected shape of each wall of the box is assumed to be given by an expression of the form:

$$w = \sin(\pi x/a)\left[a_1 \sin(\pi y/b) + a_2(1 - \cos(2\pi y/b))\right] \tag{2.19}$$

The cosine term represents the influence of the corner restraint. The complete procedure to obtain the theoretical critical stress is presented in Appendix I.

2.2.3 THEORETICAL POST-BUCKLING

The above analysis deals with elastic buckling and gives the critical stress. After exceeding this stress the deflection increases rapidly, but the plate can support the increasing load by a redistribution of the stress. The limiting capacity is reached when the stress at the supported edges reaches the yield strength. An approximate expression that determines the ultimate load is represented below.

The theory assumes a perfect plate and linear material behaviour, but real plates are not completely flat before loading and materials are nonlinear as the yield strength is approached. The result is that the deflection increases from the beginning of the load application, and buckling is not a sharp action, furthermore the stress distribution is not uniform from the beginning of loading, with higher stress at the edges. The true initial buckling stress, σ_c, differs from the ideal elastic value, σ_{cr}, and is given by a curve based on experiments, of the form shown in Fig 2-1, taken from CSA-S136-M94 for columns.

After buckling the stress distribution is shown in Fig 1-7 and the total load is given by:

$$F_{Ult} = \int \sigma \, t dy \tag{2.20}$$

which is the area under the actual stress distribution curve. It can be seen that in the limiting condition the plate may be approximated by two strips carrying the yield strength as describe in 2.2.1.

In the general case, the width of plate, when the critical stress is equal to the yield strength, is obtained from:

$$\sigma_y = \frac{\pi^2 E}{\lambda^2} = \frac{\pi^2 E}{\left(m \, b/t\right)^2} \tag{2.21}$$

from which:

$$b = \frac{\pi \, t}{m}\sqrt{\frac{E}{\sigma_y}} = b_{eff} \tag{2.22}$$

The total axial force on the flat plate is then $\sigma_y b_{eff}\, t$. Von Karman (1940) proposed that this value of the axial force remained constant for all greater values of b, thus when b>b_{eff} the mean axial stress at the ultimate load is:

$$\sigma_{av} = \sigma_y b_{eff} t / bt = \left(\sigma_{cr}\sigma_y\right)^{1/2} \tag{2.23}$$

From tests, this expression has been shown to be unconservative. It is proposed to replace σ_{cr} by the true buckling stress σ_c from the buckling curve shown in Fig 2-4.

The normalized average stress can then be expressed by:

$$\frac{\sigma_{av}}{\sigma_y} = \left(\frac{\sigma_c}{\sigma_y}\right)^{1/2} = \bar{\sigma}^{\,1/2} \tag{2.24}$$

and the ultimate force is given by:

$$F_{ult} = \bar{\sigma}^{\,1/2} \sigma_y b\ t \tag{2.25}$$

The resulting relationship is compared with the code formula [Winter (1967)] in Fig 2-4

In this study it is proposed that in the general case the ultimate load is given by:

$$F_{ult} = \left(\sigma_c \sigma_y\right)^{1/2} s\ t \tag{2.26}$$

in which the buckling stress, σ_c, will be that for the element of the box, taking into account the corner radius and the adjoining walls, and s is the total length of the walls:

$$s = 2\ (a+b) - (8 - 2\ \pi)\ R \tag{2.27}$$

2.3 CHANNEL SECTION

2.3.1 CODE PROCEDURES

A channel section is considered to be an assembly of individual plates simply supported at all edges except at the free edges of the flanges. In this way the design is simplified to the design of one plate simply supported on both long edges and two plates simply supported along one long edge and free the other.

The current method used in Canadian codes is based on the effective areas of these individual plates. The following procedure is adopted:

- Only the flat widths (w) are considered to buckle locally.
- The corners are treated as simple supports.
- Below a specified limit for the flat width there is no buckling.
- For greater widths, after initial local buckling, zones at the edges of the flat width are assumed to carry the yield strength.
- Radiused corners are assumed to carry the yield strength but are otherwise disregarded.
- The web of a channel is treated in the same manner as the elements of a box section.
- For flanges, called "unstiffened elements", the critical buckling stress, neglecting any restraint by the web, is given by (ASCE-8-90)

$$\sigma_{cr} = \frac{0.43\ \pi^2 E\ t^2}{12\ (1-\nu^2) w^2} = \frac{\pi^2 E}{\lambda^2} \tag{2.28}$$

Using Poisson's ratio, v=0.3, this gives:

$$\lambda = 5\ \left(\frac{w}{t}\right) \tag{2.29}$$

2.3.2 PROPOSED ANALYTICAL MODEL

The following dimensions are used for obtaining theoretically the critical stress of a channel:

a: flange width
b: web width
c: halfwave length of buckled element
R: radius at the corner
t: thickness

As with the box channel the energy method is used to obtain the critical stress. The strain energy is supplied by:

- Deflection of the web, U_B
- Bending and twisting of the flange, U_W
- Twisting at the corners, U_T

The change in strain energy in the member is equal to the work done, thus (Timoshenko) :

$$U_B + U_W + U_T - T = 0 \qquad \textbf{(2.30)}$$

The complete procedure for finding the theoretical critical stress is presented in Appendix I.

Should the ratio of the web depth to the flange width exeed three, for uniform stress, the web is less stable than the flange, and it is restrained by the flanges. This is shown as the "Web Mode" in Fig 2-5. For smaller ratios, the flange is less stable and is restrained by the web shown as the "Flange Mode" in Fig 2-5.

2.3.4 THEORETICAL POST-BUCKLING

Up to this point the analysis has been concerned with the theoretical local elastic buckling stress. In a concentrically loaded column, flange buckling leads to collapse at the critical local buckling stress as there is no mechanism to develop postbuckling strength.

If the web buckles first it possesses postbuckling strength and the average limiting strength for the web area based on the box section calculation, becomes:

$$\sigma_{avr} = \left(\sigma_w \sigma_y\right)^{1/2} \tag{2.31}$$

where σ_w is the actual buckling stress for the web obtained from equation 2.2, using $\bar{\lambda}$ for the web with m=1.65.

CHAPTER 3

FINITE ELEMENT STUDIES

3.1 INTRODUCTION

The more complex a section is, the more difficult is evaluation with theoretical analysis. This is the reason that, today, many plate stability problems in practical engineering are evaluated by numerical methods such as the finite element method, which give approximate solutions for the ruling equations. In the finite element method the exact differential equation at a point is replaced by an algebraic expression consisting of the value of the function at that point and at adjacent points. In other words, the analytical solution describes the behaviour of the system as a continuous system, while the finite element solution gives an discrete solution of the function. In general if a continuous system is replaced by a discrete system the analytical function is replaced by numerical values which represent the function at each point.

In this study finite element methods provide a means to obtain an independent check on the results of an analytical approach and on the validity of code procedures. Box and channel sections were analyzed using the FEM program ABAQUS to obtain:

- The critical elastic buckling stress using the Eigenvalue method
- The ultimate, postbuckling capacity, using controlled displacement

3.2 EIGENVALUE METHOD

The eigenvalue represents the ideal elastic critical stress for initial buckling, and is used here to compare the values obtained for different boundary conditions. The formation of the eigenvalue problem is based on stability analysis. The procedure may be stated as follows. Given a system with an elastic stiffness matrix ($K_{(b)}^{NM}$), a loading pattern defined by the vector (Q^{M}), and an initial stress and load stiffness matrix ($K_{(Q)}^{NM}$), find load multipliers (λ_i), and buckling mode shapes (ϕ_i^{M}), which satisfy:

$$\left[K_{(b)}^{NxM} + \lambda_i \; K_{(Q)}^{NxM}\right] \phi_i^{M} = 0 \qquad \textbf{(3.1)}$$

in which N and M refer to degrees of the freedom of whole system and i refers to the ith mode. The critical buckling loads are then given by ($\lambda_i Q^{M}$). Usually only the smallest load multiplier and its associated mode shape are of interest.

As an illustration of the procedure of the eigenvalue method a simply supported plate is considered. Assume a square thin elastic plate, simply supported on all four edges is loaded by an axial compression force in one direction. (Fig 3-1)

The plate is divided into 20 elements (eight-node elements with 4 node on the corner and 4 node on mid points). Due to symmetry, only a quarter of the plate need to be considered. Briefly, the elastic stiffness matrix $[k_n]$, is formed by adding all the element stiffness matrices which is given by:

$$[\delta_n]^T[k_n][\delta_n] = \sum\left(\iint[\phi]^T[D][\phi]\,dxdy - \iint[\alpha]^T[N][\alpha]\,dxdy\right) \qquad \textbf{(3.2)}$$

in which [δ] is the matrix of the deflection on 4 nodes of the element:

$$[\delta] = \begin{bmatrix} w_1 \\ w_2 \\ w_3 \\ w_4 \end{bmatrix} \qquad \textbf{(3.3)}$$

[ϕ] , [α] are given by:

$$[\alpha] = \begin{bmatrix} \dfrac{\partial w}{\partial x} \\ \dfrac{\partial w}{\partial y} \end{bmatrix} \qquad \textbf{(3.4)} \qquad\qquad [\phi] = \begin{bmatrix} \dfrac{\partial^2 w}{\partial x^2} \\ \dfrac{\partial^2 w}{\partial y^2} \\ \dfrac{\partial^2 w}{\partial x \partial y} \end{bmatrix} \qquad \textbf{(3.5)}$$

[D] is the material constant matrix:

$$[D]=\begin{bmatrix} D & vD & 0 \\ vD & D & 0 \\ 0 & 0 & D/2(1-v) \end{bmatrix} \tag{3.6}$$

and [N] is the external work matrix on the element, given by:

$$[N]=\begin{bmatrix} N_x & N_{xy} \\ N_{xy} & N_y \end{bmatrix} \tag{3.7}$$

Consequently to determine the critical load it is necessary to obtain the non-zero solution of:

$$\{[k_n]-[N_x][I]\}[\Delta]=0 \tag{3.8}$$

in which $[\Delta]$ consists of the section nodal deflections and [I] is the index matrix.

This is done by setting the determinant of the matrix equal to zero and solving for the smallest root of the resulting equation.

3.3 ULTIMATE LOAD

To determine the collapse load for shells, a load –displacement analysis is performed. This checks that the eigenvalue buckling prediction is accurate and at the same time investigates the behavior after buckling, and up to the collapse load.

The collapse load is defined as the maximum value in the load - displacement curve. To find the maximum load, a stepwise increasing load or displacement is applied. If the applied load is incremented it is called "load control", and if the axial shortening is incremented it is called "displacement control". Briefly, for "load control" an equilibrium system is assumed to which a small increment of load is added. This unbalance causes a displacement in the system which can be represent as:

$$u = u_0 + \Delta u \qquad \textbf{(3.9)}$$

where u_0, is the initial displacement and Δu, is a small increment which can be evaluated based on the increment in load.

This displacement becomes the initial displacement for the next step with a new load increment. It is the same process for "displacement control" by assuming steps in displacement.

3.4 ABAQUS PROGRAM

3.4.1 INTRODUCTION

The program which is used for numeric evaluation is ABAQUS. This program is a general finite element program. It is an interactive preprocessor used to create finite element models for shells. It has a variety of analysis types. Those of the interested in this study are eigenvalue extraction and static stress analysis, which are used for pre- and post-buckling. The program accepts the input which includes:

- Model Data
- History Data

The data to define a finite element model are:

- the elements: number, properties
- nodes: number
- material properties

History Data represents the initial condition or sequence of events or loading for the model. History data for eigenvalue method is basically an arbitrary initial load based on this method, and has only one step. For load - displacement analysis it represents the properties at each step which include both load and displacement.

3.4.2 INPUT OF THE PROGRAM

For executing the program, based on the method used, the following input is required:

- DEFINING OF MODEL:
  - Elements and Nodes: The number and type of element (classified by the number of nodes in each element
  - Shell: The elements in each shell and the number of layer in each shell with their thicknesses.
  - Material: The elastic modulus, yield strength and Poisson ratio for each layer of the shell
  - Boundary and Symmetric Condition: The conditions on each boundary and any symmetry
- DEFINING OF HISTORICAL DATA
  - Eigenvalue method: An initial stress distribution on the specific boundary is required. (Appendix III– List 1)
  - Load - Displacement analysis : In case of Load Control an initial and a step increment stress distribution on the required elements.

For the case of Displacement Control an initial and a step increment strain distribution on the required elements. (Appendix III– List 2)

3.4.3 OUTPUT OF THE PROGRAM

For each case by executing the eigenvalue section of the program, ABAQUS predicts the buckling modes and corresponding eigenvalue. Also a list of stresses and deflections is provided in the output of the program.

The load-displacement analysis results for each case are typically provided in n steps from zero load to a maximum which is part of the input. At each step the stress and strain distribution over the section is provided in the output.

CHAPTER 4
COMPARING THE RESULTS

The numerical, finite element results are compared with the theoretical predictions and the Codes rules. The finite element study was made for box and channel sections in the following ranges:

BOX SECTION	**RANGE**
Ratio of widths, a/b (a < b):	0.25, 0.5, 1
Ratio of width / thickness, b/t	40, 50, 66, 100, 200
Ratio of corner radius / width, R/b	0 to a/2
CHANNEL SECTION	
Ratio of web / flange width, a/b	1, 2, 4
Ratio of flange width / thickness, b/t	40, 50, 66, 100, 200
Ratio of corner radius / flange width, R/b	0 to b/2

4.1 TYPICAL EXAMPLE

To show the procedure for each case the following typical box section is chosen (Fig 4-1):

$$a = 100\ mm$$
$$b = 100\ mm$$
$$c = 100\ mm$$
$$R = 5\ mm$$
$$t = 1\ mm$$

$$\nu = 0.3$$
$$E = 200000\ MPa$$
$$\sigma_y = 350\ MPa$$

4.1.1 THEORETICAL CALCULATION

D is given by:

$$D = \frac{E\,t^3}{12\,(1-\nu^2)} = 1.83 \times 10^4\ N.mm \tag{4.1}$$

Warping factor α=0.044, and the warping constant H is given by (see appendix II for details):

$$H = \alpha\, b\, t\, R^4 = 0.044 \times 100 \times 1 \times 5^4 = 2750\ mm^6 \tag{4.2}$$

The elastic critical stress obtained from the theoretical analysis is:

$$\sigma_{cr} = \frac{N_{cr}}{t} = 82.4\ N.mm^{-2} \tag{4.3}$$

The normalized slenderness is:

$$\bar{\lambda} = \left(\frac{350}{82.4}\right)^{1/2} = 2.06 \tag{4.4}$$

Thus, according to the CSA standard, the true buckling stress for $\bar{\lambda} > 1/\sqrt{0.6} = 1.29$, is:

$$\sigma_c = \frac{82.4}{1.2} = 68.7\ N.mm^{-2} \tag{4.5}$$

The predicted mean stress at collapse, according to the method proposed in this thesis (Equation 2.24) is then:

$$\sigma_{av} = (\sigma_c \sigma_y)^{1/2} = (68.7 \times 350)^{1/2} = 155\ N.mm^{-2} \tag{4.6}$$

The true length of the walls is:

$$s = 2\ (a+b-4\ R)\ +4\ {}^{\pi}\!/_{2} R = 2\ (200-20)\ +4\ {}^{\pi}\!/_{2}\ 5 = 391\ mm \qquad \textbf{(4.7)}$$

Then the collapse load is:

$$F_{ult} = \sigma_{av} s\ t = 155 \times 391 \times 1 = 60700\ N \qquad \textbf{(4.8)}$$

4.1.2 CODE PREDICTIONS

The flat width is :

$$w = b-2\ R = 100-2\times 5 = 90\ mm \qquad \textbf{(4.9)}$$

giving a slenderness of :

$$\lambda = 1.65\ {}^{w}\!/_{t} = 1.65 \times {}^{90}\!/_{1} = 149 \qquad \textbf{(4.10)}$$

The critical buckling stress is given by:

$$\sigma_{cr} = \frac{\pi^2 E}{\lambda^2} = \frac{\pi^2 200000}{149^2} = 89.5\ N.mm^{-2} \qquad \textbf{(4.11)}$$

Then:

$$\bar{\lambda} = \left(\frac{\sigma_y}{\sigma_{cr}}\right)^{1/2} = \left(\frac{350}{89.50}\right)^{½} = 1.98 \qquad \textbf{(4.12)}$$

Leading to:

$$\rho = \frac{1-0.22/\ \bar{\lambda}}{\bar{\lambda}} = \frac{1-0.22/1.98}{1.98} = 0.448 \qquad \textbf{(4.13)}$$

and:

$$b_{eff} = \rho\ \omega = 0.448 \times 90 = 40.3\ mm \tag{4.14}$$

The ultimate load from the Code is given by:

$$F_{ult} = 4\ \sigma_y \left(b_{eff} + {}^{\pi\ R}\!/_{2} \right) t = 4 \times 350 \left(40.3 + {}^{\pi \times 5}\!/_{2} \right) \times 1 = 67400\ N \tag{4.15}$$

Thus the predicted average stress at collapse is:

$$\sigma_{av} = \frac{F_{ult}}{t\ s} = \frac{67400}{1 \times 391} = 172\ N\ mm^{-2} \tag{4.16}$$

4.1.3 FINITE ELEMENT RESULTS

4.1.3.1 EIGENVALUE RESULT

The eigenvalue is determined using load-control. Based on the input shown in Appendix III–List.1 the elastic critical stress for this case is (Fig 4.2):

$$\sigma_{cr}^{ABAQUS} = 85.7\ N/mm^2 \tag{4.17}$$

4.1.3.2 POSTBUCKLING STRENGTH

The ultimate load is determined using displacement control, Appendix III-List.2 shows the input format. At each step, the stress distribution across the boundary element set is obtained, and the average stress is evaluated. For the typical example being demonstrated, the stress distribution across the section at the ultimate load is shown in Fig 4.3.

Fig 4.4 shows the relationship between the mean stress and axial shortening. The highest stress in this curve represents the ultimate average stress, which is:

$$\sigma_{av}^{ABAQUS} = 162\ N.mm^{-2} \tag{4.18}$$

The ultimate force is given by:

$$F_{ul}^{ABAQUS} = \sigma_{ab}^{ABAQUS} s\ t\ = 162 \times 391 \times 1 = 63500\ N \tag{4.19}$$

4.2 RESULTS FOR BOX SECTIONS

The results are given in the figures listed in following table:

Fig No	CASES			
		a/b	b/t	R/b
Fig 4.5	Critical	1	40	0 to 0.5
Fig 4.6	Critical	1	50	0 to 0.5
Fig 4.7	Critical	1	66	0 to 0.5
Fig 4.8	Critical	1	100	0 to 0.5
Fig 4.9	Critical	1	200	0 to 0.5
Fig 4.10	Critical	0.5	40	0 to 0.25
Fig 4.11	Critical	0.5	50	0 to 0.25
Fig 4.12	Critical	0.5	66	0 to 0.25
Fig 4.13	Critical	0.5	100	0 to 0.25
Fig 4.14	Critical	0.5	200	0 to 0.25
Fig 4.15	Critical	0.25	40	0 to 0.125
Fig 4.16	Critical	0.25	50	0 to 0.125
Fig 4.17	Critical	0.25	66	0 to 0.125
Fig 4.18	Critical	0.25	100	0 to 0.125
Fig 4.19	Critical	0.25	200	0 to 0.125
Fig 4.20	Ultimate	1	40	0 to 0.5
Fig 4.21	Ultimate	1	50	0 to 0.5
Fig 4.22	Ultimate	1	66	0 to 0.5
Fig 4.23	Ultimate	1	100	0 to 0.5
Fig 4.24	Ultimate	1	200	0 to 0.5
Fig 4.25	Ultimate	0.5	40	0 to 0.25
Fig 4.26	Ultimate	0.5	50	0 to 0.25
Fig 4.27	Ultimate	0.5	66	0 to 0.25
Fig 4.28	Ultimate	0.5	100	0 to 0.25
Fig 4.29	Ultimate	0.5	200	0 to 0.25
Fig 4.30	Ultimate	0.25	40	0 to 0.125
Fig 4.31	Ultimate	0.25	50	0 to 0.125
Fig 4.32	Ultimate	0.25	66	0 to 0.125
Fig 4.33	Ultimate	0.25	100	0 to 0.125
Fig 4.34	Ultimate	0.25	200	0 to 0.125

In each figure the Code, theory and ABAQUS result for critical and ultimate stresses are shown.

Table 4-1 shows the summary of the results for all the cases. In this table how the Code and the theory differ from ABAQUS is shown as a percentage error.

The **m factors** used in equation 1.1 are represented in Fig 4-35 to 4-37, and values normalized with respect to 1.65, for box sections, are shown in Fig 4-38 to 4-40, as they vary with R/b.

Finally following figure shows the normalized mean stress at the ultimate load for theory, ABAQUS and Code predictions.

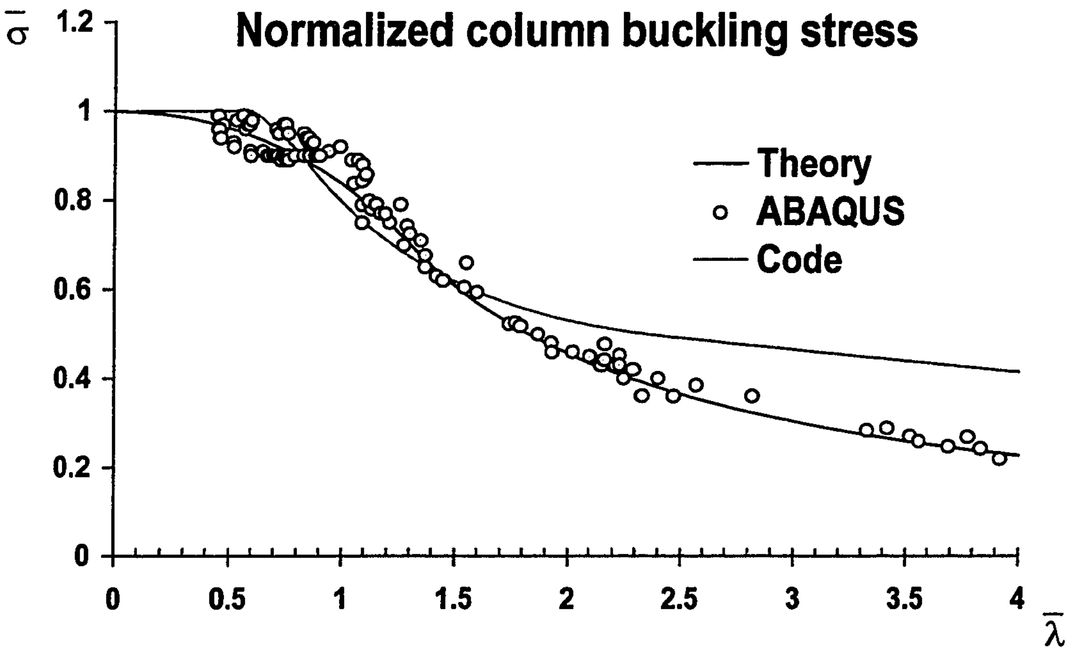

The extreme cases based on the percentage error between Code and ABAQUS result are shown in following table:

a/b	b/t	R/b	Critical stress	(N/mm²)		Code Error	Theory Error
			Code	Theory	ABAQUS		
1	40	0.3	2832	1435	1578	-79%	9%
0.25	200	0.1	28	72	81	65%	11%
a/b	b/t	R/b	Ultimate stress	(N/mm²)		Code Error	Theory Error
			Code	Theory	ABAQUS		
1	200	0.3	174	134	145	-20%	7%
0.25	200	0.125	106	160	177	40%	10%

4.3 RESULTS FOR CHANNEL SECTIONS

The results are given in the figures listed in following table:

Fig No	Case			
		a/b	b/t	R/b
Fig 4.42	Critical	1	40	0 to 0.25
Fig 4.43	Critical	1	50	0 to 0.25
Fig 4.44	Critical	1	66	0 to 0.25
Fig 4.45	Critical	1	100	0 to 0.25
Fig 4.46	Critical	1	200	0 to 0.25
Fig 4.47	Critical	0.5	40	0 to 0.25
Fig 4.48	Critical	0.5	50	0 to 0.25
Fig 4.49	Critical	0.5	66	0 to 0.25
Fig 4.50	Critical	0.5	100	0 to 0.25
Fig 4.51	Critical	0.5	200	0 to 0.25
Fig 4.52	Critical	0.25	40	0 to 0.25
Fig 4.53	Critical	0.25	50	0 to 0.25
Fig 4.54	Critical	0.25	66	0 to 0.25
Fig 4.55	Critical	0.25	100	0 to 0.25
Fig 4.56	Critical	0.25	200	0 to 0.25

In each figure the Code, theory and ABAQUS predictions for critical stresses are shown.
Table 4-2 shows the summary of the results for all the cases. In this table how the Code and the theory differ from ABAQUS is shown as percentage errors.
The **m factors** are represented in Fig 4-57 to 4-59 and normalized values with respect to 5 for the flanges, are shown in Fig 4-60 to 4-62 as they vary with R/b.
Finally Fig 4.41 shows the normalized mean stress at the ultimate load for theory, ABAQUS and Code results.

The extreme cases based on the percentage error between Code and ABAQUS result are shown in following table:

a/b	b/t	R/b	Critical stress (N/mm^2)			Code	Theory
			Code	Theory	ABAQUS	Error	Error
1	200	0.1	16	69	74	78%	7%

4.4 CONCLUSIONS

4.4.1 BOX SECTIONS

The influence that the radii at the corners has on the elastic and ultimate buckling stress of the box sections is important and should not be neglected, as in the current codes.

For boxes with a low width to thickness ratio, 66 or less, failure occurred close to the yield strength. In these situations the buckling stress is more influenced by the ratio of the widths, (a/b) than R/b. For a high width to thickness ratio, more than 66 when the failure stress is lower than yield strength, both the ratio of the widths and R/b are very influential on the failure. By neglecting the b/a ratio and R/b the Code can be 65% conservative to 79% unsafe.

4.4.2 CHANNEL SECTIONS

The influence that the ratio of the web to flange, b/a, has on the buckling capacity of the section is important and must be considered. For the channels with a web to flange ratio less than 3 failure occurred by flange buckling mode, and the critical stress represents the ultimate stress. For a web to flange ratio more than 3 web buckling occurred first. In this case there is a possibility for the channel to carry an ultimate load in exceed of critical elastic value. By neglecting the b/a ratio the Code can be varied from over 34% to 54% conservative while by neglecting R/b, the Code can be 78% conservative.

4.4.3 FINAL COMMENTS

An inappropriate interpretation of the ratio of the width for the cold-formed sections and the neglect of the influence of the corner radii on the buckling capacity as in the current codes, can lead to unsafe design or overdesign.

4.4.4 FUTURE RESEARCH

To follow the present work, which is just done for two major forms of cold-formed section (box, channel) it is recommended that other be investigated.

APPENDIX I

ANALYSIS

I.1 INTRODUCTION

In this chapter the steps of the procedure are described. The software which is used for parametric calculation is Mathcad which has the ability to solve algebraic equations. To obtain the result for each specific case the numerical values of the parameters are substituted in the final algebraic expressions.

I.2 BOX SECTION

After buckling the deflection of the elements is assumed to be modeled by trigonometric expressions as follows: (shown in Fig I.1)

Side a:

$$w_a = \left[a_3 \cdot \sin\left(\pi \cdot \frac{x}{a}\right) + a_4 \cdot \left(1 - \cos\left(\pi \cdot \frac{2 \cdot x}{a}\right)\right)\right] \cdot \sin\left(\pi \cdot \frac{z}{c}\right) \qquad \text{(I-1)}$$

Side b :

$$w_b = \left[a_1 \cdot \sin\left(\pi \cdot \frac{y}{b}\right) - a_2 \cdot \left(1 - \cos\left(\pi \cdot \frac{2 \cdot y}{b}\right)\right)\right] \cdot \sin\left(\pi \cdot \frac{z}{c}\right) \qquad \text{(I-2)}$$

where a_1, a_2, a_3, a_4 define the buckled shape and a < b.

As it was explained in Chapter 2 the strain energy due to deflection in a plate supported on all edges, is given by :

$$U = \frac{D}{2} \cdot \int \int \left[\left[\left(\frac{d^2 \cdot w}{dx^2} \right) + \left(\frac{d^2 \cdot w}{dy^2} \right) \right]^2 \right] dx\, dy \qquad \text{(I-3)}$$

Considering the affect of the corner radii on the width of the plates for side b the strain energy due to bending is given by:

$$U_b = \frac{D}{2} \cdot \int_0^c \int_\beta^{b-\beta} \left[\left[\left(\frac{d^2 \cdot w}{dy^2} \right) + \left(\frac{d^2 \cdot w}{dz^2} \right) \right]^2 \right] dy\, dz \qquad \text{(I-4)}$$

$$= \frac{1}{48} \cdot D \cdot \frac{\pi^4}{(c^3 \cdot b^4)} \cdot \left[-12 \cdot \sin\left[2 \cdot \pi \cdot \frac{(b-\beta)}{b}\right] \cdot b^5 \cdot a_2{}^2 - 6 \cdot b^5 \cdot a_1{}^2 \cdot \cos\left[\pi \cdot \frac{(b-\beta)}{b}\right] \cdot \sin\left[\pi \cdot \frac{(b-\beta)}{b}\right]\right]$$

$$\cdot + 84 \cdot \cos\left[\pi \cdot \frac{(b-\beta)}{b}\right] \cdot b^3 \cdot a_1 \cdot a_2 \cdot c^2 - 48 \cdot \sin\left[2 \cdot \pi \cdot \frac{(b-\beta)}{b}\right] \cdot b^3 \cdot a_2{}^2 \cdot c^2 + 6 \cdot b^5 \cdot a_1{}^2 \cdot \pi + 18 \cdot a_2{}^2 \cdot b^5 \cdot \pi$$

$$\cdot + 6 \cdot a_1{}^2 \cdot c^4 \cdot \cos\left[\pi \cdot \frac{(b-\beta)}{b}\right] \cdot \sin\left[\pi \cdot \frac{(b-\beta)}{b}\right] \cdot b - 16 \cdot b \cdot a_1 \cdot a_2 \cdot c^4 \cdot \cos\left[3 \cdot \pi \cdot \frac{(b-\beta)}{b}\right]$$

$$\cdot - 4 \cdot b^5 \cdot a_1 \cdot a_2 \cdot \cos\left[3 \cdot \pi \cdot \frac{(b-\beta)}{b}\right] + 36 \cdot \cos\left[\pi \cdot \frac{(b-\beta)}{b}\right] \cdot b^5 \cdot a_1 \cdot a_2$$

$$\cdot + 48 \cdot b \cdot a_1 \cdot a_2 \cdot c^4 \cdot \cos\left[\pi \cdot \frac{(b-\beta)}{b}\right] + 48 \cdot a_2{}^2 \cdot c^4 \cdot \cos\left[2 \cdot \pi \cdot \frac{(b-\beta)}{b}\right] \cdot \sin\left[2 \cdot \pi \cdot \frac{(b-\beta)}{b}\right] \cdot b$$

in which β is given by:

$$\beta = R \cdot \left(1 - \frac{1}{\sqrt{2}}\right) \qquad \text{(I-5)}$$

and for side a it is given by:

$$U_a=\frac{D}{2}\cdot\int_0^c\int_\beta^{a-\beta}\left[\left[\left(\frac{d^2\cdot w}{dx^2}\right)+\left(\frac{d^2\cdot w}{dz^2}\right)\right]^2\right]dx\,dz \tag{I-6}$$

$$=\frac{1}{48}\cdot D\cdot\frac{\pi^4}{(c^3\cdot a^4)}\cdot\left[-12\cdot\sin\left[2\cdot\pi\cdot\frac{(a-\beta)}{a}\right]\cdot a^5\cdot a_4{}^2-6\cdot a^5\cdot a_3{}^2\cdot\cos\left[\pi\cdot\frac{(a-\beta)}{a}\right]\cdot\sin\left[\pi\cdot\frac{(a-\beta)}{a}\right]\right]$$

$$\cdot+84\cdot\cos\left[\pi\cdot\frac{(a-\beta)}{a}\right]\cdot a^3\cdot a_3\cdot a_4\cdot c^2-48\cdot\sin\left[2\cdot\pi\cdot\frac{(a-\beta)}{a}\right]\cdot a^3\cdot a_4{}^2\cdot c^2+6\cdot a^5\cdot a_3{}^2\cdot\pi+18\cdot a_4{}^2\cdot a^5\cdot\pi$$

$$\cdot+6\cdot a_3{}^2\cdot c^4\cdot\cos\left[\pi\cdot\frac{(a-\beta)}{a}\right]\cdot\sin\left[\pi\cdot\frac{(a-\beta)}{a}\right]\cdot a-16\cdot a\cdot a_3\cdot a_4\cdot c^4\cdot\cos\left[3\cdot\pi\cdot\frac{(a-\beta)}{a}\right]$$

$$\cdot-4\cdot a^5\cdot a_3\cdot a_4\cdot\cos\left[3\cdot\pi\cdot\frac{(a-\beta)}{a}\right]+36\cdot\cos\left[\pi\cdot\frac{(a-\beta)}{a}\right]\cdot a^5\cdot a_3\cdot a_4$$

$$\cdot+48\cdot a\cdot a_3\cdot a_4\cdot c^4\cdot\cos\left[\pi\cdot\frac{(a-\beta)}{a}\right]+48\cdot a_4{}^2\cdot c^4\cdot\cos\left[2\cdot\pi\cdot\frac{(a-\beta)}{a}\right]\cdot\sin\left[2\cdot\pi\cdot\frac{(a-\beta)}{a}\right]\cdot a$$

The external work due to uniform axial force given by:

$$T=\frac{N}{2}\cdot\int\int\left(\frac{dw}{dy}\right)^2dx\,dy \tag{I-7}$$

The external work for side b is given by :

$$T_b=\frac{N}{2}\cdot\int_0^c\int_\beta^{b-\beta}\left(\frac{dw}{dz}\right)^2dy\,dz \tag{I-8}$$

$$=\frac{1}{48}\cdot N\cdot\pi\cdot\frac{b}{c}\cdot\left[-6\cdot a_1{}^2\cdot\cos\left[\pi\cdot\frac{(b-\beta)}{b}\right]\cdot\sin\left[\pi\cdot\frac{(b-\beta)}{b}\right]+3\cdot a_2{}^2\cdot\cos\left[2\cdot\pi\cdot\frac{(b-\beta)}{b}\right]\cdot\sin\left[2\cdot\pi\cdot\frac{(b-\beta)}{b}\right]\right]$$

$$\cdot -6\cdot a_1{}^2\cdot\cos\left(\pi\cdot\frac{\beta}{b}\right)\cdot\sin\left(\pi\cdot\frac{\beta}{b}\right)+18\cdot a_2{}^2\cdot\pi\cdot\beta-4\cdot a_1\cdot a_2\cdot\cos\left(3\cdot\pi\cdot\frac{\beta}{b}\right)+6\cdot a_1{}^2\cdot\pi\cdot\beta+36\cdot\cos\left(\pi\cdot\frac{\beta}{b}\right)\cdot a_1\cdot a_2$$

$$\cdot -6\cdot a_1{}^2\cdot\pi+36\cdot\cos\left[\pi\cdot\frac{(b-\beta)}{b}\right]\cdot a_1\cdot a_2+6\cdot a_1{}^2\cdot\pi\cdot\beta-12\cdot\sin\left(2\cdot\pi\cdot\frac{\beta}{b}\right)\cdot a_2{}^2$$

and for side a is given by:

$$T_a=\frac{N}{2}\cdot\int_0^c\int_\beta^{a-\beta}\left(\frac{dw}{dz}\right)^2 dx\,dz \tag{I-9}$$

$$=\frac{1}{48}\cdot N\cdot\pi\cdot\frac{a}{c}\cdot\left[-6\cdot a_3{}^2\cdot\cos\left[\pi\cdot\frac{(a-\beta)}{a}\right]\cdot\sin\left[\pi\cdot\frac{(a-\beta)}{a}\right]+3\cdot a_4{}^2\cdot\cos\left[2\cdot\pi\cdot\frac{(a-\beta)}{a}\right]\cdot\sin\left[2\cdot\pi\cdot\frac{(a-\beta)}{a}\right]\right]$$

$$\cdot -6\cdot a_3{}^2\cdot\cos\left(\pi\cdot\frac{\beta}{a}\right)\cdot\sin\left(\pi\cdot\frac{\beta}{a}\right)+18\cdot a_4{}^2\cdot\pi\cdot\beta-4\cdot a_3\cdot a_4\cdot\cos\left(3\cdot\pi\cdot\frac{\beta}{a}\right)+6\cdot a_3{}^2\cdot\pi\cdot\beta+36\cdot\cos\left(\pi\cdot\frac{\beta}{a}\right)\cdot a_3\cdot a_4$$

$$\cdot +36\cdot\cos\left[\pi\cdot\frac{(a-\beta)}{a}\right]\cdot a_3\cdot a_4+6\cdot a_3{}^2\cdot\pi\cdot\beta-6\cdot a_3{}^2\cdot\pi-12\cdot\sin\left(2\cdot\pi\cdot\frac{\beta}{a}\right)\cdot a_4{}^2$$

The warping constant is given by:

$$H=\int\left(\bar{\varpi}_s-\varpi_s\right)^2\cdot t\,ds \tag{I-10}$$

Where $(\bar{\varpi}_s-\varpi_s)$ is the net displacement normal to a cross section due to warping and the length s is measured along the element wall.

(For evaluation of H see Appendix II)

The strain energy due to warping for the corner between sides a and b is given by:

$$U_H = E \cdot H \cdot \int_0^c \left(\frac{d^2 \cdot \phi}{dz^2}\right)^2 dz \qquad \text{(I-11)}$$

in which

$$\phi = \left(\frac{dw}{dy}\right)_{y=0} \qquad \text{(I-12)}$$

This leads to:

$$U_H = \frac{1}{4} \cdot E \cdot H \cdot \frac{\pi^6}{c^3} \cdot \frac{a_1^2}{b^2} \qquad \text{(I-13)}$$

The energy balance for the whole section is given by:

$$U_a + U_b + U_H - (T_a + T_b) = 0 \qquad \text{(I-14)}$$

This equation has five unknowns, N,a_1,a_2,a_3,a_4. At each corner the tangents to the deflected plates must be perpendicular to each other. This provides the third equation which gives a_3 in terms of a_1 :

$$\left(\frac{\delta w}{\delta x}\right)_{x=0} = \left(\frac{\delta w}{\delta y}\right)_{y=0}$$

thus

$$a_1 \cdot \sin\left(\pi \cdot \frac{z}{c}\right) \cdot \frac{\pi}{b} = a_3 \cdot \sin\left(\pi \cdot \frac{z}{c}\right) \cdot \frac{\pi}{a}$$

$$a_3 = a_1 \cdot \frac{a}{b}$$ (I-15)

Considering the bending moment for sides a and b, to provide equal moments at the corner for both plates the following equation must be valid:

$$\left(\frac{\delta^2 \cdot w}{\delta x^2}\right)_{x=0} = \left(\frac{\delta^2 \cdot w}{\delta y^2}\right)_{y=0}$$

$$-4 \cdot a_2 \cdot \frac{\pi^2}{b^2} \cdot \sin\left(\pi \cdot \frac{z}{c}\right) = -4 \cdot a_4 \cdot \frac{\pi^2}{a^2} \cdot \sin\left(\pi \cdot \frac{z}{c}\right)$$

$$a_4 = \frac{a^2}{b^2} \cdot a_2$$ (I-16)

Substituting the value of a_3 and a_4 in term of a_1, a_2, leads to an equation with three parameters. Differentiating with respect to a_1 and a_2 gives two equations. To find the theoretical critical stress the determinant of these equations is equated to zero.

Differentiating with respect to a_1 gives:

$$F_{11}(N) \cdot a_1 + F_{12}(N) \cdot a_2 = 0$$ (I-17)

Differentiating with respect to a_2 gives:

$$F_{21}(N) \cdot a_1 + F_{22}(N) \cdot a_2 = 0$$ (I-18)

Equating the determinant of equations 5-17 and 5-18 to zero leads to:

$$F_{11}(N)\cdot F_{22}(N) - F_{12}(N)\cdot F_{21}(N) = 0 \qquad \text{(I-19)}$$

in which

$$F_{11}(N) = \frac{1}{48}\cdot D\cdot\frac{\pi^4}{(c^3\cdot b^4)}\cdot\left[-12\cdot\cos\left[\pi\cdot\frac{(b-\beta)}{b}\right]\cdot b^5\cdot\sin\left[\pi\cdot\frac{(b-\beta)}{b}\right]+12\cdot b^5\cdot\pi+12\cdot c^4\cdot\cos\left[\pi\cdot\frac{(b-\beta)}{b}\right]\cdot\sin\left[\pi\cdot\frac{(b-\beta)}{b}\right]\cdot b\right] \qquad \text{(I-20)}$$

$$+\frac{1}{48}\cdot N\cdot\pi\cdot\frac{b}{c}\cdot\left[-12\cdot\cos\left[\pi\cdot\frac{(b-\beta)}{b}\right]\cdot\sin\left[\pi\cdot\frac{(b-\beta)}{b}\right]-12\cdot\pi+24\cdot\pi\cdot\beta-12\cdot\cos\left(\pi\cdot\frac{\beta}{b}\right)\cdot\sin\left(\pi\cdot\frac{\beta}{b}\right)\right]$$

$$+\frac{1}{2}\cdot E\cdot H\cdot\frac{\pi^6}{c^3\cdot b^2}$$

$$+\frac{1}{48}\cdot D\cdot\frac{\pi^4}{(c^3\cdot b^4)}\cdot\left[-12\cdot b^4\cdot a\cdot\cos\left[\pi\cdot\frac{(b-\beta)}{b}\right]\cdot\sin\left[\pi\cdot\frac{(b-\beta)}{b}\right]+12\cdot b^4\cdot a\cdot\pi+12\cdot a\cdot c^4\cdot\cos\left[\pi\cdot\frac{(b-\beta)}{b}\right]\cdot\sin\left[\pi\cdot\frac{(b-\beta)}{b}\right]\right]$$

$$+\frac{1}{48}\cdot N\cdot\pi\cdot\frac{b}{c}\cdot\left[-12\cdot\frac{a}{b}\cdot\cos\left[\pi\cdot\frac{(b-\beta)}{b}\right]\cdot\sin\left[\pi\cdot\frac{(b-\beta)}{b}\right]-12\cdot\frac{a}{b}\cdot\pi+24\cdot\frac{a}{b}\cdot\pi\cdot\beta-12\cdot\frac{a}{b}\cdot\cos\left(\pi\cdot\frac{\beta}{b}\right)\cdot\sin\left(\pi\cdot\frac{\beta}{b}\right)\right]$$

$$+\frac{1}{2}\cdot E\cdot H\cdot\frac{\pi^6}{c^3\cdot b^2}$$

$$F_{21}(N) = \frac{1}{48}\cdot D\cdot\frac{\pi^4}{(c^3\cdot b^4)}\cdot\left[-4\cdot b^5\cdot\cos\left[3\cdot\pi\cdot\frac{(b-\beta)}{b}\right]+168\cdot\cos\left[\pi\cdot\frac{(b-\beta)}{b}\right]\cdot b^3\cdot c^2+72\cdot\cos\left[\pi\cdot\frac{(b-\beta)}{b}\right]\cdot b^5\right] \qquad \text{(I-21)}$$

$$+\frac{1}{48}\cdot N\cdot\pi\cdot\frac{b}{c}\cdot\left[36\cdot\cos\left[\pi\cdot\frac{(b-\beta)}{b}\right]-4\cdot\cos\left(3\cdot\pi\cdot\frac{\beta}{b}\right)+36\cdot\cos\left(\pi\cdot\frac{\beta}{b}\right)\right]$$

$$+\frac{1}{48}\cdot D\cdot\frac{\pi^4}{(c^3\cdot b^4)}\cdot\left[-4\cdot b^4\cdot a\cdot\cos\left[3\cdot\pi\cdot\frac{(b-\beta)}{b}\right]+168\cdot\cos\left[\pi\cdot\frac{(b-\beta)}{b}\right]\cdot b^2\cdot a\cdot c^2+72\cdot b^4\cdot a\cdot\cos\left[\pi\cdot\frac{(b-\beta)}{b}\right]\right]$$

$$+\frac{1}{48}\cdot N\cdot\pi\cdot\frac{b}{c}\cdot\left[36\cdot\frac{a}{b}\cdot\cos\left[\pi\cdot\frac{(b-\beta)}{b}\right]-4\cdot\frac{a}{b}\cdot\cos\left(3\cdot\pi\cdot\frac{\beta}{b}\right)+36\cdot\frac{a}{b}\cdot\cos\left(\pi\cdot\frac{\beta}{b}\right)\right]$$

$$F_{12}(N)=\frac{1}{48}\cdot D\cdot\frac{\pi^4}{\left(c^3\cdot b^4\right)}\cdot\left[-4\cdot b^5\cdot\cos\left[3\cdot\pi\cdot\frac{(b-\beta)}{b}\right]+84\cdot\cos\left[\pi\cdot\frac{(b-\beta)}{b}\right]\cdot b^3\cdot c^2+36\cdot\cos\left[\pi\cdot\frac{(b-\beta)}{b}\right]\cdot b^5\right] \tag{I-22}$$

$$\cdot+\frac{1}{48}\cdot N\cdot\pi\cdot\frac{b}{c}\left[36\cdot\cos\left[\pi\cdot\frac{(b-\beta)}{b}\right]-4\cdot\cos\left(3\cdot\pi\cdot\frac{\beta}{b}\right)+36\cdot\cos\left(\pi\cdot\frac{\beta}{b}\right)+48\cdot b\cdot c^4\cdot\cos\left[\pi\cdot\frac{(b-\beta)}{b}\right]+16\cdot b\cdot c^4\cdot\cos\left[3\cdot\pi\cdot\frac{(b-\beta)}{b}\right]\right]$$

$$\cdot+\frac{1}{48}\cdot D\cdot\frac{\pi^4}{\left(c^3\cdot b^4\right)}\cdot\left[-4\cdot b^3\cdot a^2\cdot\cos\left[3\cdot\pi\cdot\frac{(b-\beta)}{b}\right]+84\cdot\cos\left[\pi\cdot\frac{(b-\beta)}{b}\right]\cdot b\cdot a^2\cdot c^2+36\cdot\cos\left[\pi\cdot\frac{(b-\beta)}{b}\right]\cdot b^3\cdot a^2\right]$$

$$\cdot+\frac{1}{48}\cdot D\cdot\frac{\pi^4}{\left(c^3\cdot b^4\right)}\cdot\left[\frac{16}{b}\cdot a^2\cdot c^4\cdot\cos\left[3\cdot\pi\cdot\frac{(b-\beta)}{b}\right]+\frac{48}{b}\cdot a^2\cdot c^4\cdot\cos\left[\pi\cdot\frac{(b-\beta)}{b}\right]\right]$$

$$\cdot+\frac{1}{48}\cdot N\cdot\pi\cdot\frac{b}{c}\cdot\left[36\cdot\cos\left[\pi\cdot\frac{(b-\beta)}{b}\right]\cdot\frac{a^2}{b^2}-4\cdot\frac{a^2}{b^2}\cdot\cos\left(3\cdot\pi\cdot\frac{\beta}{b}\right)+36\cdot\cos\left(\pi\cdot\frac{\beta}{b}\right)\cdot\frac{a^2}{b^2}\right]$$

$$F_{22}(N)=\frac{1}{48}\cdot D\cdot\frac{\pi^4}{\left(c^3\cdot b^4\right)}\cdot\left[-24\cdot\sin\left[2\cdot\pi\cdot\frac{(b-\beta)}{b}\right]\cdot b^5-192\cdot\sin\left[2\cdot\pi\cdot\frac{(b-\beta)}{b}\right]\cdot b^3\cdot c^2+72\cdot b^5\cdot\pi\right] \tag{I-23}$$

$$\cdot+\frac{1}{48}\cdot N\cdot\pi\cdot\frac{b}{c}\cdot\left[6\cdot\cos\left[2\cdot\pi\cdot\frac{(b-\beta)}{b}\right]\cdot\sin\left[2\cdot\pi\cdot\frac{(b-\beta)}{b}\right]+36\cdot\pi+36\cdot\pi\cdot\beta-24\cdot\sin\left(2\cdot\pi\cdot\frac{\beta}{b}\right)\right]$$

$$\cdot+\frac{1}{48}\cdot D\cdot\frac{\pi^4}{\left(c^3\cdot b^4\right)}\cdot\left[-24\cdot\sin\left[2\cdot\pi\cdot\frac{(b-\beta)}{b}\right]\cdot b^3\cdot a^2-192\cdot\sin\left[2\cdot\pi\cdot\frac{(b-\beta)}{b}\right]\cdot b\cdot a^2\cdot c^2+72\cdot b^3\cdot a^2\cdot\pi\right]$$

$$\cdot+\frac{1}{48}\cdot N\cdot\pi\cdot\frac{b}{c}\cdot\left[6\cdot\frac{a^2}{b^2}\cdot\cos\left[2\cdot\pi\cdot\frac{(b-\beta)}{b}\right]\cdot\sin\left[2\cdot\pi\cdot\frac{(b-\beta)}{b}\right]+36\cdot\frac{a^2}{b^2}\cdot\pi+36\cdot\frac{a^2}{b^2}\cdot\pi\cdot\beta-24\cdot\sin\left(2\cdot\pi\cdot\frac{\beta}{b}\right)\cdot\frac{a^2}{b^2}\right]$$

The critical theoretical buckling force is evaluated from $F_{11(N)}$ to $F_{22(N)}$ as:

$$N_{cr}=\mathrm{root}\left(F_{11}(N)\cdot F_{22}(N)-F_{12}(N)\cdot F_{21}(N),N\right) \tag{I-24}$$

I.3 CHANNEL SECTION

For a channel section the procedure is divided into two phases. Depending on the ratio of web width to flange width, the critical buckling stress for the web may be smaller or larger than the critical stress for the flange. The true buckling stress is that of the combined section, but the buckling mode may be described as "flange mode" or "web mode" .

I.3.1 FLANGE MODE

Assuming the flange buckles first, the deflection of the elements after buckling is given by: (shown in Fig I.2)

Web :

$$w_{web}=\left[a_1\cdot\sin\left(\pi\cdot\frac{y}{b}\right)+a_2\cdot\left(1-\cos\left(\frac{2\cdot\pi\cdot y}{b}\right)\right)\right]\cdot\sin\left(\pi\cdot\frac{z}{c}\right) \tag{I-25}$$

Flange:

$$w_{flange}=\left[\theta\cdot x+a_3\cdot\left(1-\cos\left(\frac{\pi\cdot x}{2\cdot a}\right)\right)\right]\cdot\sin\left(\pi\cdot\frac{z}{c}\right) \tag{I-26}$$

where θ , a_1, a_2, a_3 define the buckled shape.

The strain energy due to bending for the web is given by:

$$U_{web}=\frac{D}{2}\cdot\int_0^c\int_\beta^{b-\beta}\left[\left[\left(\frac{d^2}{dy^2}w\right)+\left(\frac{d^2}{dz^2}w\right)\right]^2-2\cdot(1-\nu)\cdot\left[\frac{d^2}{dy^2}w\cdot\frac{d^2}{dz^2}w-\left(\frac{d}{dyz}w\right)^2\right]\right]dy\,dz$$

$$=\frac{1}{48}\cdot D\cdot\frac{\pi^4}{(c^3\cdot b^4)}\cdot\left[-12\cdot\sin\left[2\cdot\pi\cdot\frac{(b-\beta)}{b}\right]\cdot b^5\cdot a_2{}^2-6\cdot b^5\cdot a_1{}^2\cdot\cos\left[\pi\cdot\frac{(b-\beta)}{b}\right]\cdot\sin\left[\pi\cdot\frac{(b-\beta)}{b}\right]\right] \quad \text{(I-27)}$$

$$.-84\cdot\cos\left[\pi\cdot\frac{(b-\beta)}{b}\right]\cdot b^3\cdot a_1\cdot a_2\cdot c^2-48\cdot\sin\left[2\cdot\pi\cdot\frac{(b-\beta)}{b}\right]\cdot b^3\cdot a_2{}^2\cdot c^2+6\cdot b^5\cdot a_1{}^2\cdot\pi+18\cdot a_2{}^2\cdot b^5\cdot\pi$$

$$.+6\cdot a_1{}^2\cdot c^4\cdot\cos\left[\pi\cdot\frac{(b-\beta)}{b}\right]\cdot\sin\left[\pi\cdot\frac{(b-\beta)}{b}\right]\cdot b+16\cdot b\cdot a_1\cdot a_2\cdot c^4\cdot\cos\left[3\cdot\pi\cdot\frac{(b-\beta)}{b}\right]$$

$$.+4\cdot b^5\cdot a_1\cdot a_2\cdot\cos\left[3\cdot\pi\cdot\frac{(b-\beta)}{b}\right]-36\cdot\cos\left[\pi\cdot\frac{(b-\beta)}{b}\right]\cdot b^5\cdot a_1\cdot a_2$$

$$.+48\cdot a_2{}^2\cdot c^4\cdot\cos\left[2\cdot\pi\cdot\frac{(b-\beta)}{b}\right]\cdot\sin\left[2\cdot\pi\cdot\frac{(b-\beta)}{b}\right]\cdot b-48\cdot b\cdot a_1\cdot a_2\cdot c^4\cdot\cos\left[\pi\cdot\frac{(b-\beta)}{b}\right]$$

where:

$$\beta=R\left(1-\frac{1}{\sqrt{2}}\right) \quad \text{(I-28)}$$

For the flange the strain energy is given by:

$$U_{flange}=\frac{D}{2}\cdot\int_0^c\int_\beta^a\left[\left[\left(\frac{d^2}{dx^2}w\right)+\left(\frac{d^2}{dz^2}w\right)\right]^2-2\cdot(1-\nu)\cdot\left[\frac{d^2}{dx^2}w\cdot\frac{d^2}{dz^2}w-\left(\frac{d}{dxz}w\right)^2\right]\right]dx\,dz$$

$$=\frac{D}{384\cdot a^3\cdot c^3}\cdot\left(96\cdot\sin\left(\frac{1}{2}\cdot\pi\cdot\frac{\beta}{a}\right)\cdot a^3\cdot a_3{}^2\cdot c^2\cdot\pi^5+6\cdot a_3{}^2\cdot c^4\cdot\pi^3\cdot\cos\left(\frac{1}{2}\cdot\pi\cdot\frac{\beta}{a}\right)\cdot\sin\left(\frac{1}{2}\cdot\pi\cdot\frac{\beta}{a}\right)\cdot a\right. \quad \text{(I-29)}$$

$$.+144\cdot a_3{}^2\cdot a^4\cdot\pi^4\cdot\beta+96\cdot\theta\cdot a_3\cdot a^4\cdot\pi^4\cdot\beta^2-144\cdot a_3{}^2\cdot a^4\cdot\pi^6\cdot\beta-384\cdot\sin\left(\frac{1}{2}\cdot\pi\cdot\frac{\beta}{a}\right)\cdot a^5\cdot a_3{}^2\cdot\pi^2$$

$$.+32\cdot\theta^2\cdot a^5\cdot\pi^6-144\cdot a_3{}^2\cdot a^3\cdot\pi^4+144\cdot a_3{}^2\cdot a^3\cdot\pi^6+96\cdot a^2\cdot a_3\cdot\theta\cdot c^2\cdot\pi^3-768\cdot a^4\cdot\theta\cdot a_3\cdot\pi^2$$

$$.-3\cdot a_3{}^2\cdot c^3\cdot\pi^4+96\cdot a\cdot a_3{}^2\cdot c^2\cdot\pi^3-96\cdot a\cdot a_3{}^2\cdot c^2\cdot\pi^5+192\cdot a^4\cdot a_3\cdot\theta\cdot c^2\cdot\pi^4\cdot\cos\left(\frac{1}{2}\cdot\pi\cdot\frac{\beta}{a}\right)$$

$$.-96\cdot a^3\cdot a_3\cdot\theta\cdot c^2\cdot\pi^3\cdot\sin\left(\frac{1}{2}\cdot\pi\cdot\frac{\beta}{a}\right)\cdot\beta-768\cdot a^6\cdot\theta\cdot a_3\cdot\cos\left(\frac{1}{2}\cdot\pi\cdot\frac{\beta}{a}\right)$$

The external work for the web is given by:

$$T_{web}=\frac{N}{2}\cdot\int_{0}^{c}\int_{\beta}^{b-\beta}\left(\frac{d}{dz}w\right)^{2}dy\,dz \tag{I-30}$$

$$=\frac{1}{48}\cdot N\cdot\pi\cdot\frac{b}{c}\cdot\left[-6\cdot a_1^{2}\cdot\cos\left[\pi\cdot\frac{(b-\beta)}{b}\right]\cdot\sin\left[\pi\cdot\frac{(b-\beta)}{b}\right]+3\cdot a_2^{2}\cdot\cos\left[2\cdot\pi\cdot\frac{(b-\beta)}{b}\right]\cdot\sin\left[2\cdot\pi\cdot\frac{(b-\beta)}{b}\right]\right]$$

$$.-6\cdot a_1^{2}\cdot\cos\left(\pi\cdot\frac{\beta}{b}\right)\cdot\sin\left(\pi\cdot\frac{\beta}{b}\right)+18\cdot a_2^{2}\cdot\pi\cdot\beta+4\cdot a_1\cdot a_2\cdot\cos\left(3\cdot\pi\cdot\frac{\beta}{b}\right)+6\cdot a_1^{2}\cdot\pi\cdot\beta-36\cdot\cos\left(\pi\cdot\frac{\beta}{b}\right)\cdot a_1\cdot a_2$$

$$.-6\cdot a_1^{2}\cdot\pi+6\cdot a_1^{2}\cdot\pi\cdot\beta-36\cdot\cos\left[\pi\cdot\frac{(b-\beta)}{b}\right]\cdot a_1\cdot a_2-12\cdot\sin\left(2\cdot\pi\cdot\frac{\beta}{b}\right)\cdot a_2^{2}$$

and for flange it is given by:

$$T_{flange}=\frac{N}{2}\cdot\int_{0}^{c}\int_{\beta}^{a}\left(\frac{d}{dz}w\right)^{2}dx\,dz \tag{I-31}$$

$$=\frac{N\cdot\pi\cdot a}{24\cdot c}\cdot\left(-24\cdot a_3^{2}-24\cdot\theta\cdot a\cdot a_3+6\cdot\theta\cdot a\cdot a_3\cdot\pi+2\cdot\theta^{2}\cdot\pi\cdot a^{2}+9\cdot a_3^{2}\cdot\pi\right)$$

$$.+\frac{N}{24\cdot c}\cdot\left(-9\cdot a_3^{2}\cdot\pi^{2}\cdot\beta+24\cdot a_3^{2}\cdot\sin\left(\frac{1}{2}\cdot\pi\cdot\frac{\beta}{a}\right)\cdot\pi\cdot a-6\cdot\theta\cdot\pi^{2}\cdot a_3\cdot\beta^{2}-2\cdot\theta^{2}\cdot\pi^{2}\cdot\beta^{3}\right)$$

$$.+24\cdot\theta\cdot a\cdot a_3\cdot\pi\cdot\sin\left(\frac{1}{2}\cdot\pi\cdot\frac{\beta}{a}\right)\cdot\beta+48\cdot\theta\cdot a^{2}\cdot a_3\cdot\cos\left(\frac{1}{2}\cdot\pi\cdot\frac{\beta}{a}\right)-6\cdot a_3^{2}\cdot\pi\cdot\cos\left(\frac{1}{2}\cdot\pi\cdot\frac{\beta}{a}\right)\cdot\sin\left(\frac{1}{2}\cdot\pi\cdot\frac{\beta}{a}\right)\cdot a$$

The strain energy due to twisting at one corner is given by:

$$U_H=\frac{E\cdot H}{2}\cdot\int_{0}^{c}\left(\frac{d^{2}}{dz^{2}}\phi\right)^{2}dz \tag{I-32}$$

in which

$$\phi=\left(\frac{d}{dy}w\right)_{y=0}=\theta\cdot\sin\left(\pi\cdot\frac{z}{c}\right) \tag{I-33}$$

This leads to:

$$U_H = \frac{1}{2} \cdot E \cdot H \cdot \frac{\pi^6}{c^3} \cdot \frac{{a_1}^2}{b^2} \qquad \text{(I-34)}$$

The energy balance for the whole section is given by:

$$U_{web} + 2 \cdot U_{flange} + 2 \cdot U_H - \left(T_{web} + 2 \cdot T_{flange}\right) = 0 \qquad \text{(I-35)}$$

This equation has five unknowns N, θ, a_1, a_2, a_3. At each corner the tangent to the plates must be perpendicular to each other. Thus:

$$\left(\frac{dw_{flange}}{dx}\right)_{x=0} = \left(\frac{dw_{web}}{dy}\right)_{y=0}$$

$$a_1 \cdot \frac{\pi}{b} \cdot \sin\left(\pi \cdot \frac{z}{c}\right) = \theta \cdot \sin\left(\pi \cdot \frac{z}{c}\right)$$

$$\theta = a_1 \cdot \frac{\pi}{b} \qquad \text{(I-36)}$$

Equal bending moment at the corner for both plate gives:

$$\left(\frac{d^2 \cdot w_{flange}}{dx^2}\right)_{x=0} = \left(\frac{d^2 \cdot w_{web}}{dy^2}\right)_{y=0}$$

$$4 \cdot a_2 \cdot \frac{\pi^4}{b^2} \cdot \sin\left(\pi \cdot \frac{z}{c}\right) = \frac{1}{4} \cdot a_3 \cdot \frac{\pi^4}{a^2} \cdot \sin\left(\pi \cdot \frac{z}{c}\right)$$

$$a_3 = 16 \cdot \frac{a^2}{b^2} \cdot a_2 \tag{I-37}$$

Finally by substituting the value of a_3 and θ in term of a_1, a_2, leads to an equation with three parameters and the rest of the procedure is the same as that for the box section.

I.3.2 WEB MODE

Assuming the web buckles first, the deflection of the elements after buckling is given by: (shown in Fig I.3)

Web :

$$w_{web} = \left[a_1 \cdot \sin\left(\pi \cdot \frac{y}{b}\right) - a_2 \cdot \left(1 - \cos\left(\frac{2 \cdot \pi \cdot y}{b}\right)\right)\right] \cdot \sin\left(\pi \cdot \frac{z}{c}\right) \tag{I-38}$$

Flange:

$$w_{flange} = \left[\theta \cdot x - a_3 \cdot \left(1 - \cos\left(\pi \cdot \frac{\pi \cdot x}{2 \cdot a}\right)\right)\right] \cdot \sin\left(\pi \cdot \frac{z}{c}\right) \tag{I-39}$$

where θ , a_1, a_2, a_3 define the buckled shape.

The strain energy due to bending for the web is given by:

$$U_{web} = \frac{D}{2} \cdot \int_0^c \int_\beta^{b-\beta} \left[\left[\left(\frac{d^2}{dy^2} w \right) + \left(\frac{d^2}{dz^2} w \right) \right]^2 - 2 \cdot (1 - \nu) \cdot \left[\frac{d^2}{dy^2} w \cdot \frac{d^2}{dz^2} w - \left(\frac{d}{dyz} w \right)^2 \right] \right] dy\, dz$$

$$= \frac{1}{48} \cdot D \cdot \frac{\pi^4}{(c^3 \cdot b^4)} \cdot \left[-12 \cdot \sin\left[2 \cdot \pi \cdot \frac{(b - \beta)}{b} \right] \cdot b^5 \cdot a_2{}^2 - 6 \cdot b^5 \cdot a_1{}^2 \cdot \cos\left[\pi \cdot \frac{(b - \beta)}{b} \right] \cdot \sin\left[\pi \cdot \frac{(b - \beta)}{b} \right] \right] \tag{I-40}$$

$$+ 84\cdot\cos\left[\pi\cdot\frac{(b-\beta)}{b}\right]\cdot b^3\cdot a_1\cdot a_2\cdot c^2 - 48\cdot\sin\left[2\cdot\pi\cdot\frac{(b-\beta)}{b}\right]\cdot b^3\cdot a_2{}^2\cdot c^2 + 6\cdot b^5\cdot a_1{}^2\cdot\pi + 18\cdot a_2{}^2\cdot b^5\cdot\pi$$

$$+ 6\cdot a_1{}^2\cdot c^4\cdot\cos\left[\pi\cdot\frac{(b-\beta)}{b}\right]\cdot\sin\left[\pi\cdot\frac{(b-\beta)}{b}\right]\cdot b - 16\cdot b\cdot a_1\cdot a_2\cdot c^4\cdot\cos\left[3\cdot\pi\cdot\frac{(b-\beta)}{b}\right]$$

$$- 4\cdot b^5\cdot a_1\cdot a_2\cdot\cos\left[3\cdot\pi\cdot\frac{(b-\beta)}{b}\right] + 36\cdot\cos\left[\pi\cdot\frac{(b-\beta)}{b}\right]\cdot b^5\cdot a_1\cdot a_2$$

$$- 48\cdot b\cdot a_1\cdot a_2\cdot c^4\cdot\cos\left[\pi\cdot\frac{(b-\beta)}{b}\right] + 48\cdot a_2{}^2\cdot c^4\cdot\cos\left[2\cdot\pi\cdot\frac{(b-\beta)}{b}\right]\cdot\sin\left[2\cdot\pi\cdot\frac{(b-\beta)}{b}\right]\cdot b$$

and for flange it is given by:

$$U_{flange} = \frac{D}{2}\cdot\int_0^c\int_\beta^a\left[\left[\left(\frac{d^2}{dx^2}w\right)+\left(\frac{d^2}{dz^2}w\right)\right]^2 - 2\cdot(1-\nu)\cdot\left[\frac{d^2}{dx^2}w\cdot\frac{d^2}{dz^2}w - \left(\frac{d}{dxz}w\right)^2\right]\right]dx\,dz$$

$$= \frac{D}{384\cdot a^3\cdot c^3}\cdot\left(96\cdot\sin\left(\frac{1}{2}\cdot\pi\cdot\frac{\beta}{a}\right)\cdot a^3\cdot a_3{}^2\cdot c^2\cdot\pi^5 + 6\cdot a_3{}^2\cdot c^4\cdot\pi^3\cdot\cos\left(\frac{1}{2}\cdot\pi\cdot\frac{\beta}{a}\right)\cdot\sin\left(\frac{1}{2}\cdot\pi\cdot\frac{\beta}{a}\right)\cdot a\right. \qquad \text{(I-41)}$$

$$+ 144\cdot a_3{}^2\cdot a^4\cdot\pi^4\cdot\beta - 96\cdot\theta\cdot a_3\cdot a^4\cdot\pi^4\cdot\beta^2 - 144\cdot a_3{}^2\cdot a^4\cdot\pi^6\cdot\beta - 384\cdot\sin\left(\frac{1}{2}\cdot\pi^2\cdot\frac{\beta}{a}\right)\cdot a^5\cdot a_3{}^2\cdot\pi^2$$

$$+ 32\cdot\theta^2\cdot a^5\cdot\pi^6 - 144\cdot a_3{}^2\cdot a^3\cdot\pi^4 + 144\cdot a_3{}^2\cdot a^3\cdot\pi^6 - 96\cdot a^2\cdot a_3\cdot\theta\cdot c^2\cdot\pi^3 + 768\cdot a^4\cdot\theta\cdot a_3\cdot\cos\left(\frac{1}{2}\cdot\pi^2\right)\cdot\pi^2$$

$$- 3\cdot a_3{}^2\cdot c^3\cdot\pi^4 - 96\cdot a\cdot a_3{}^2\cdot c^2\cdot\pi^3 - 96\cdot a\cdot a_3{}^2\cdot c^2\cdot\pi^5 + 96\cdot a^3\cdot a_3\cdot\theta\cdot c^2\cdot\pi^3\cdot\sin\left(\frac{1}{2}\cdot\pi\cdot\frac{\beta}{a}\right)\cdot\beta$$

$$- 192\cdot a^4\cdot a_3\cdot\theta\cdot c^2\cdot\pi^4\cdot\cos\left(\frac{1}{2}\cdot\pi\cdot\frac{\beta}{a}\right) + 768\cdot a^6\cdot\theta\cdot a_3\cdot\cos\left(\frac{1}{2}\cdot\pi^2\cdot\frac{\beta}{a}\right)$$

The external work for the web is given by :

$$T_{web}=\frac{N}{2}\cdot\int_{0}^{c}\int_{\beta}^{b-\beta}\left(\frac{d}{dz}w\right)^{2}dy\,dz \tag{I-42}$$

$$=\frac{1}{48}\cdot N\cdot\pi\cdot\frac{b}{c}\cdot\left[-6\cdot a_1^{2}\cdot\cos\left[\pi\cdot\frac{(b-\beta)}{b}\right]\cdot\sin\left[\pi\cdot\frac{(b-\beta)}{b}\right]+3\cdot a_2^{2}\cdot\cos\left[2\cdot\pi\cdot\frac{(b-\beta)}{b}\right]\cdot\sin\left[2\cdot\pi\cdot\frac{(b-\beta)}{b}\right]\right]$$

$$-6\cdot a_1^{2}\cdot\cos\left(\pi\cdot\frac{\beta}{b}\right)\cdot\sin\left(\pi\cdot\frac{\beta}{b}\right)+18\cdot a_2^{2}\cdot\pi\cdot\beta-4\cdot a_1\cdot a_2\cdot\cos\left(3\cdot\pi\cdot\frac{\beta}{b}\right)+6\cdot a_1^{2}\cdot\pi\cdot\beta+36\cdot\cos\left(\pi\cdot\frac{\beta}{b}\right)\cdot a_1\cdot a_2$$

$$-12\cdot\sin\left(2\cdot\pi\cdot\frac{\beta}{b}\right)\cdot a_2^{2}-6\cdot a_1^{2}\cdot\pi+6\cdot a_1^{2}\cdot\pi\cdot\beta+36\cdot\cos\left[\pi\cdot\frac{(b-\beta)}{b}\right]\cdot a_1\cdot a_2+18\cdot a_2^{2}\cdot\pi$$

and for flange it is given by:

$$T_{flange}=\frac{N}{2}\cdot\int_{0}^{c}\int_{\beta}^{a}\left(\frac{d}{dz}w\right)^{2}dx\,dz \tag{I-43}$$

$$=\frac{N\cdot\pi\cdot a}{24\cdot c}\cdot\left(-24\cdot a_3^{2}+24\cdot\theta\cdot a\cdot a_3-6\cdot\theta\cdot a\cdot a_3\cdot\pi+2\cdot\theta^{2}\cdot\pi\cdot a^{2}+9\cdot a_3^{2}\cdot\pi\right)$$

$$+\frac{N}{24\cdot c}\cdot\left(-9\cdot a_3^{2}\cdot\pi^{2}\cdot\beta+24\cdot a_3^{2}\cdot\sin\left(\frac{1}{2}\cdot\pi\cdot\frac{\beta}{a}\right)\cdot\pi\cdot a+6\cdot\theta\cdot\pi^{2}\cdot a_3\cdot\beta^{2}\right)-2\cdot\theta^{2}\cdot\pi^{2}\cdot\beta^{3}$$

$$-24\cdot\theta\cdot a\cdot a_3\cdot\pi\cdot\sin\left(\frac{1}{2}\cdot\pi\cdot\frac{\beta}{a}\right)\cdot\beta-48\cdot\theta\cdot a^{2}\cdot a_3\cdot\cos\left(\frac{1}{2}\cdot\pi\cdot\frac{\beta}{a}\right)-6\cdot a_3^{2}\cdot\pi\cdot\cos\left(\frac{1}{2}\cdot\pi\cdot\frac{\beta}{a}\right)\cdot\sin\left(\frac{1}{2}\cdot\pi\cdot\frac{\beta}{a}\right)\cdot a$$

The strain energy due to warping for a corner is given by:

$$U_{Hweb}=\frac{1}{2}\cdot E\cdot H\cdot\frac{\pi^{6}}{c^{3}}\cdot\frac{a_1^{2}}{b^{2}} \tag{I-44}$$

Using the equations I-41 and I-44 and substituting the values of a_3 and θ in term of a_1,a_2 leads to an equation with three parameters, and the rest of the procedure is the same as that for the box section.

APPENDIX II

WARPING CONSTANT

Each radiused corner of a box or channel section possesses a warping constant which depends on the geometry of the section. Based on the method of Timoshenko and Gere (1961) the following procedure is used to calculate the warping constant.

II.1 BOX SECTION

The corner is opening up as shown in Fig II.1. This is then treated as a beam "loaded" by the normal distance from the intersection of the median lines of the adjoining plates to the tangent to the corner element, as shown in Fig II.2. This normal distance is given by:

$$r = R\cdot(\sin\theta + \cos\theta - 1) \qquad \text{(II-1)}$$

The total "load" is given by:

$$V = \int_0^{\frac{\pi}{2}} R\cdot(\sin\theta + \cos\theta - 1)\cdot R\, d\theta \qquad = 43\ R^2 \qquad \text{(II-2)}$$

R_1 and R_2, the reactions of the ends of the "beam", as shown in Fig II.2, are:

$$R_1 = \frac{0.43R^2\cdot\left(\frac{a}{2} - R + \pi\cdot\frac{R}{4}\right)}{\left(\frac{a+b}{2} - 2\cdot R + \pi\cdot\frac{R}{2}\right)} \qquad \text{(II-3)}$$

$$R_2 = \frac{0.43R^2 \cdot \left(\frac{b}{2} - R + \pi \cdot \frac{R}{4}\right)}{\left(\frac{a+b}{2} - 2 \cdot R + \pi \cdot \frac{R}{2}\right)} \tag{II-4}$$

The "shear force" in the beam is shown in Fig II.2. This shear force represents the term of $(\overline{\omega}_s - \omega_s)$ in the warping constant equation:

$$H = \int (\overline{\omega}_s - \omega_s)^2 \cdot t \, ds \tag{II-5}$$

The evaluation of this integral is based on two parts which are:

1. Integration on the straight parts
2. Integration on the curve part

$$H_{straight} = \left[\left[\frac{0.43R^2 \cdot \left(\frac{a}{2} - R + \pi \cdot \frac{R}{4}\right)}{\left(\frac{a+b}{2} - 2 \cdot R + \pi \cdot \frac{R}{2}\right)}\right]^2 \cdot \left(\frac{b}{2} - R\right) + \left[\frac{0.43R^2 \cdot \left(\frac{b}{2} - R + \pi \cdot \frac{R}{4}\right)}{\left(\frac{a+b}{2} - 2 \cdot R + \pi \cdot \frac{R}{2}\right)}\right]^2 \cdot \left(\frac{a}{2} - R\right)\right] \cdot t \tag{II-6}$$

$$H_{curve} = \left[\frac{1}{2} \cdot R1^2 \cdot \pi \cdot R + \left(\frac{1}{4} \cdot \pi^2 - \pi\right) \cdot R^3 \cdot R1 + \left(\frac{1}{24} \cdot \pi^3 - \frac{1}{4} \cdot \pi^2 + 2 \cdot \pi - 5\right) \cdot R^5\right] \cdot t \tag{II-7}$$

and H is given by:

$$H = H_{straignt} + H_{curve} \qquad \text{(II-8)}$$

The warping constant H can be expressed by (Fig II.3):

$$H = \alpha \cdot b \cdot t \cdot R^4 \qquad \text{(II-9)}$$

in which:

b= longer length
α= a factor that varies with a/b and R/b shown in Fig II.4

The value of α is given closely by:

$$\alpha = 0.01 + 0.037 \cdot \frac{a}{b} - 0.057 \cdot \frac{R}{b} \qquad \text{(II-10)}$$

II.2 CHANNEL SECTION

The corner is opened up as shown in Fig II.5. The procedure is the same as that for the box; however, in the channel section the centre of rotation for the corner is no longer at the intersection of the median lines but at a distance e from this point, on the median line of the web, and is established by minimizing the warping constant as follows:

The normal distance from the centre of rotation to the element tangent is given by (Fig II.6):

$$r = R\cdot(\sin(\theta)+\cos(\theta)-1) - e\cdot\cos(\theta) \qquad \text{(II-11)}$$

The total "load" is given by:

$$V = \int_0^{\frac{\pi}{2}} \left[R\cdot(\sin(\theta)+\cos(\theta)-1) - e\cdot\cos(\theta)\right]\cdot R\, d\theta = \left(0.43\cdot R^2 - e\cdot R\right) \qquad \text{(II-12)}$$

R_1 and R_2, the reactions of the ends of the open corner beam, as shown in Fig II.6, are calculated using:

$$R_1\cdot\left(b+\frac{a}{2}-2\cdot R+\pi\cdot\frac{R}{2}\right)+e\cdot\left(\frac{b}{2}-R\right)\cdot\left[\frac{a}{2}-R+\pi\cdot\frac{R}{2}+\left(\frac{b-R}{2}\right)\right]+e\cdot R\cdot\left(\frac{a}{2}-R+\pi\cdot\frac{R}{6}\right)-0.43\cdot R^2\cdot\left(\pi\cdot\frac{R}{4}+\frac{b}{2}-R\right)=0$$

thus:

$$R_1 = \frac{(.25\cdot e\cdot a\cdot b - .46\cdot e\cdot b\cdot R + .25\cdot e\cdot b^2 - .55\cdot R^2\cdot e + 9.22\cdot 10^{-2}\cdot R^3 - .215\cdot R^2\cdot a)}{(-b - .5\cdot a + .43\cdot R)} \qquad \text{(II-13)}$$

and

$$e\cdot(b-R)+e\cdot R-0.43\cdot R^2+\frac{(.25\cdot e\cdot a\cdot b-.46\cdot e\cdot b\cdot R+.25\cdot e\cdot b^2-.55\cdot R^2\cdot e+9.22\cdot 10^{-2}\cdot R^3-.215\cdot R^2\cdot a)}{(-b-.5\cdot a+.43\cdot R)}+R_2=0$$

thus:

$$R_2=\frac{(75.\cdot e\cdot b^2+25.\cdot e\cdot a\cdot b+3.\cdot e\cdot b\cdot R-43.\cdot R^2\cdot b+9.27.\cdot R^3+55.\cdot R^2\cdot e)}{(-100.\cdot b-50.\cdot a+43.\cdot R)} \qquad \text{(II-14)}$$

The shear force in the beam, as shown in Fig II.6 represents the term of $(\bar{\omega}_s-\omega_s)$ in the warping constant given by:

$$H=\int (\bar{\omega}_s-\omega_s)^2\cdot t\,ds \qquad \text{(II-15)}$$

The evaluation of this integral is based on three parts which are (Fig II-6):

1. Integration on C part
2. Integration on D part
3. Integration on F part

$$H_C=\int_0^{b-R}(R_1+e\cdot s)^2\,ds=\frac{1}{3\cdot e}\cdot\left[(R_1+e\cdot b-e\cdot R)^3-R_1^{\,3}\right] \qquad \text{(II-16)}$$

$$H_D=\int_0^{\frac{\pi}{2}}\left[(R_1+e\cdot L)-(R^2-R^2\cdot\cos(\theta)-R^2\cdot\theta+R^2\cdot\sin(\theta)-R\cdot\sin(\theta)\cdot e)\right]^2\cdot R\,d\theta \qquad \text{(II-17)}$$

$$=\frac{1}{24}\cdot\left(24\cdot e\cdot L\cdot R^2\cdot\pi+6\cdot e^2\cdot R^2\cdot\pi+R^4\cdot\pi^3+12\cdot e^2\cdot L^2\cdot\pi+6\cdot R_1\cdot R^2\cdot\pi^2-12\cdot R^3\cdot e\cdot\pi+6\cdot e\cdot L\cdot R^2\cdot\pi^2\right)\cdot R$$

$$+\frac{1}{24}\cdot\left(48\cdot R^4\cdot\pi+12\cdot R_1^{\,2}\cdot\pi-6\cdot R^4\cdot\pi^2+48\cdot R^3\cdot e-24\cdot R_1\cdot R^2\cdot\pi-96\cdot R^4+48\cdot R_1\cdot R^2+24\cdot R_1\cdot e\cdot L\cdot\pi+48\cdot e\cdot L\cdot R^2\right)\cdot R$$

$$+\frac{1}{24}\cdot\left(-R^3-R^2\cdot e+2\cdot e^2\cdot L-2\cdot R_1\cdot R+2\cdot R_1\cdot e-2\cdot e\cdot L\cdot R\right)\cdot R^2$$

where:

$$L = b - R \tag{II-18}$$

$$H_F = R_2^{\,2} \cdot \left(\frac{a}{2} - R\right) \tag{II-19}$$

Differentiating the warping constant with respect to e, and equating it to zero gives:

$$e = \frac{\left(36.4 \cdot b \cdot a^2 \cdot R + 65 \cdot R^3 \cdot a - 21.4 \cdot R^2 \cdot a^2 - 18.3 \cdot R^4 + 46 \cdot b \cdot a \cdot R + 41.5 \cdot a \cdot b \cdot R^2 - 59.6 \cdot R^2 \cdot a \cdot b - 19.2 \cdot R^3 \cdot a\right)}{\left(105 \cdot b \cdot a^2 + 384 \cdot a \cdot b - 360 \cdot R^2 + 400 \cdot b^2 \cdot a + 424 \cdot R^2 \cdot b + 228 \cdot a \cdot R^2\right)} \tag{II-20}$$

and H is given by:

$$H = H_C + H_D + H_F \tag{II-21}$$

The warping constant H can be expressed by (Fig II.7):

$$H = \alpha \cdot b \cdot t \cdot R^4 \tag{II-22}$$

in which:

b= longer length
α= a factor that varies with a/b and R/b shown in Fig II.8

The value of α is given closely by:

$$\alpha = 0.015 + 0.014 \cdot \frac{a}{b} - 0.03 \cdot \frac{R}{b} \tag{II-23}$$

APPENDIX III LIST-1

```
*HEADING
SQUARE PLATE - ELASTIC BUDKLING  ( BUCKLE )-S8R5 2 X 2   4-2-3-1
*restart,write
*NODE
1010
1018,0.0,0.45,0.0
1024,0.05,0.5,0.0
1032,0.5,0.5,0.0
2010,0.0,0.0,3.0
2018,0.0,0.45,3.0
2024,0.05,0.5,3.0
2032,0.5,0.5,3.0
1,0.450,.050,0.0
2,0.450,.050,3.0
*NGEN,NSET=ZYEDG1
1010,1018,1
*NGEN,NSET=ZYEDG2
2010,2018,1
*NGEN,NSET=ZXEDG1
1024,1032,1
*NGEN,NSET=ZXEDG2
2024,2032,1
*NGEN,NSET=ZR1,LINE=C
1018,1024,1,1
*NGEN,NSET=ZR2,LINE=C
2018,2024,1,2
*NGEN,NSET=YZEDG
1010,2010,100
*NGEN,NSET=XZEDG
1030,2030,100
*NFILL
ZYEDG1,ZYEDG2,10,100
*NFILL
ZXEDG1,ZXEDG2,10,100
*NFILL
ZR1,ZR2,10,100
*ELEMENT,TYPE=S8R5,ELSET=ONE
1,1010,1012,1212,1210,1011,1112,1211,1110
*ELGEN,ELSET=ONE
1,11,2,1,5,200,11
*MATERIAL ,NAME=PLATE
*ELASTIC
20.E4,.3
*SHELL SECTION,MATERIAL=PLATE,ELSET=ONE
.01,3
*BOUNDARY
ZYEDG1,1
ZYEDG1,4
ZYEDG1,6
ZYEDG2,1
ZYEDG2,4
ZYEDG2,6
ZXEDG1,2
ZXEDG1,5,6
ZXEDG2,2
```

```
ZXEDG2,5,6
ZR1,1,2
ZR1,4
ZR1,6
ZR2,1,2
ZR2,4
ZR1,6
YZEDG,YSYMM
*STEP
*BUCKLE
1,,,99
*MODAL FILE
*CLOAD
1010,3,1.458
1011,3,5.833
1012,3,2.917
1013,3,5.833
1014,3,2.917
1015,3,5.833
1016,3,2.917
1017,3,5.833
1018,3,2.767
1019,3,5.236
1020,3,2.618
1021,3,5.236
1022,3,2.618
1023,3,5.236
1024,3,1.726
1025,3,1.667
1026,3,0.833
1027,3,1.667
1028,3,0.833
1029,3,1.667
1030,3,0.833
1031,3,1.667
1032,3,0.417
2010,3,-1.458
2011,3,-5.833
2012,3,-2.917
2013,3,-5.833
2014,3,-2.917
2015,3,-5.833
2016,3,-2.917
2017,3,-5.833
2018,3,-2.767
2019,3,-5.236
2020,3,-2.618
2021,3,-5.236
2022,3,-2.618
2023,3,-5.236
2024,3,-1.726
2025,3,-1.667
2026,3,-0.833
2027,3,-1.667
2028,3,-0.833
2029,3,-1.667
```

```
2030,3,-0.833
2031,3,-1.667
2032,3,-0.417
*NODE PRINT
U
*END STEP
```

APPENDIX III LIST-2

```
*HEADING
SQUARE PLATE - RIKS STEP ANALYSIS  ( STATIC )-S8R5 2 X 2   4-2-3-1
*restart,write
*NODE
1010
1018,0.0,0.45,0.0
1024,0.05,0.5,0.0
1032,0.5,0.5,0.0
2010,0.0,0.0,3.0
2018,0.0,0.45,3.0
2024,0.05,0.5,3.0
2032,0.5,0.5001,3.0
1,0.450,.050,0.0
2,0.450,.050,3.0
*NGEN,NSET=ZYEDG1
1010,1018,1
*NGEN,NSET=ZYEDG2
2010,2018,1
*NGEN,NSET=ZXEDG1
1024,1032,1
*NGEN,NSET=ZXEDG2
2024,2032,1
*NGEN,NSET=ZR1,LINE=C
1018,1024,1,1
*NGEN,NSET=ZR2,LINE=C
2018,2024,1,2
*NGEN,NSET=YZEDG
1010,2010,100
*NGEN,NSET=XZEDG
1030,2030,100
*NFILL
ZYEDG1,ZYEDG2,10,100
*NFILL
ZXEDG1,ZXEDG2,10,100
*NFILL
ZR1,ZR2,10,100
*ELEMENT,TYPE=S8R5,ELSET=ONE
1,1010,1012,1212,1210,1011,1112,1211,1110
*ELGEN,ELSET=ONE
1,11,2,1,5,200,11
*MATERIAL ,NAME=PLATE
*ELASTIC
20.E4,.3
*SHELL SECTION,MATERIAL=PLATE,ELSET=ONE
.01,3
*BOUNDARY
ZYEDG1,1
ZYEDG1,6
ZYEDG2,ZSYMM
ZXEDG1,2
ZXEDG1,6
ZXEDG2,ZSYMM
ZR1,1,2
ZR1,6
ZR2,ZSYMM
YZEDG,YSYMM
*STEP,NLGEOM,INC=400
*STATIC,RIKS
, , , ,1030,3,.2
```

```
*MODAL FILE
*CLOAD
1010,3,.0166666
1011,3,.0666666
1012,3,.0333333
1013,3,.0666666
1014,3,.0333333
1015,3,.0666666
1016,3,.0333333
1017,3,.0666666
1018,3,.0333333
1019,3,.0666666
1020,3,.0333333
1021,3,.0666666
1022,3,.0333333
1023,3,.0666666
1024,3,.0333333
1025,3,.0666666
1026,3,.0333333
1027,3,.0666666
1028,3,.0333333
1029,3,.0666666
1030,3,.0166666
*PRINT,RESIDUAL=NO
*NODE filE,NSET=N2030
U
*END STEP
```

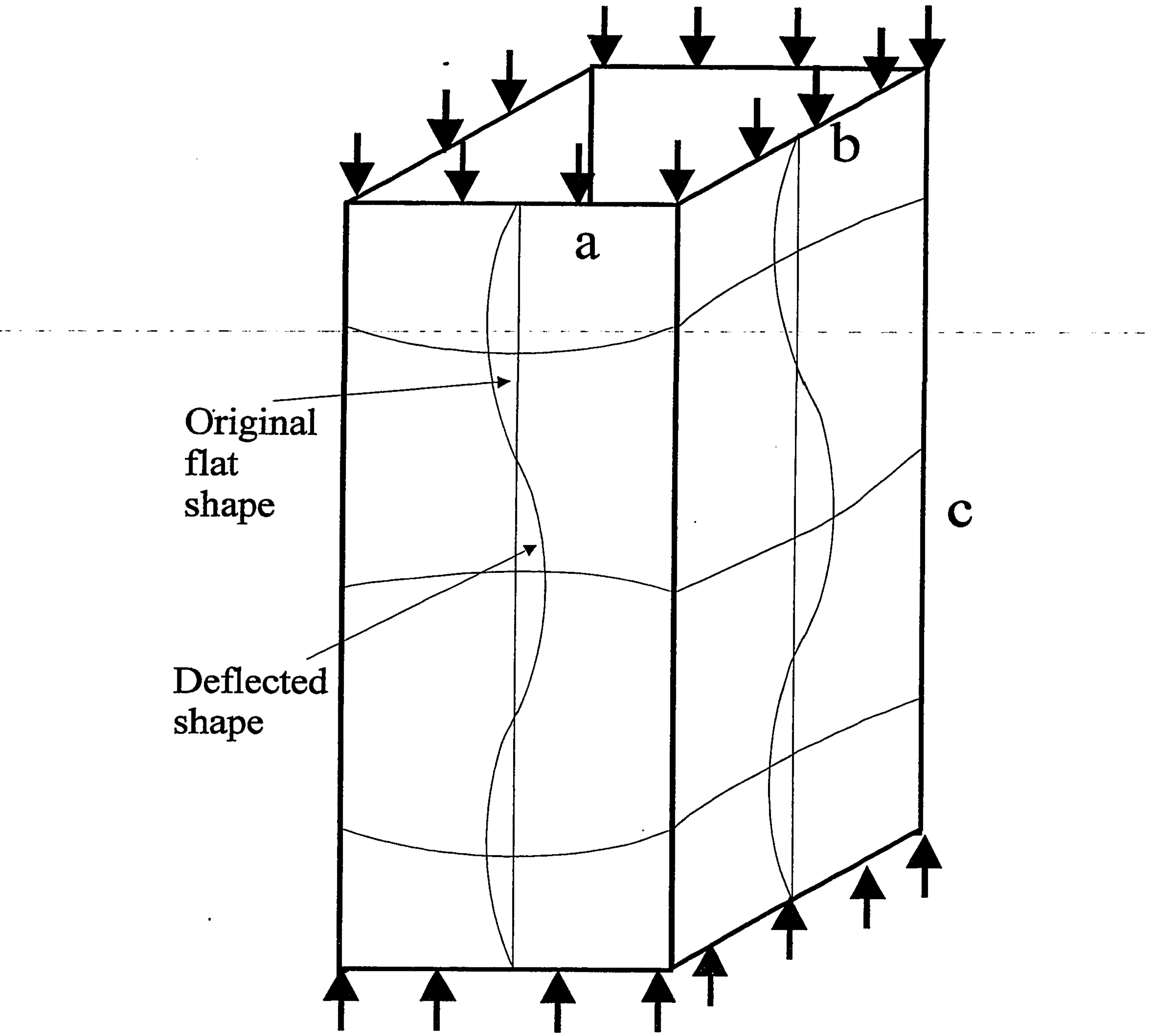

Fig D.1 Local buckling of a box section

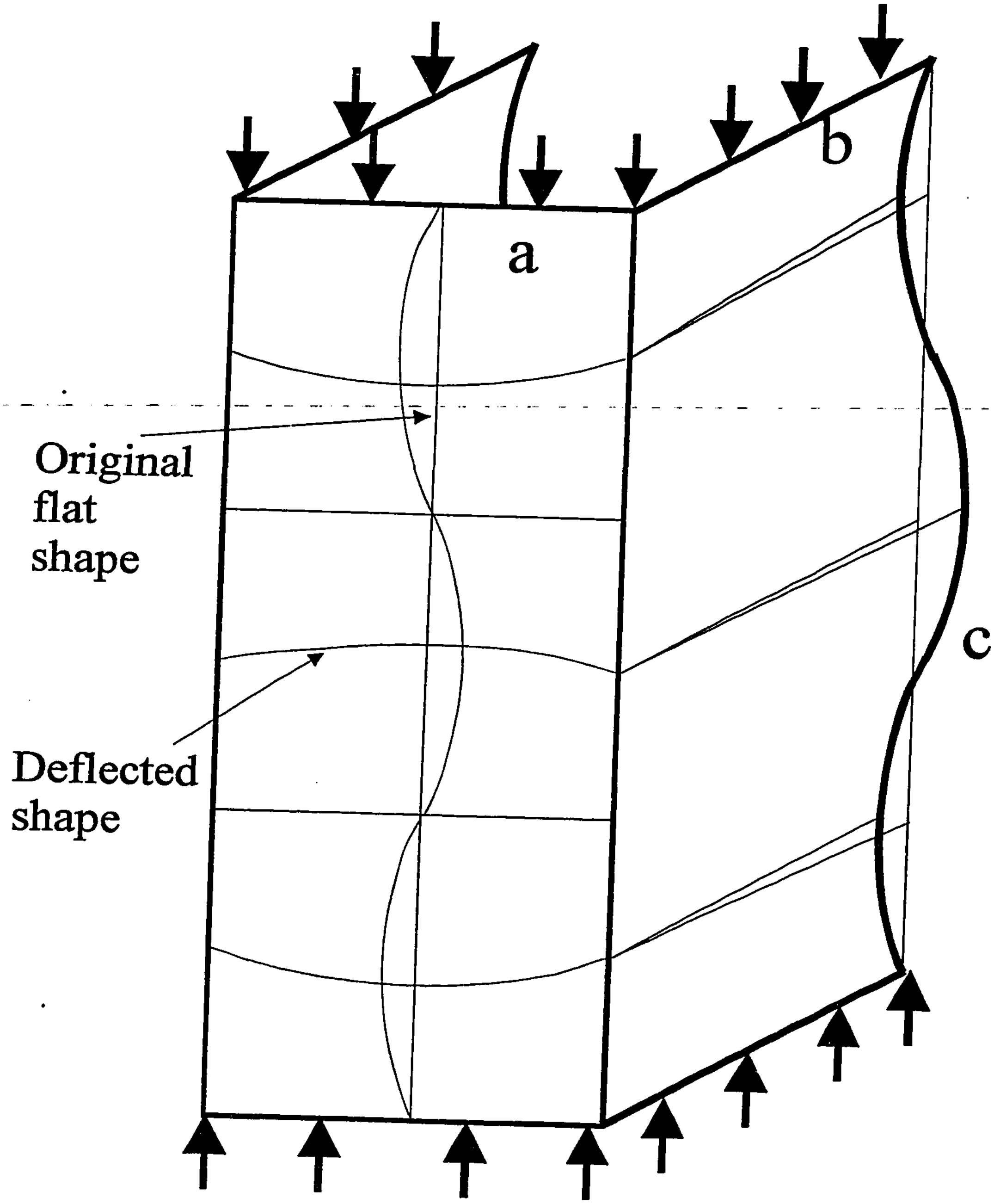

Fig D-2 Local buckling for a channel section

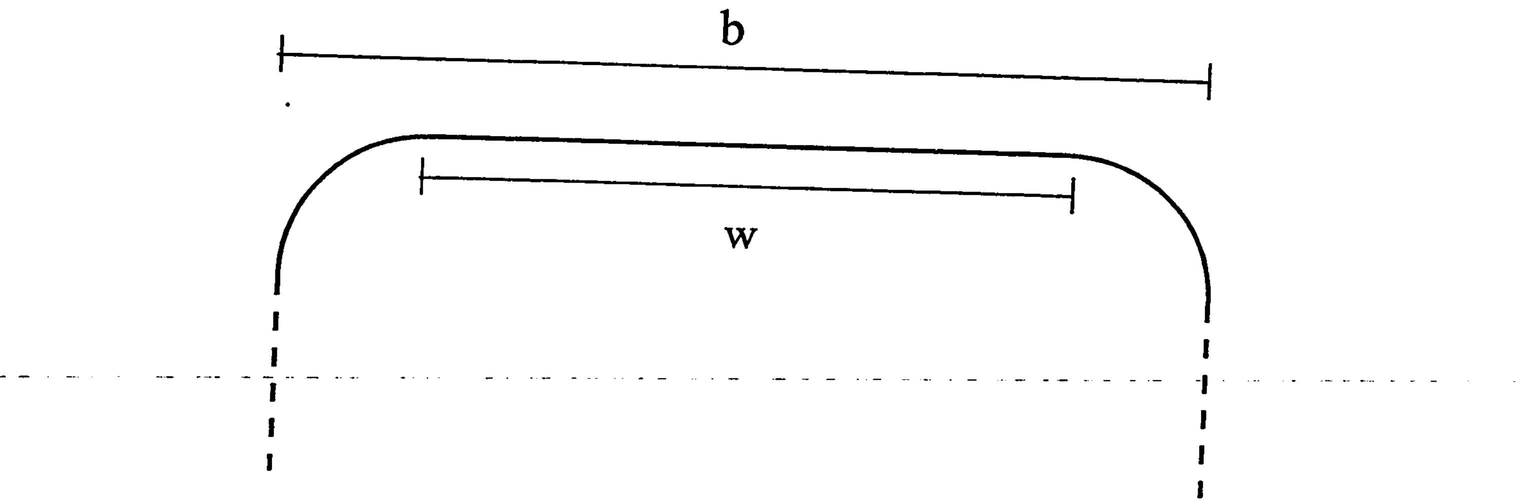

Overal width b, and flat width w

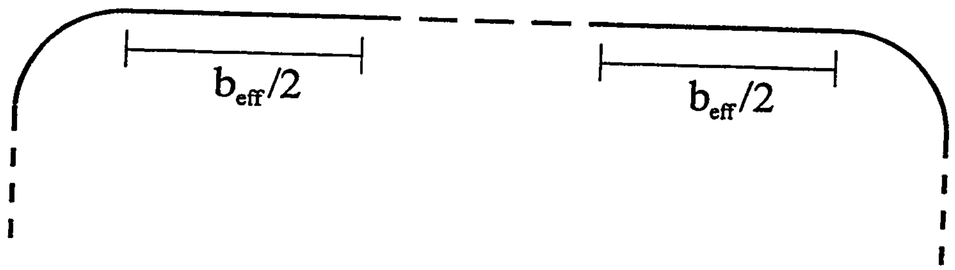

Effective width, b_{eff}

Fig D-3 Flat, overall and effective widths

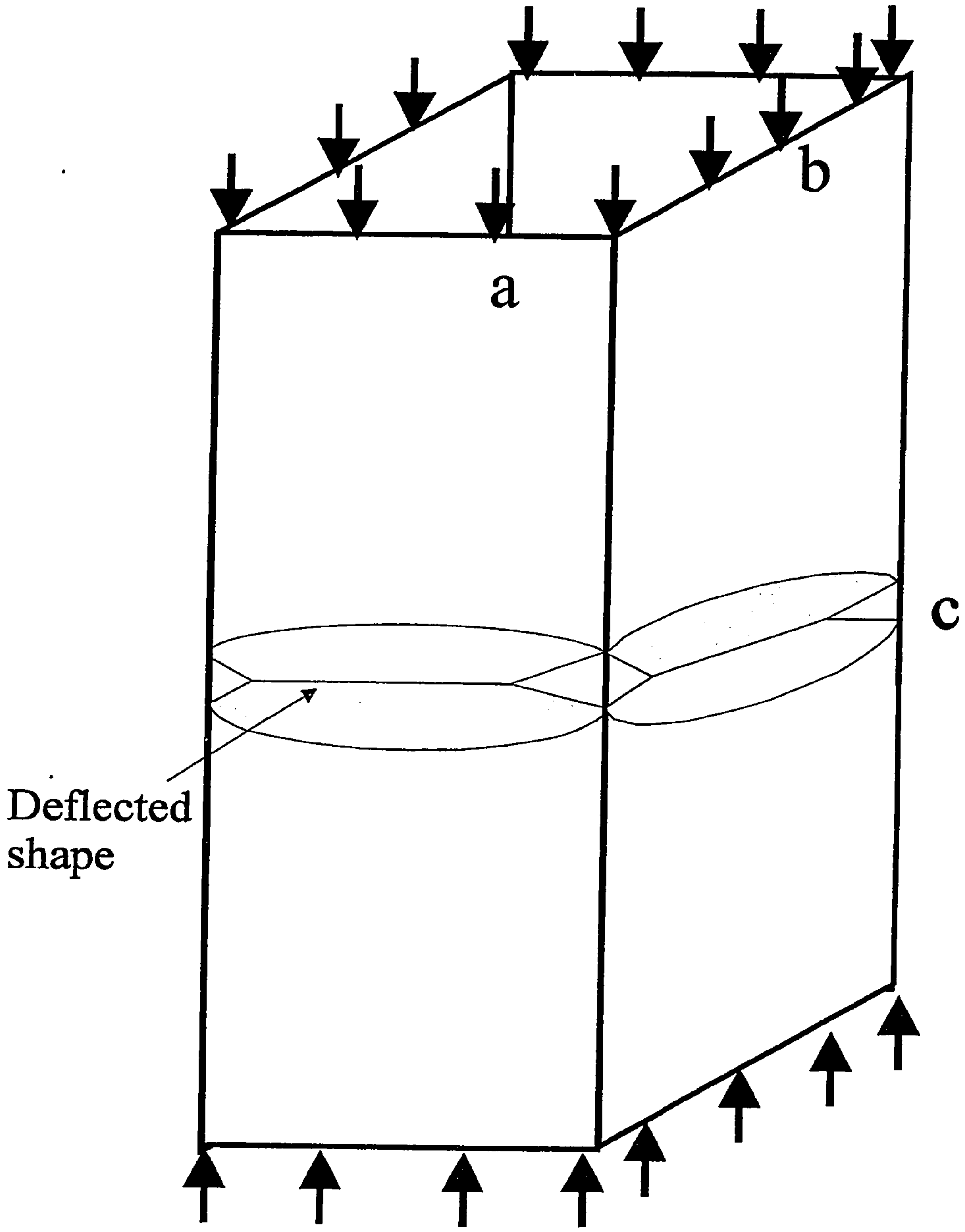

Fig D-4 Collapse mode for a box section

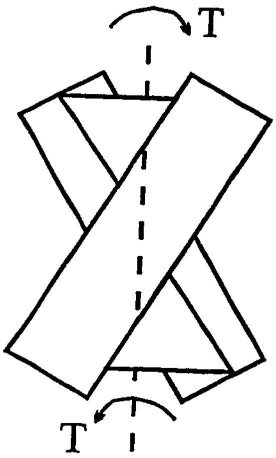

Twisting without restrain

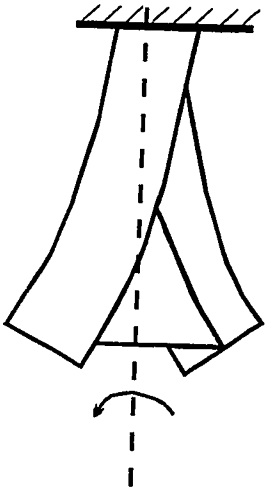

Twisting with fixed end

Fig D-5 Warping for I beam

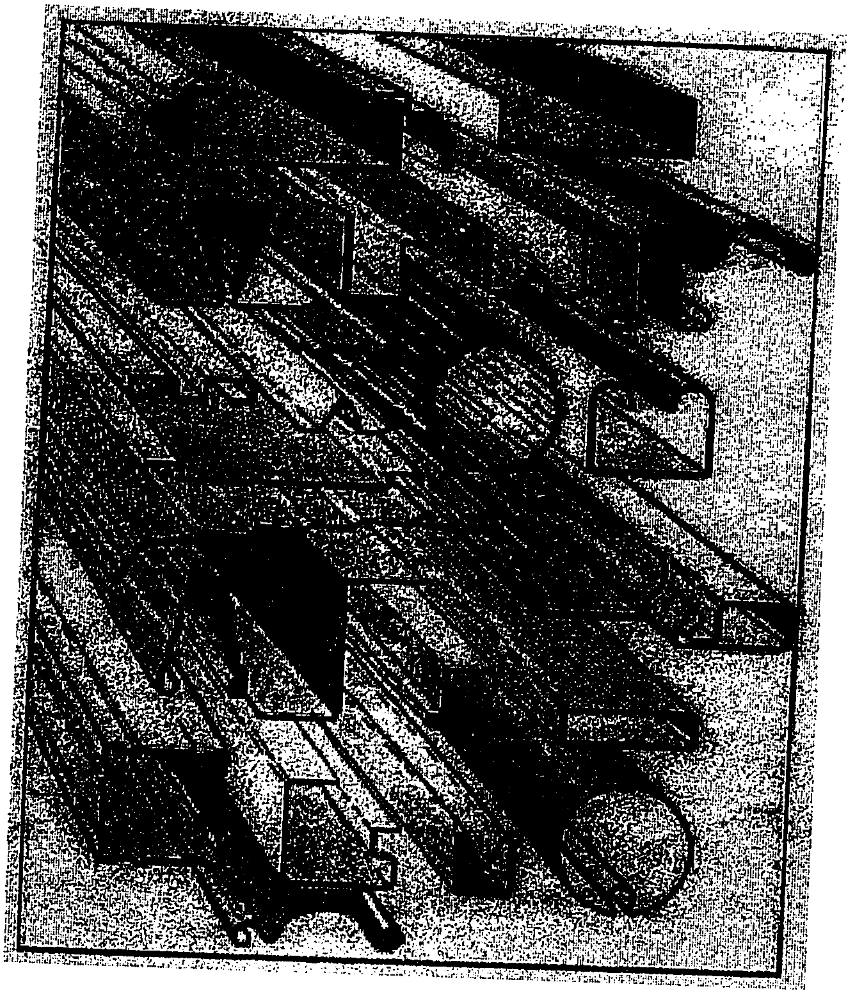

Fig 1-1 Cold-formed sections

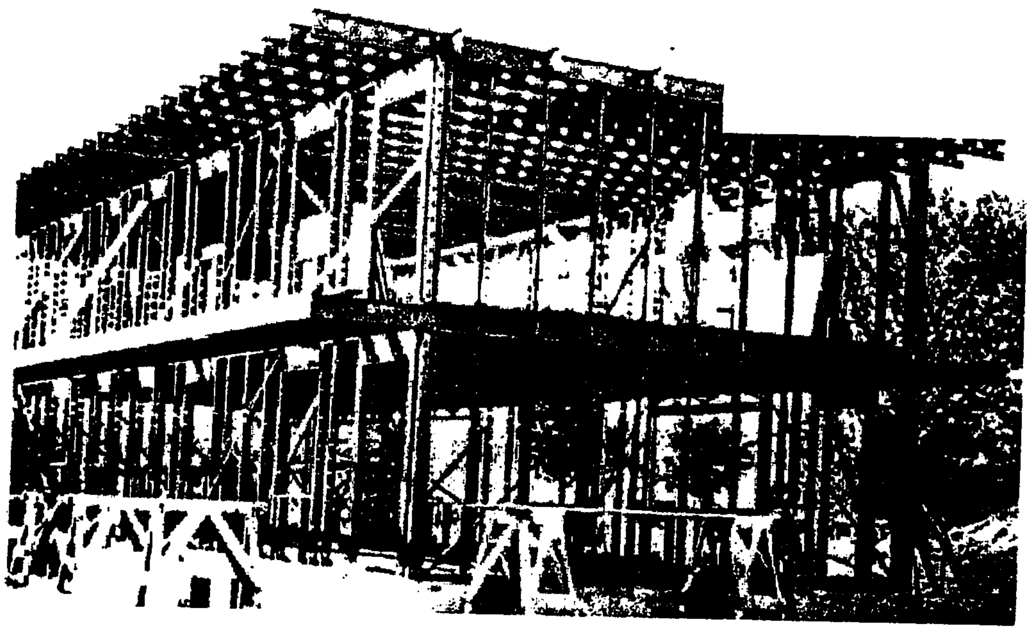

Fig 1-2 Cold-formed steel structure (Pen Metal Company)

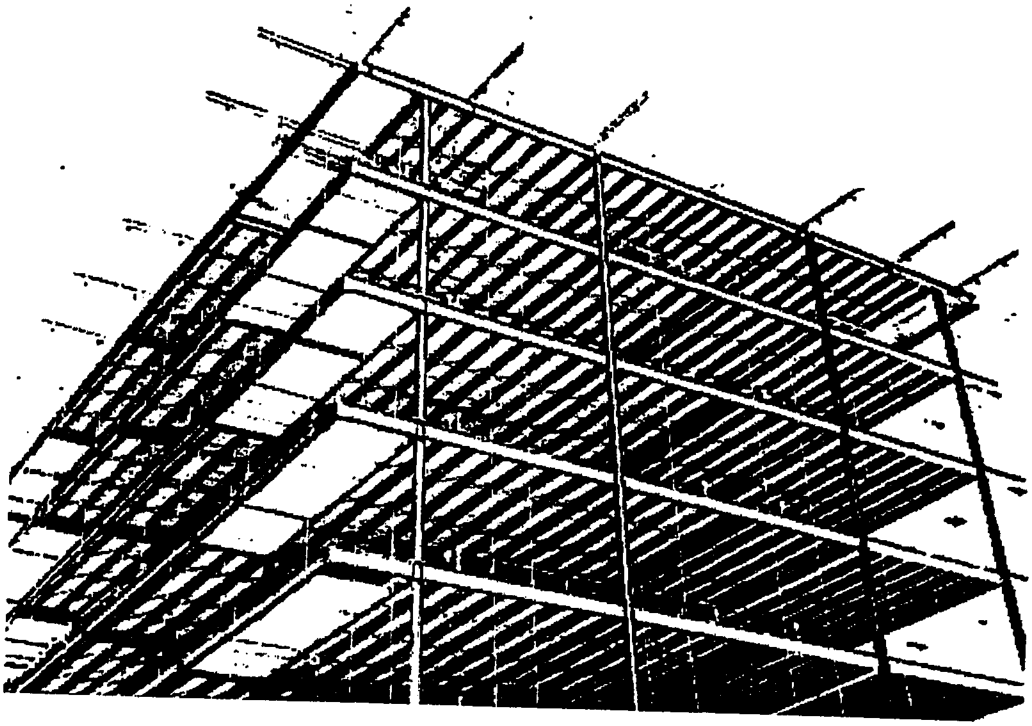

Fig 1-3 Cold-formed and hot-rolled steel structure (Stran-Steel Corporation)

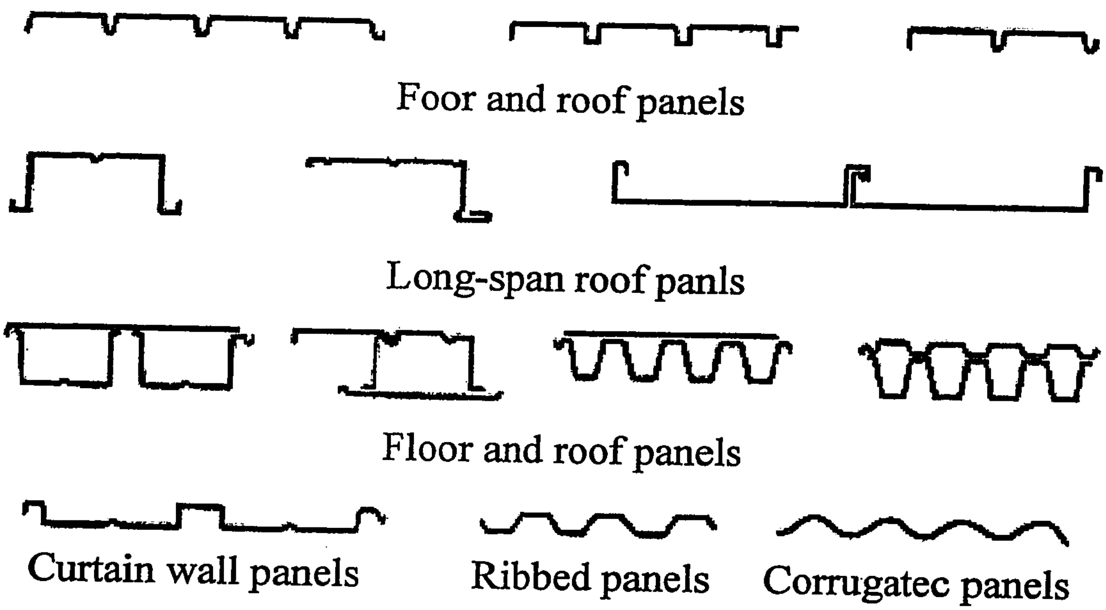

Fig 1-4 Typical cold-formed panels

Fig 1-5 Force-Shortening relationship for column and plate

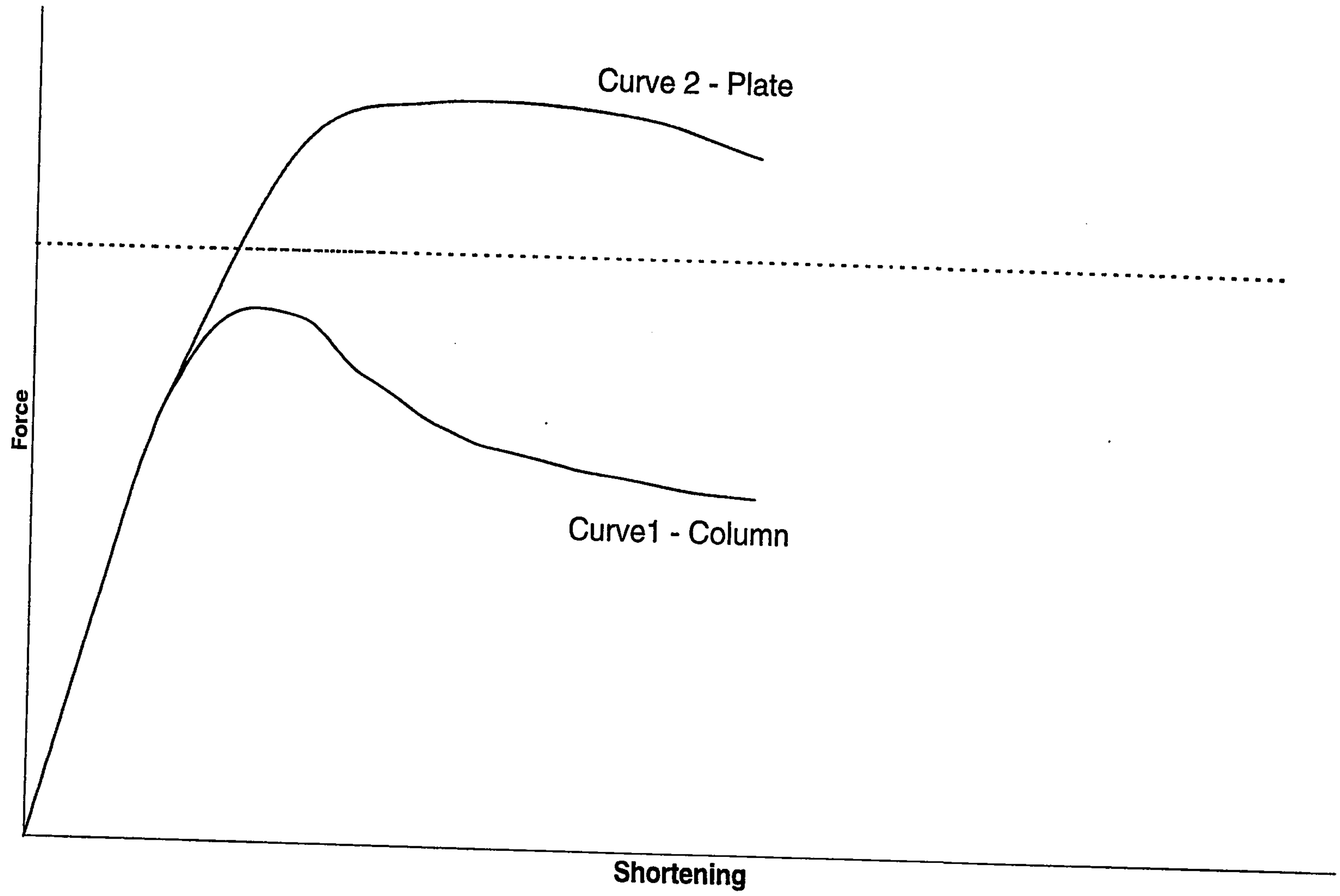

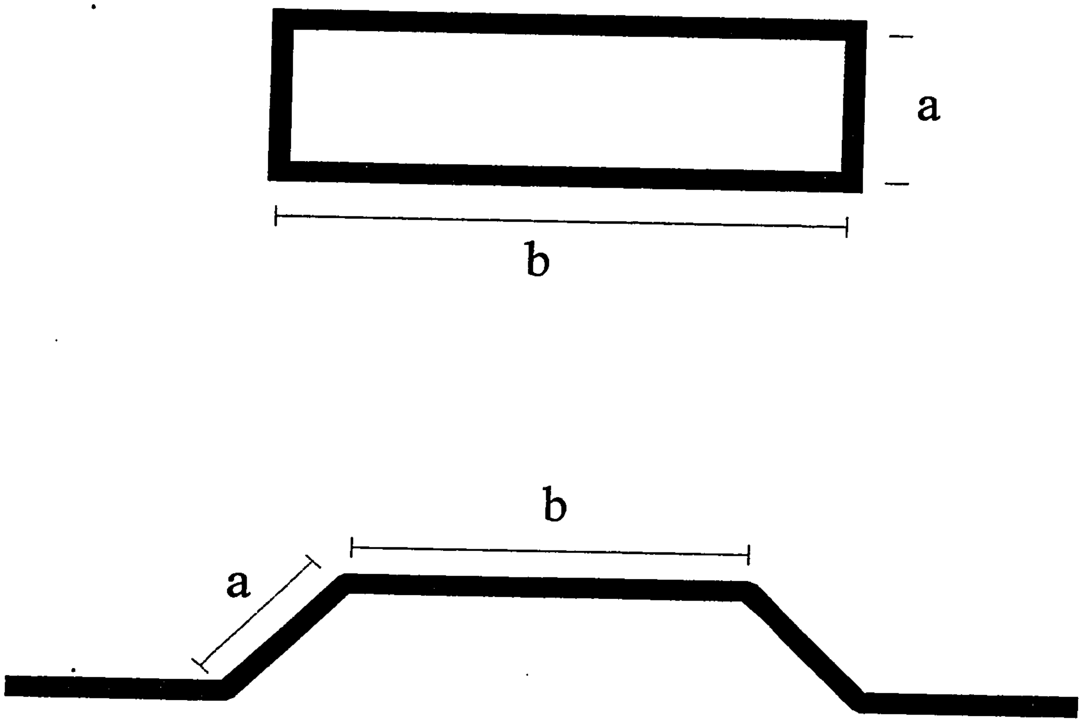

Fig 1-6 Box and panel section dimensions

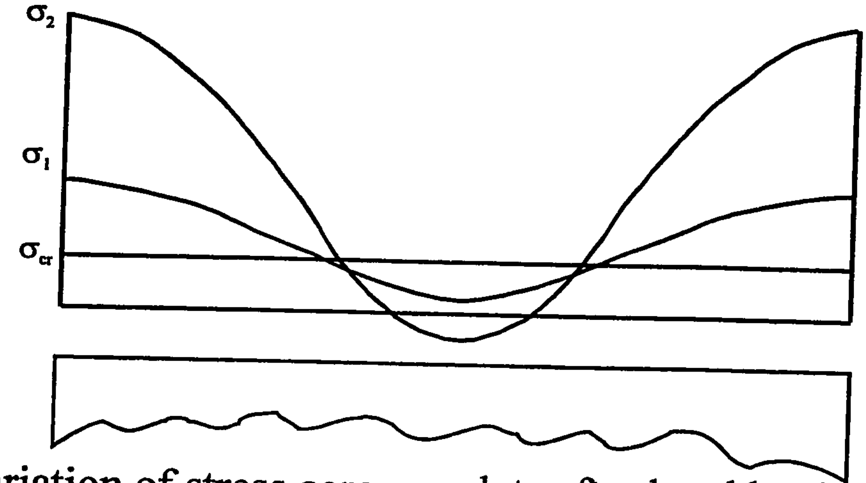

Variation of stress across a plate after local buckling

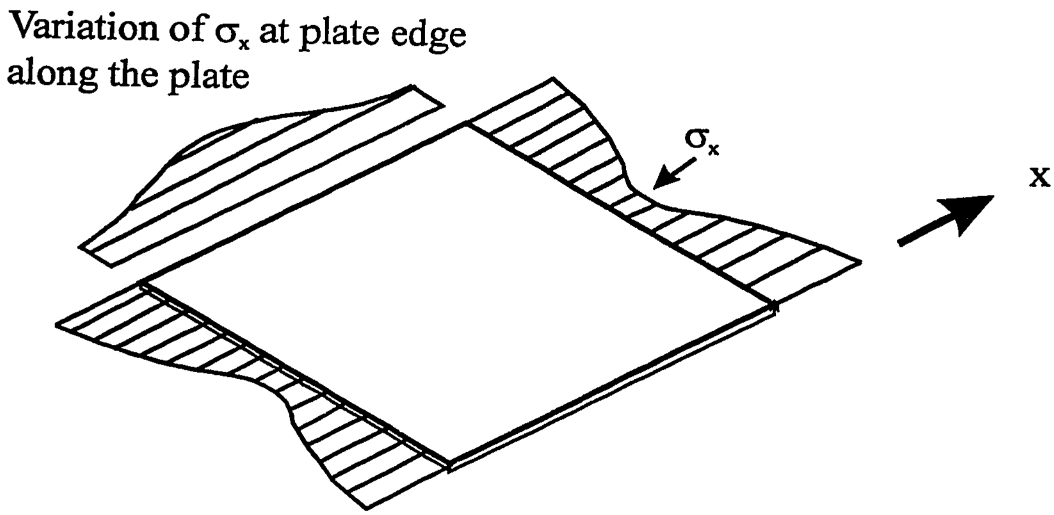

Fig 1.7 Stress distribution on a simply supported plate

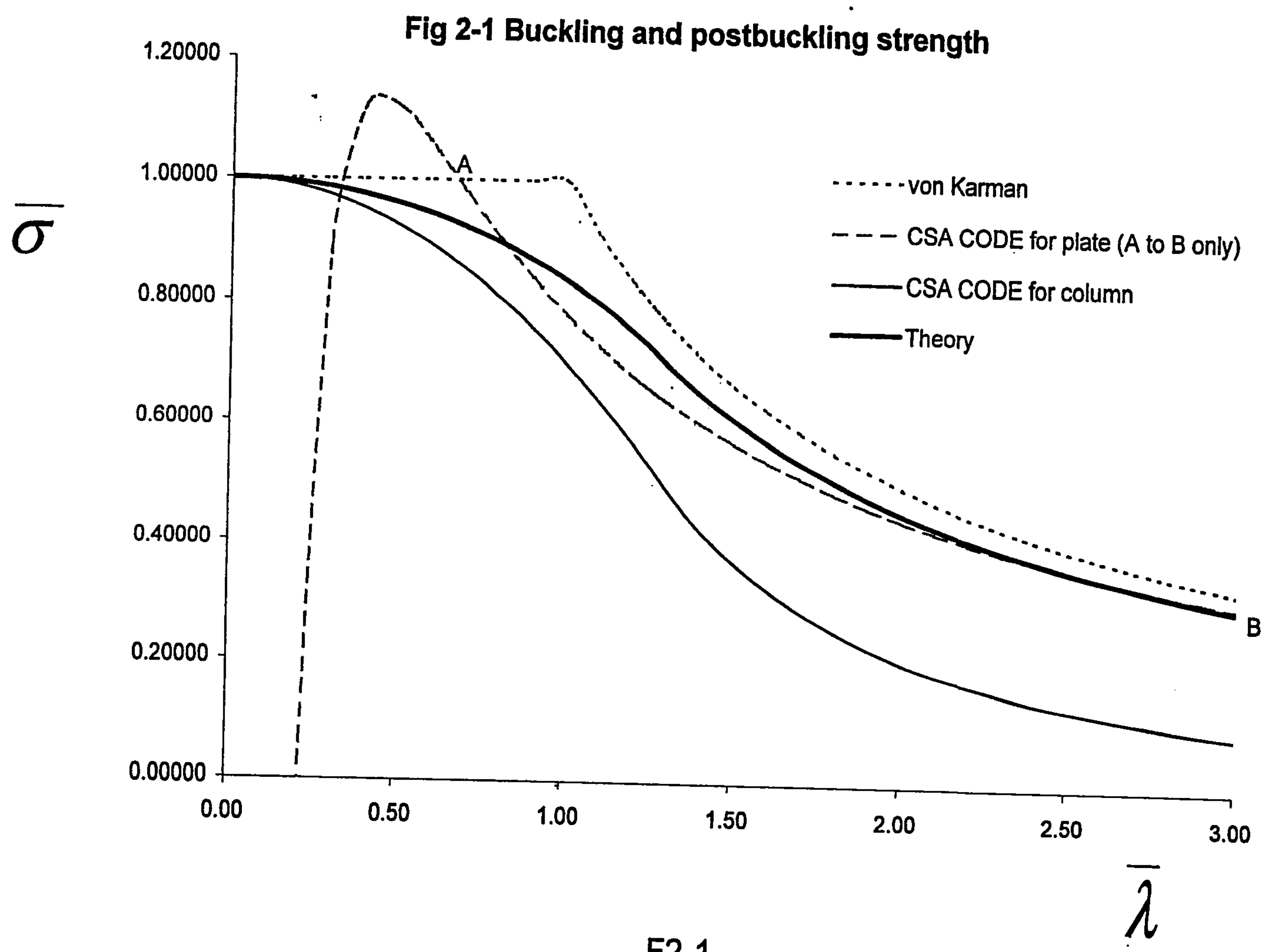
Fig 2-1 Buckling and postbuckling strength
$\overline{\sigma}$
1.20000
1.00000
0.80000
0.60000
0.40000
0.20000
0.00000
0.00
0.50
1.00
1.50
2.00
2.50
3.00
$\overline{\lambda}$
A
B
von Karman
CSA CODE for plate (A to B only)
CSA CODE for column
Theory

F2-1

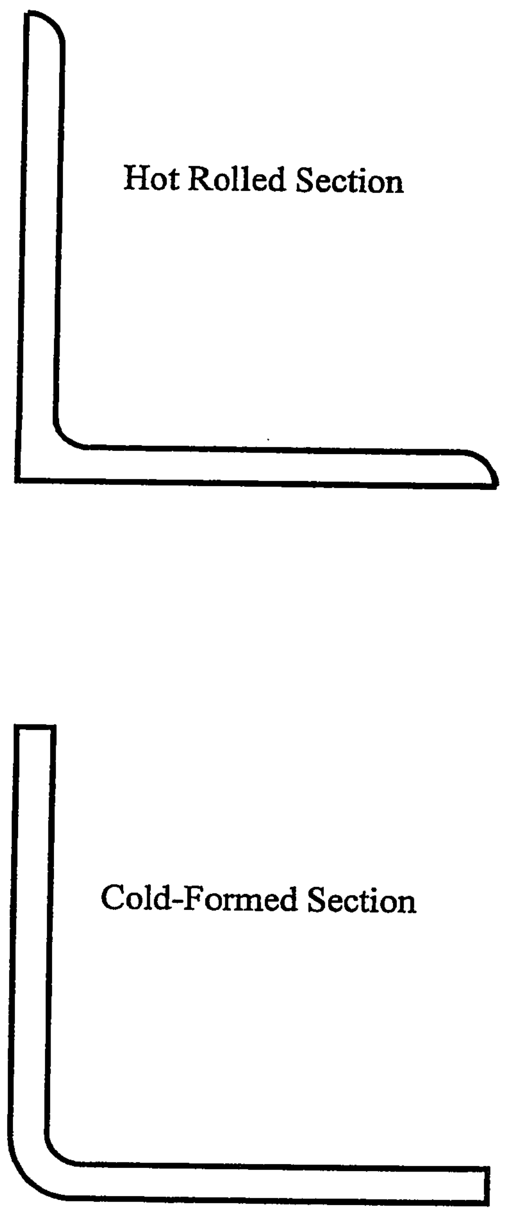

Fig 2-2 Cold-formed and hot-rolled corners

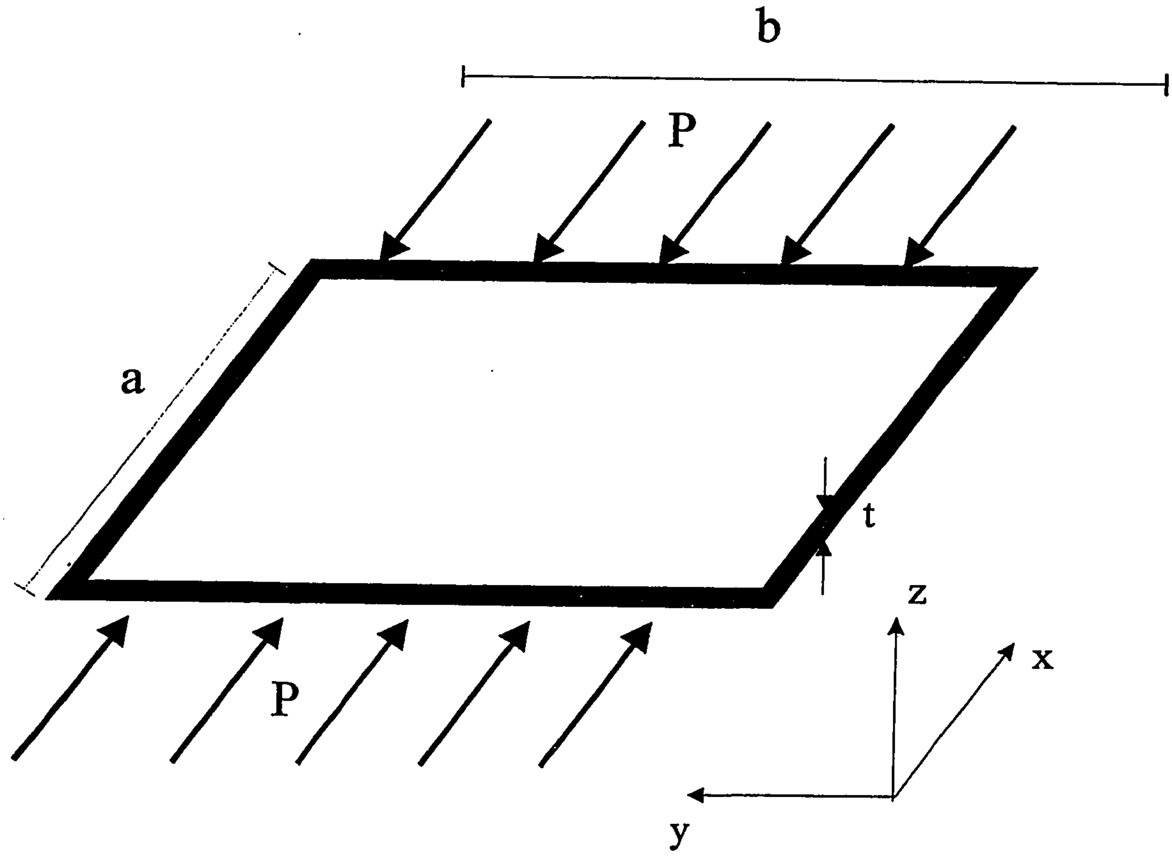

Fig 2-3 Simply supported plate

F2-3

Fig 2-4 Postbuckling curve

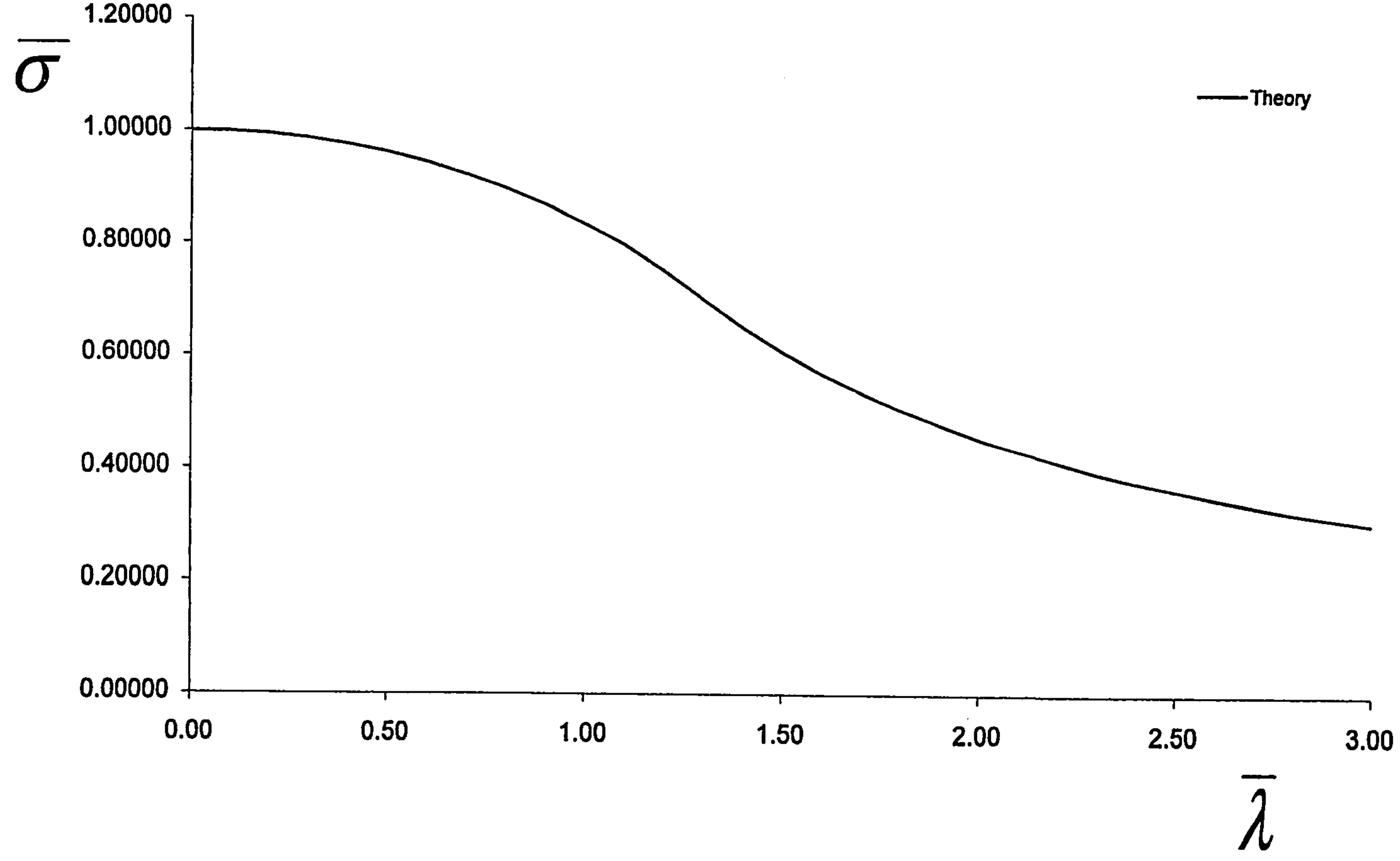

F2-4

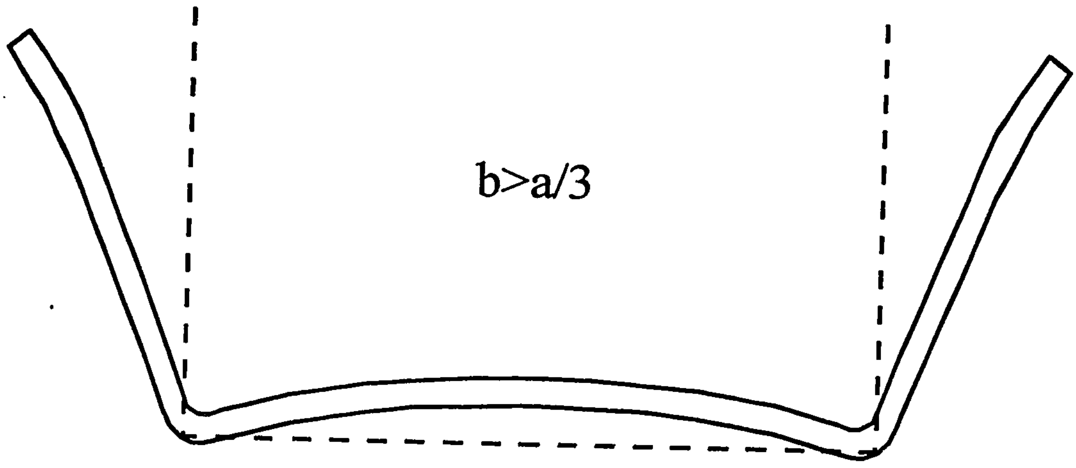

Flange buckling mode

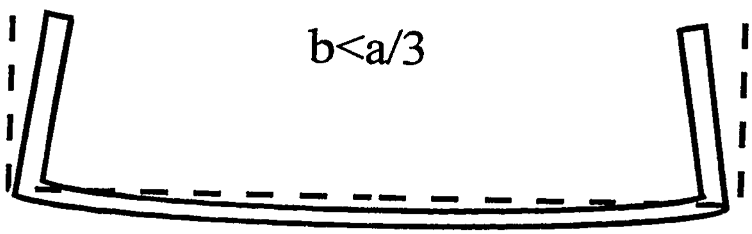

Web buckling mode

Fig 2-5 Buckling modes of a channel

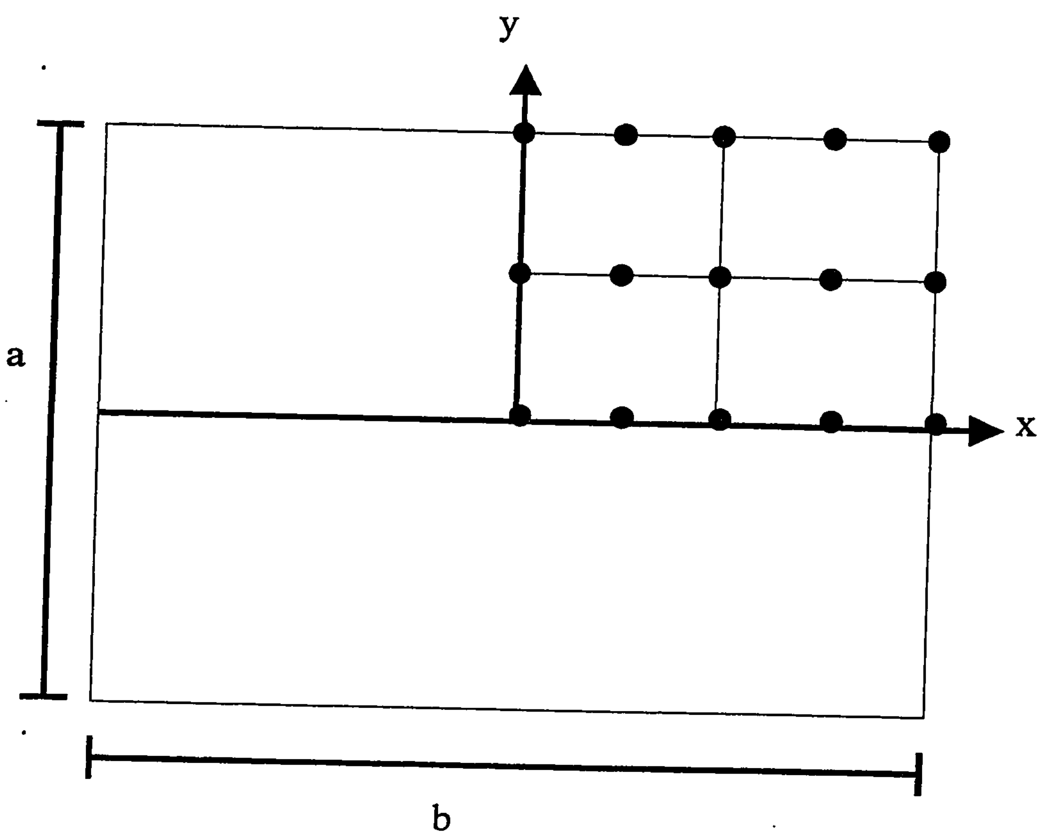

Fig 3-1 Sample plate for ABAQUS

$t = 1$ mm
$E = 200000$ N/mm^2
$\nu = 0.3$

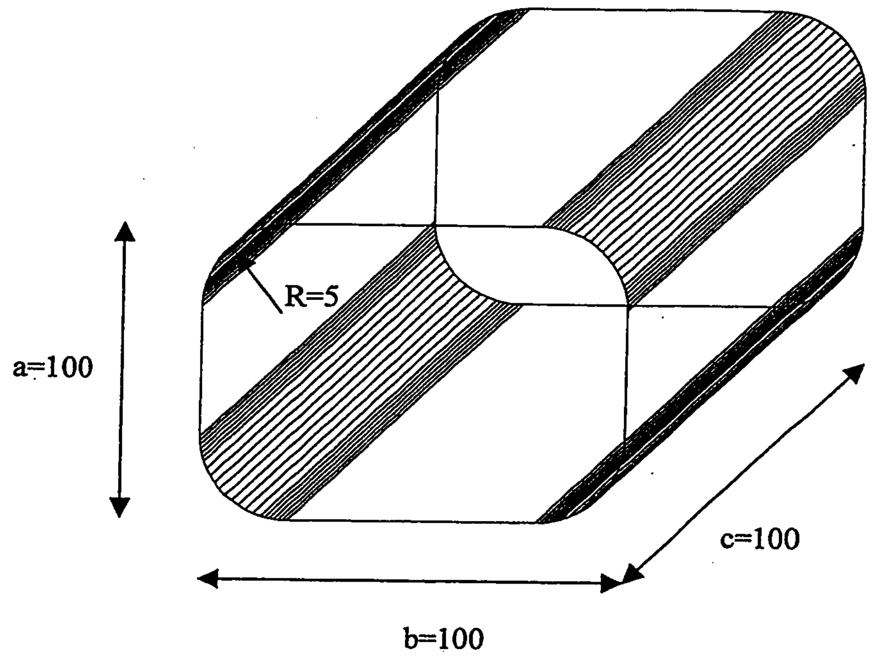

Fig 4-1 Typical box section

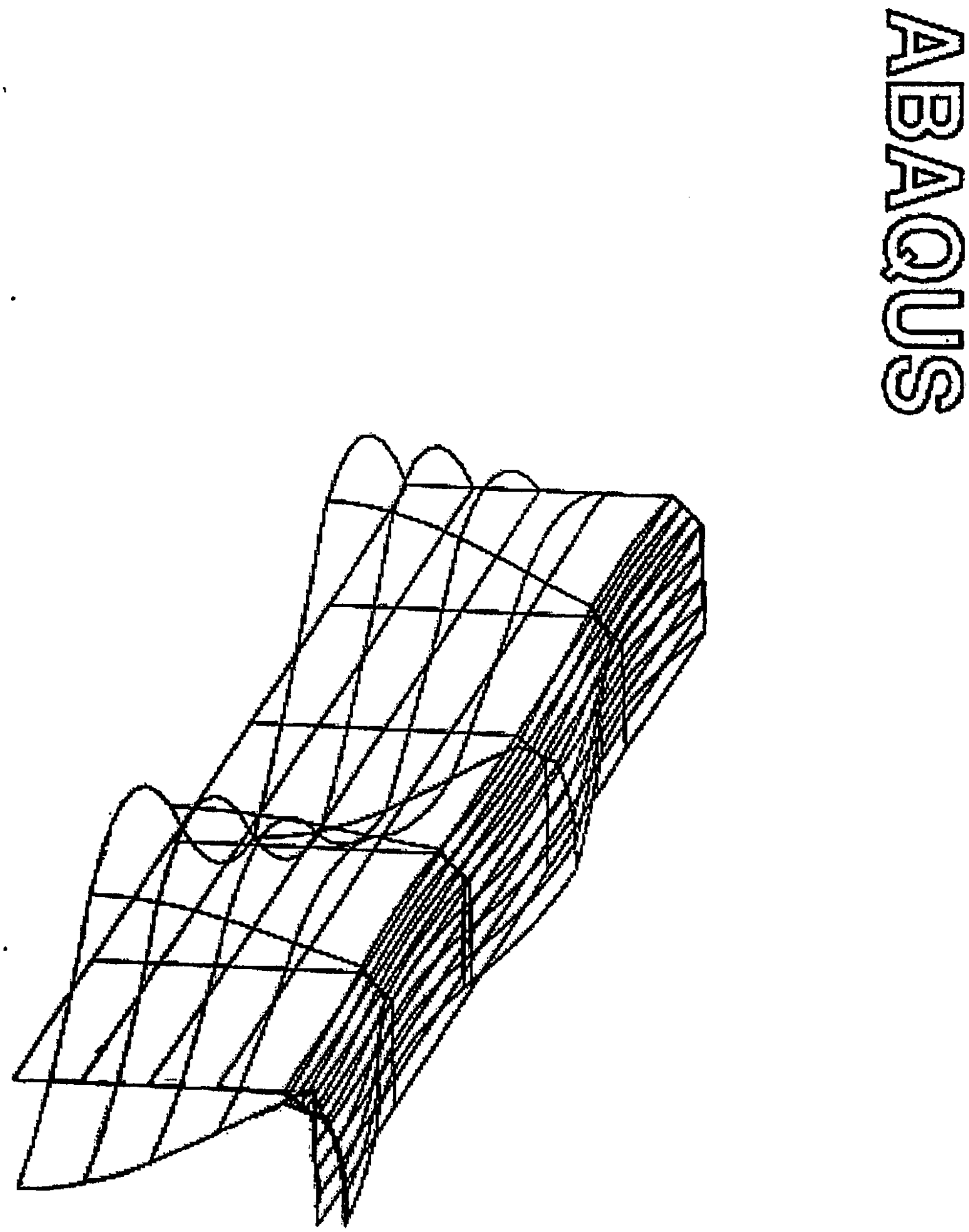

Fig 4-2 Typical ABAQUS elastic buckling

Fig 4-3 Stress distribution across the wall of a box section
b/a=1, b/t=100, R/b=0.05

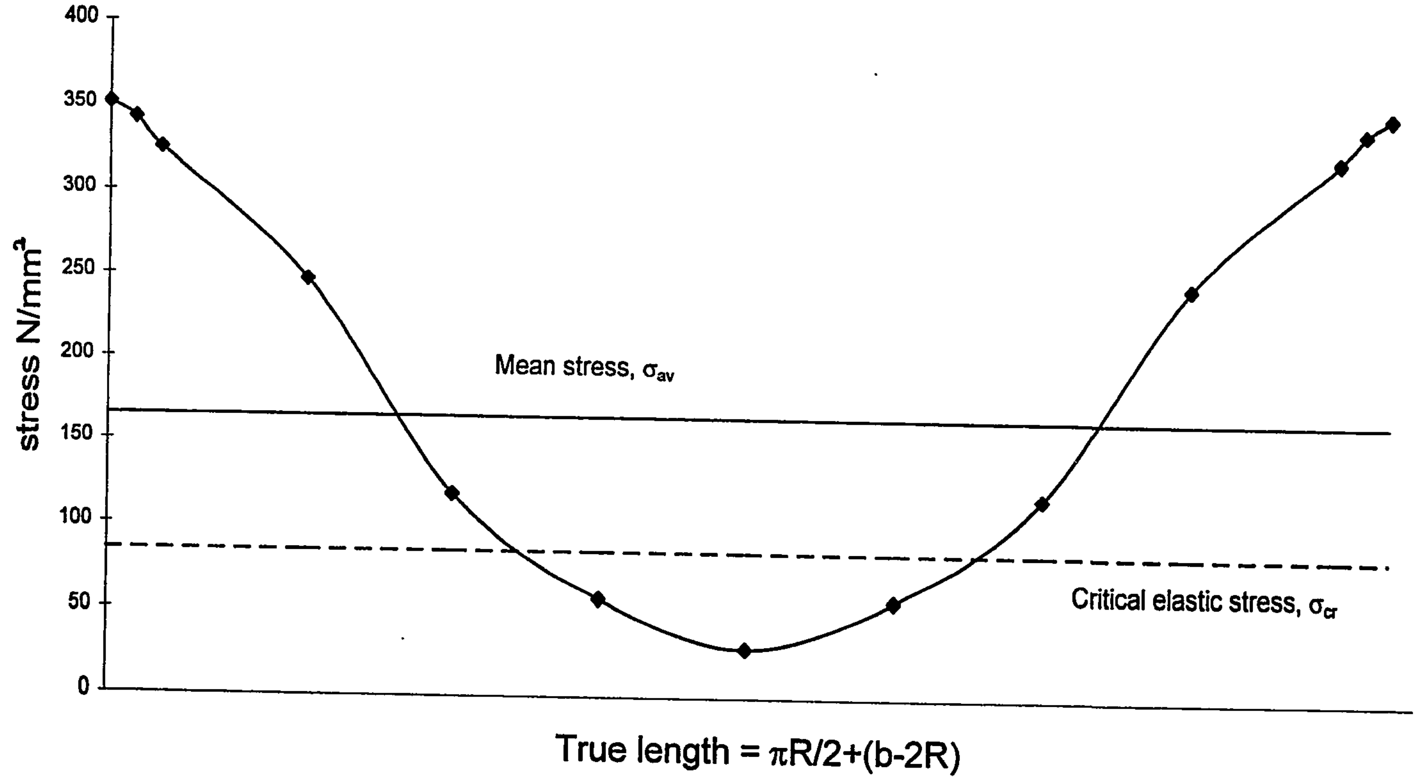

a = 100 mm

b = 100 mm

c = 100 mm

t = 1 mm

R = 5 mm

E = 200000 N/mm^2

critical_stress = 86 N/mm^2

ultimate_stress = 165 N/mm^2

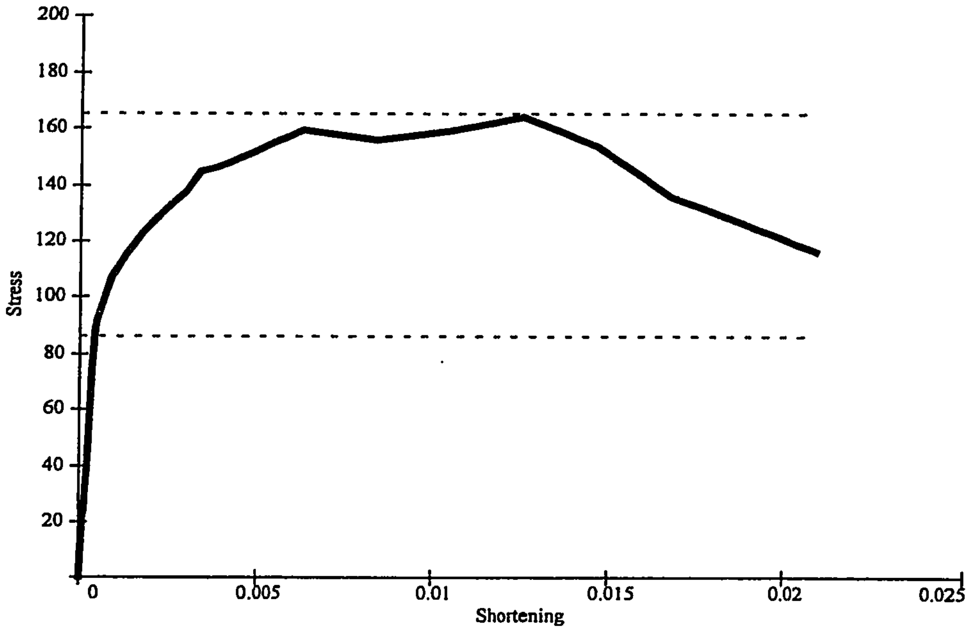

Fig 4-4 Mean stress and axial shortening for each step for a box section

Fig 4-5 Critical stress for a box section, a/b=1 b/t=40

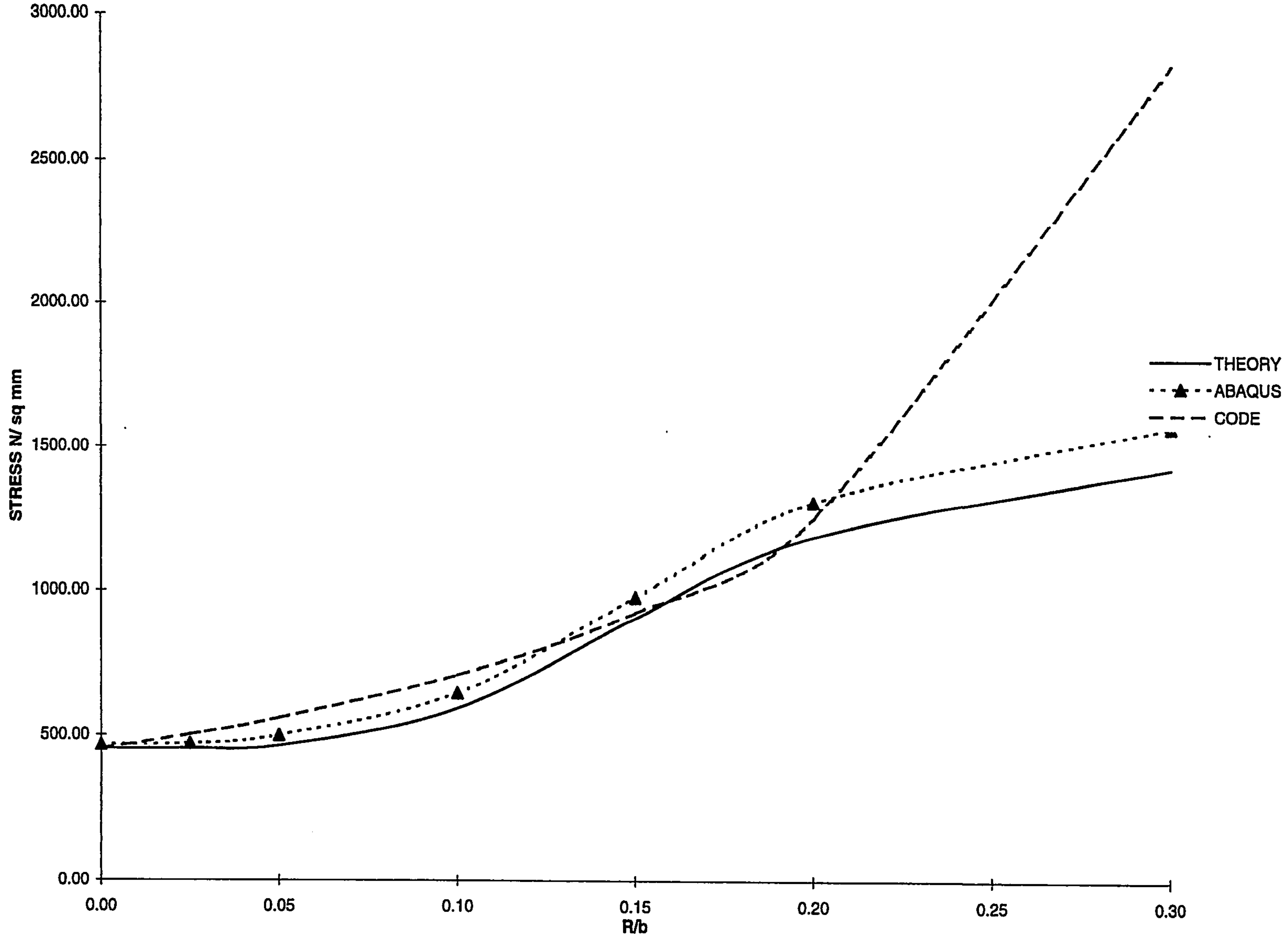

F4-5

Fig 4-6 Critical stress for a box section, a/b=1 b/t=50

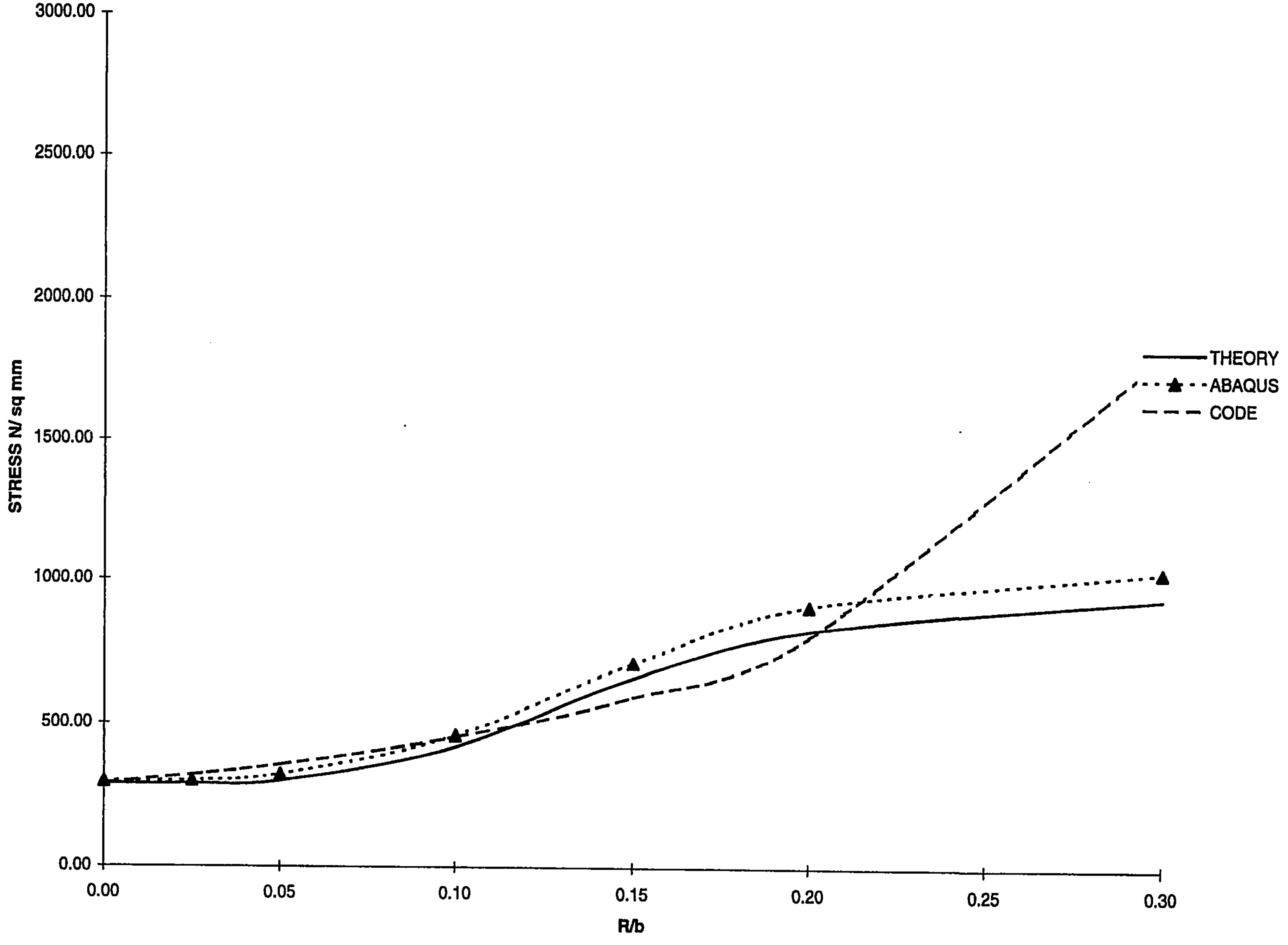

F4-6

Fig 4-7 Critical stress for a box section, a/b=1 b/t=66

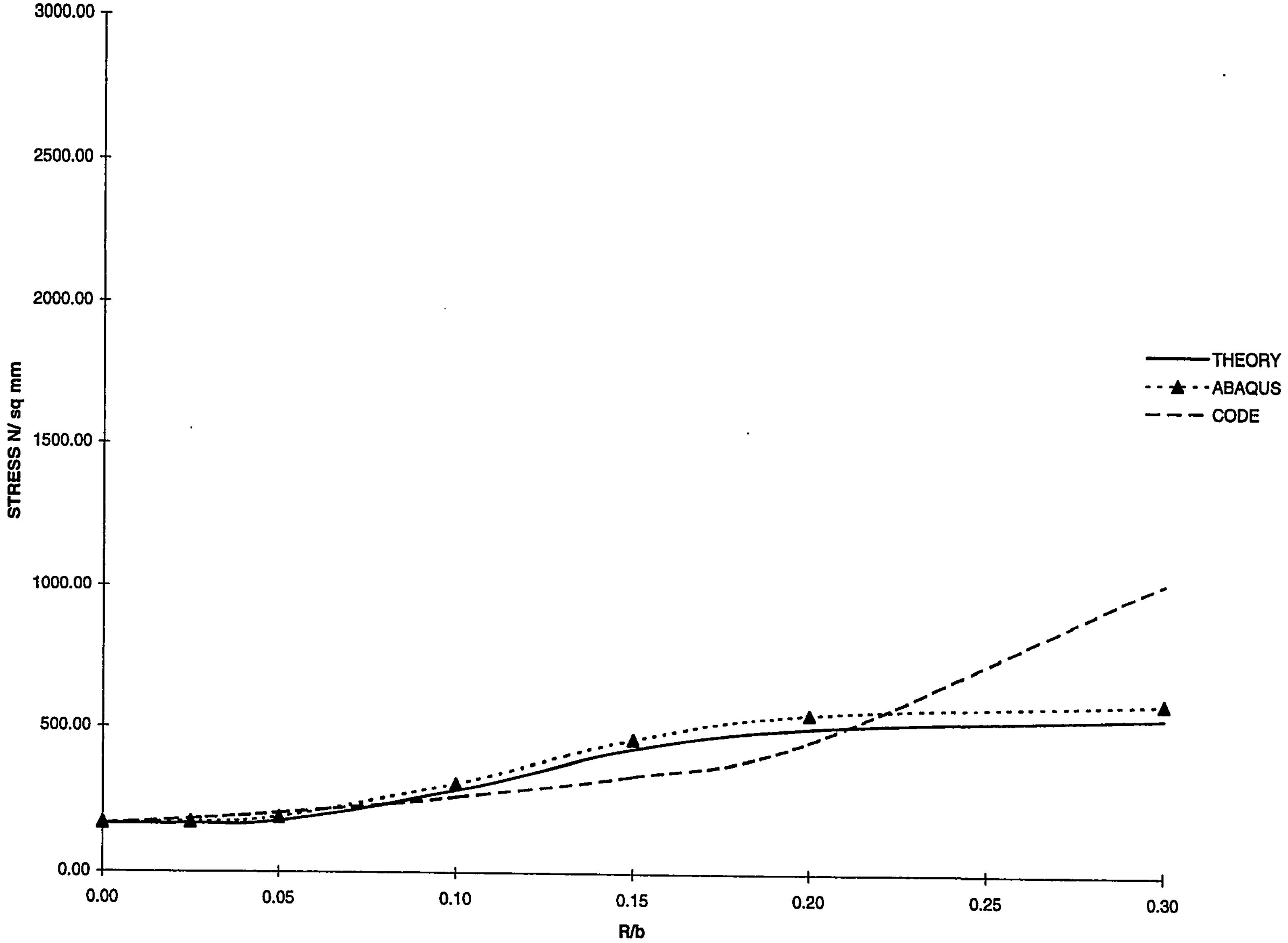

F4-7

Fig 4-8 Critical stress for a box section, a/b=1 b/t=100

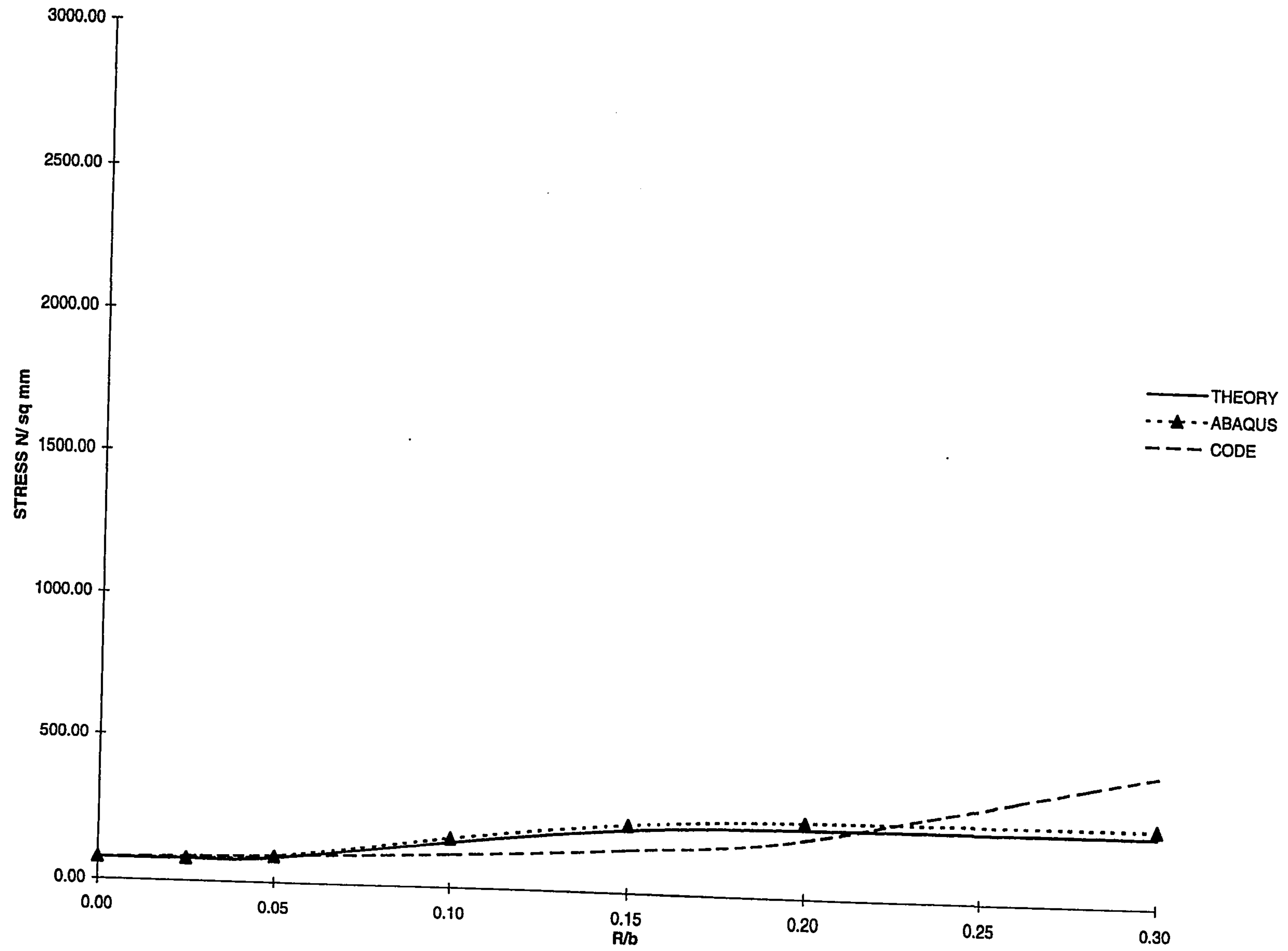

F4-8

Fig 4-9 Critical stress for a box section, a/b=1 b/t=200

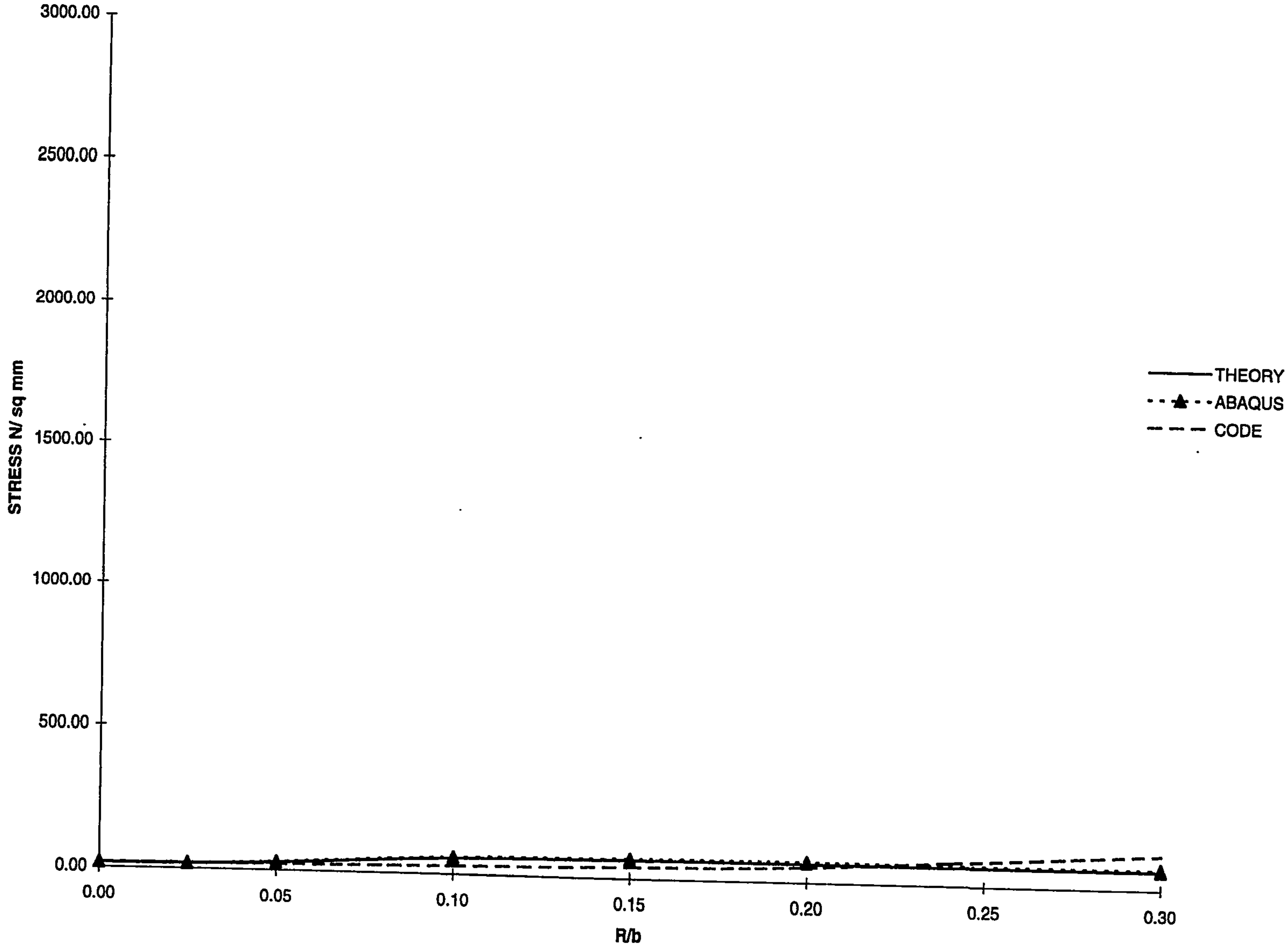

Fig 4-10 Critical stress for a box section, a/b=0.5 b/t=40

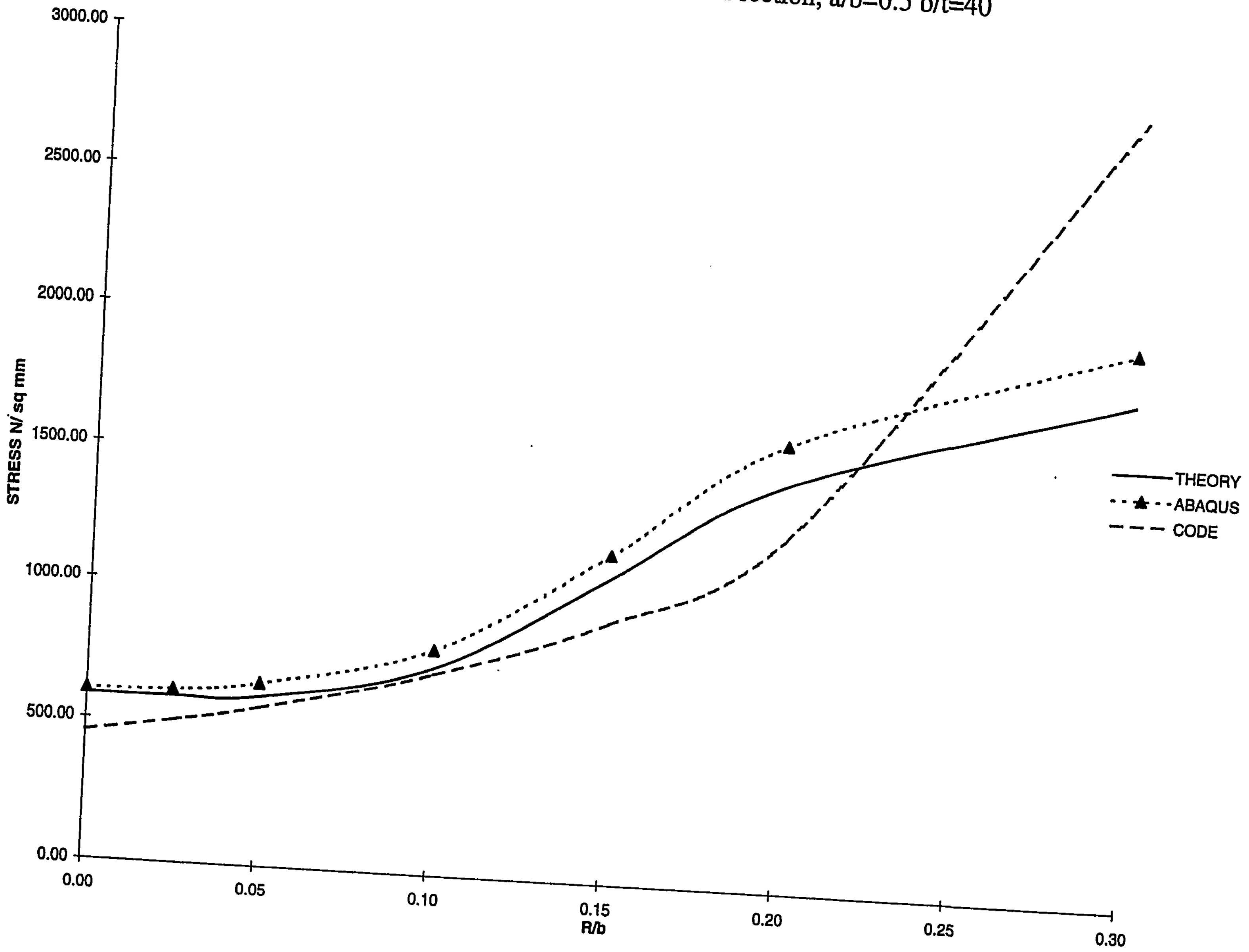

F4-10

Fig 4-11 Critical stress for a box section, a/b=0.5 b/t=50

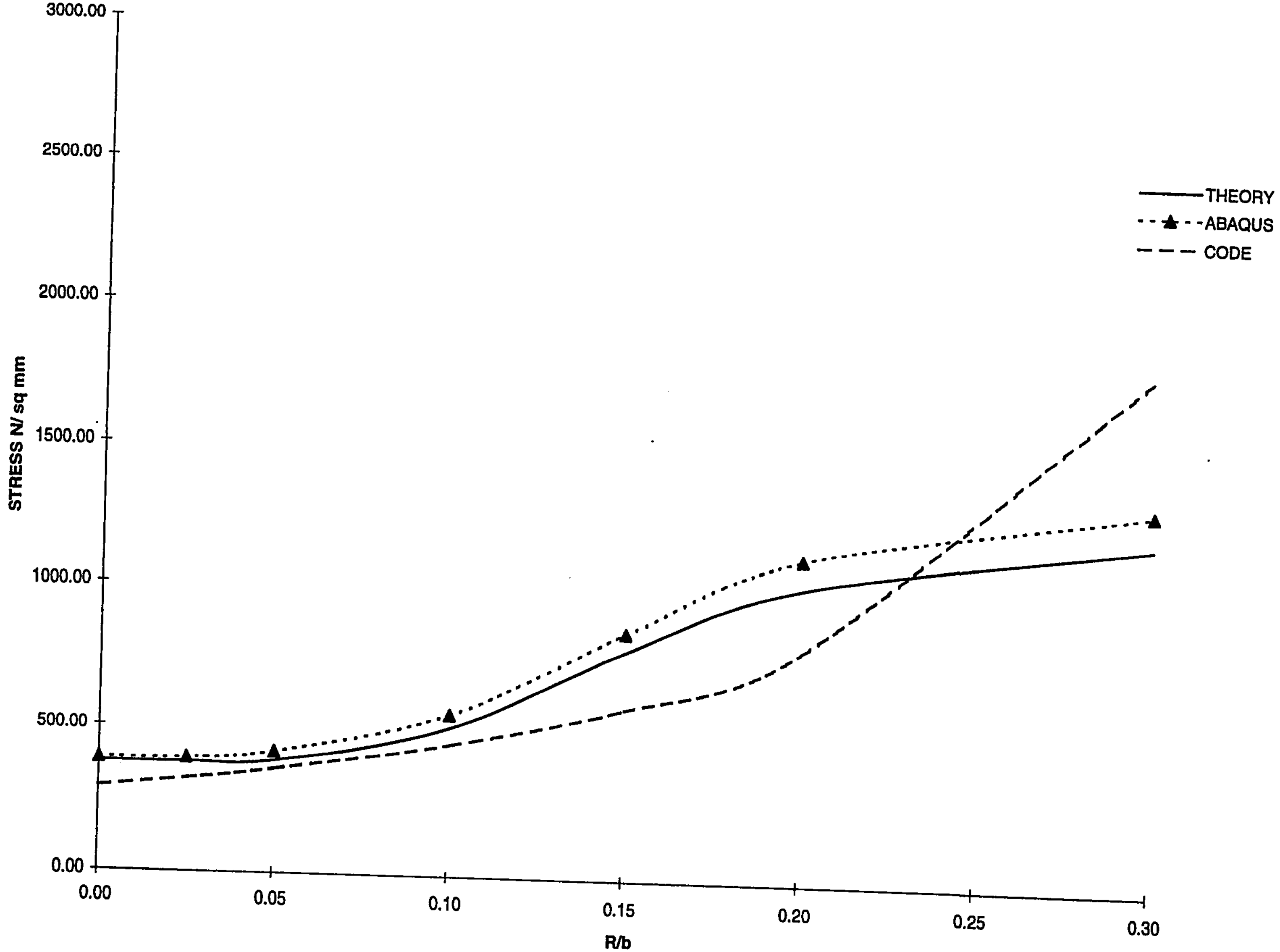

Fig 4-12 Critical stress for a box section, a/b=0.5 b/t=66

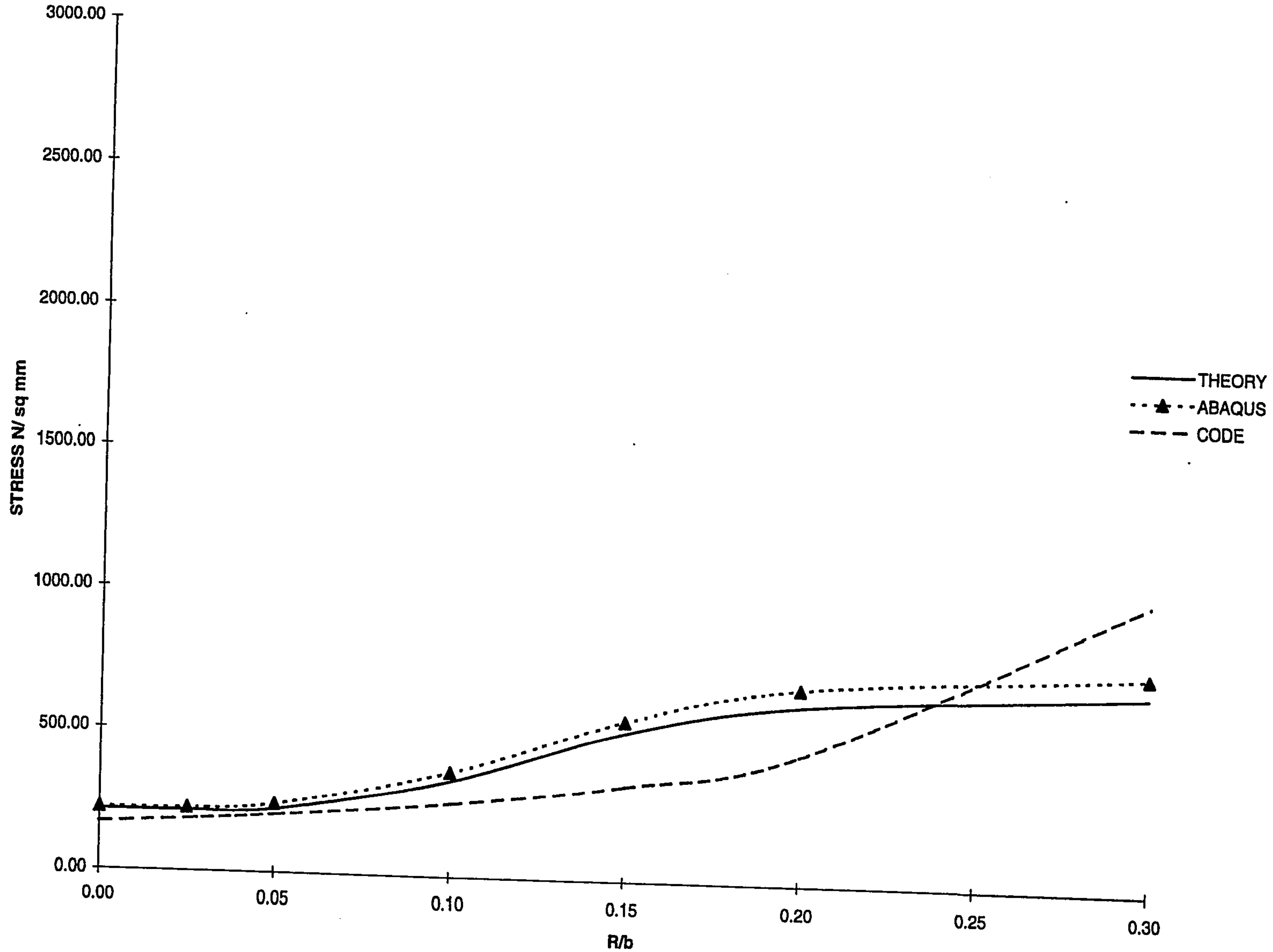

F4-12

Fig 4-13 Critical stress for a box section, a/b=0.5 b/t=100

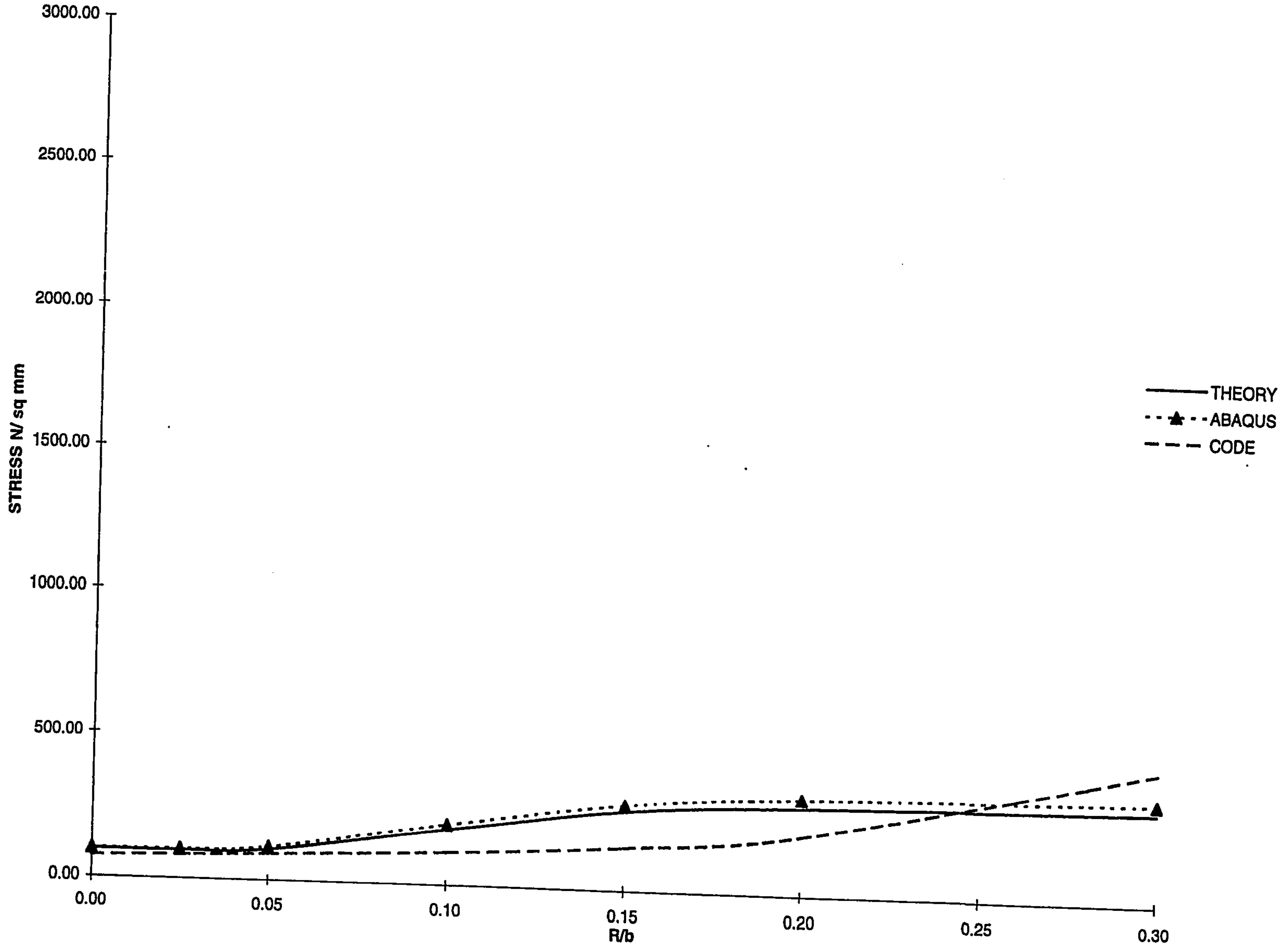

Fig 4-14 Critical stress for a box section, a/b=0.5 b/t=200

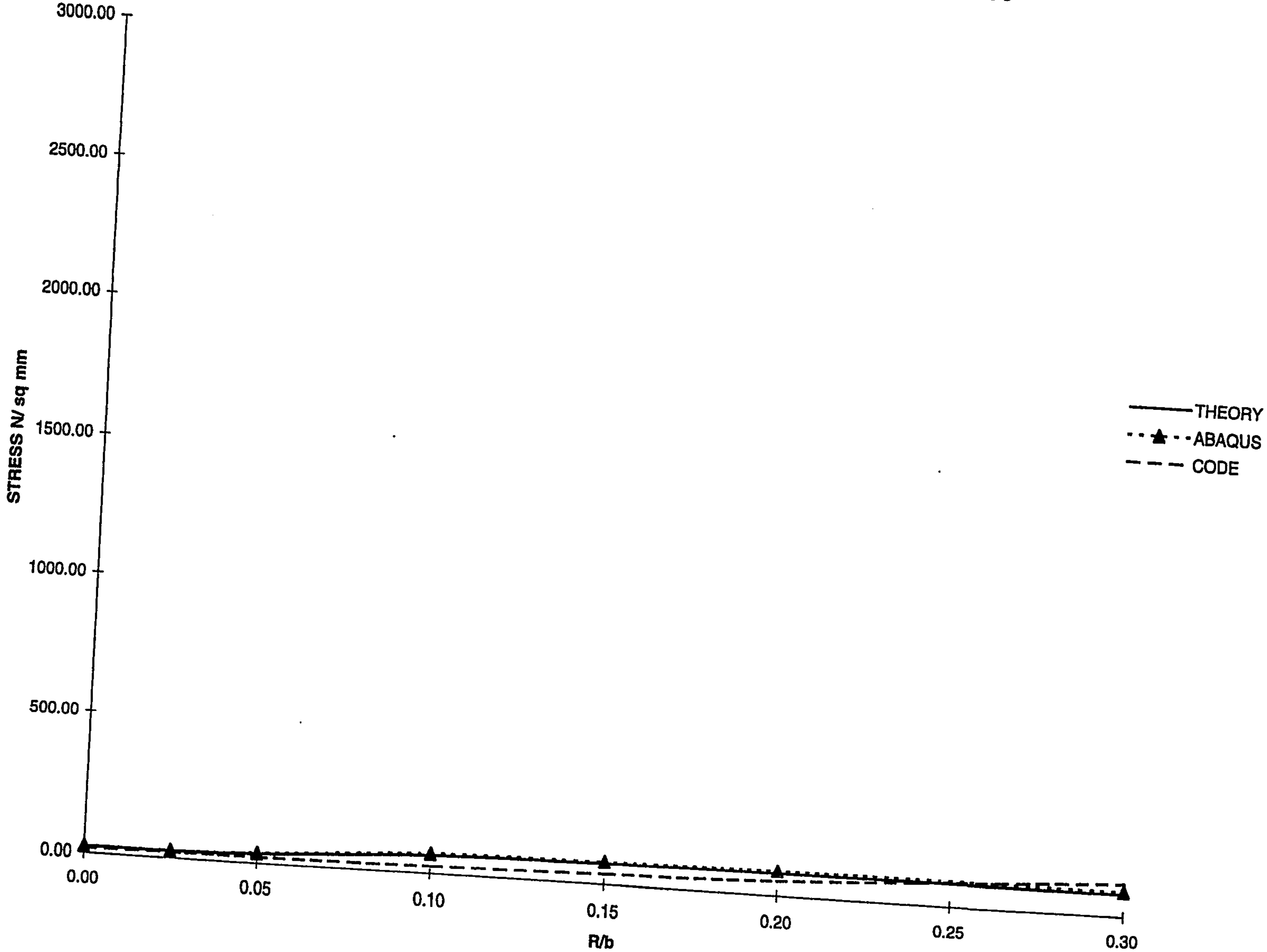

Fig 4-15 Critical stress for a box section, a/b=0.25 b/t=40

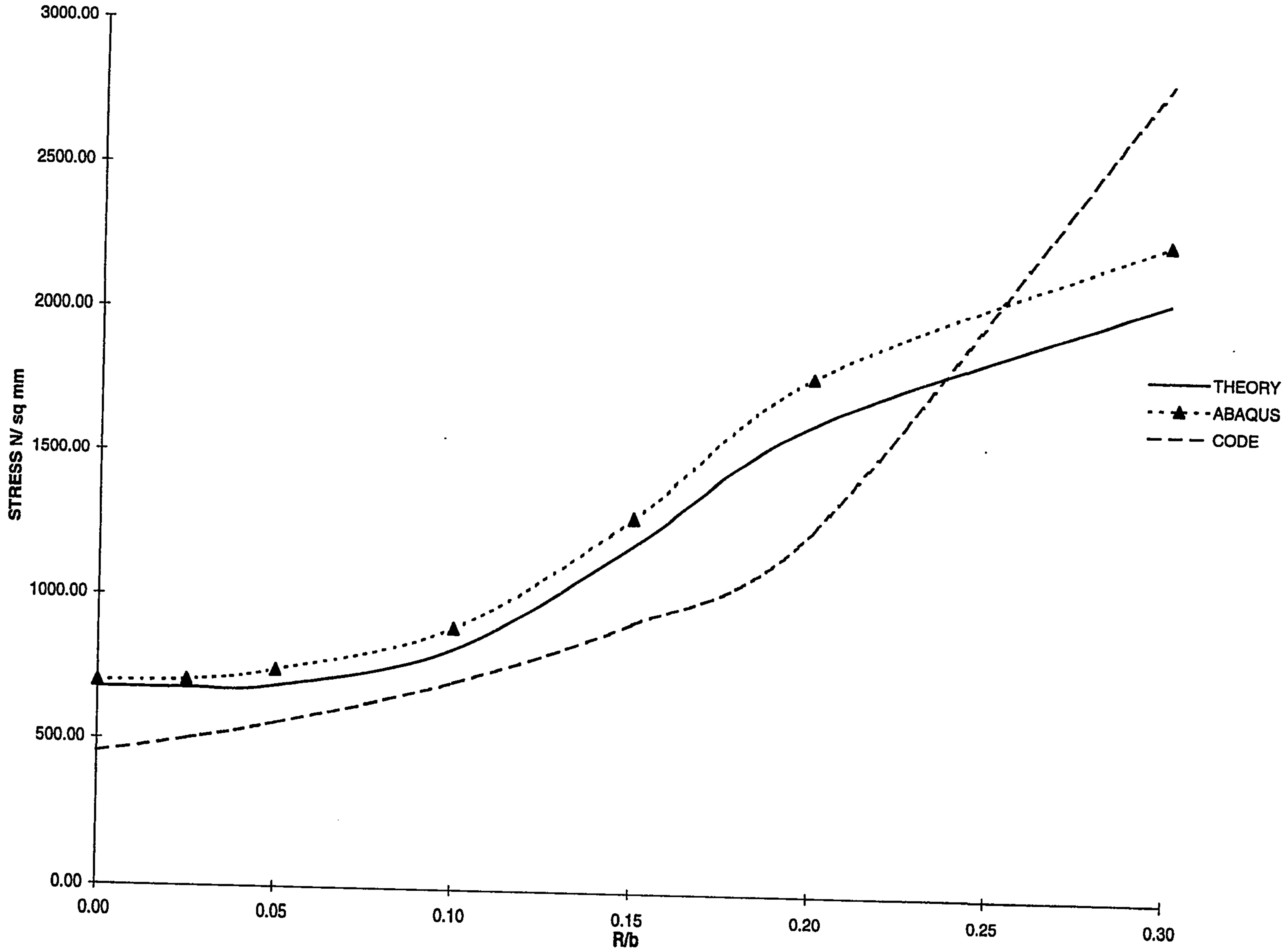

Fig 4-16 Critical stress for a box section, a/b=0.25 b/t=50

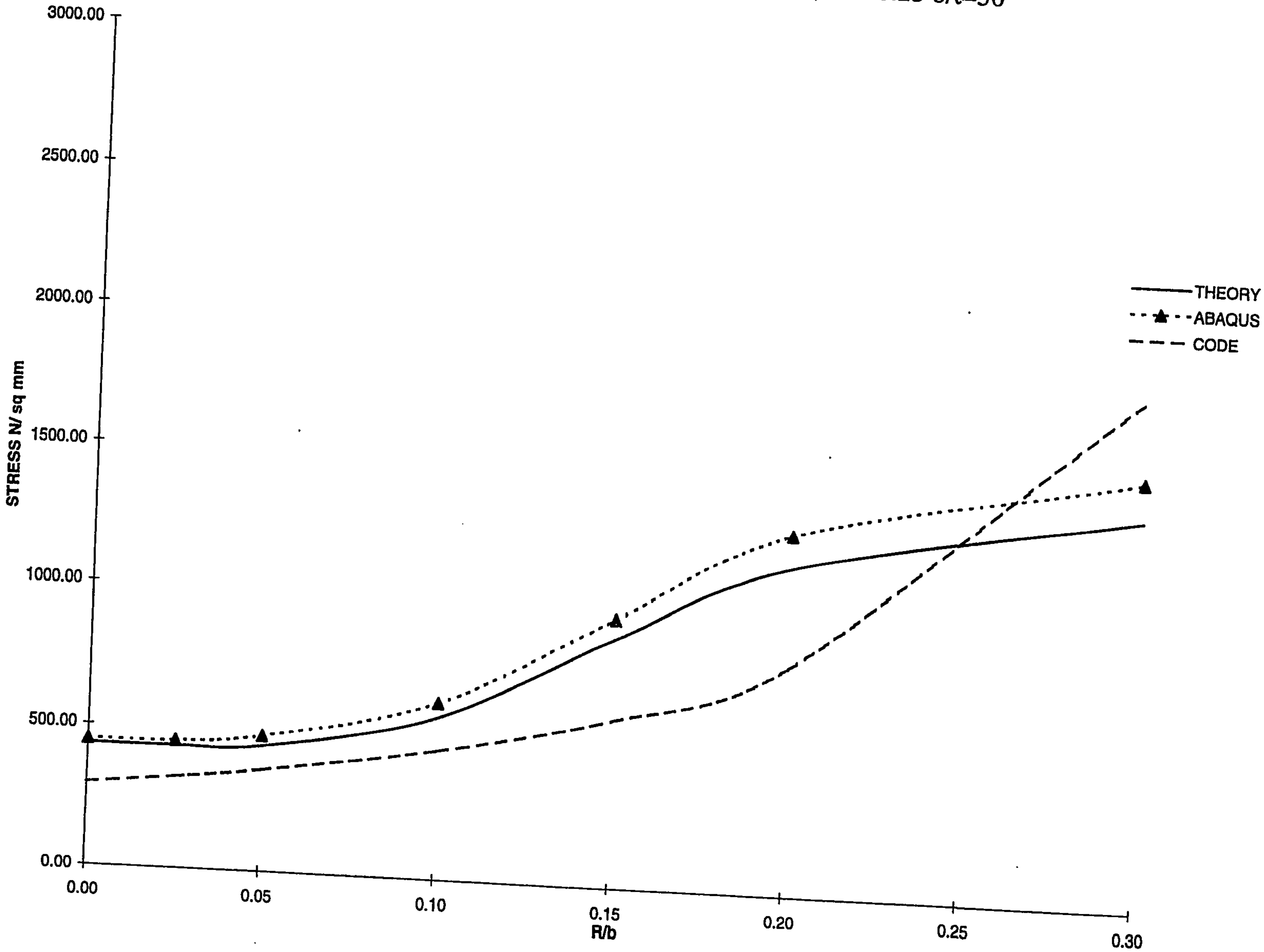

Fig 4-17 Critical stress for a box section, a/b=0.25 b/t=66

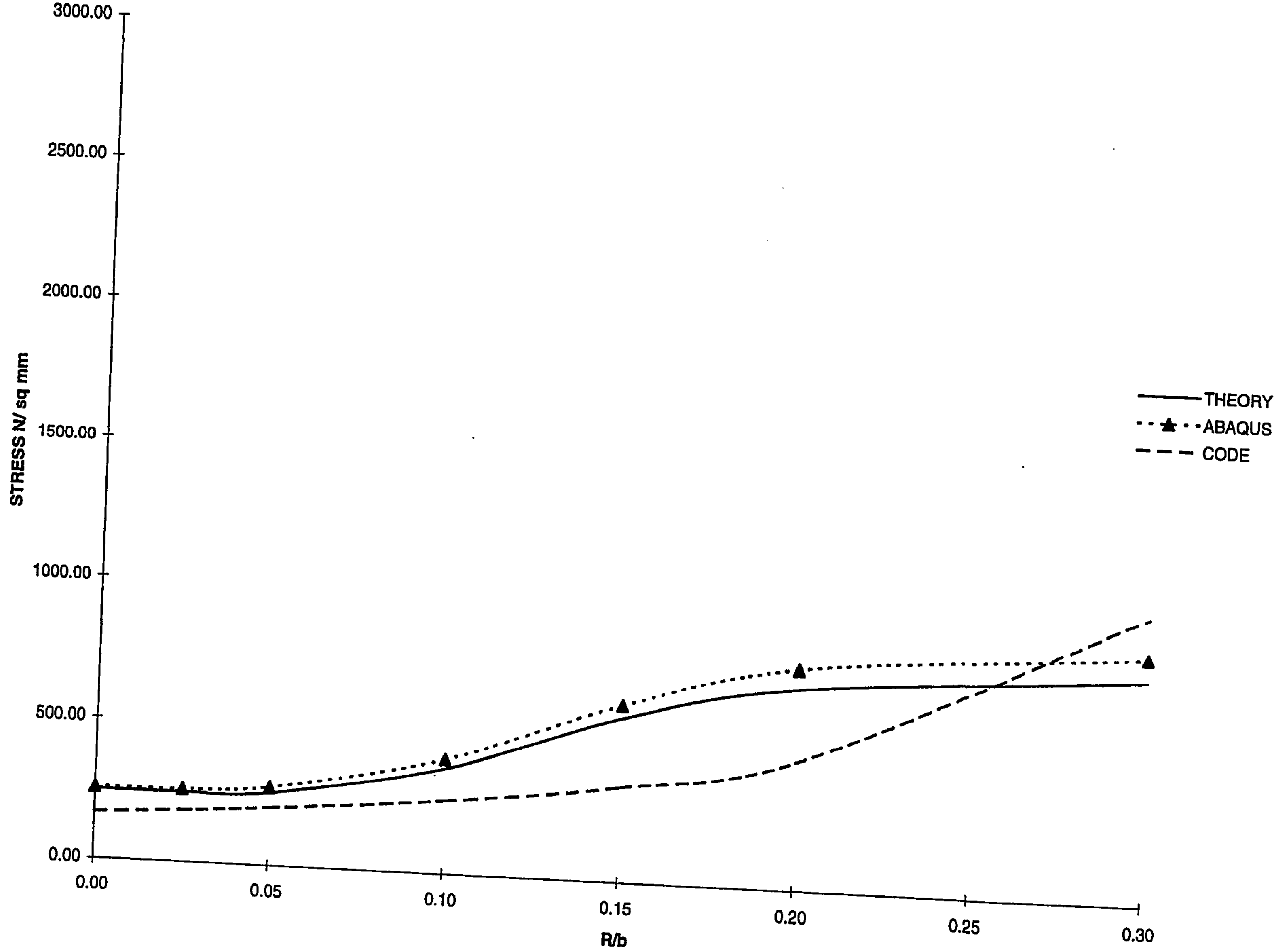

Fig 4-18 Critical stress for a box section, a/b=0.25 b/t=100

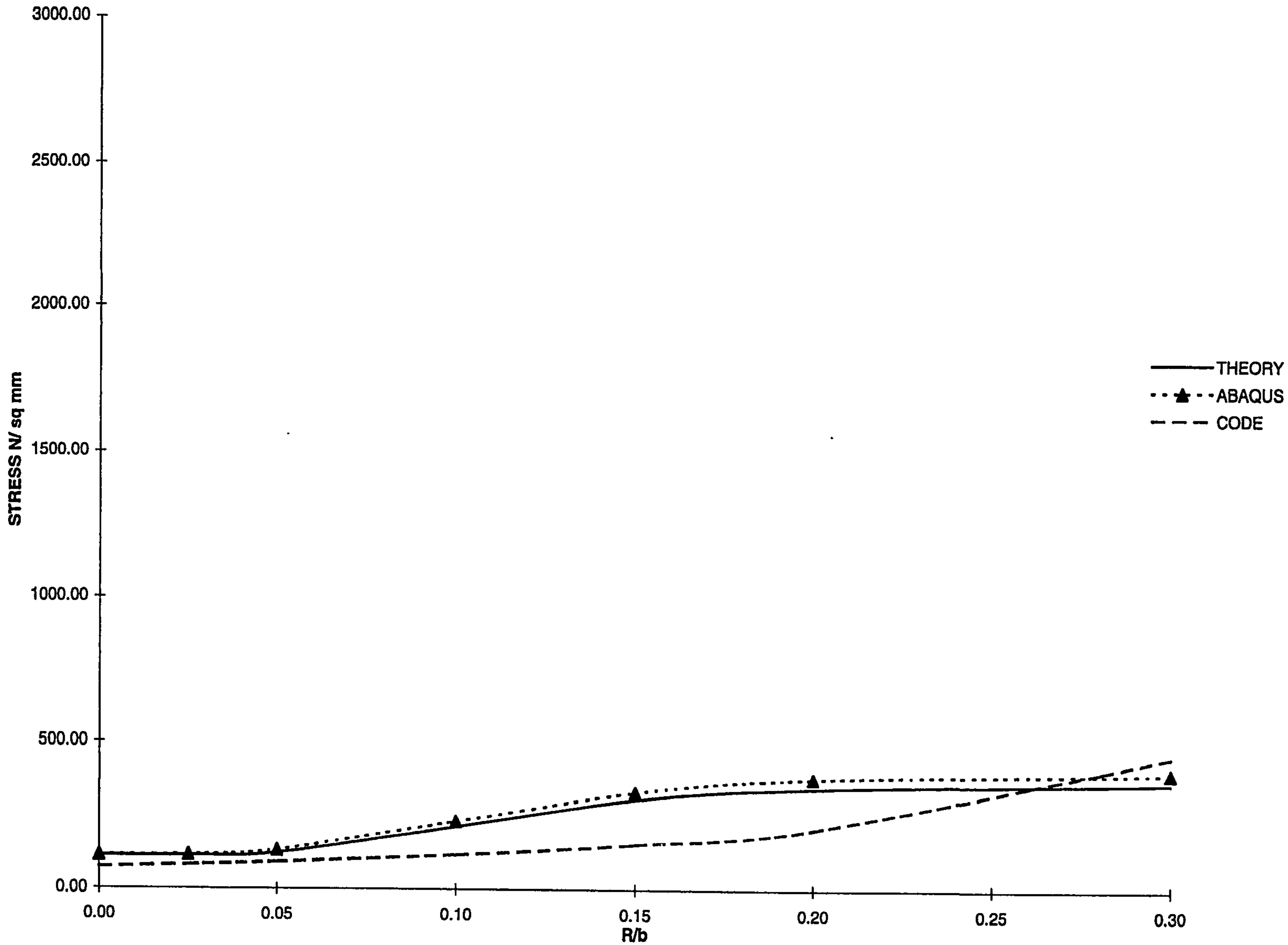

Fig 4-19 Critical stress for a box section, a/b=0.5 b/t=200

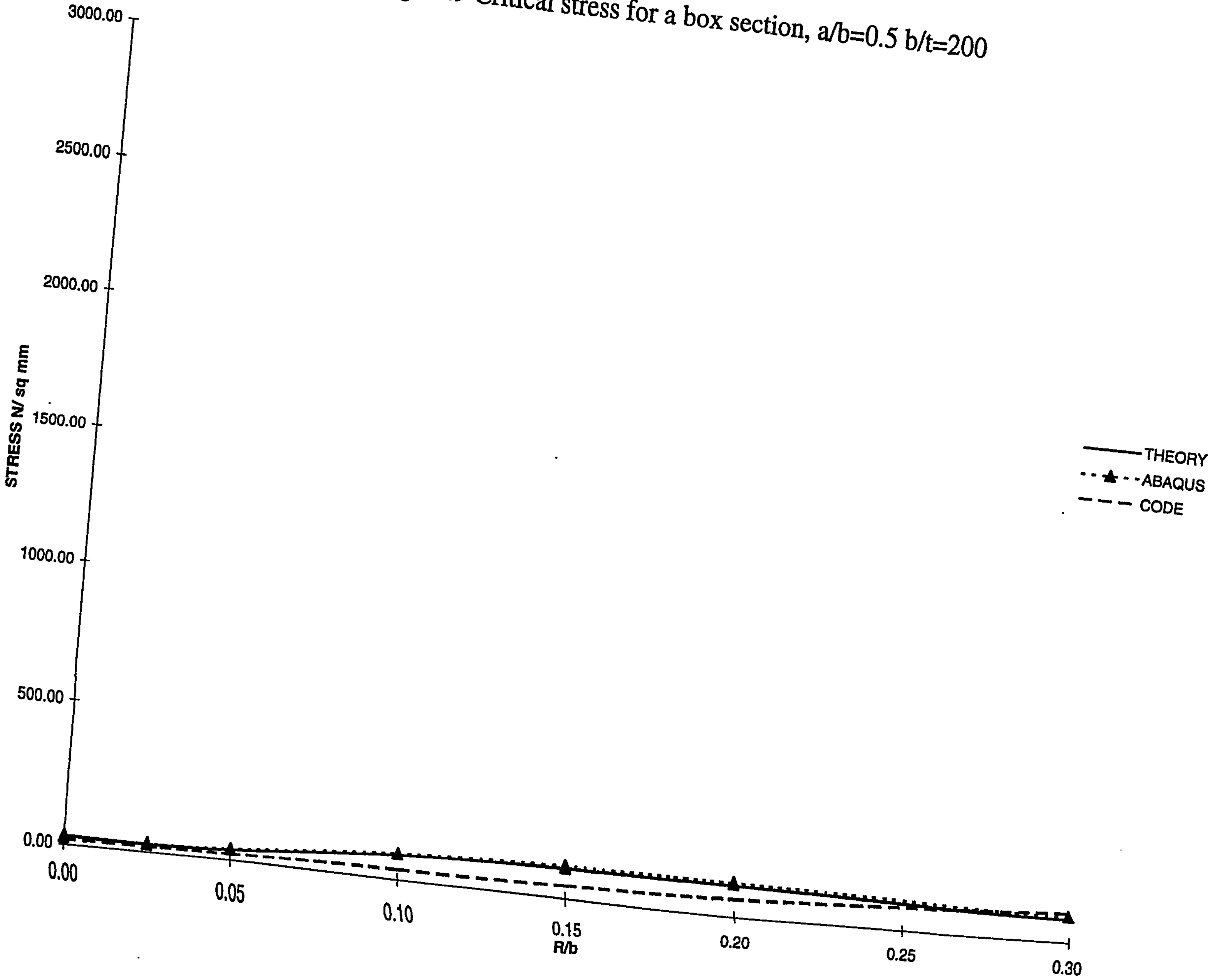

Fig 4-20 Ultimate stress for a box section, a/b=1 b/t=40

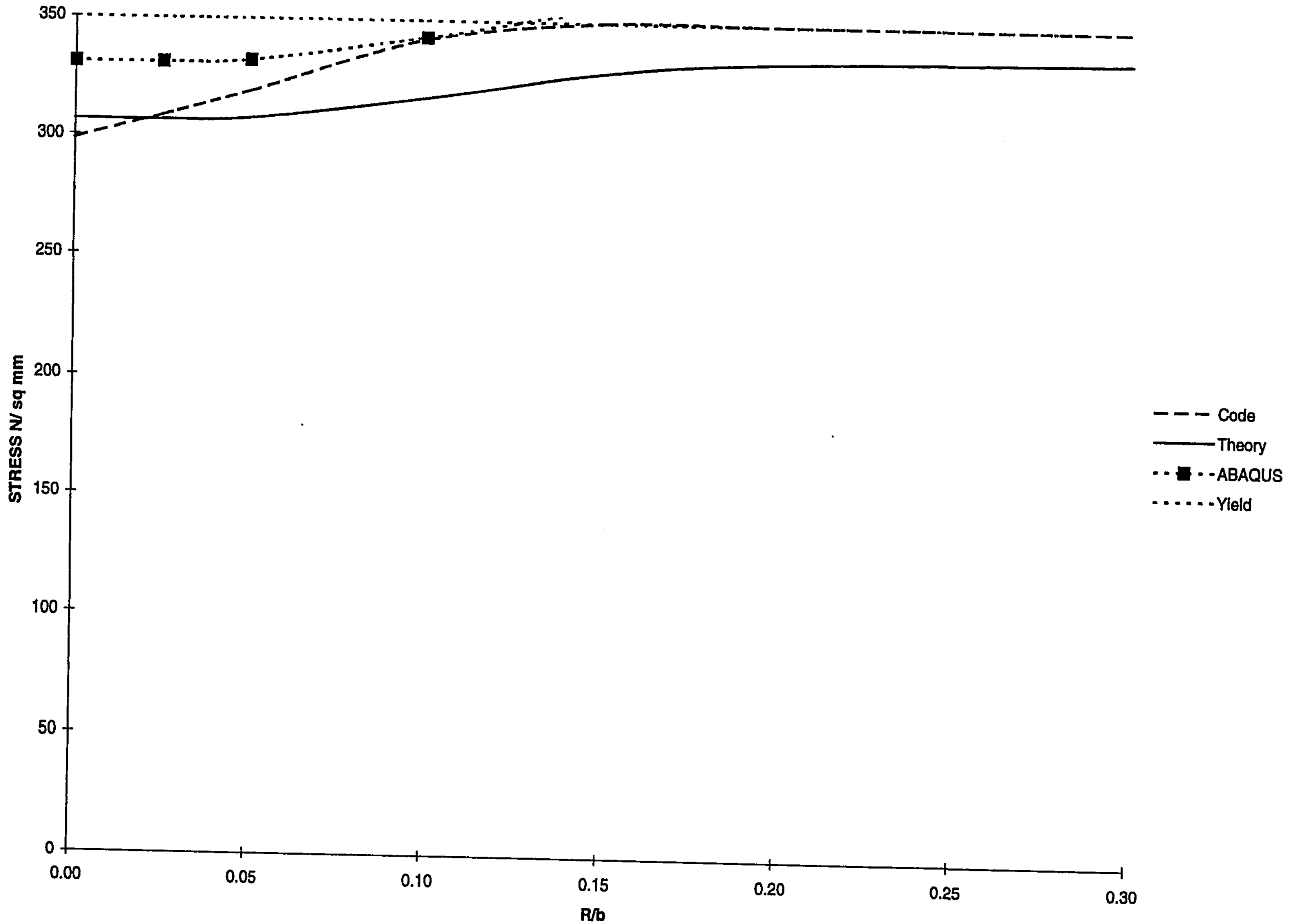

F4-20

Fig 4-21 Ultimate stress for a box section, a/b=1 b/t=50

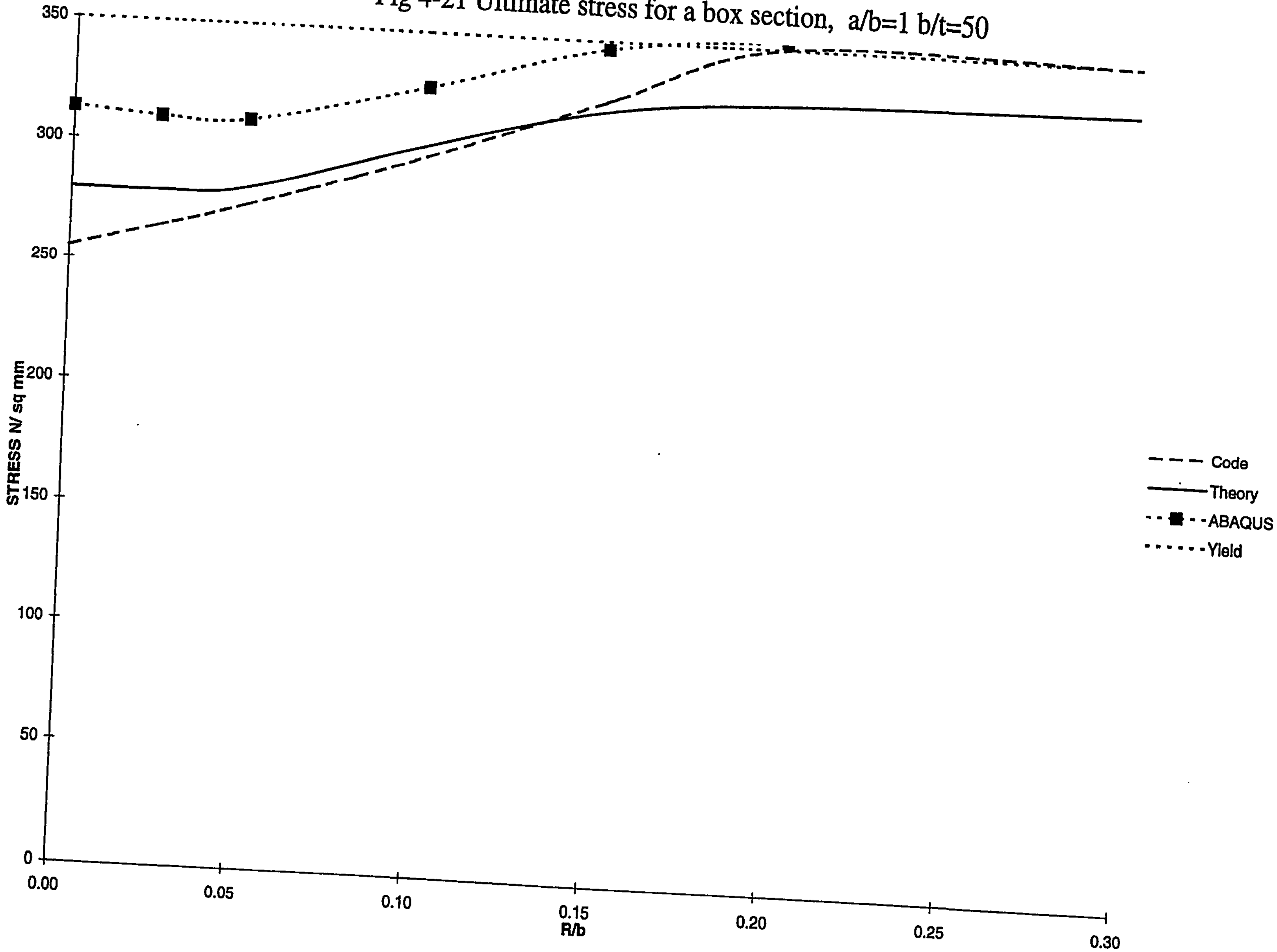

F4-21

Fig 4-22 Ultimate stress for a box section, a/b=1 b/t=66

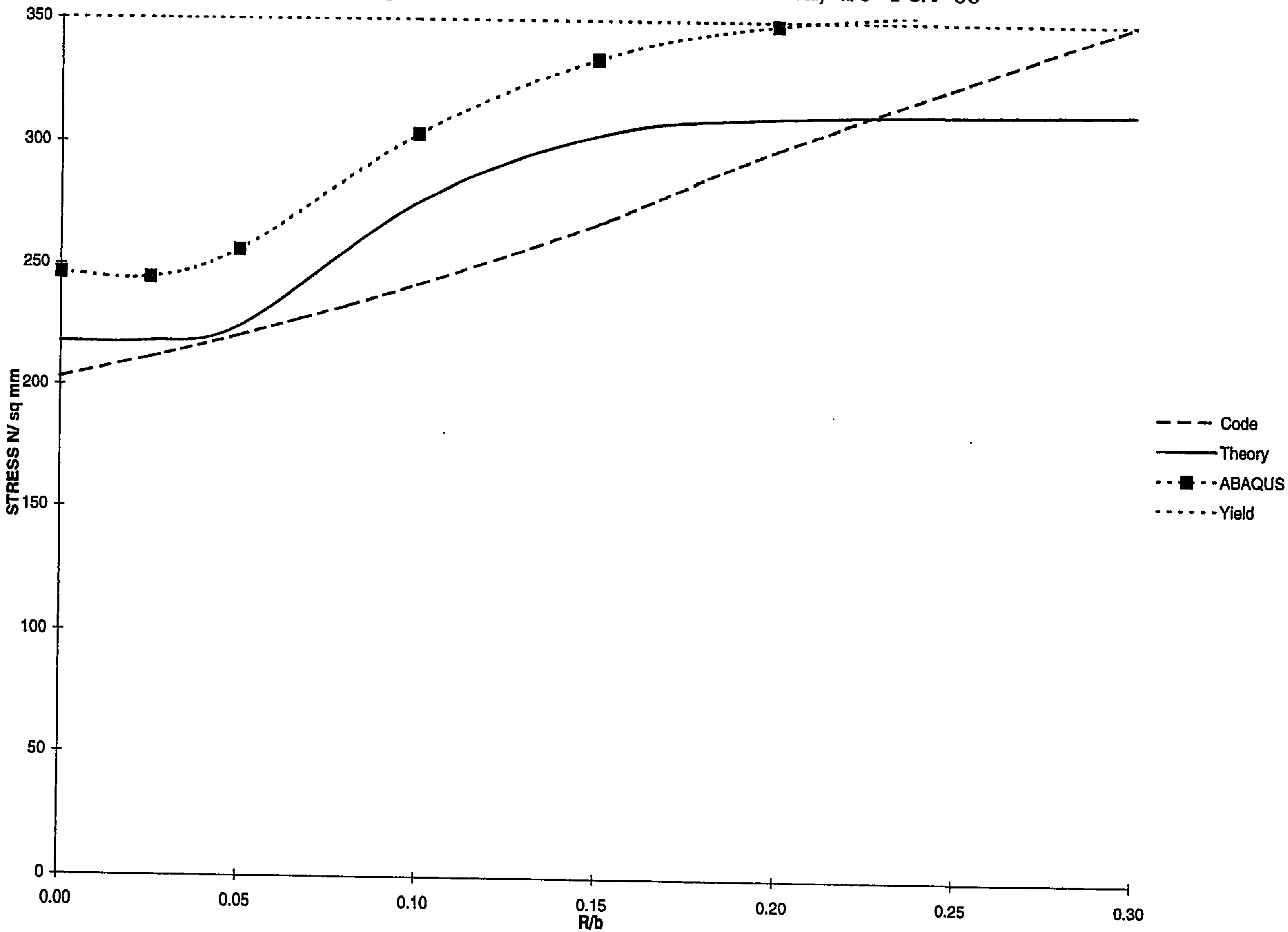

F4-22

Fig 4-23 Ultimate stress for a box section, a/b=1 b/t=100

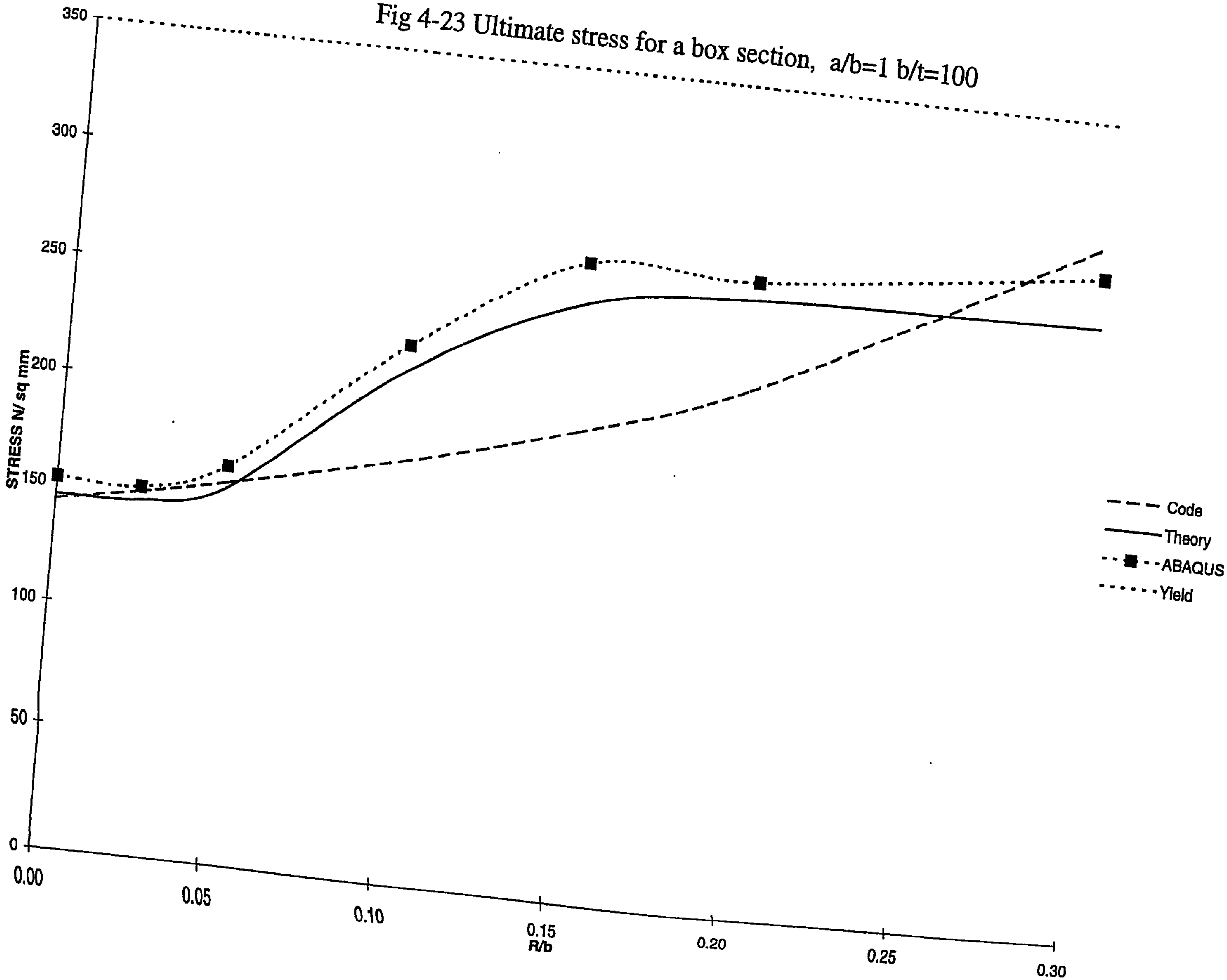

Fig 4-24 Ultimate stress for a box section, a/b=1 b/t=200

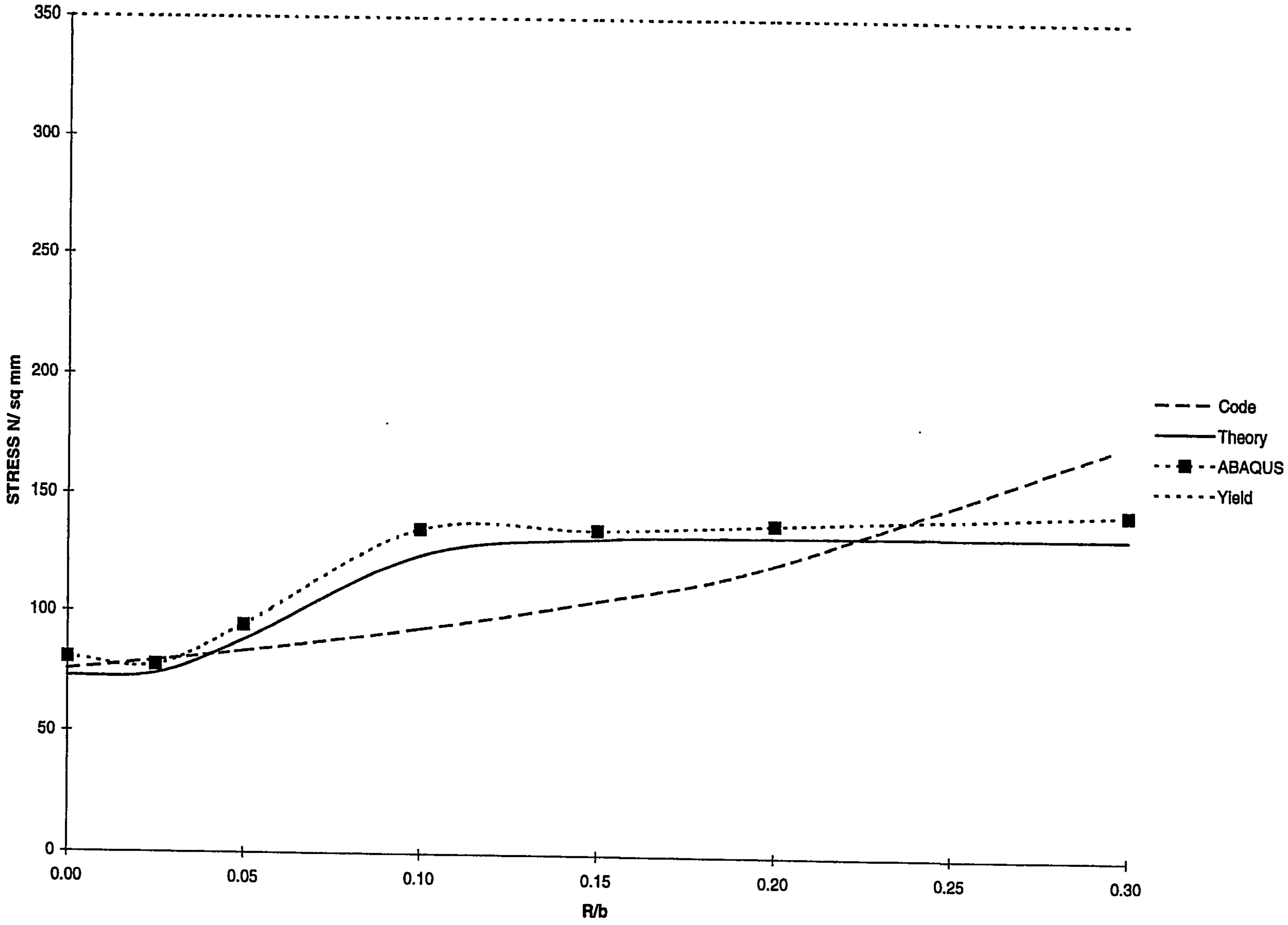

Fig 4-25 Ultimate stress for a box section, a/b=0.5 b/t=40

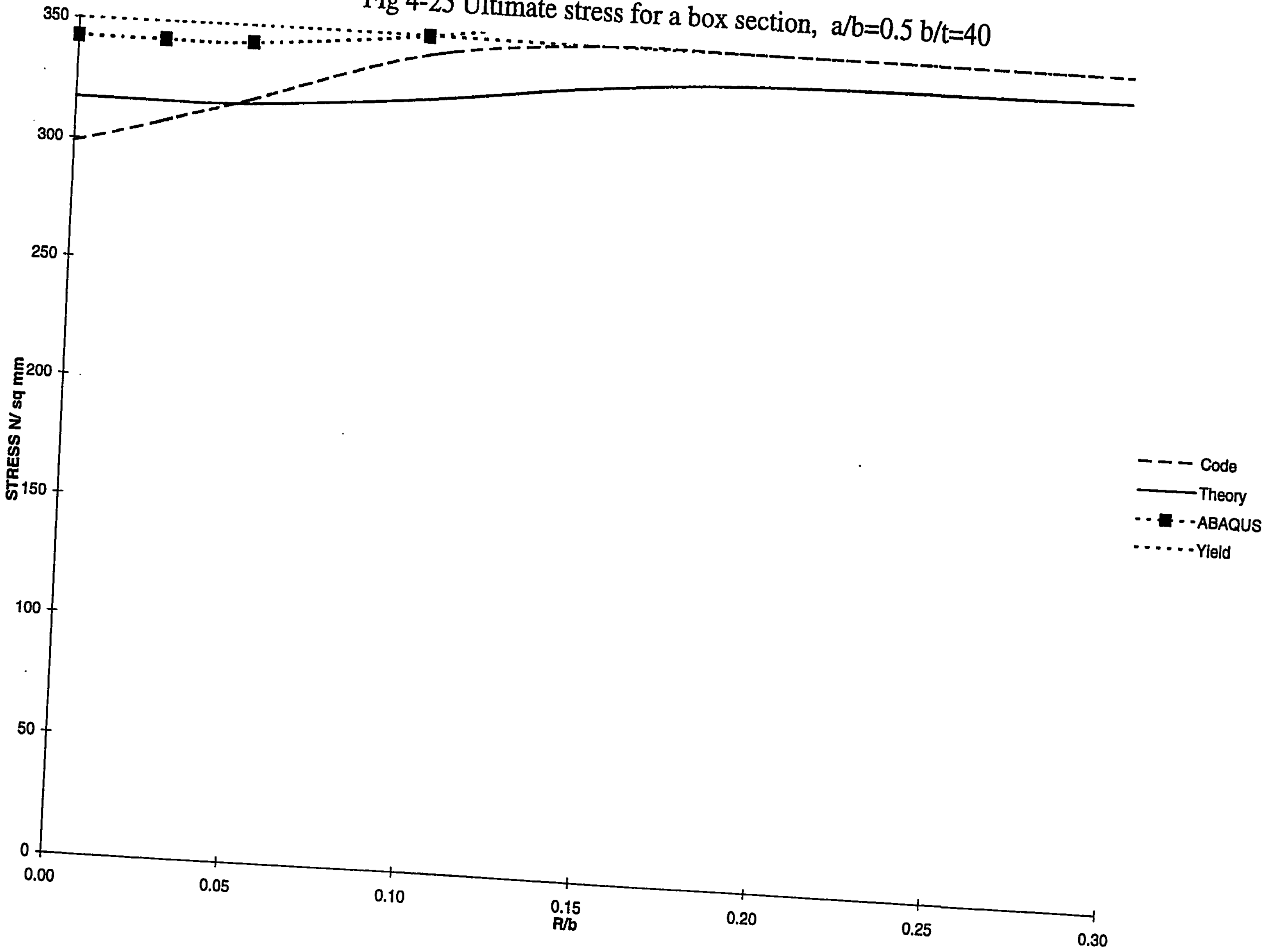

F4-25

Fig 4-26 Ultimate stress for a box section, a/b=0.5 b/t=50

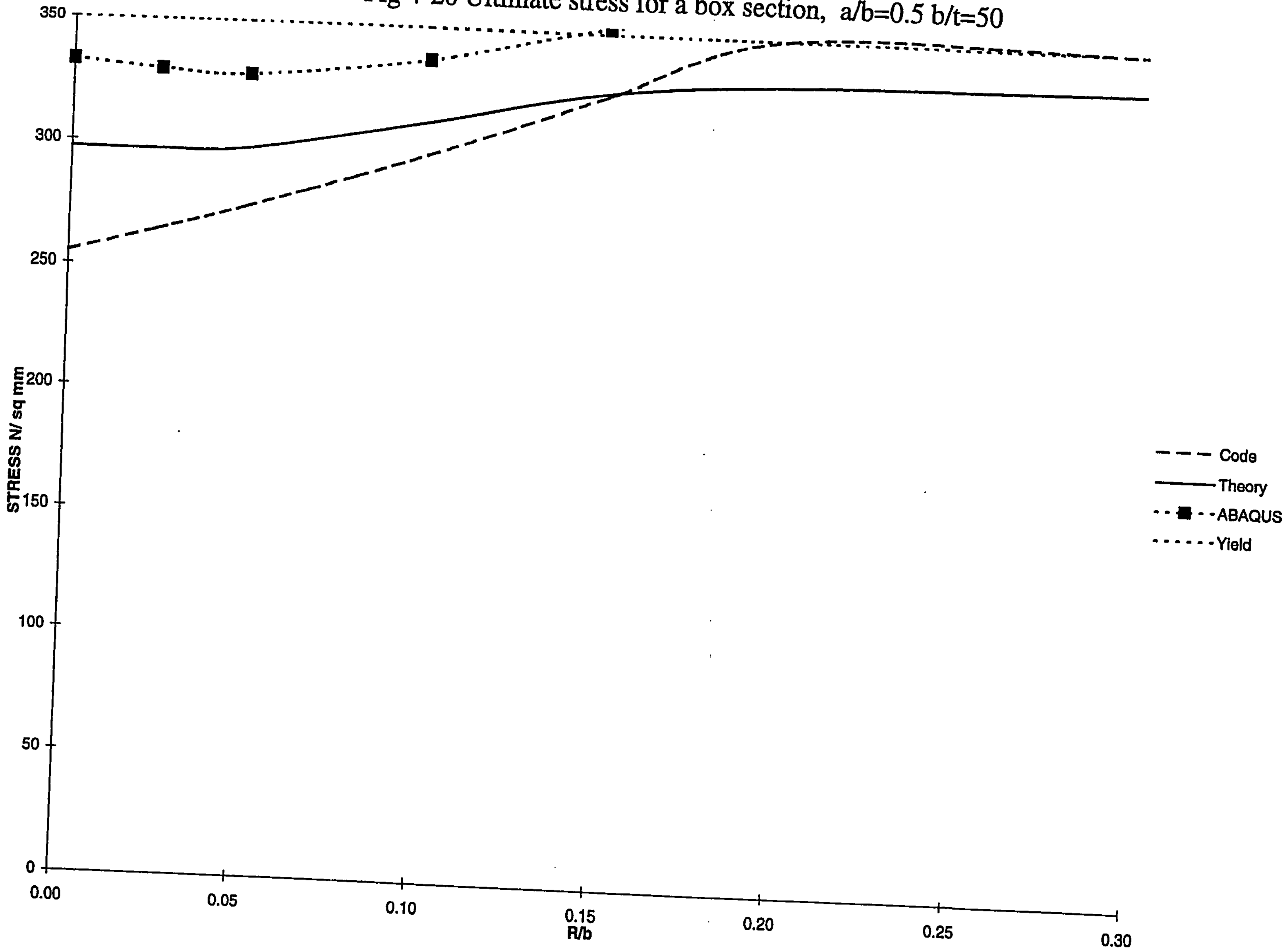

F4-26

Fig 4-27 Ultimate stress for a box section, a/b=0.5 b/t=66

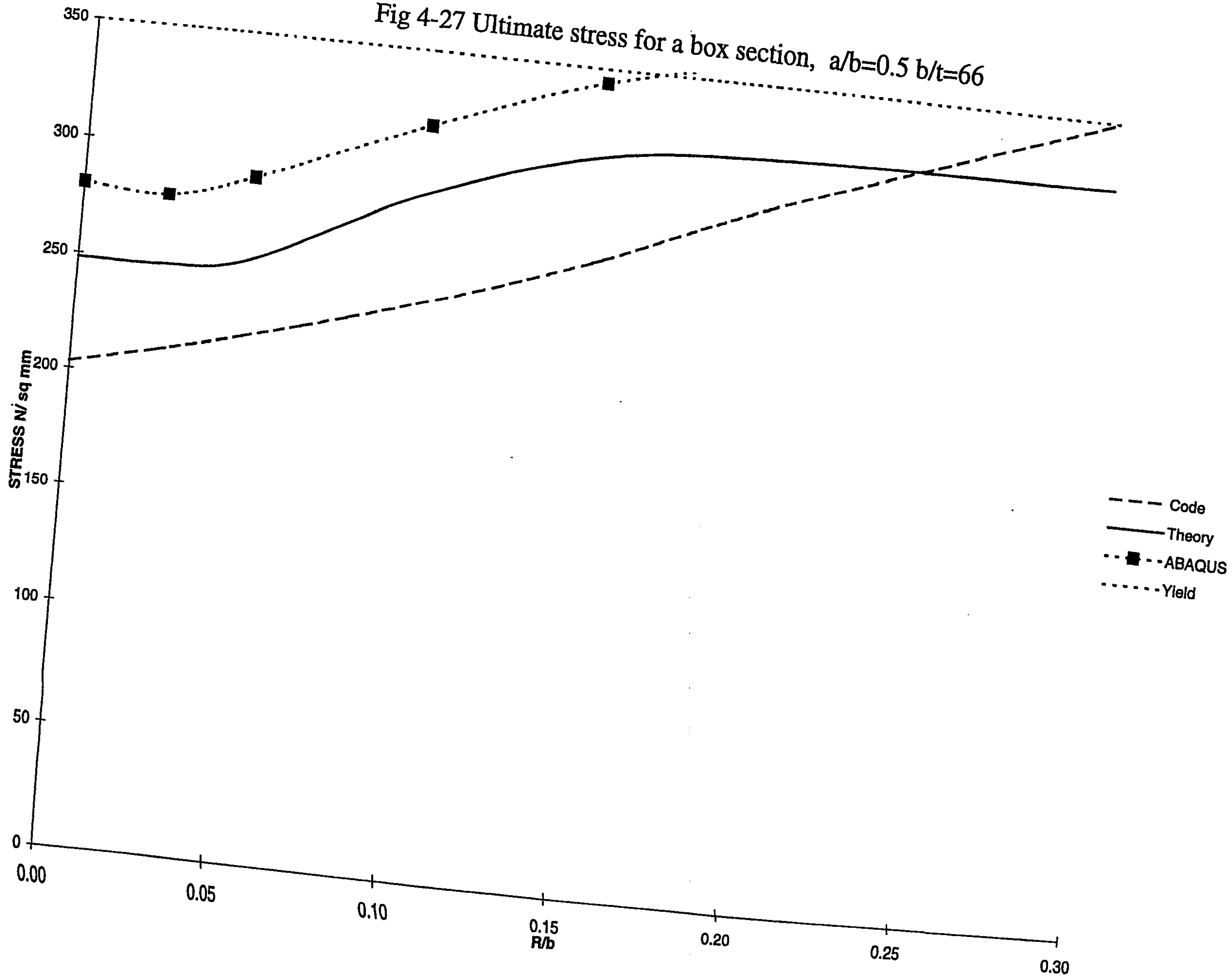

F4-27

Fig 4-28 Ultimate stress for a box section, a/b=0.5 b/t=100

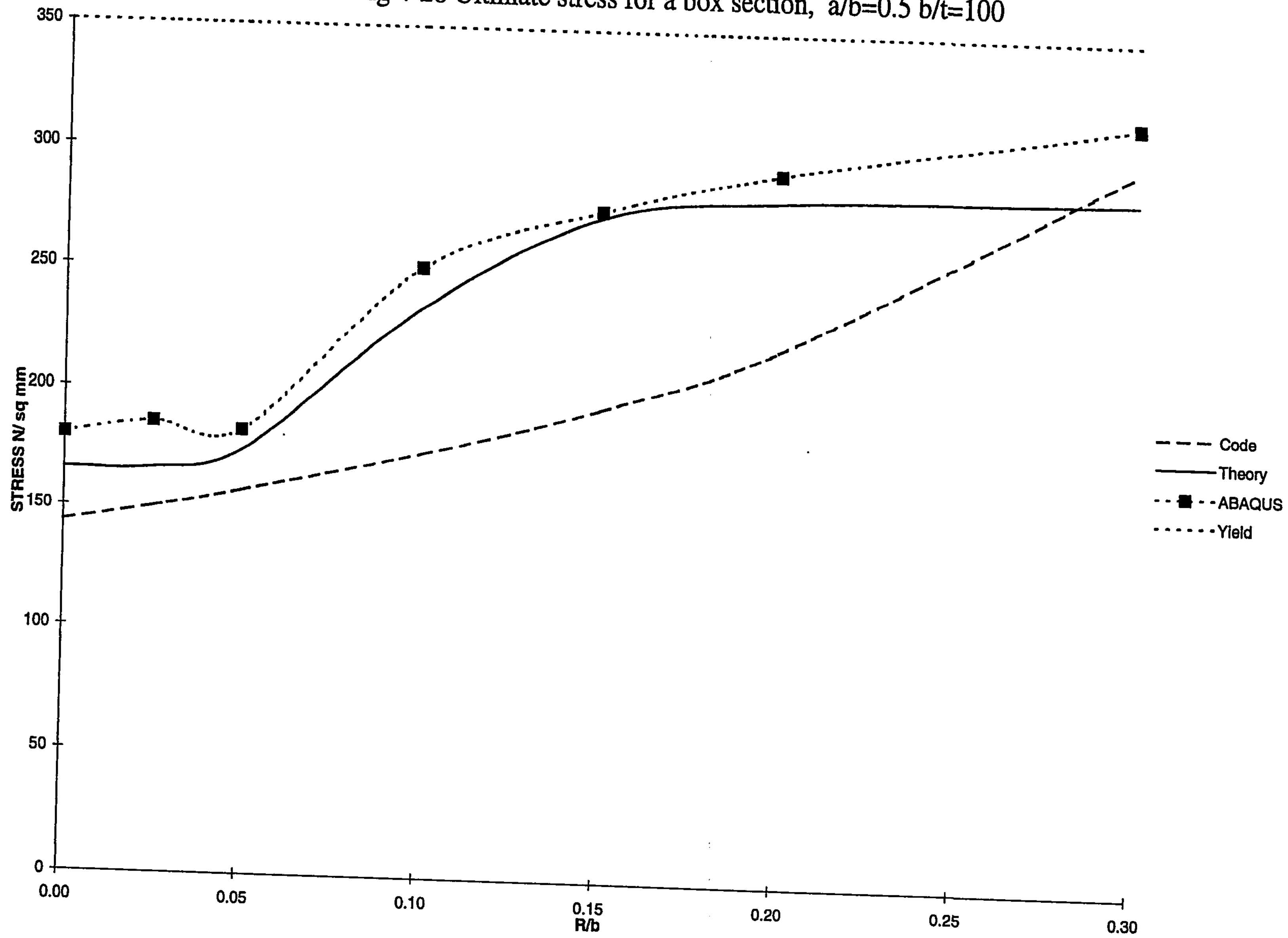

F4-28

Fig 4-29 Ultimate stress for a box section, a/b=0.5 b/t=200

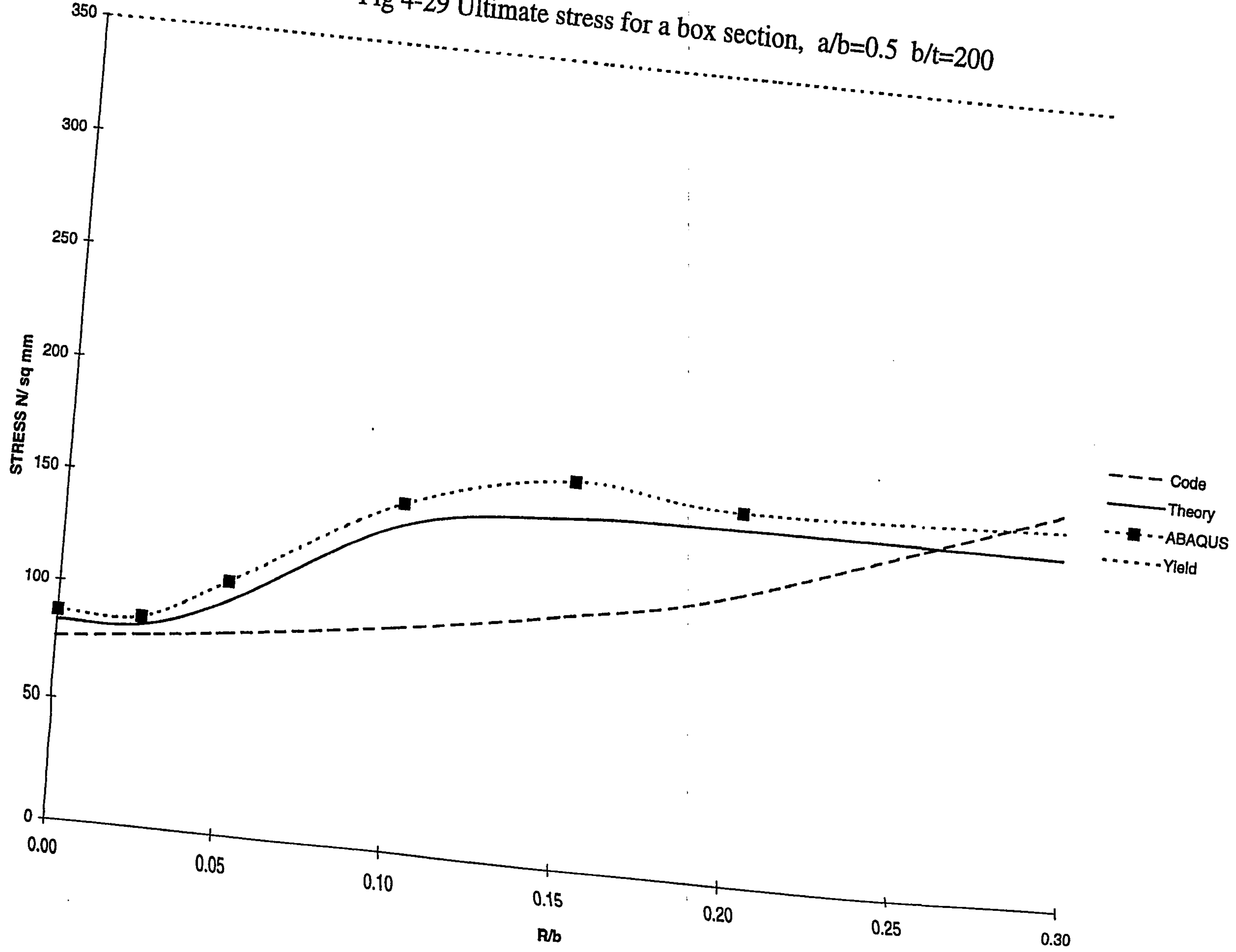

Fig 4-30 Ultimate stress for a box section, a/b=0.25 b/t=40

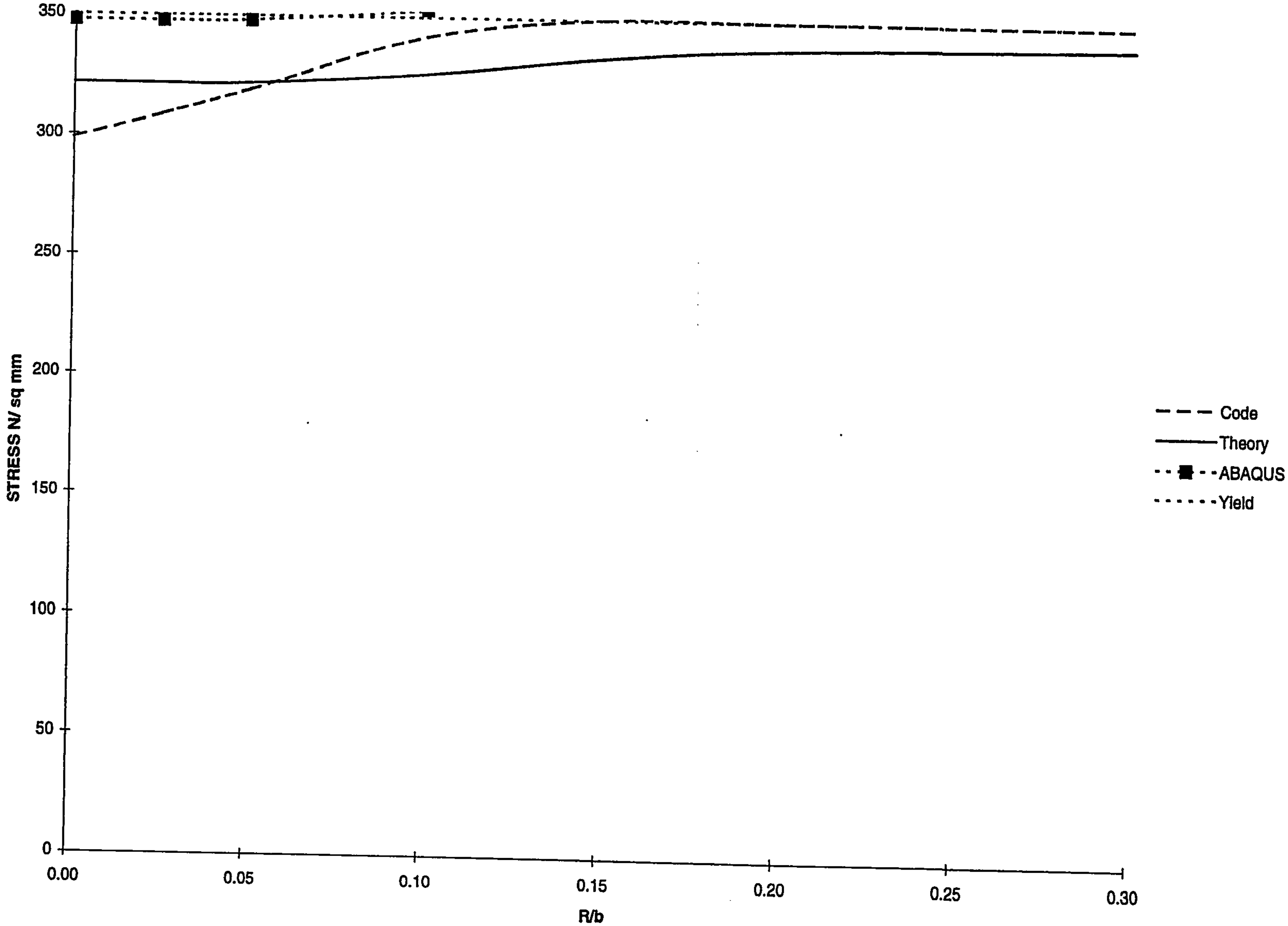

F4-30

Fig 4-31 Ultimate stress for a box section, a/b=0.25 b/t=50

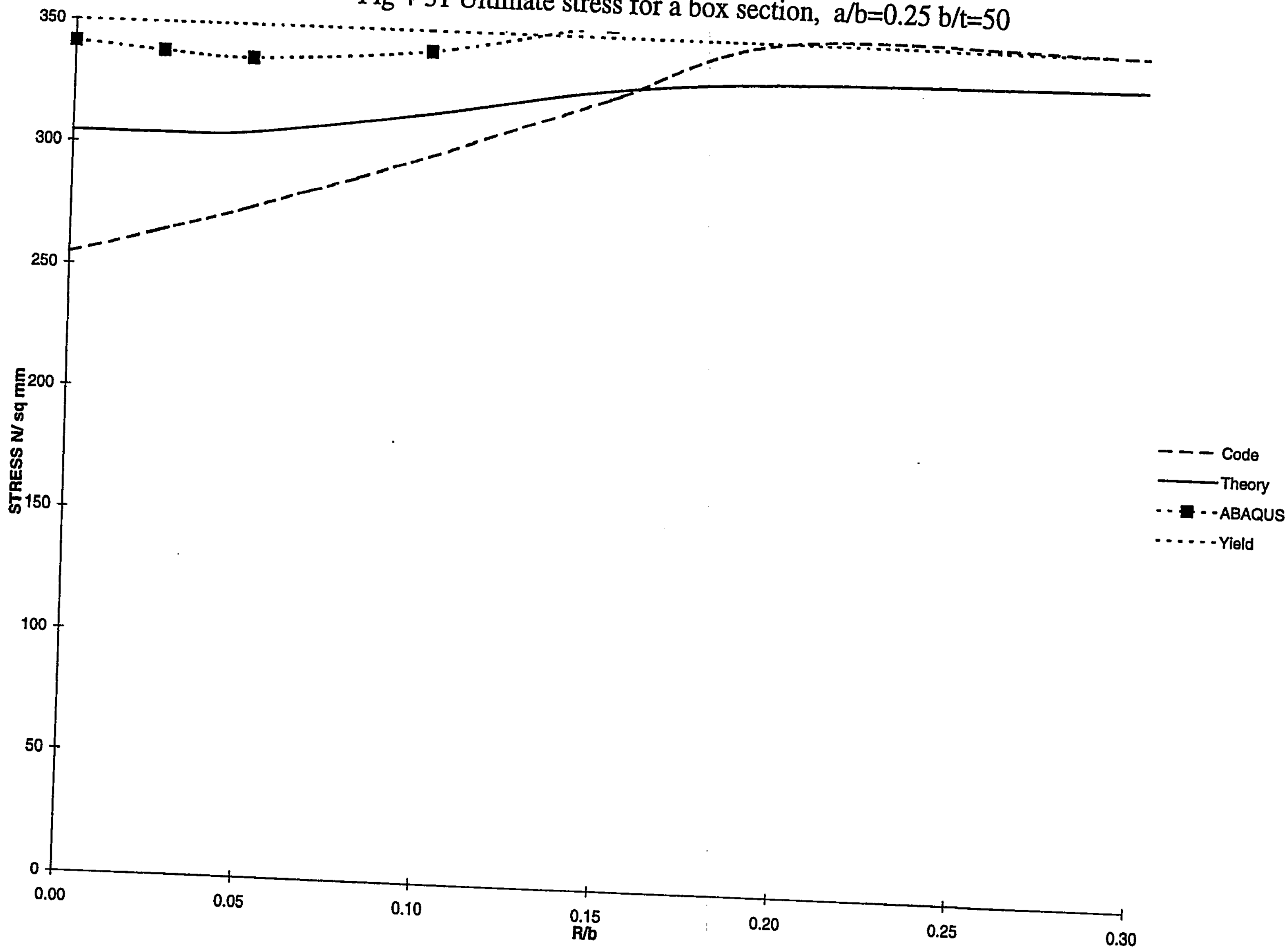

Fig 4-32 Ultimate stress for a box section, a/b=0.25 b/t=66

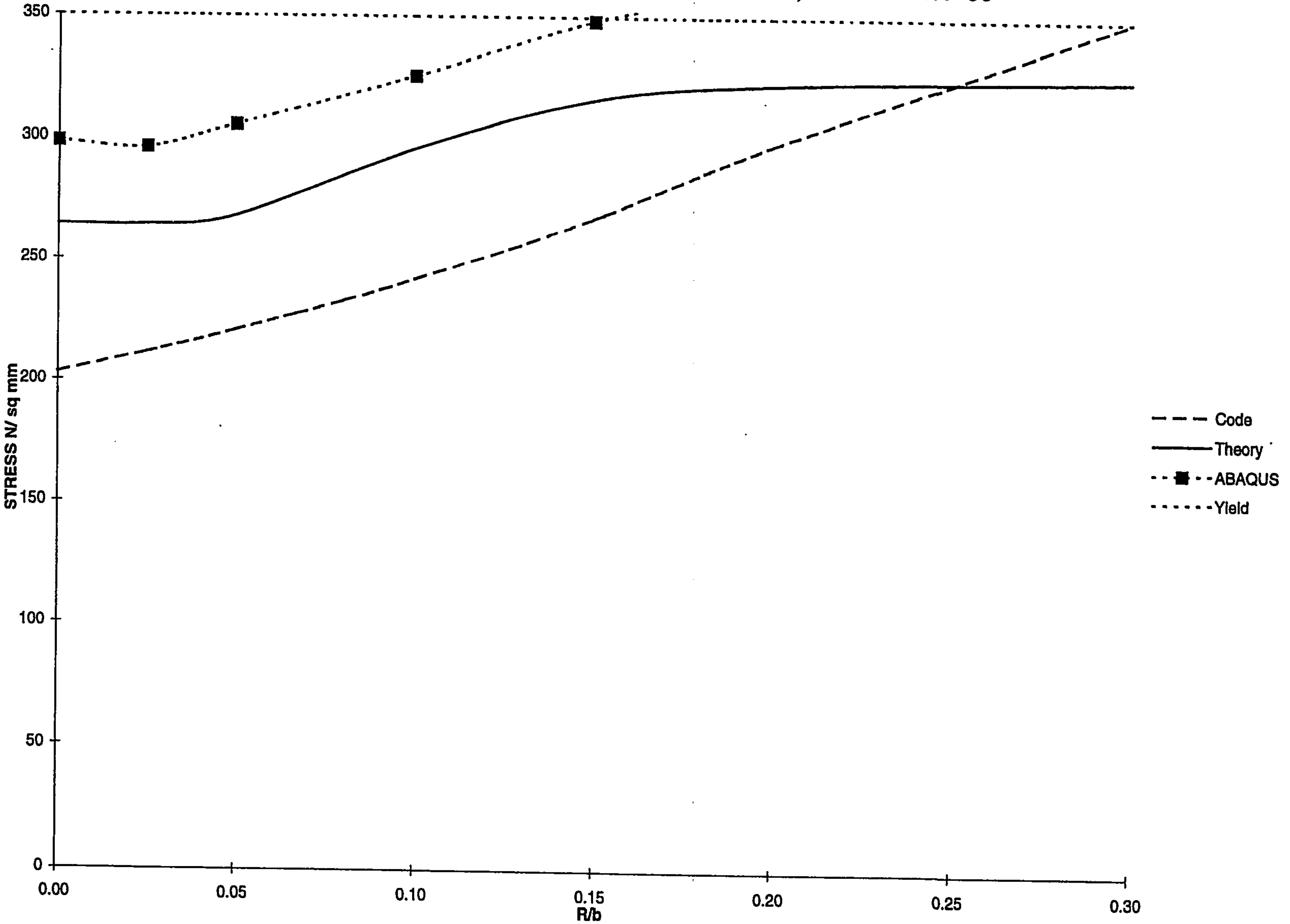

F4-32

Fig 4-33 Ultimate stress for a box section, a/b=0.25 b/t=100

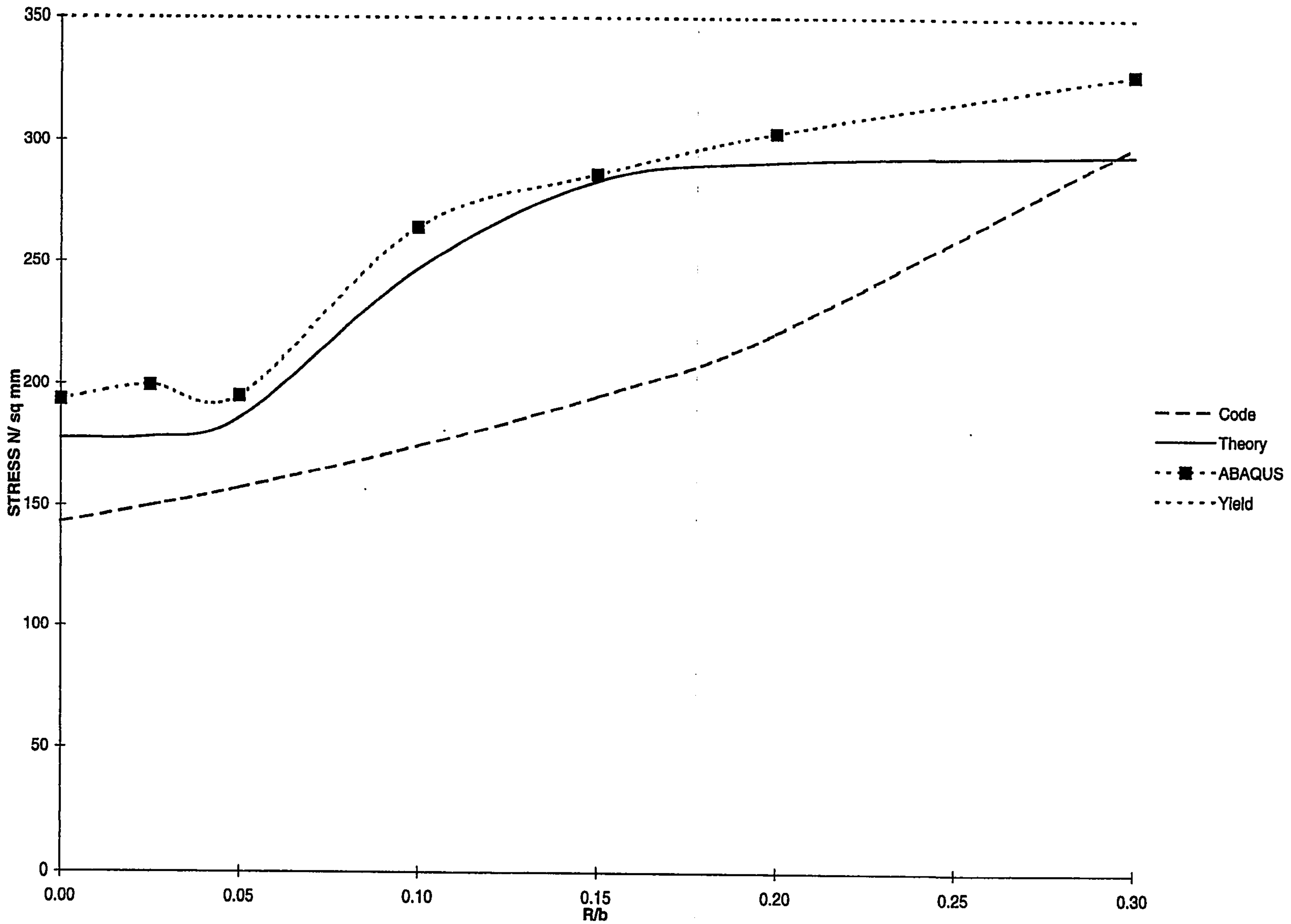

Fig 4-34 Ultimate stress for a box section, a/b=0.25 b/t=200

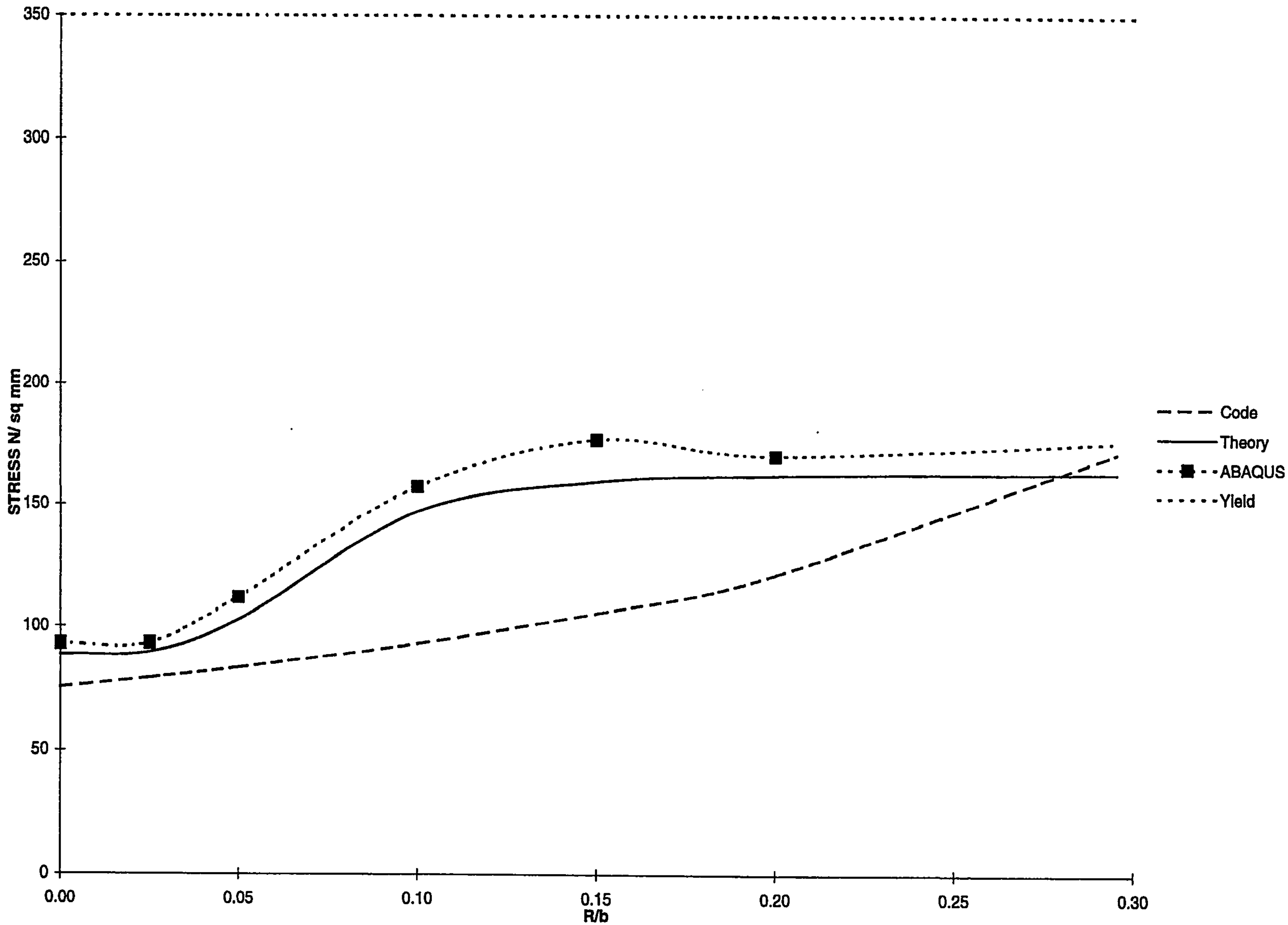

Fig 4-35 m factors for box sections (a/b=1)
(Theory)

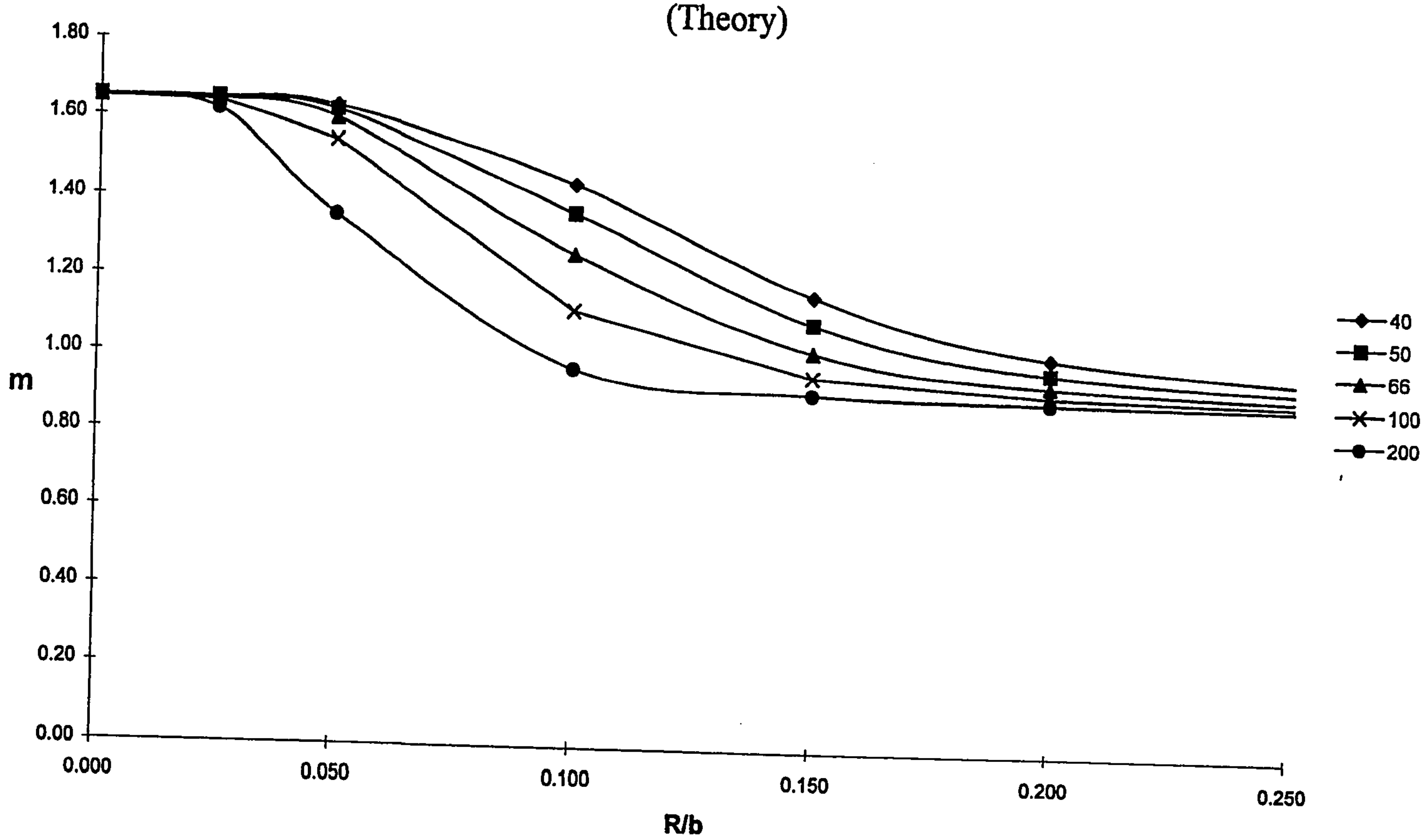

F4-35

Fig 4-36 m factors for box sections (a/b=0.5)
(Theory)

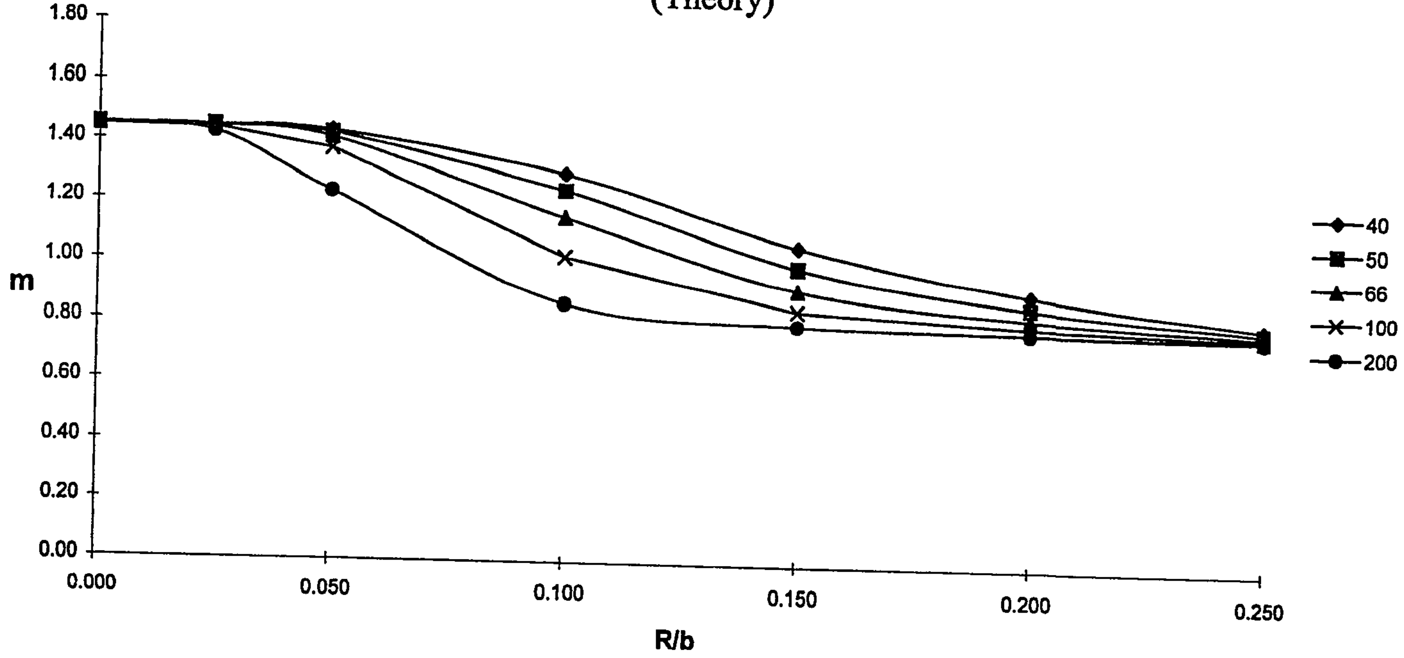

F4-36

Fig 4-37 m factors for box sections (a/b=0.25)
(Theory)

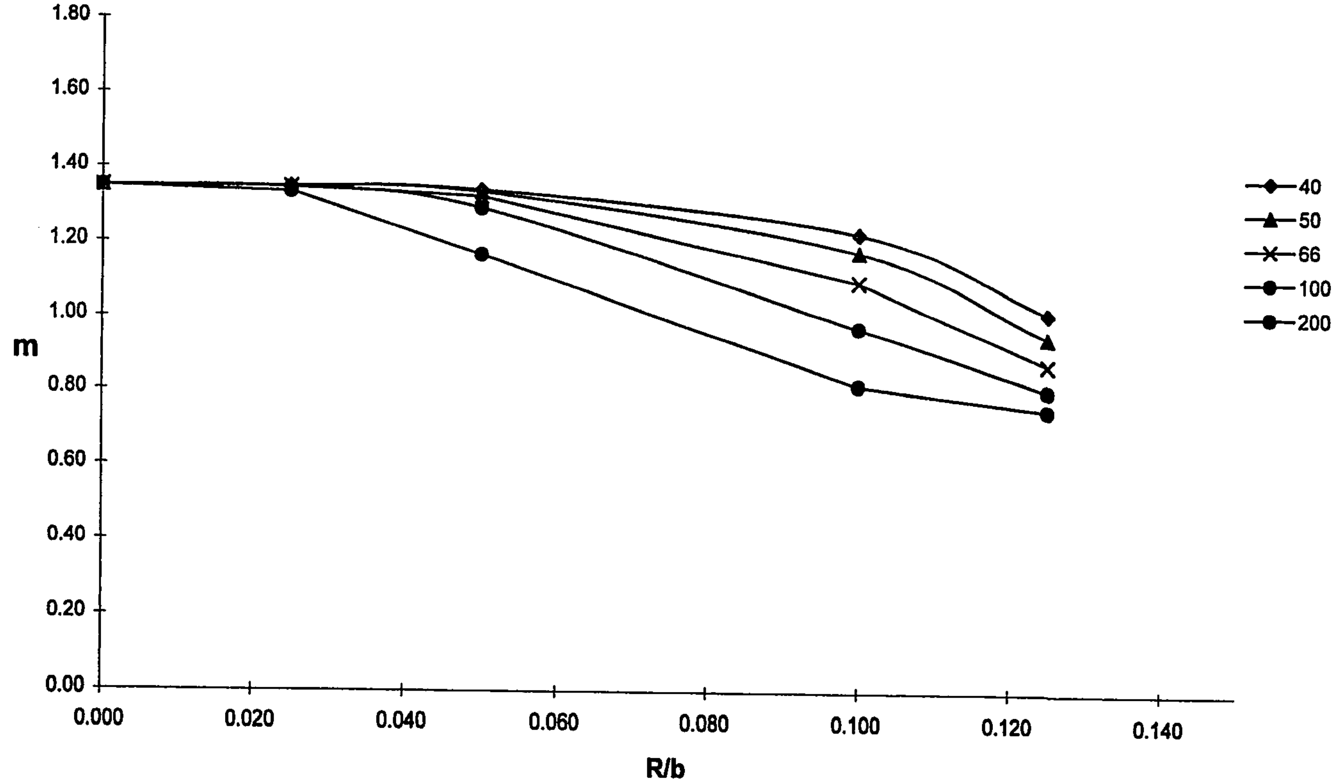

F4-37

Fig 4-38 Normalized m for box sections (a/b=1)

m=m / 1.65

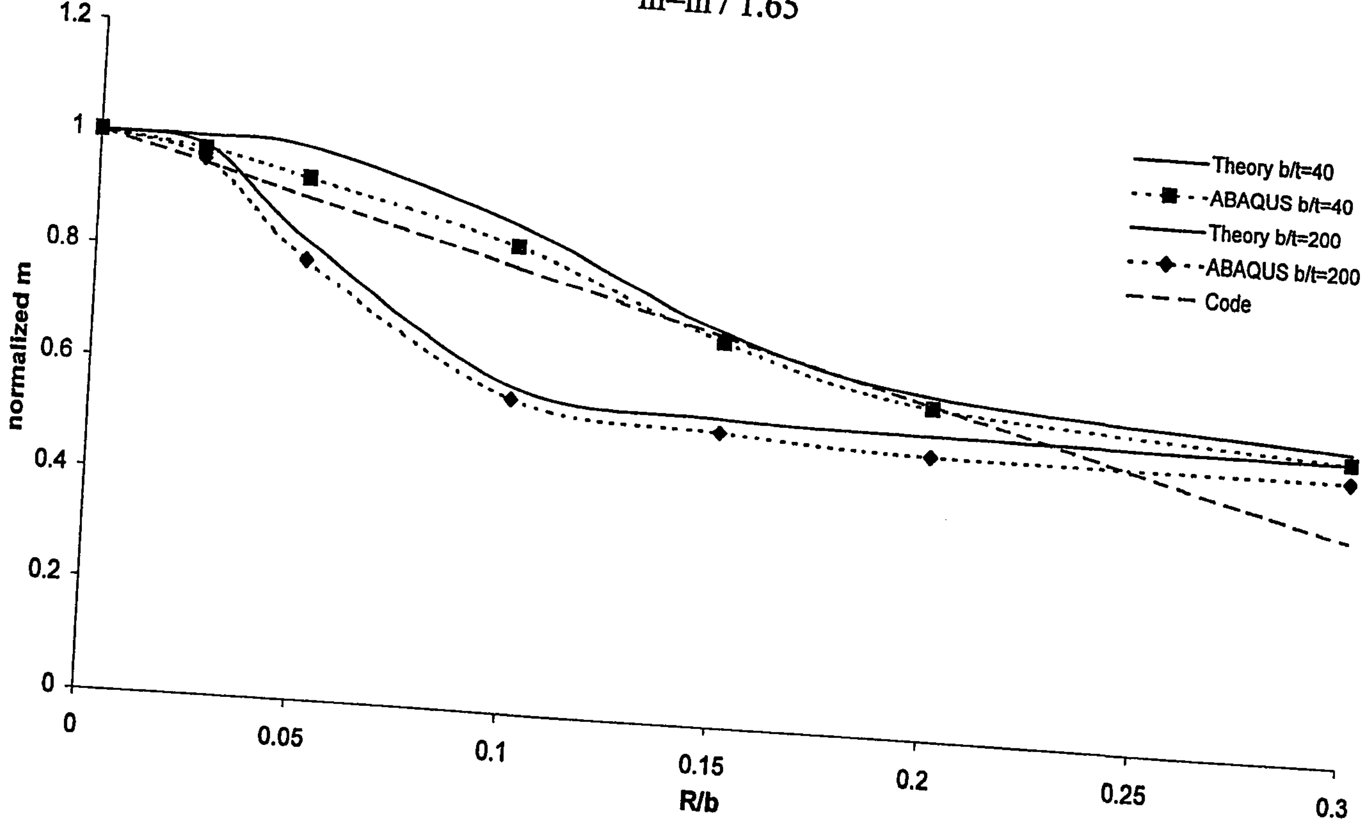

F4-38

Fig 4-39 Normalized m for box section (a/b=0.5)
m=m / 1.65

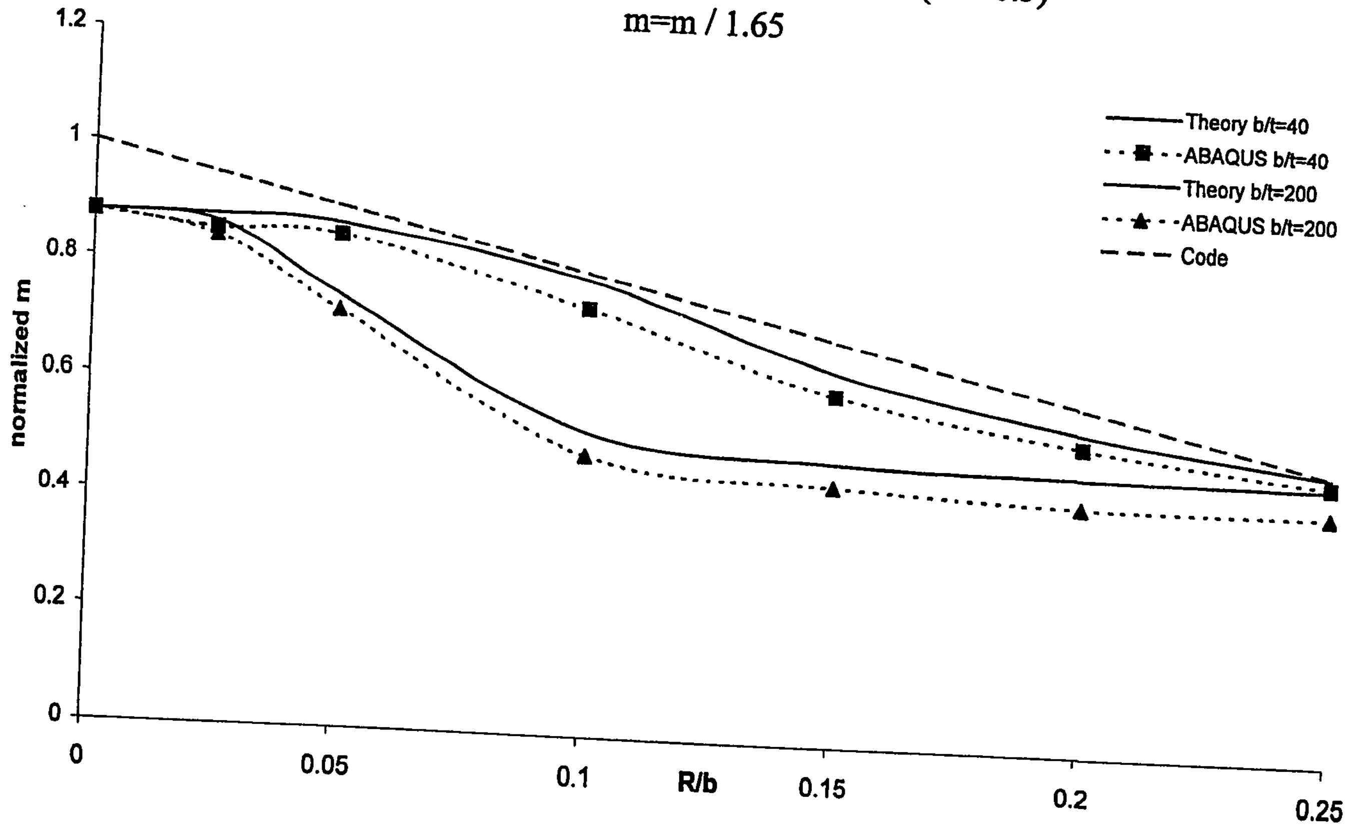

F4-39

Fig 4-40 Normalized m for box section (a/b=0.25)
m=m / 1.65

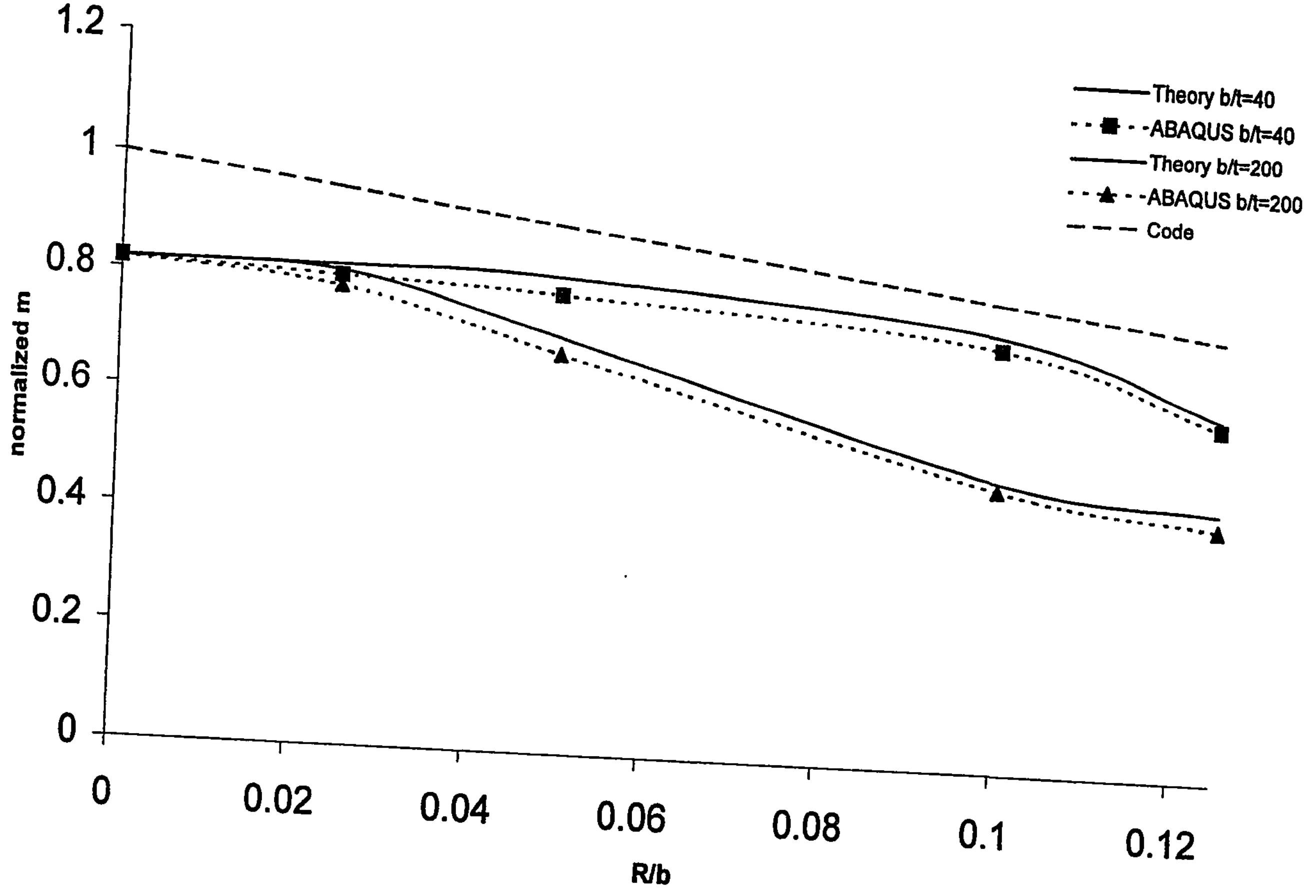

F4-40

Fig 4-41 Normalized mean postbuckling strength for box sections

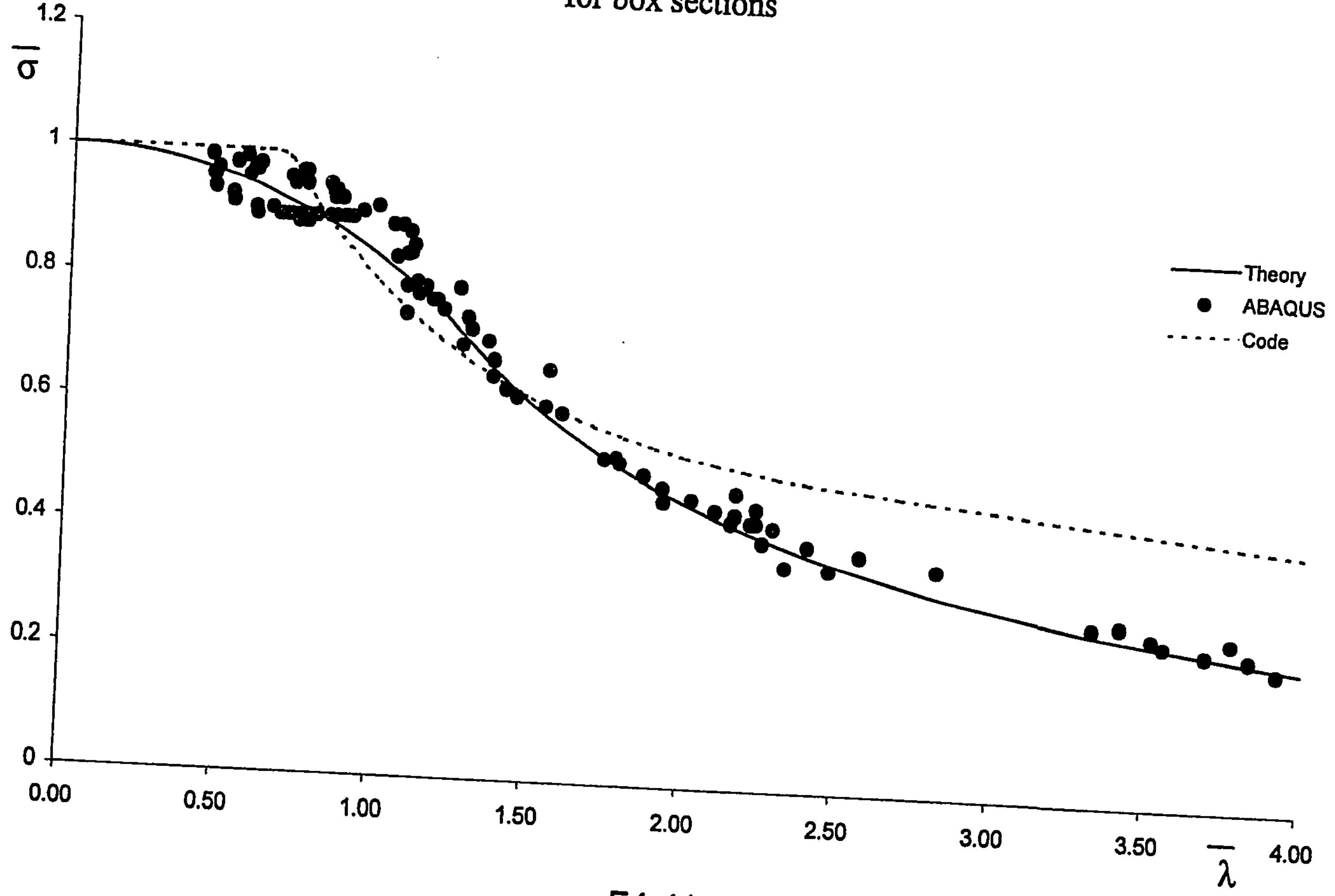

F4-41

Fig 4-42 Critical stress for a channel section, b/a=1 b/t=40

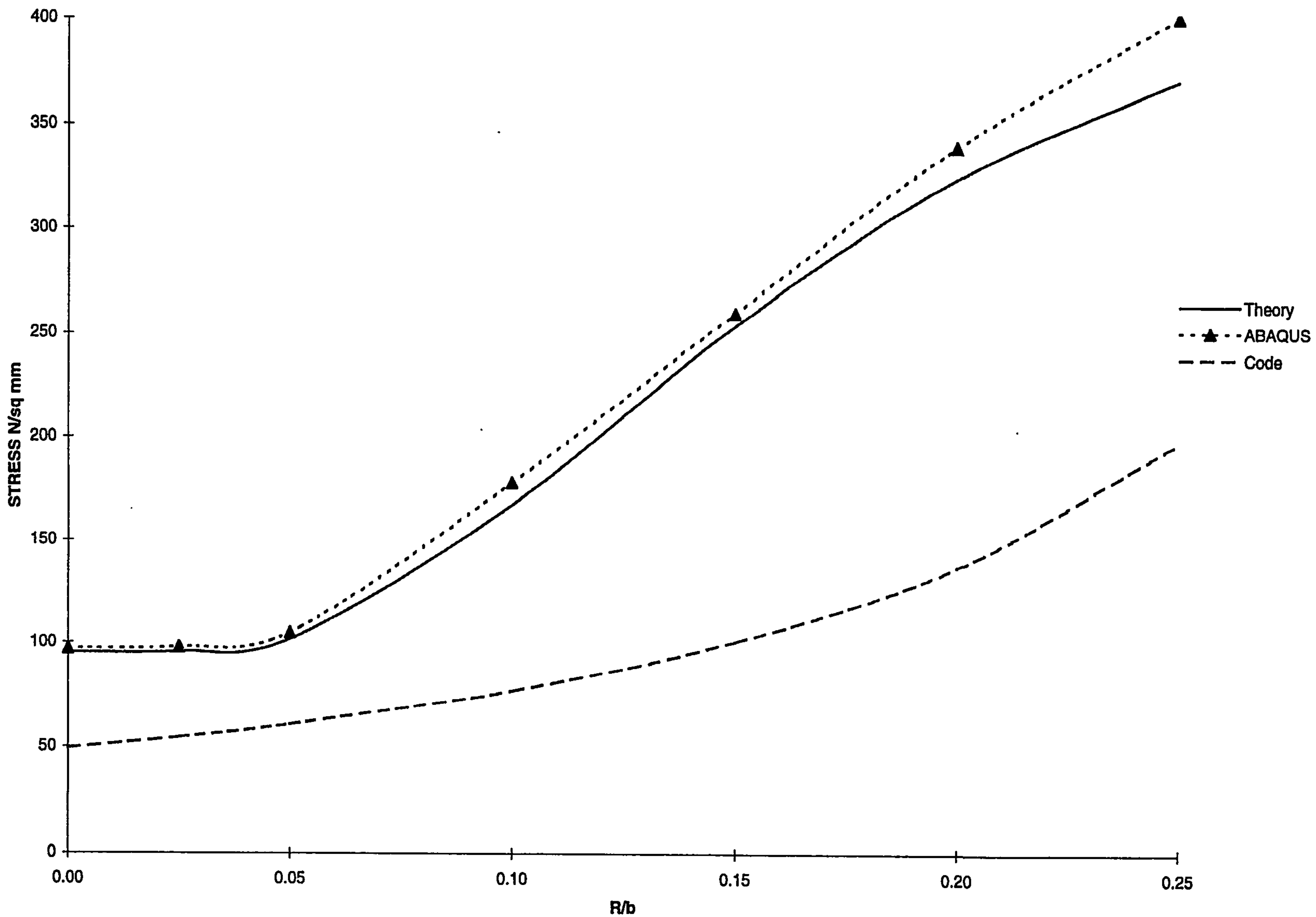

F4-42

Fig 4-43 Critical stress for a channel section, b/a=1 b/t=50

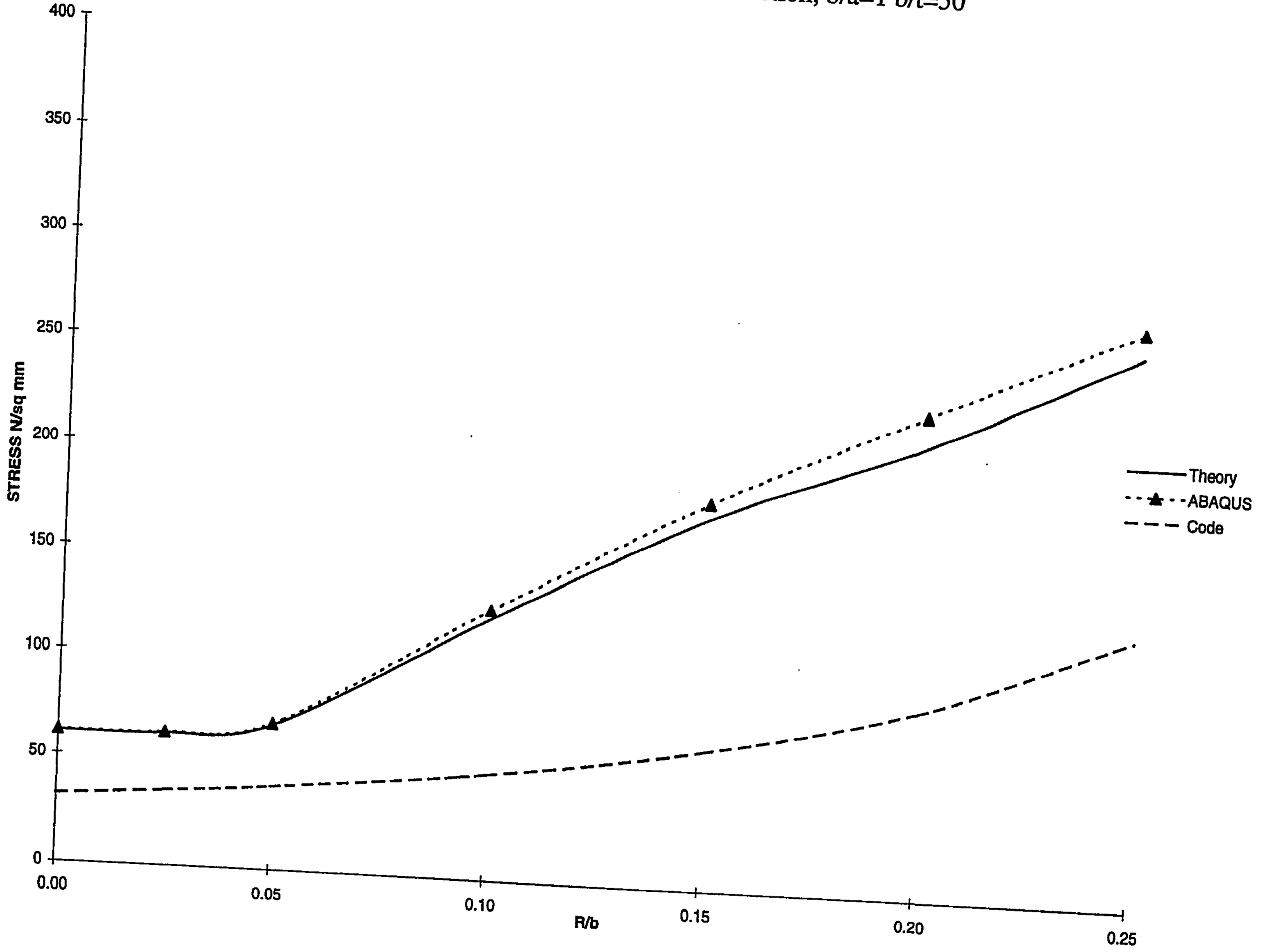

F4-43

Fig 4-44 Critical stress for a channel section, b/a=1 b/t=66

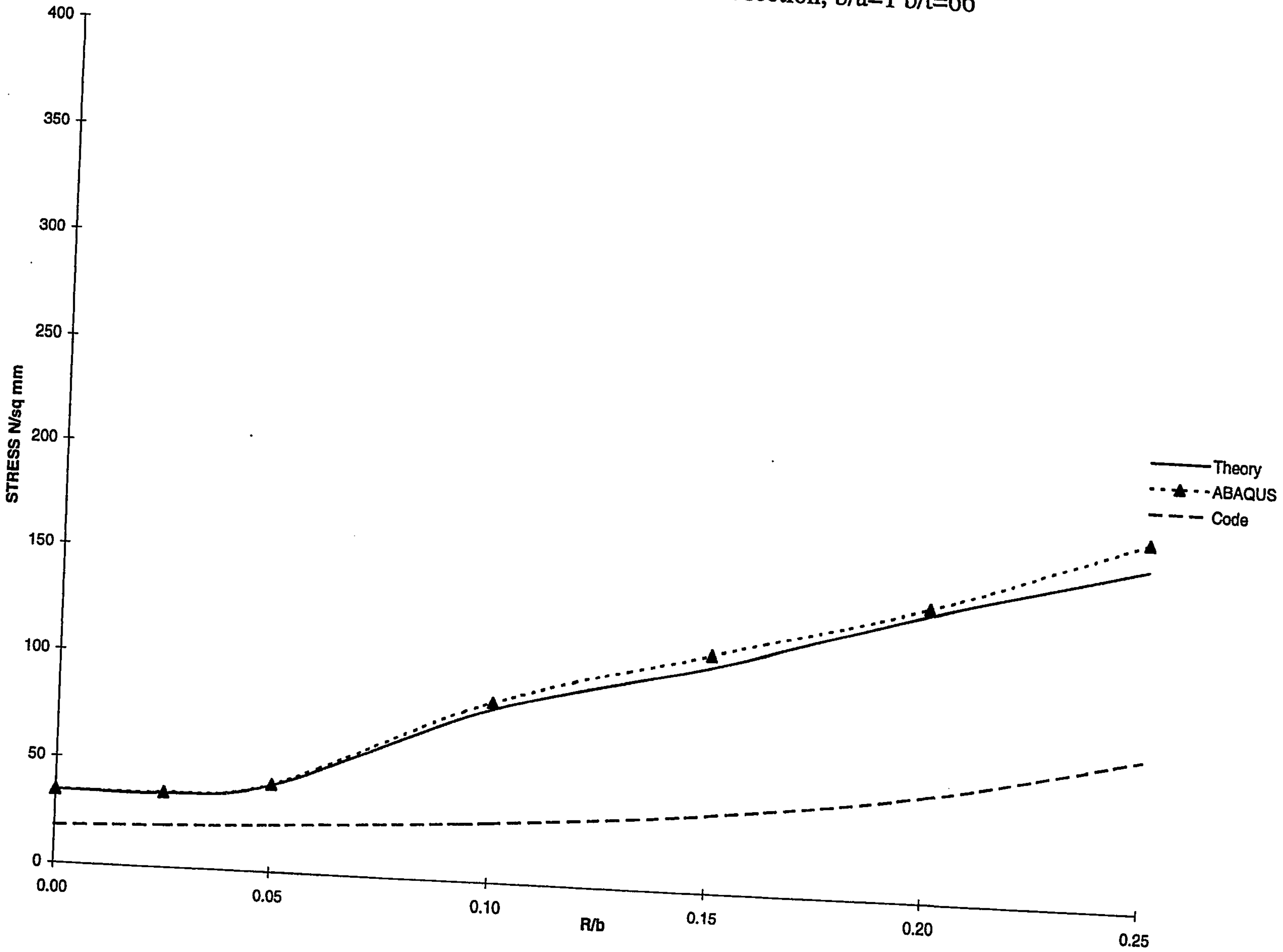

F4-44

Fig 4-45 Critical stress for a channel section, b/a=1 b/t=100

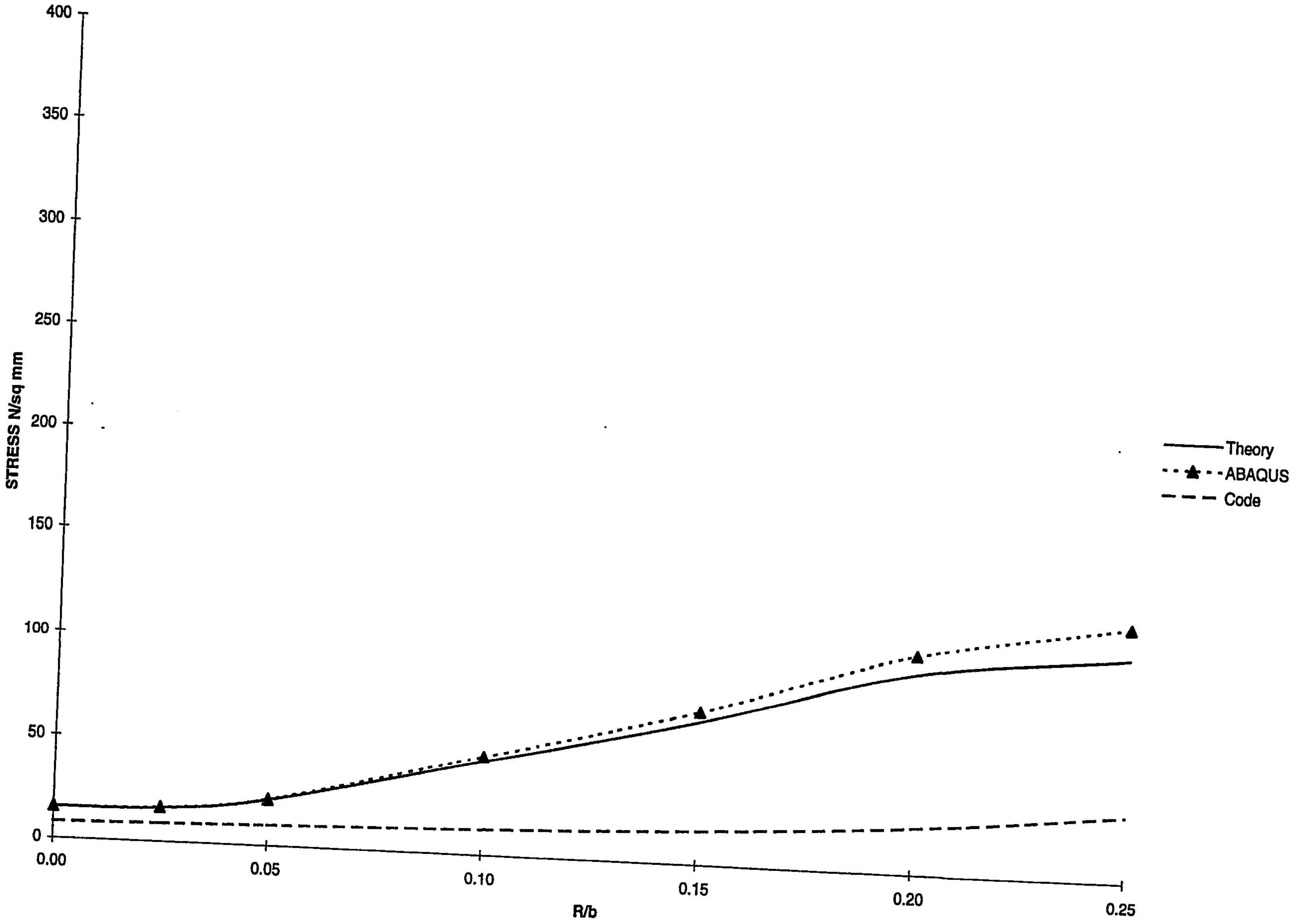

F4-45

Fig 4-46 Critical stress for a channel section, a/b=1 b/t=200

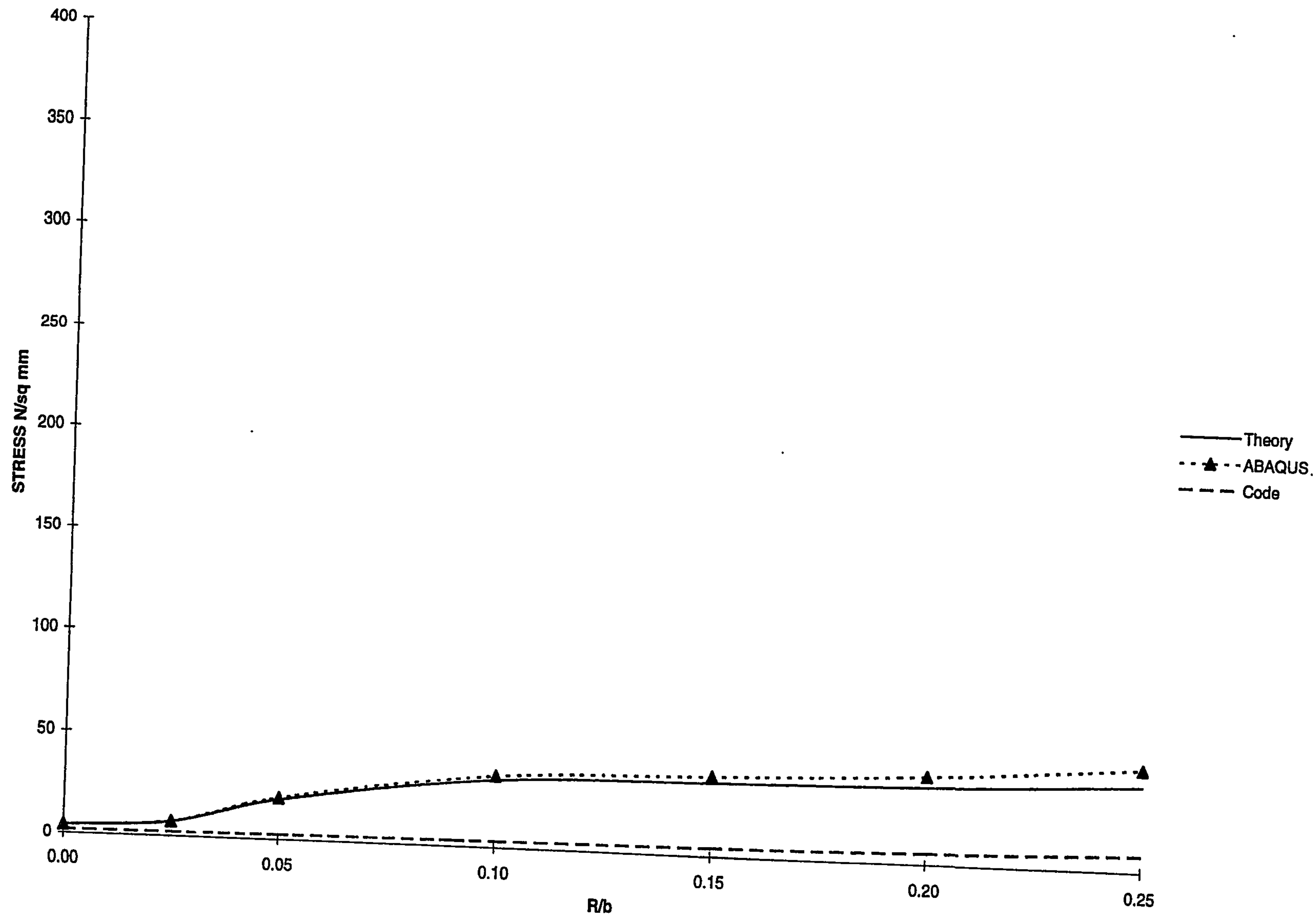

F4-46

Fig 4-47 Critical stress for a channel section, b/a=0.5 b/t=40

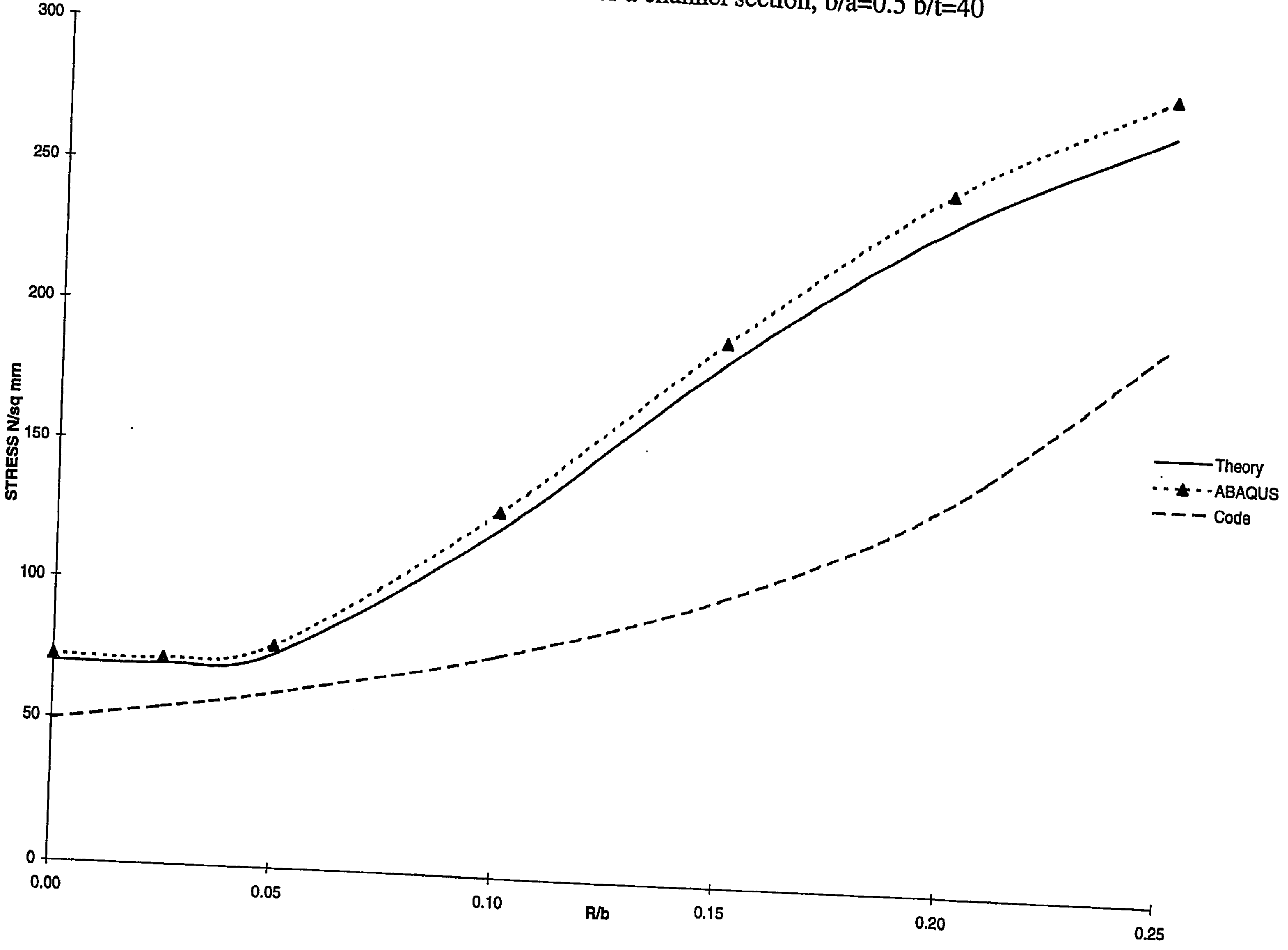

F4-47

Fig 4-48 Critical stress for a channel section, b/a=0.5 b/t=50

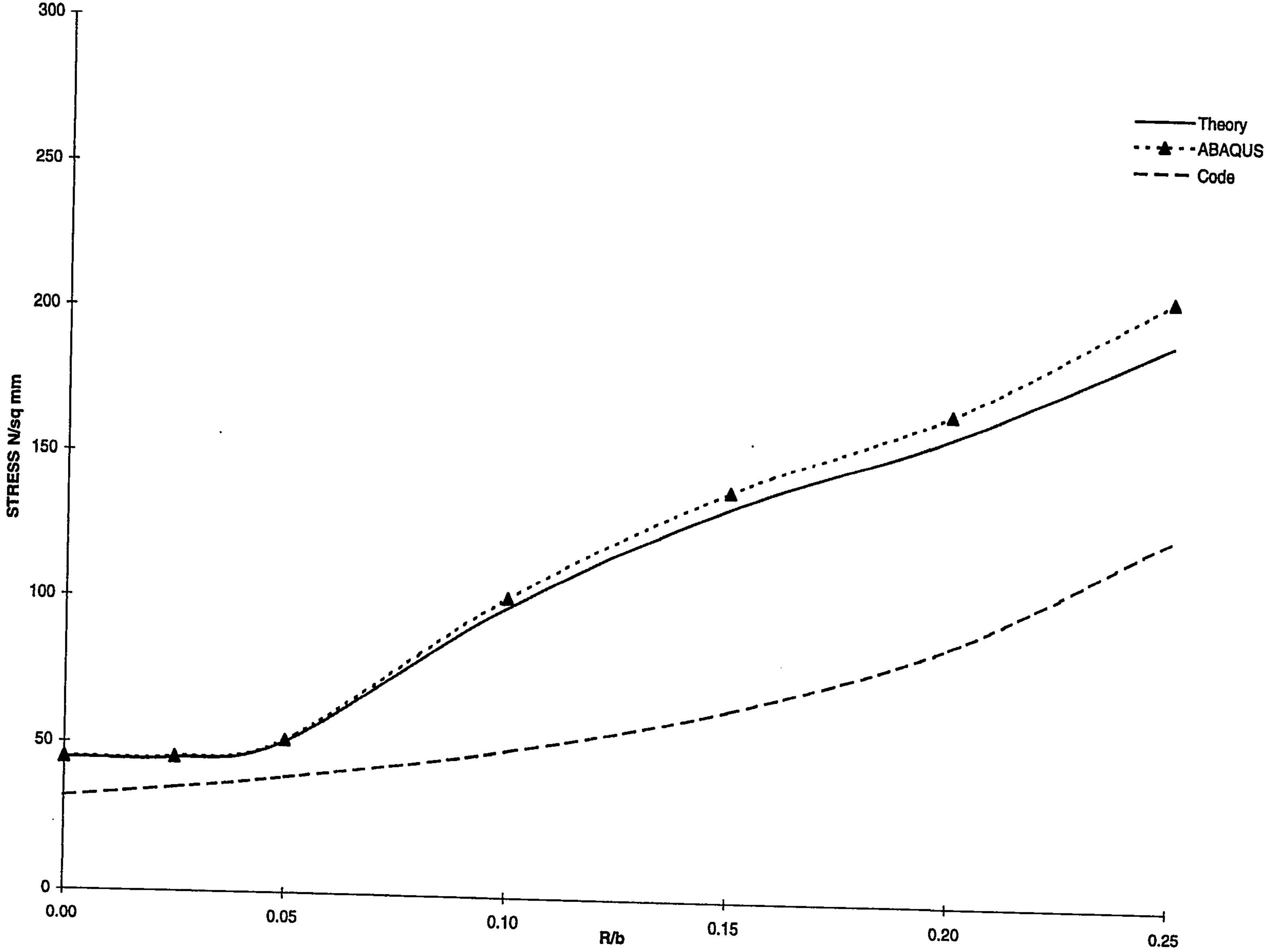

F4-48

Fig 4-49 Critical stress for a cannel section, b/a=0.5 b/t=66

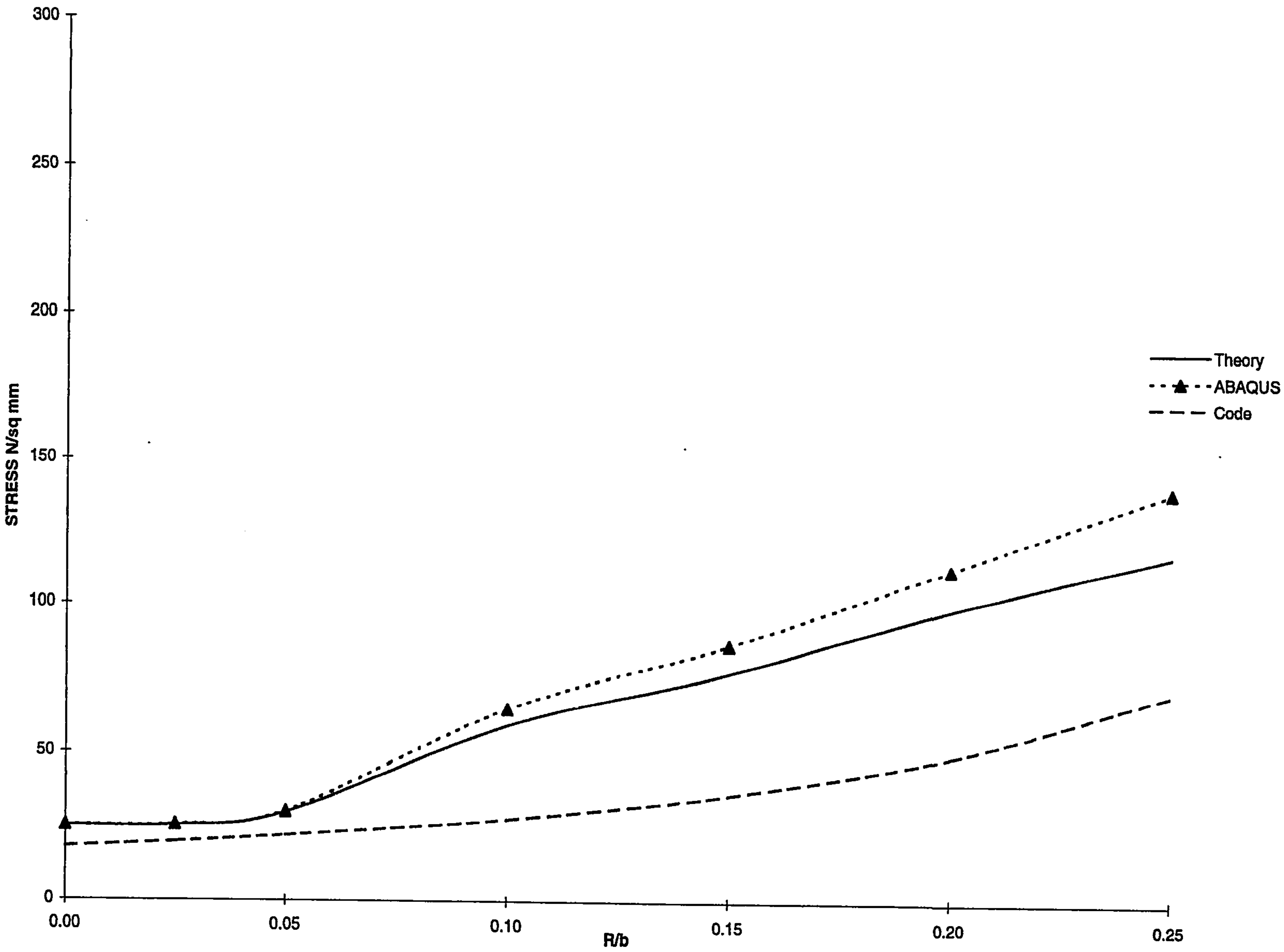

F4-49

Fig 4-50 Critical stress for a channel section, b/a=0.5 b/t=100

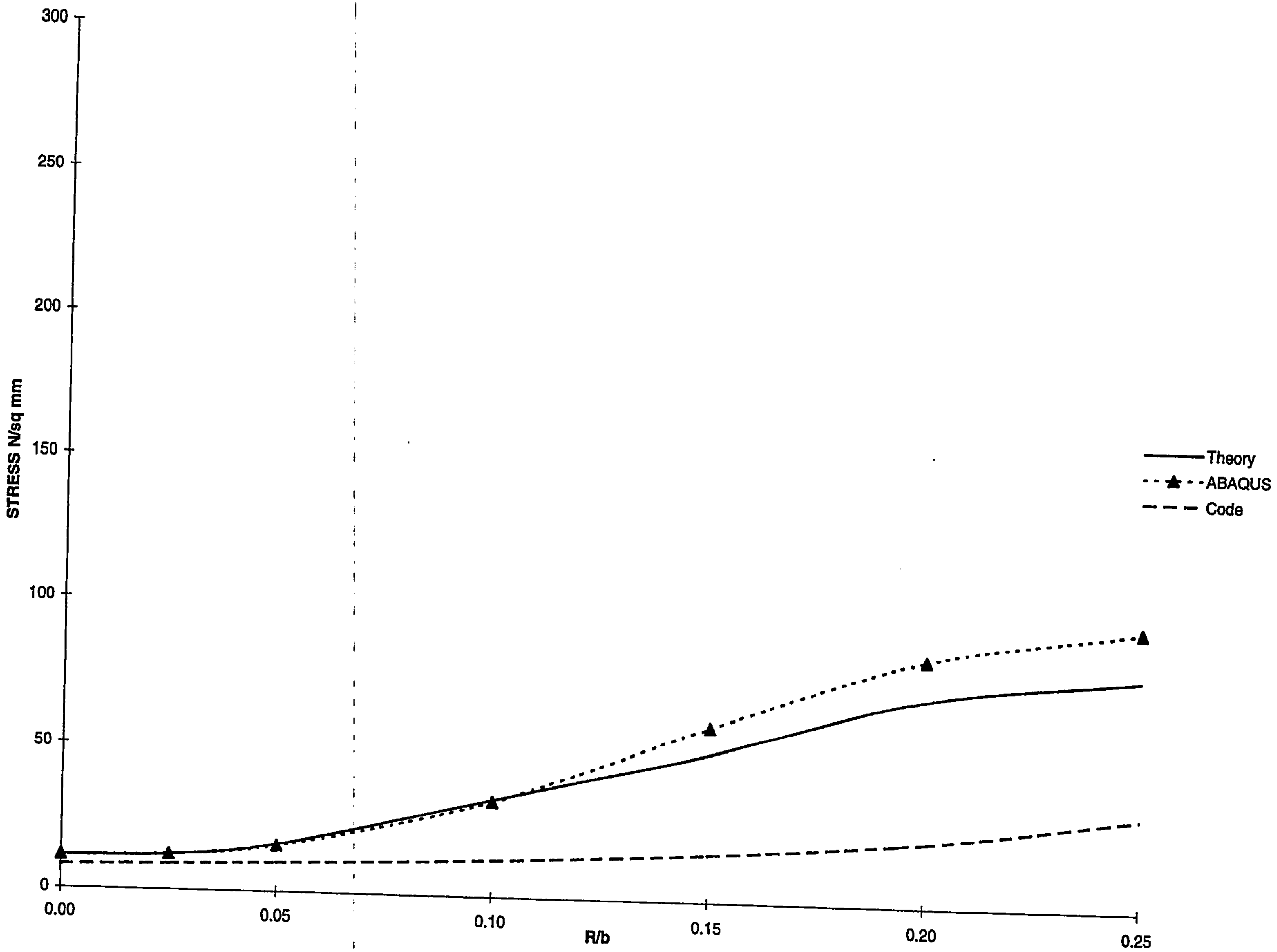

F4-50

Fig 4-51 Critical stress for a channel section, b/a=0.5 b/t=200

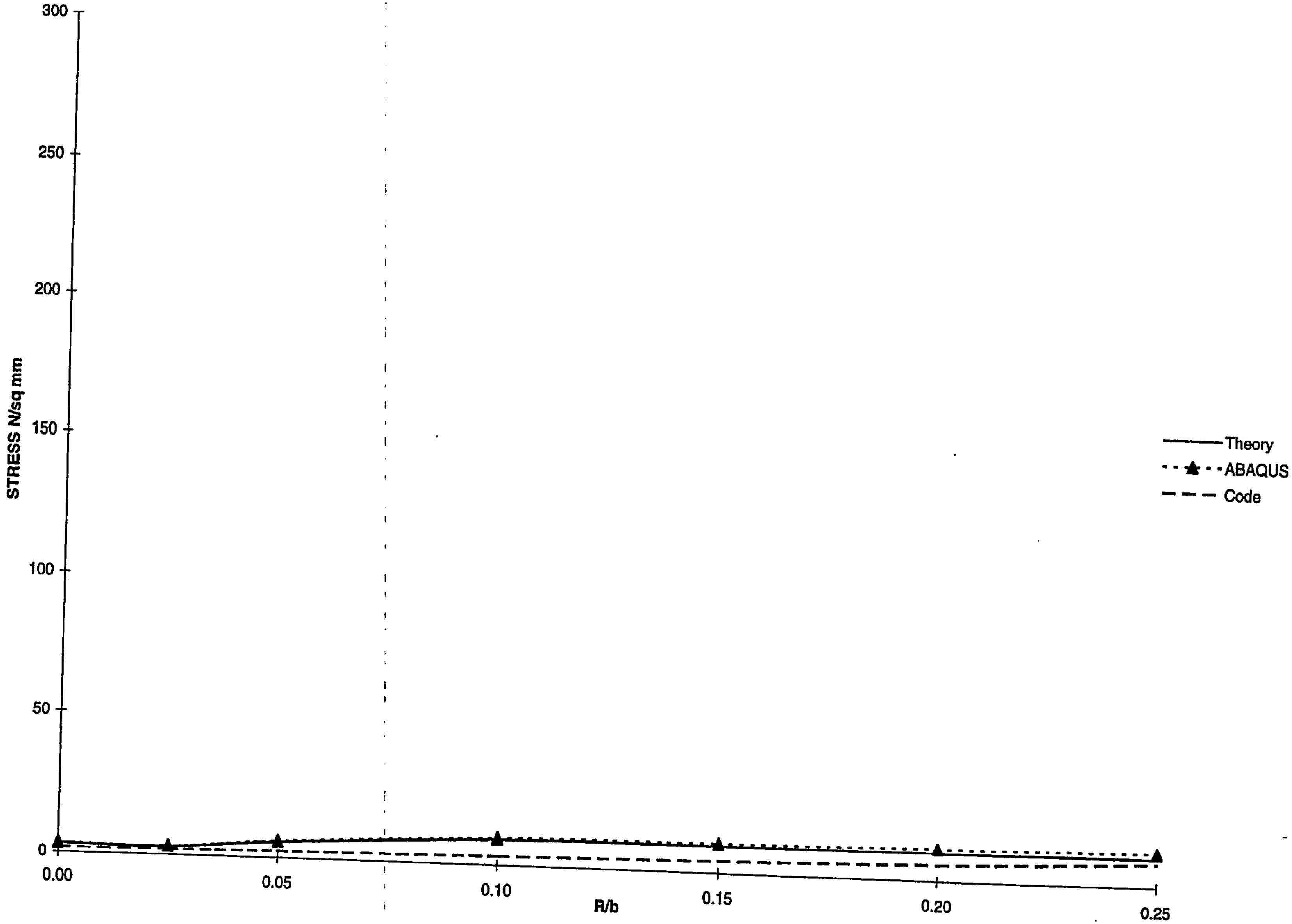

F4-51

Fig 4-52 Critical stress for a channel section, b/a=0.25 b/t=40

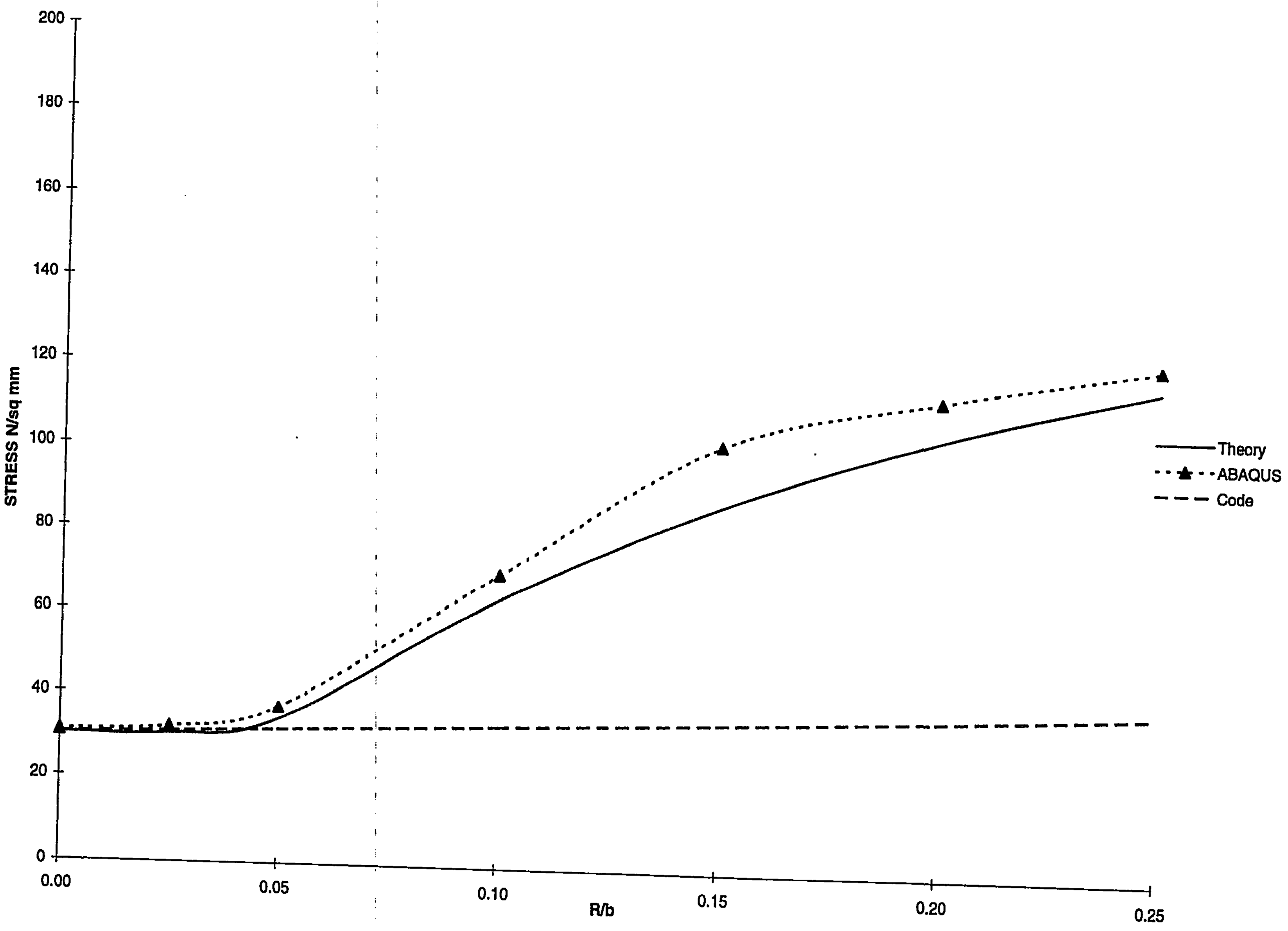

F4-52

Fig 4-53 Critical stress for a channel section, b/a=0.25 b/t=50

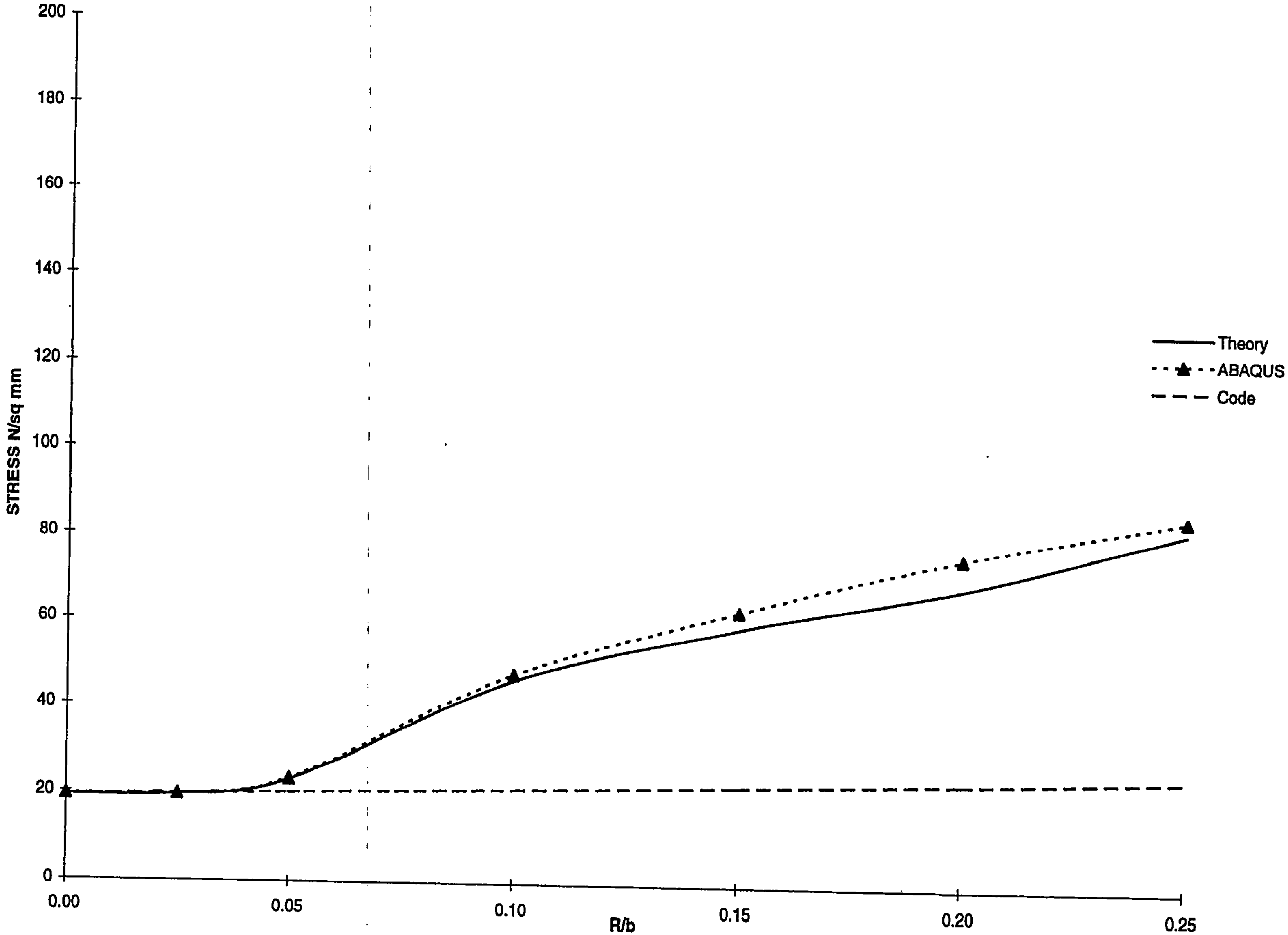

F4-53

Fig 4-54 Critical stress for a channel section, b/a=0.25 b/t=66

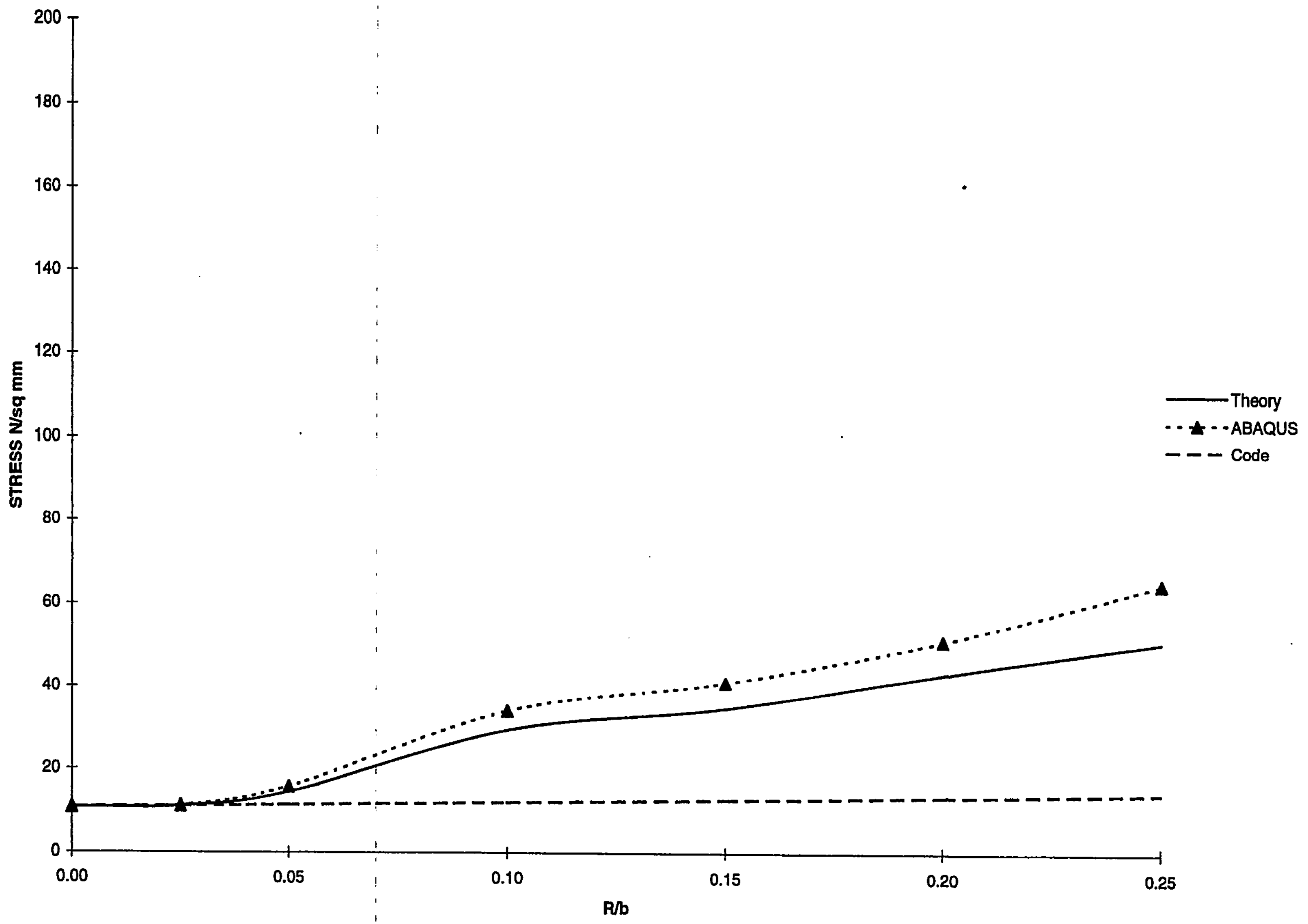

F4-54

Fig 4-55 Critical stress for a channel section, b/a=0.25 b/t=100

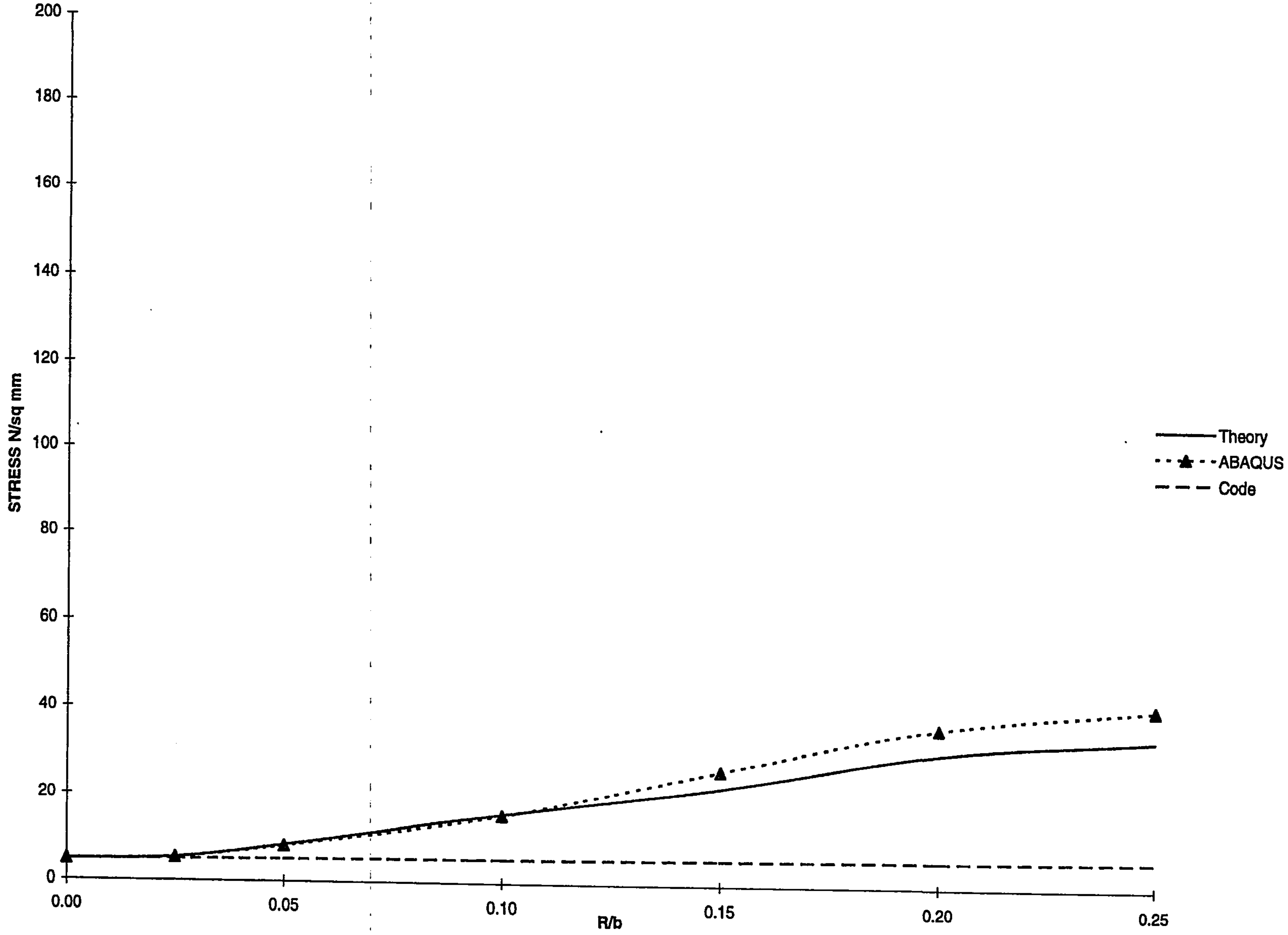

F4-55

Fig 4-56 Critical stress for a channel section, b/a=0.25 b/t=200

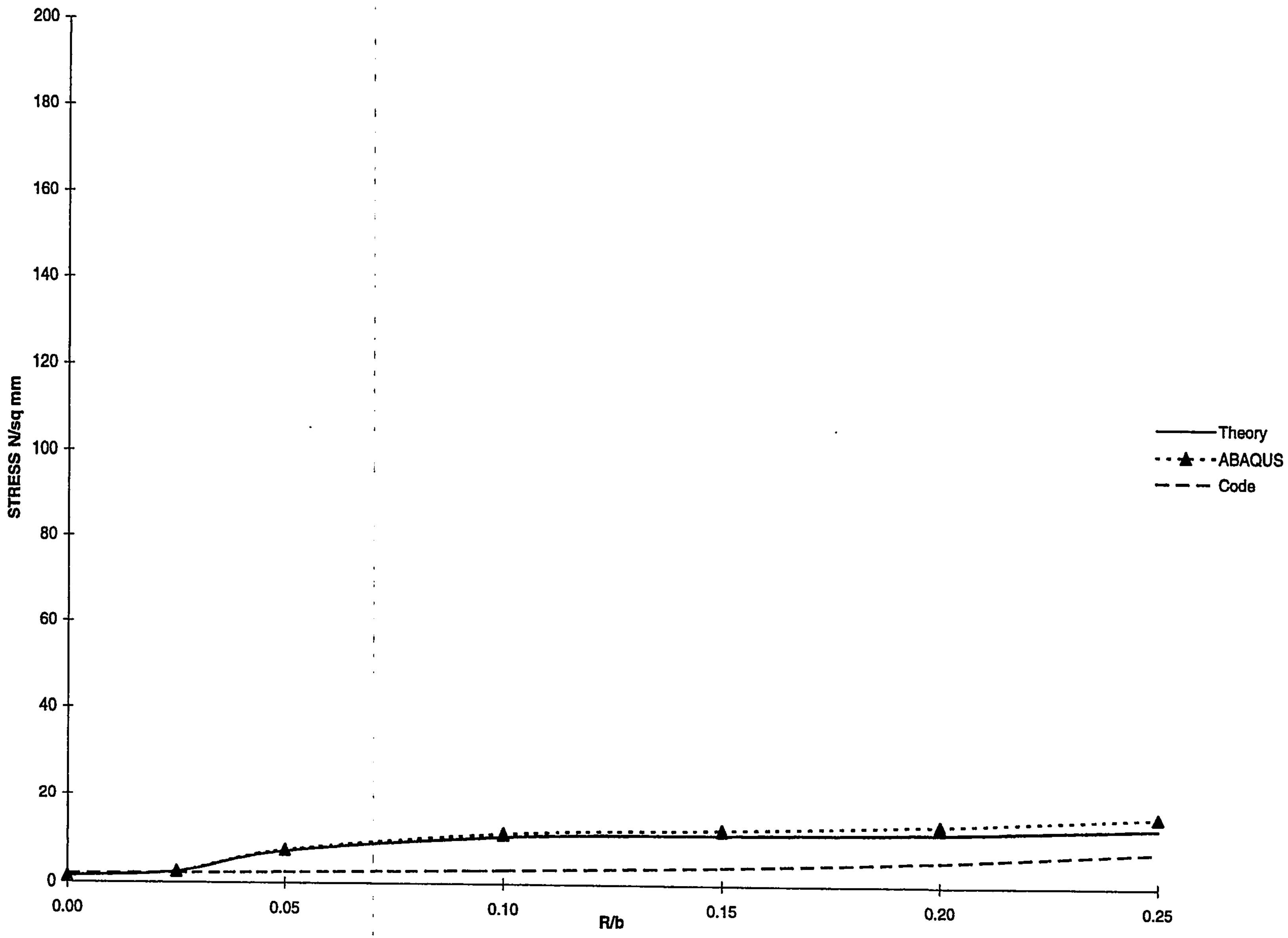

F4-56

Fig 4-57 m factors for a channel sections, a/b=1
(Theory)

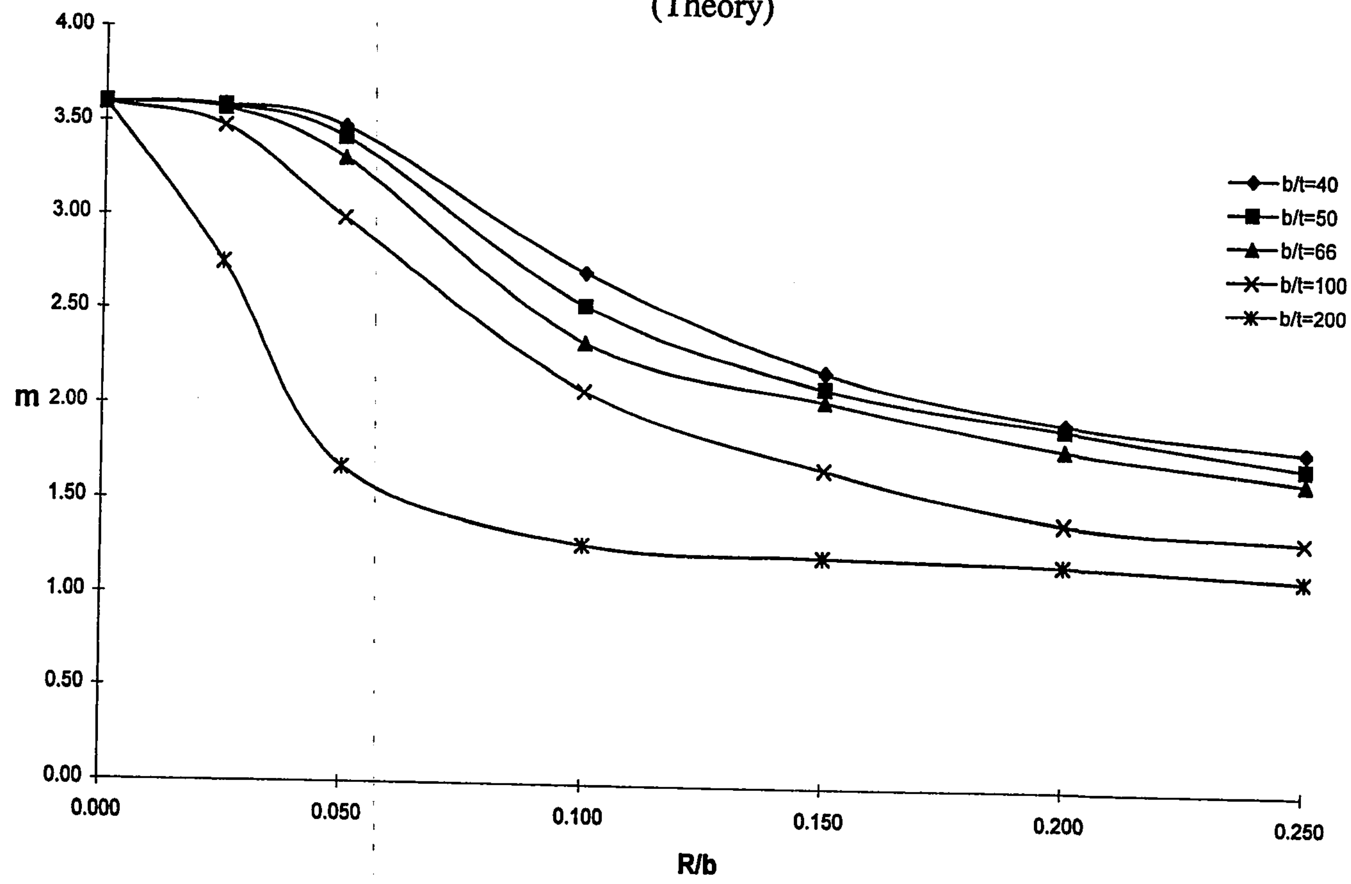

F4-57

Fig 4-58 m factors for a channel sections, b/a=0.5
(Theory)

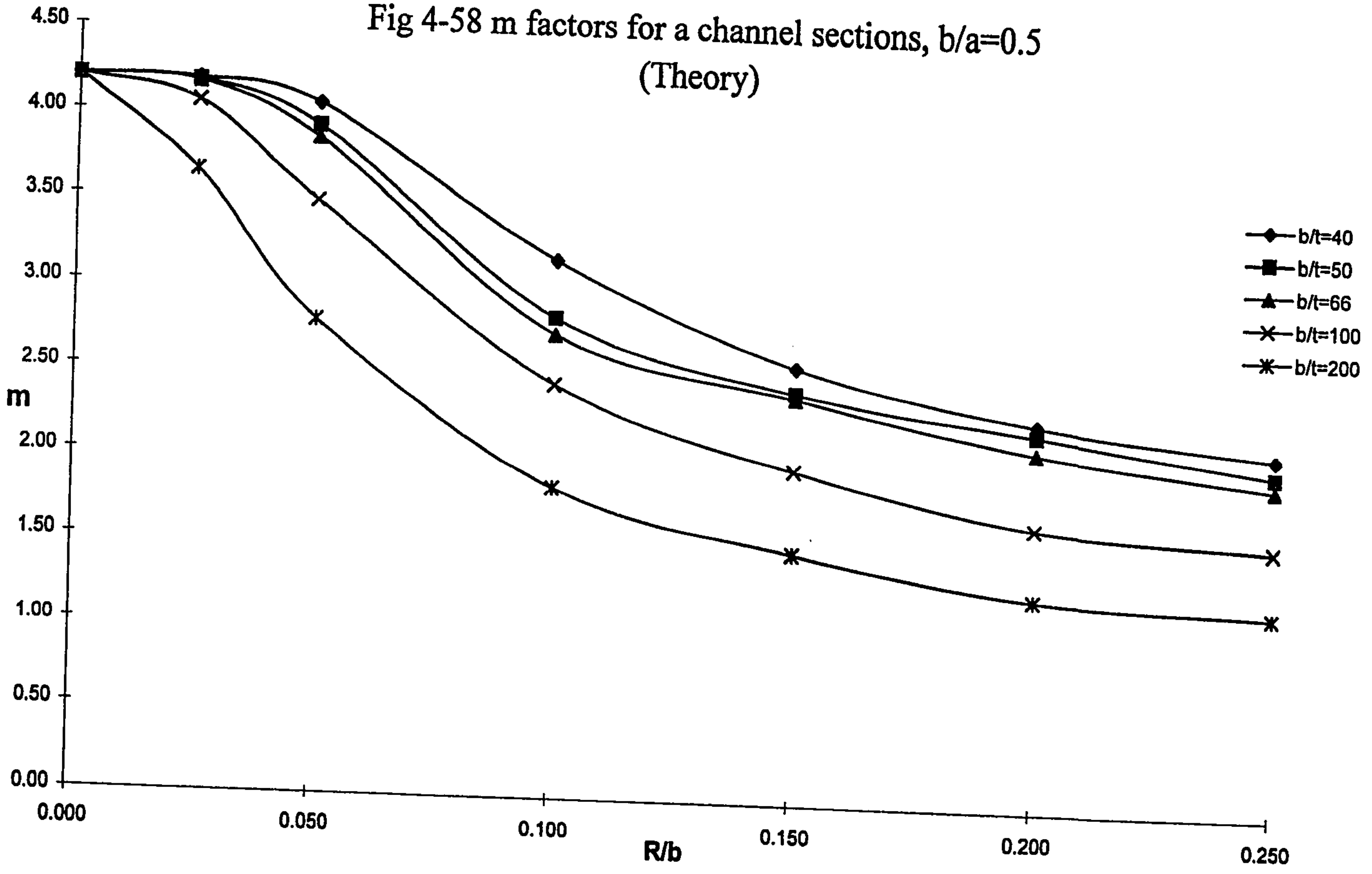

F4-58

Fig 4-59 m factors for a channel sections, b/a=0.25
(Theory)

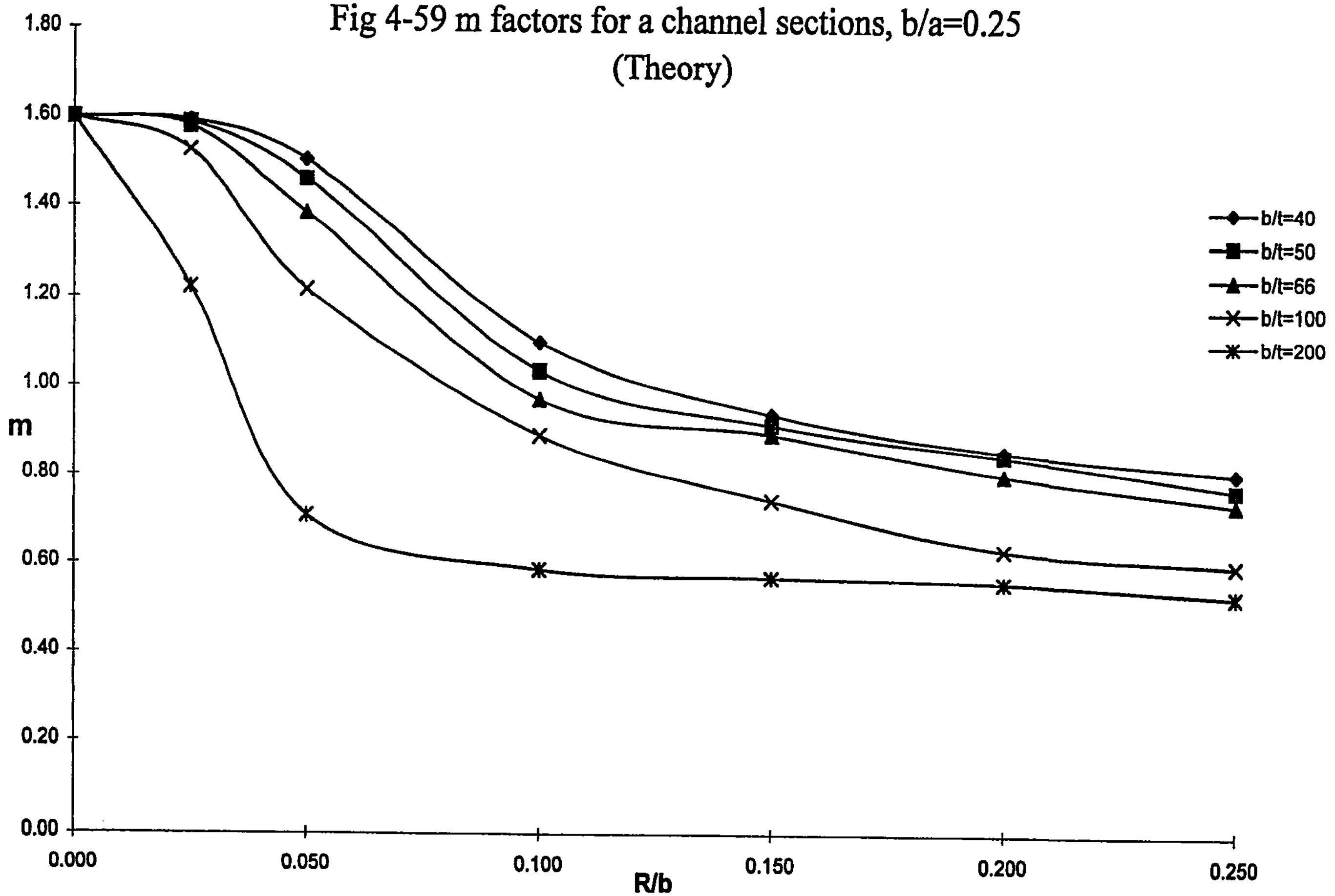

F4-59

Fig 4-60 Normalized m for channel sections, (a/b=1)

m=m / 5

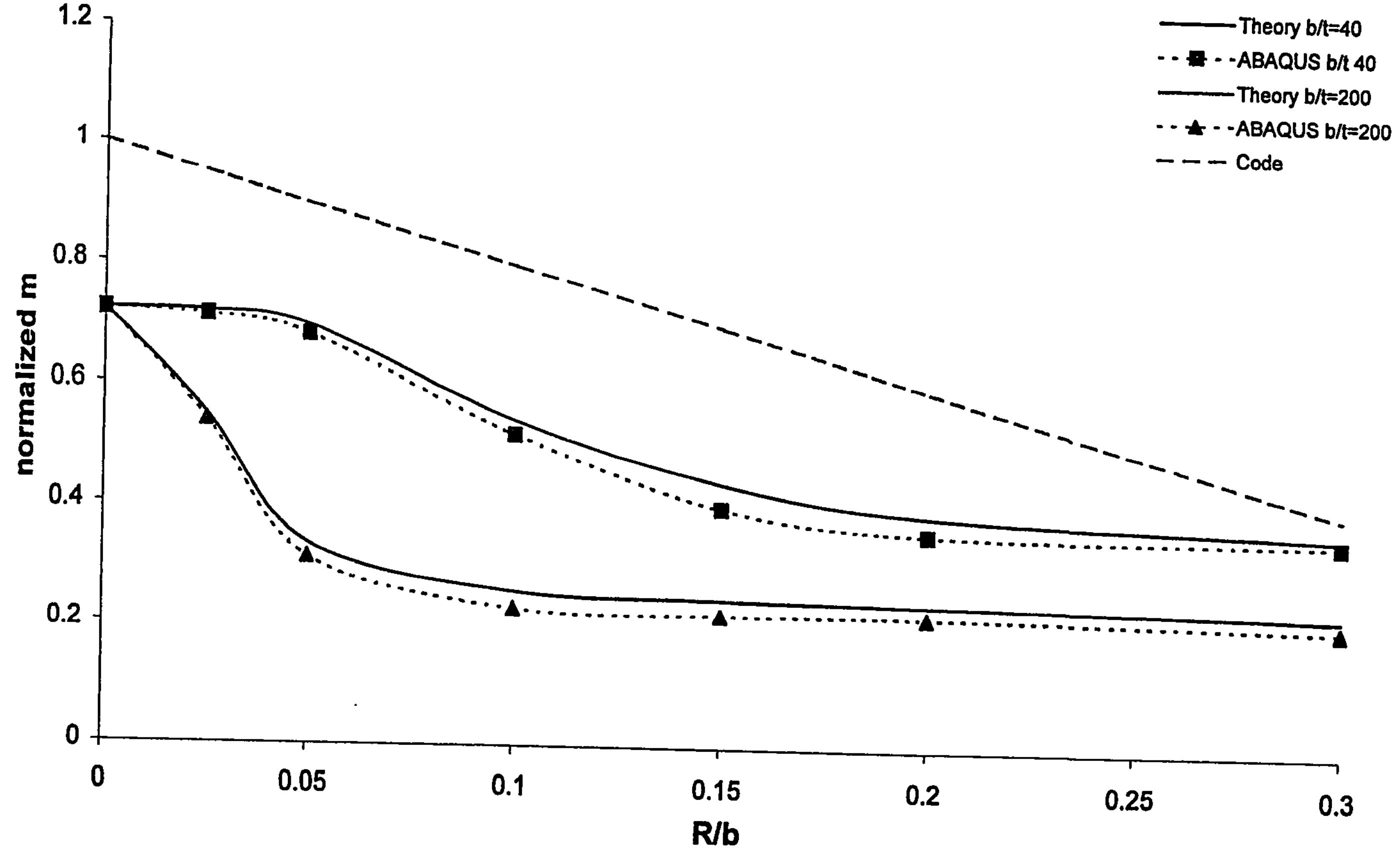

F4-60

Fig 4-61 Normalized m for channel sections, (a/b=0.5)

m=m / 5

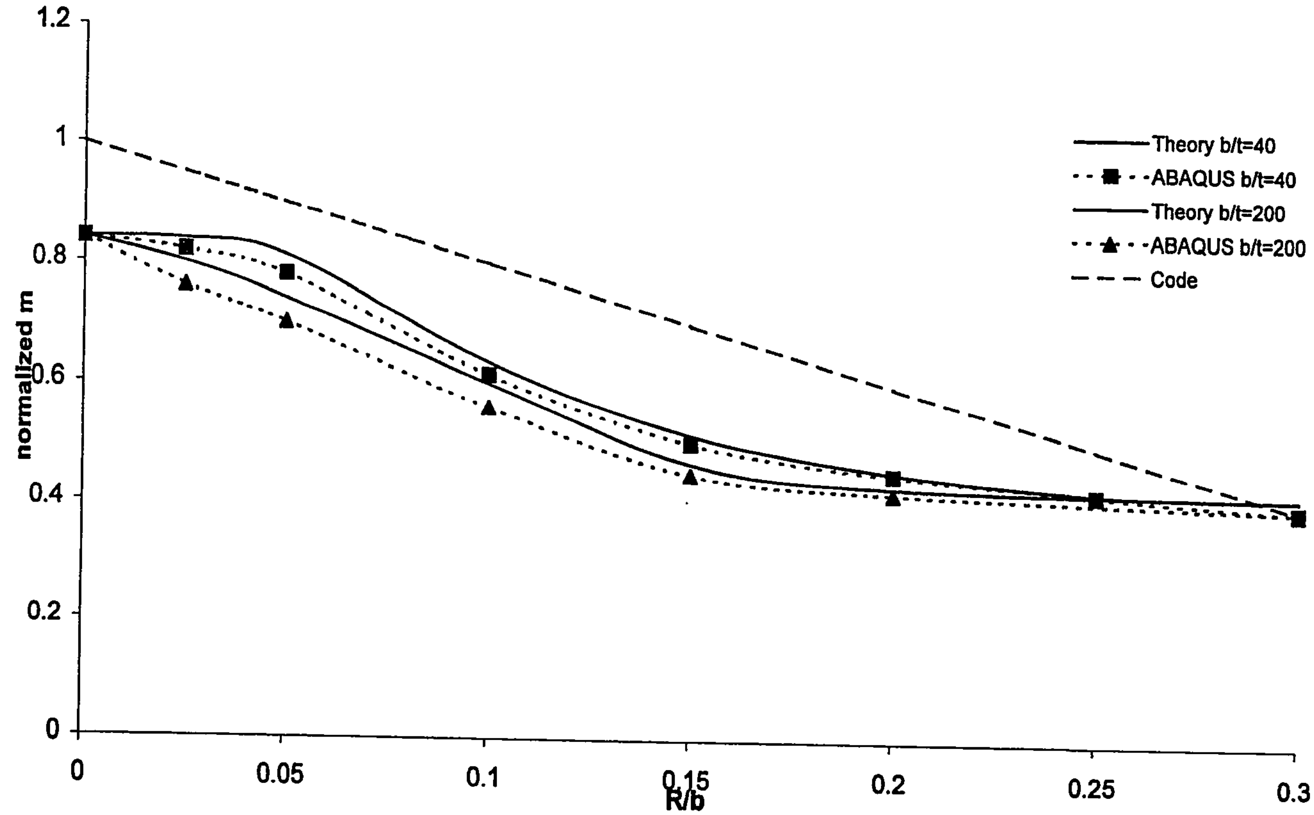

F4-61

Fig 4-62 Normalized m for channel sections, (a/b=0.25)

m =m / 5

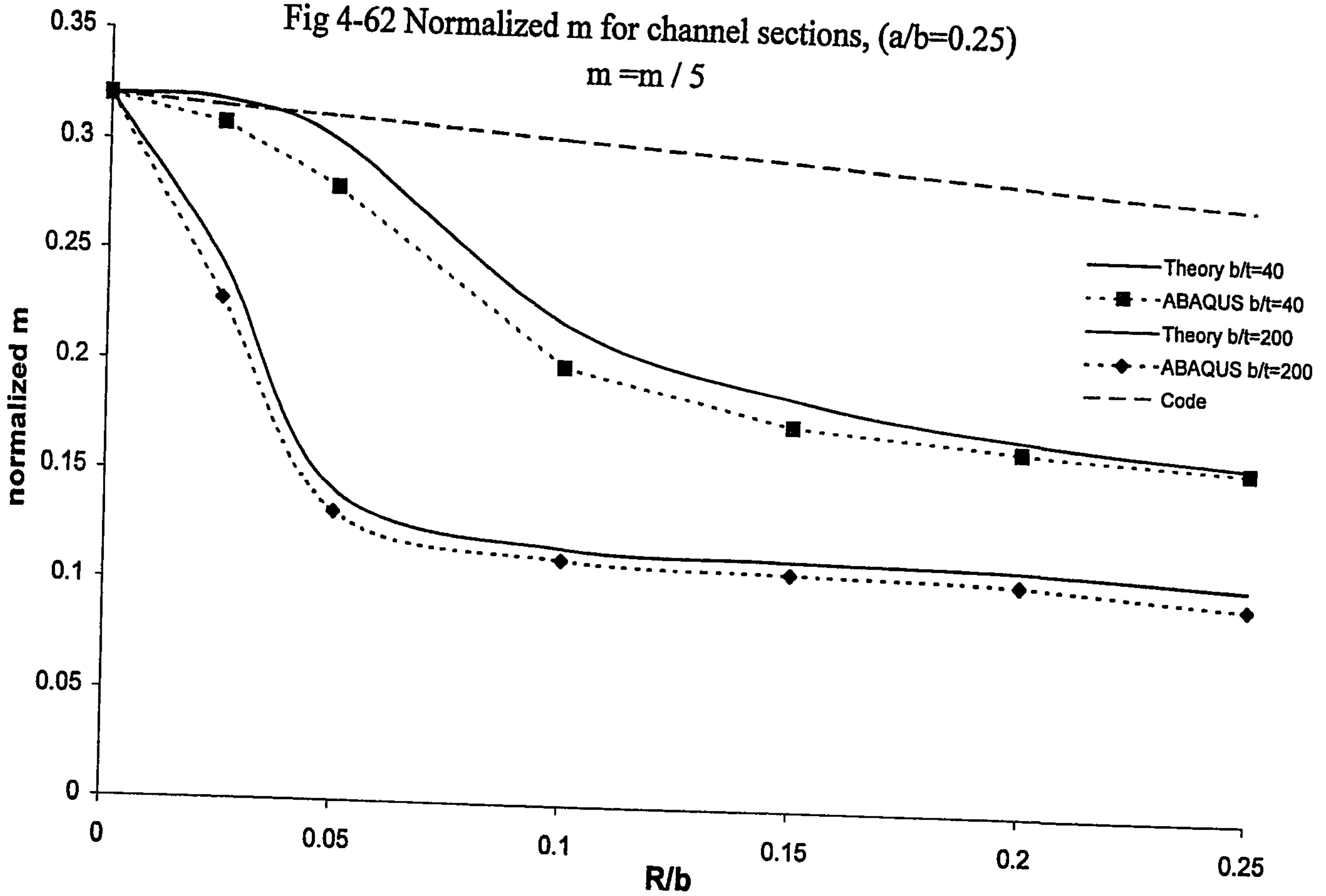

F4-62

Fig 4-63 Normalized mean strength for channel sections

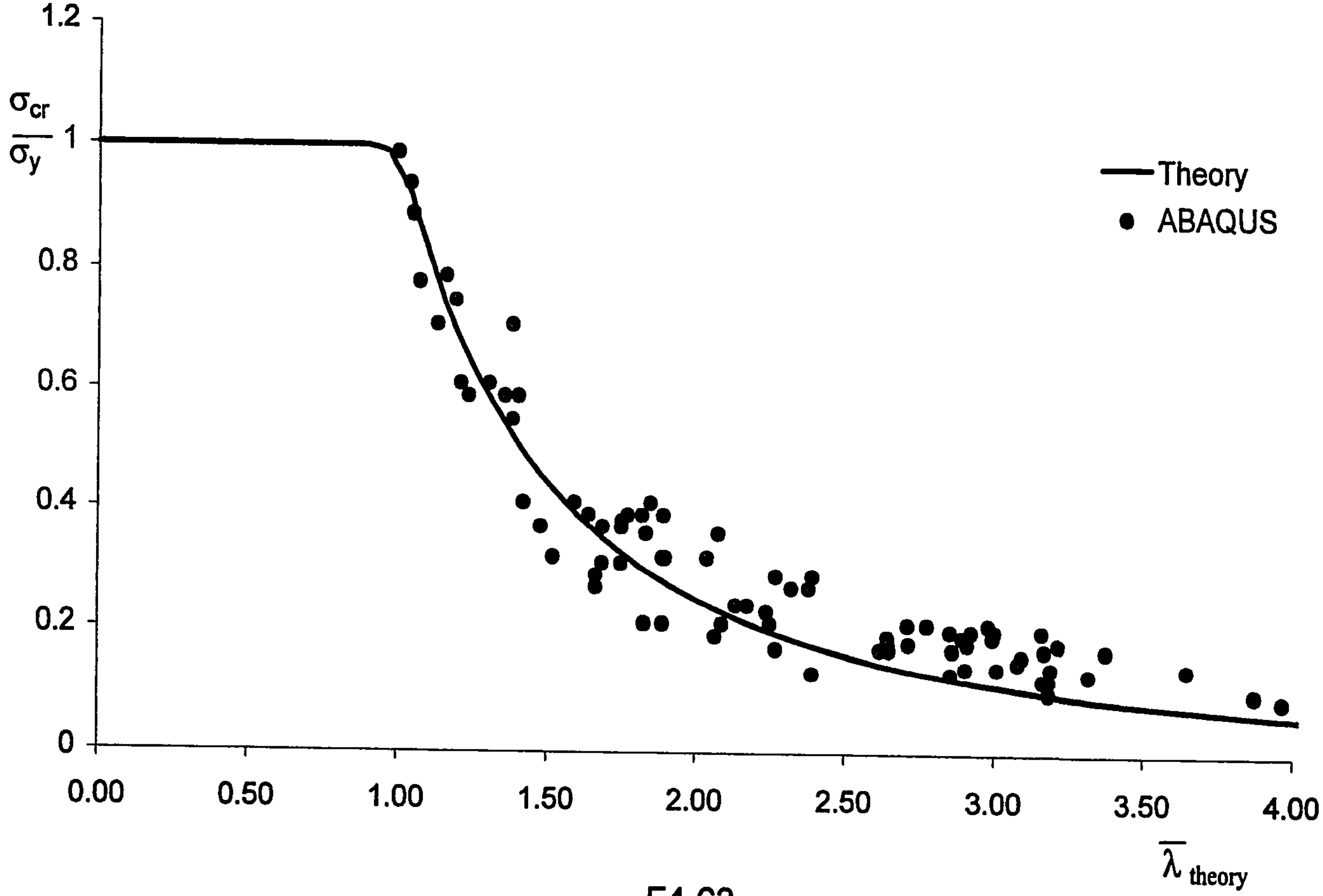

F4-63

Side a:

$$f(x,z) := \left[a_3 \cdot \sin\left(\pi \cdot \frac{x}{a}\right) + a_4 \cdot \left(1 - \cos\left(\pi \cdot \frac{2 \cdot x}{a}\right)\right)\right] \cdot \sin\left(\pi \cdot \frac{z}{c}\right)$$

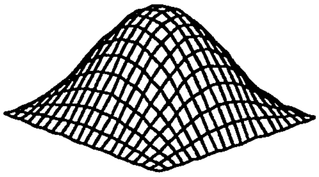

N X-Y-Z 45 degree view

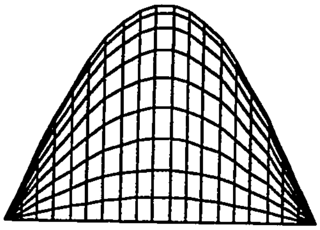

N Down X axis

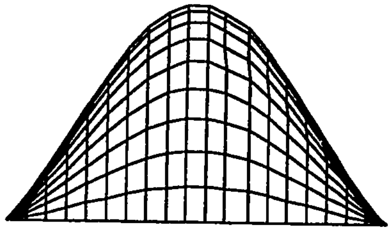

N Down Z axis

Side b :

$$f(y,z) := \left[a_1 \cdot \sin\left(\pi \cdot \frac{y}{b}\right) - a_2 \cdot \left(1 - \cos\left(\pi \cdot \frac{2 \cdot y}{b}\right)\right)\right] \cdot \sin\left(\pi \cdot \frac{z}{c}\right)$$

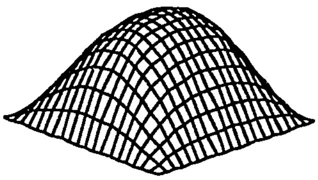

M X-Y-Z 45 degree view

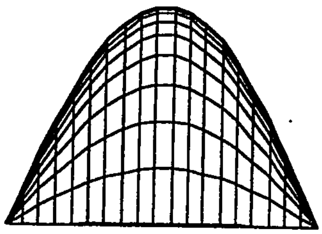

M Down Y axis

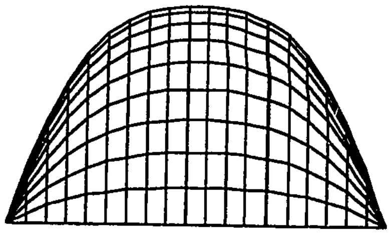

M Down Z axis

Fig I-1 Deflection of a box section

Flange:

$$f(x,z) := \left[\theta\cdot x + a_{3}\cdot\left(1 - \cos\left(\frac{\pi\cdot x}{2\cdot a}\right)\right)\right]\cdot\sin\left(\pi\cdot\frac{z}{c}\right)$$

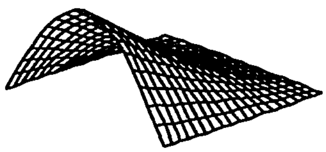

N X-Y-Z 45 degree view

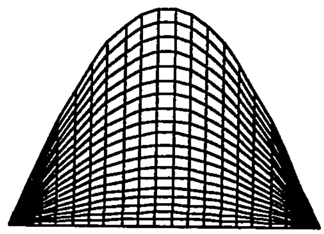

N Down X axis

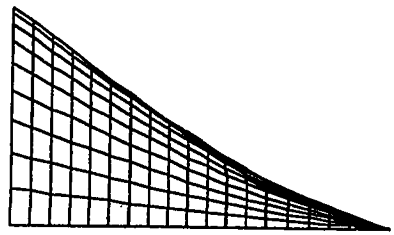

N Down Z axis

Web :

$$f(y,z) := \left[a_{1}\cdot\sin\left(\pi\cdot\frac{y}{b}\right) - a_{2}\cdot\left(1 - \cos\left(\frac{2\cdot\pi\cdot y}{b}\right)\right)\right]\cdot\sin\left(\pi\cdot\frac{z}{c}\right)$$

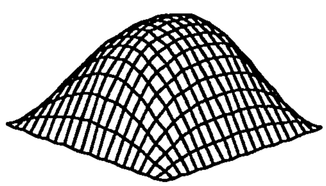

M X-Y-Z 45 degree view

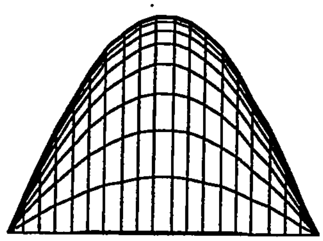

M Down Y axis

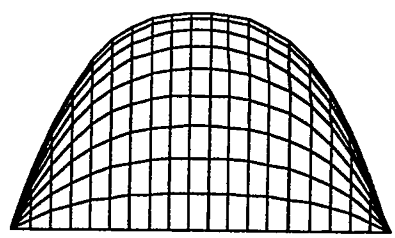

M Down Z axis

Fig I-2 Deflection of a channel section (flange mode)

Flange:

$$f(x,z) := \left[0\cdot\theta\cdot x - a_3\cdot\left(1-\cos\left(\pi\cdot\frac{\pi\cdot x}{2\cdot a}\right)\right)\right]\cdot\sin\left(\pi\cdot\frac{z}{c}\right)$$

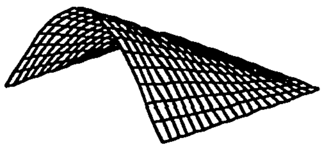

N X-Y-Z 45 degree view

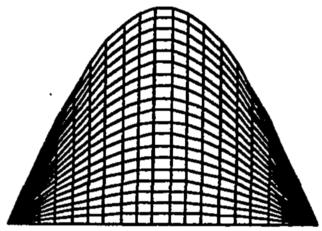

N Down X axis

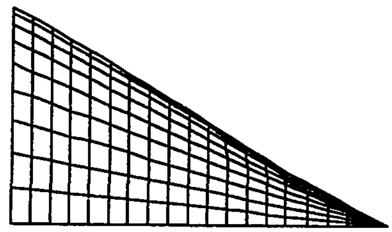

N Down Z axis

Web :

$$f(y,z) := \left[a_1\cdot\sin\left(\pi\cdot\frac{y}{b}\right) + a_2\cdot\left(1-\cos\left(\frac{2\cdot\pi\cdot y}{b}\right)\right)\right]\cdot\sin\left(\pi\cdot\frac{z}{c}\right)$$

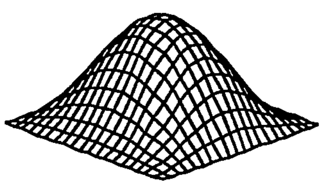

M X-Y-Z 45 degree view

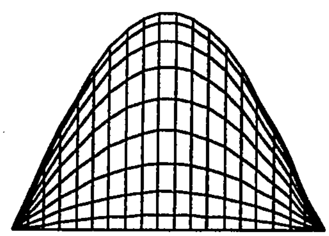

M Down Y axis

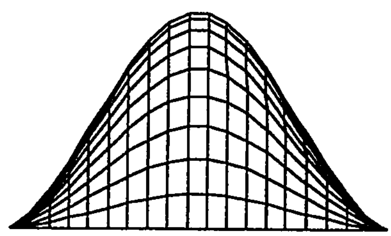

M Down Z axis

Fig I-3 Deflection of a channel section (web mode)

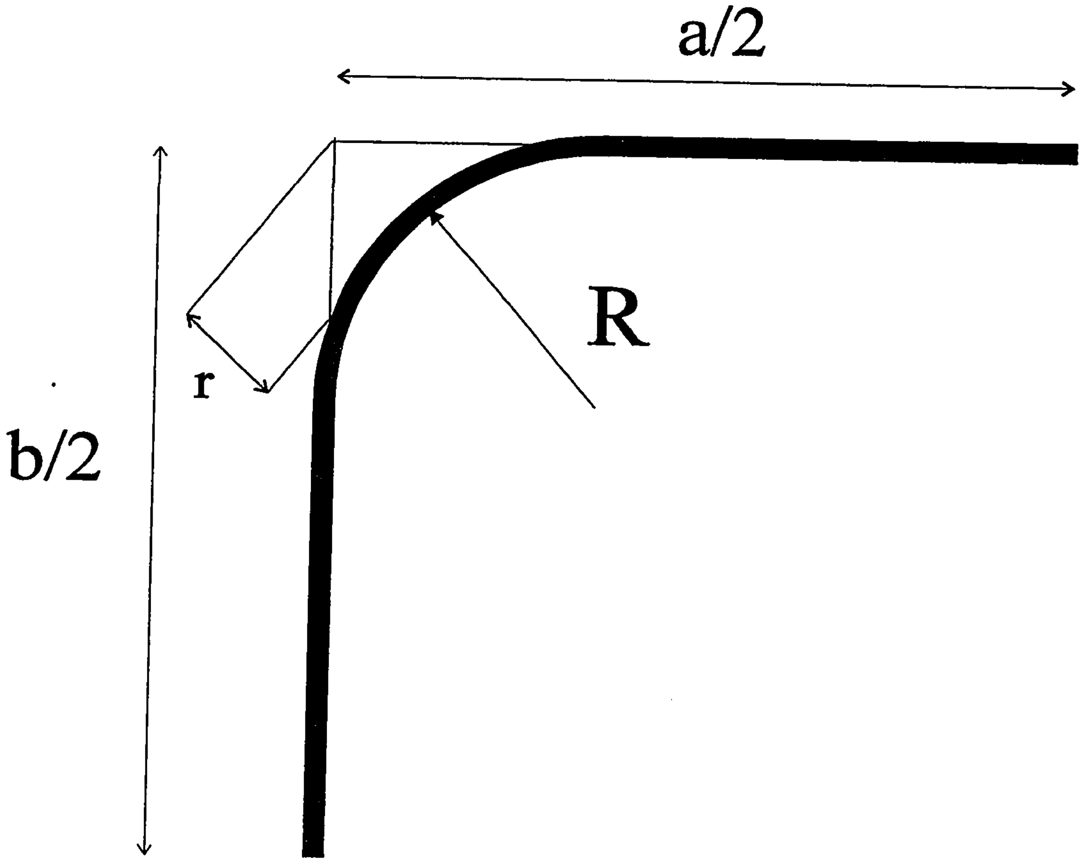

Fig II-1 Corner of a box section

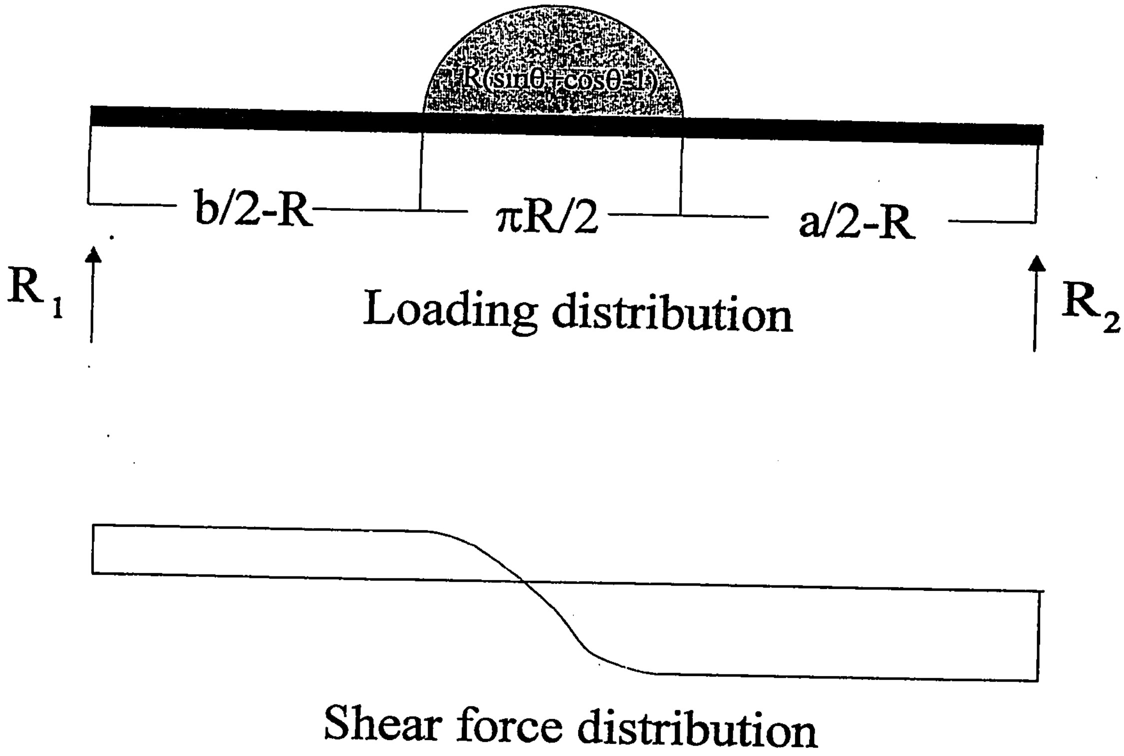

FigII-2 Warping constant construction
for the cormer of a box setion

Fig II-3 Warping constant for box sections (t=1)

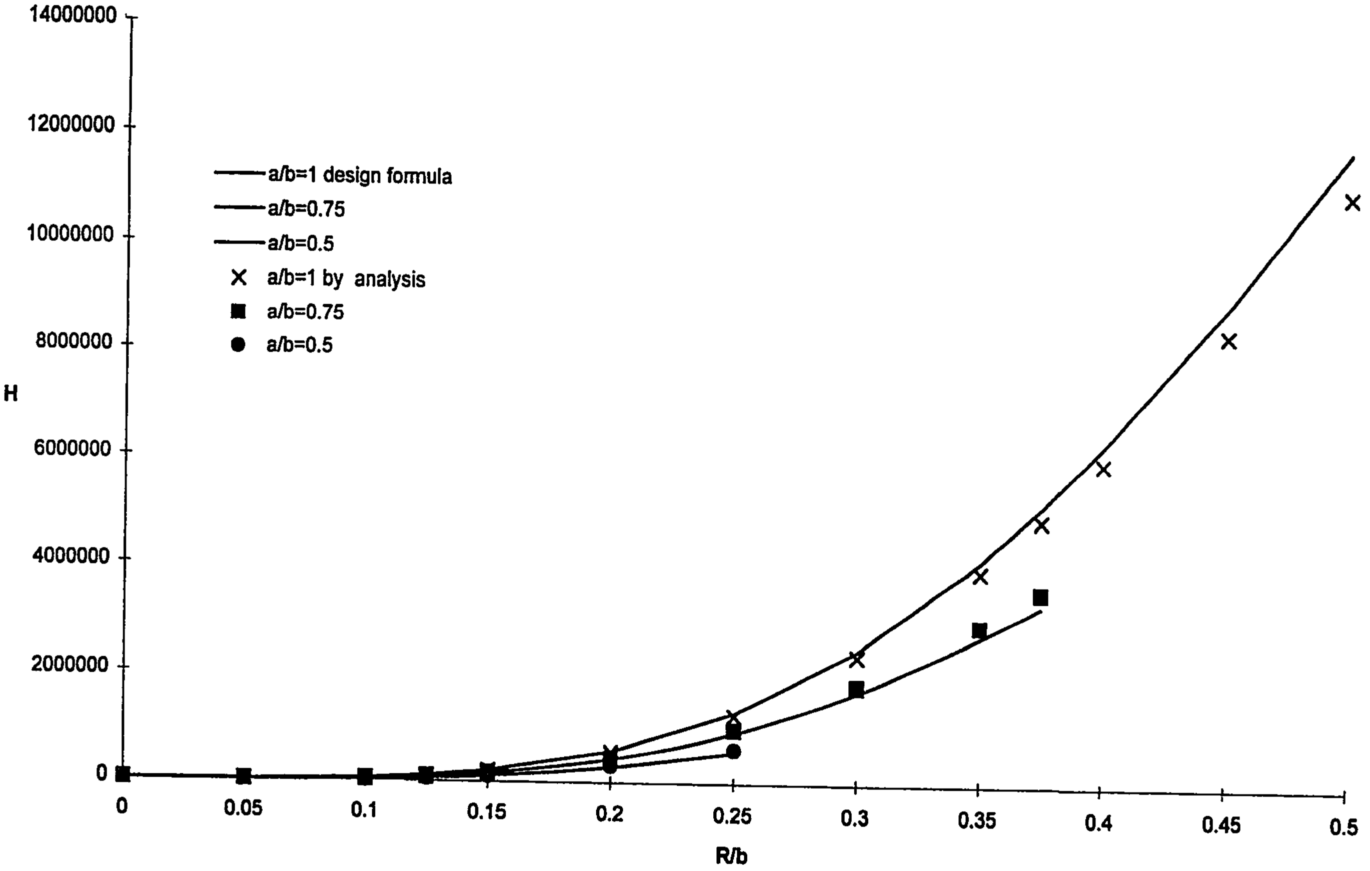

Fig II-4 Warping factor α for box sections

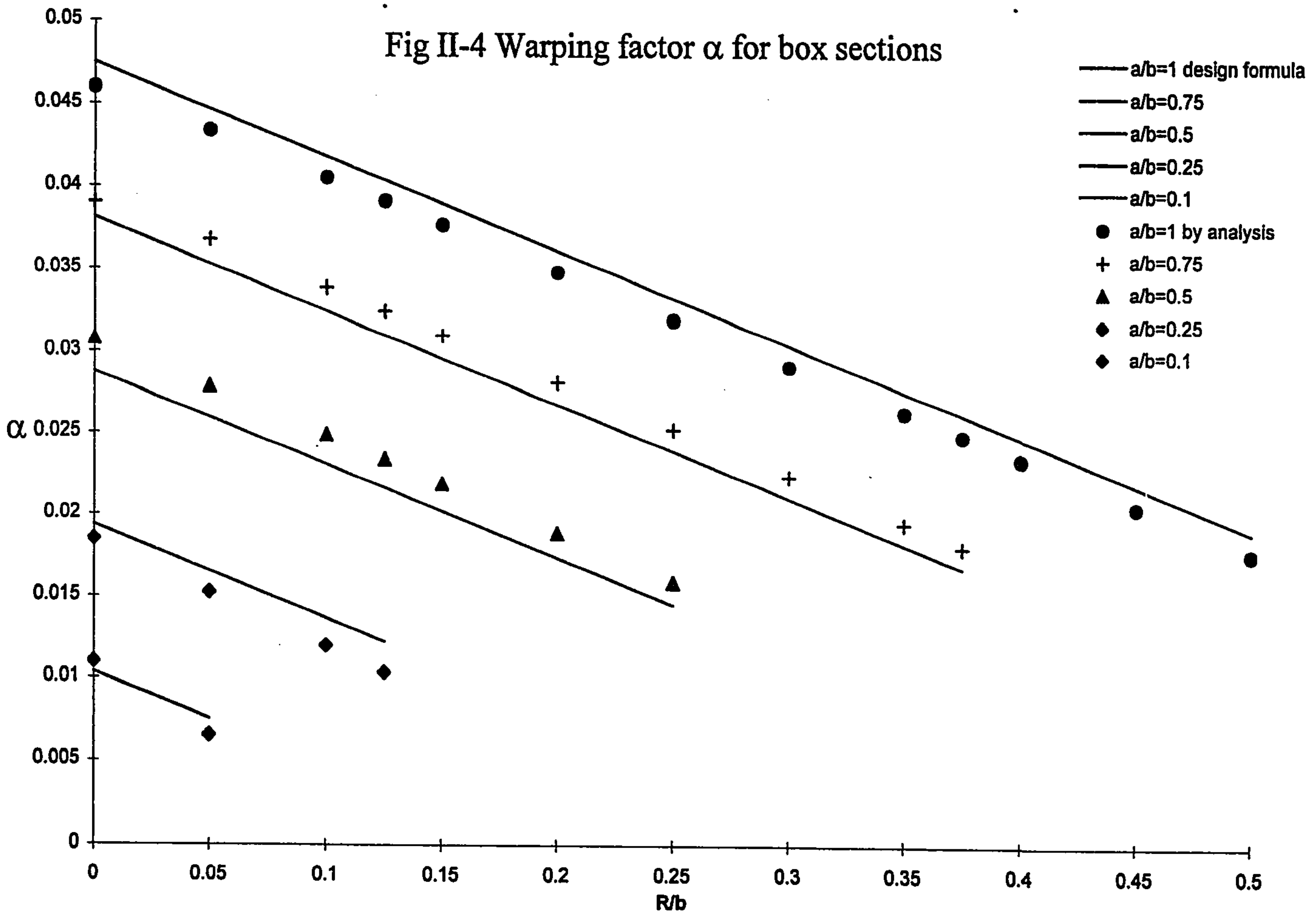

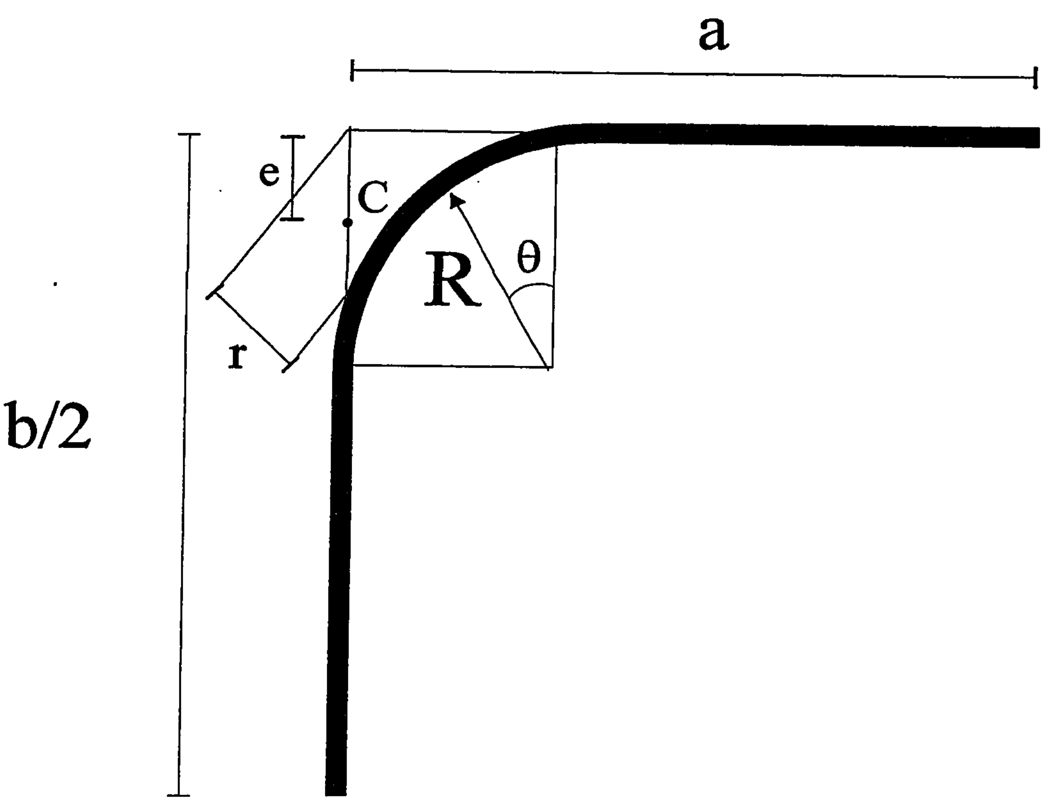

Fig II-5 Corner of a channel section

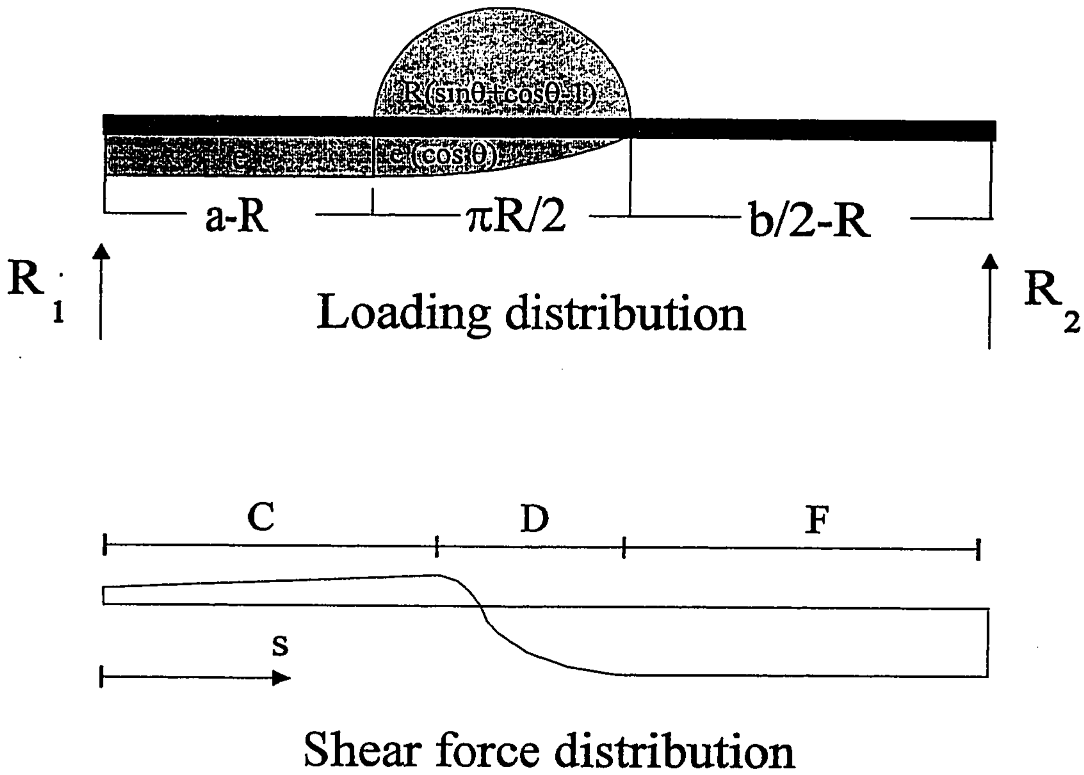

Fig II-6 Warping constant construction for the corner of a channel section

Fig II-7 Warping constant for channel sections (t=1)

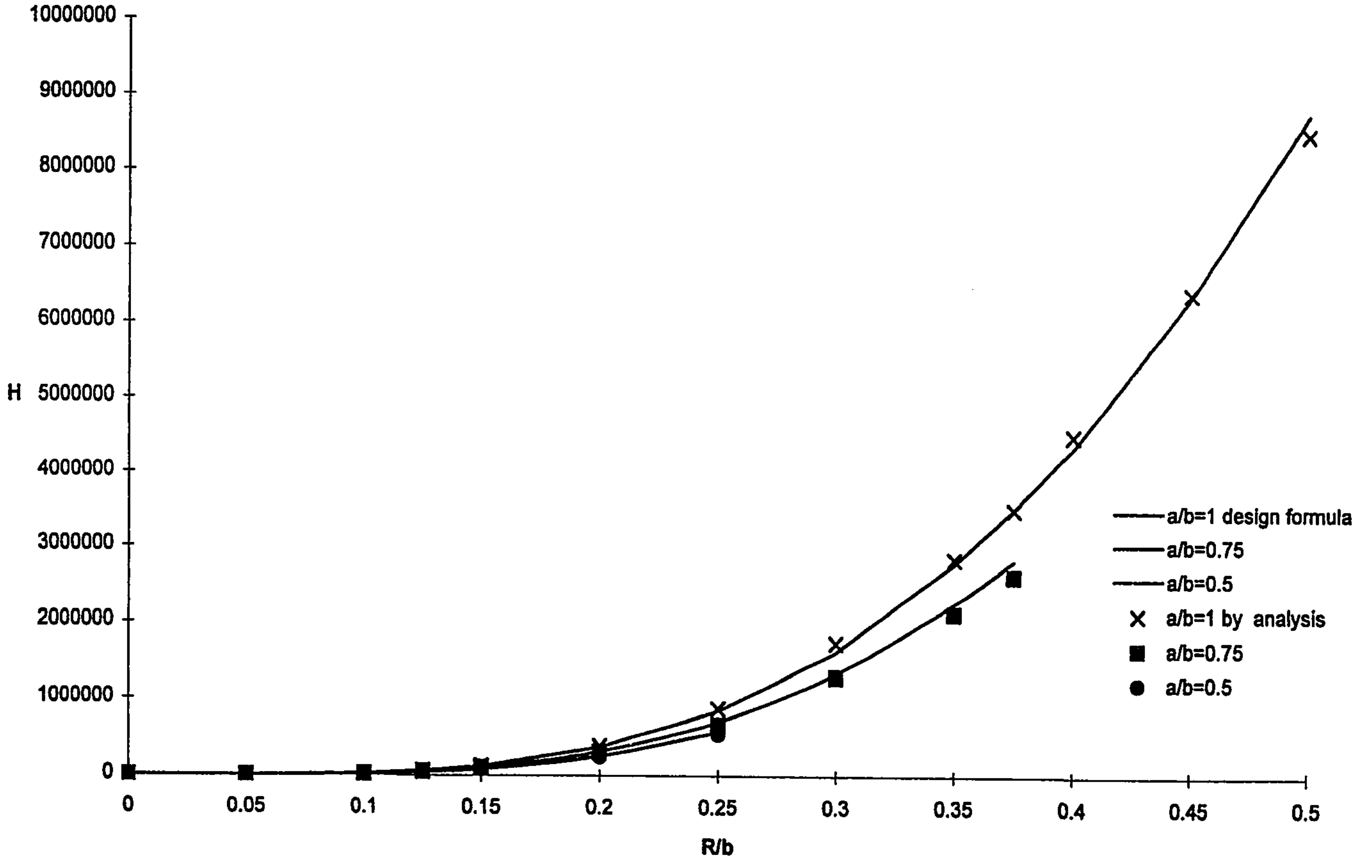

Fig II-8 Warping factor α for channel sections

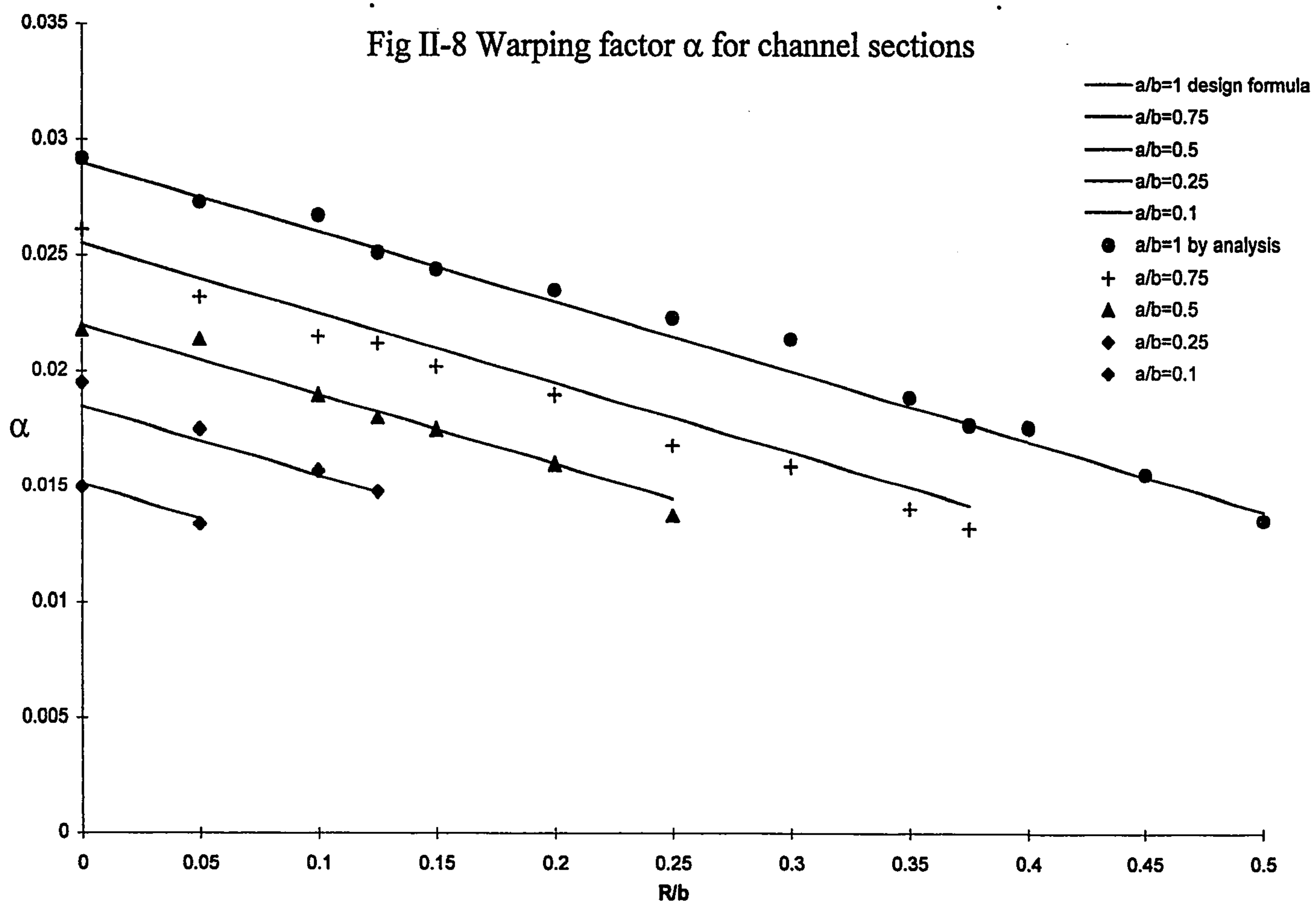

Table 4-1 Summary of results for box sections

			CRITICAL			Code	Theory	ULTIMATE				
			CODE	THEORY	ABAQUS			CODE	THEORY	ABAQUS		
1	40	0.000	453	453	467	3%	3%	299	307	331	10%	7%
1	40	0.025	502	454	472	-6%	4%	309	310	331	7%	6%
1	40	0.050	559	464	501	-12%	7%	319	312	332	4%	6%
1	40	0.100	708	593	646	-10%	8%	342	313	343	0%	9%
1	40	0.150	925	921	978	5%	6%	350	329	355	2%	7%
1	40	0.200	1259	1212	1314	4%	8%	350	340	361	3%	6%
1	40	0.300	2832	1435	1578	-79%	9%	350	337	364	4%	7%
1	50	0.000	290	287	299	3%	4%	255	280	313	19%	11%
1	50	0.025	321	293	302	-6%	3%	265	280	311	15%	10%
1	50	0.050	358	310	324	-10%	4%	275	282	311	11%	9%
1	50	0.100	453	402	459	1%	12%	299	303	327	9%	7%
1	50	0.150	592	675	712	17%	5%	325	327	347	6%	6%
1	50	0.200	806	845	910	11%	7%	350	337	353	1%	5%
1	50	0.300	1813	951	1035	-75%	8%	350	330	356	2%	7%
1	66	0.000	163	163	168	3%	3%	203	218	246	18%	12%
1	66	0.025	181	164	170	-6%	4%	212	219	245	14%	11%
1	66	0.050	201	173	187	-8%	7%	221	225	256	14%	12%
1	66	0.100	255	278	303	16%	8%	243	276	304	20%	9%
1	66	0.150	333	420	460	28%	9%	268	304	334	20%	9%
1	66	0.200	453	487	549	17%	11%	299	311	348	14%	11%
1	66	0.300	1020	530	594	-72%	11%	350	314	358	2%	12%

Table 4-1 Summary of results for box sections

[illegible]			normalized [illegible]			normalized [illegible] stress		
CODE	THEORY	ABAQUS	CODE	THEORY	ABAQUS	CODE	THEORY	ABAQUS
1.65	1.65	1.65	0.88	0.88	0.87	0.85	0.88	0.95
1.57	1.65	1.64	0.83	0.88	0.86	0.88	0.89	0.95
1.49	1.63	1.59	0.79	0.87	0.84	0.91	0.89	0.95
1.32	1.44	1.40	0.70	0.77	0.74	0.98	0.89	0.98
1.16	1.16	1.14	0.62	0.62	0.60	1.00	0.94	1.02
0.99	1.01	0.98	0.53	0.54	0.52	1.00	0.97	1.03
0.66	0.93	0.90	0.35	0.49	0.47	1.00	0.96	1.04
1.65	1.65	1.65	1.10	1.10	1.08	0.73	0.80	0.89
1.57	1.63	1.64	1.04	1.09	1.08	0.76	0.80	0.89
1.49	1.59	1.58	0.99	1.06	1.04	0.79	0.81	0.89
1.32	1.39	1.33	0.88	0.93	0.87	0.85	0.87	0.94
1.16	1.08	1.07	0.77	0.72	0.70	0.93	0.93	0.99
0.99	0.96	0.95	0.66	0.64	0.62	1.00	0.96	1.01
0.66	0.91	0.89	0.44	0.61	0.58	1.00	0.94	1.02
1.65	1.65	1.65	1.46	1.46	1.44	0.58	0.62	0.70
1.57	1.65	1.64	1.39	1.46	1.43	0.61	0.62	0.70
1.49	1.60	1.56	1.32	1.42	1.37	0.63	0.64	0.73
1.32	1.26	1.23	1.17	1.12	1.07	0.69	0.79	0.87
1.16	1.03	1.00	1.03	0.91	0.87	0.77	0.87	0.95
0.99	0.95	0.91	0.88	0.85	0.80	0.85	0.89	1.00
0.66	0.92	0.88	0.59	0.81	0.77	1.00	0.90	1.02

Table 4-1 Summary of results for box sections

[illegible]	[illegible]	[illegible]	CRITICAL CODE	THEORY	ABAQUS	Code Error	Theory Error	ULTIMATE CODE	THEORY	ABAQUS	Code Error	Theory Error
1	100	0.000	73	72	75	3%	4%	143	145	153	6%	5%
1	100	0.025	80	75	76	-6%	1%	150	146	152	1%	4%
1	100	0.050	90	83	89	0%	7%	157	155	164	4%	6%
1	100	0.100	113	154	172	34%	10%	174	214	225	23%	5%
1	100	0.150	148	210	233	36%	10%	195	251	268	27%	7%
1	100	0.200	201	228	258	22%	12%	221	260	268	17%	3%
1	100	0.300	453	234	268	-69%	13%	299	264	285	-5%	7%
1	200	0.000	18	18	19	3%	3%	76	73	81	6%	10%
1	200	0.025	20	18	20	-3%	8%	79	74	78	-2%	5%
1	200	0.050	22	28	29	23%	3%	84	88	95	12%	7%
1	200	0.100	28	52	58	51%	10%	93	124	135	31%	8%
1	200	0.150	37	57	64	42%	11%	106	132	136	22%	3%
1	200	0.200	50	62	67	25%	7%	122	133	139	12%	4%
1	200	0.300	113	60	68	-68%	11%	174	134	145	-20%	7%

Table 4-1 Summary of results for box sections

[illegible]			Normalized [illegible]			Normalized shear stress		
CODE	THEORY	ABAQUS	CODE	THEORY	ABAQUS	CODE	THEORY	ABAQUS
1.65	1.65	1.65	2.20	2.20	2.16	0.41	0.42	0.44
1.57	1.62	1.63	2.09	2.16	2.14	0.43	0.42	0.43
1.49	1.54	1.51	1.98	2.06	1.98	0.45	0.44	0.47
1.32	1.13	1.09	1.76	1.51	1.43	0.50	0.61	0.64
1.16	0.97	0.93	1.54	1.29	1.23	0.56	0.72	0.77
0.99	0.93	0.89	1.32	1.24	1.16	0.63	0.74	0.77
0.66	0.92	0.87	0.88	1.22	1.14	0.85	0.75	0.81
1.65	1.65	1.65	4.39	4.39	4.33	0.22	0.21	0.23
1.57	1.66	1.61	4.17	4.41	4.23	0.23	0.21	0.22
1.49	1.33	1.33	3.95	3.54	3.48	0.24	0.25	0.27
1.32	0.97	0.94	3.52	2.59	2.47	0.27	0.35	0.39
1.16	0.93	0.89	3.08	2.48	2.33	0.30	0.38	0.39
0.99	0.89	0.87	2.64	2.38	2.29	0.35	0.38	0.40
0.66	0.91	0.87	1.76	2.42	2.28	0.50	0.38	0.41

Table 4-1 Summary of results for box sections

a/b	b/t	R/b	CRITICAL CODE	THEORY	ABAQUS	Code Error	Theory Error	ULTIMATE CODE	THEORY	ABAQUS	Code Error	Theory Error
0.5	40	0.000	450	590	604	26%	2%	299	321	343	13%	6%
0.5	40	0.025	510	587	611	17%	4%	309	320	343	10%	7%
0.5	40	0.050	559	597	645	13%	7%	319	322	343	7%	6%
0.5	40	0.100	708	730	796	11%	8%	342	323	350	2%	8%
0.5	40	0.150	925	1085	1171	21%	7%	350	327	359	3%	9%
0.5	40	0.200	1259	1462	1608	22%	9%	350	343	364	4%	6%
0.5	40	0.250	2832	1822	2004	-41%	9%	350	330	367	5%	10%
0.5	50	0.000	290	372	387	25%	4%	255	297	333	23%	11%
0.5	50	0.025	321	379	391	18%	3%	265	297	330	20%	10%
0.5	50	0.050	358	380	417	14%	9%	275	299	328	16%	9%
0.5	50	0.100	453	517	558	19%	7%	299	311	337	11%	8%
0.5	50	0.150	592	793	857	31%	7%	325	326	352	8%	7%
0.5	50	0.200	806	1050	1129	29%	7%	350	335	358	2%	6%
0.5	50	0.300	1813	1190	1323	-37%	10%	350	334	361	3%	7%
0.5	66	0.000	158	211	218	27%	3%	203	248	280	28%	12%
0.5	66	0.025	191	212	220	13%	4%	212	249	278	24%	11%
0.5	66	0.050	201	222	239	16%	7%	221	254	289	24%	12%
0.5	66	0.100	255	334	364	30%	8%	243	290	319	24%	9%
0.5	66	0.150	333	520	562	41%	7%	268	313	344	22%	9%
0.5	66	0.200	453	635	692	34%	8%	299	319	358	17%	11%
0.5	66	0.300	1020	699	764	-34%	8%	350	322	368	5%	12%

Table 4-1 Summary of results for box sections

[illegible]			normalized [illegible]			normalized shear stress		
CODE	THEORY	ABAQUS	CODE	THEORY	ABAQUS	CODE	THEORY	ABAQUS
1.65	1.45	1.45	0.88	0.77	0.76	0.85	0.92	0.98
1.55	1.45	1.44	0.83	0.77	0.76	0.88	0.91	0.98
1.48	1.44	1.40	0.79	0.77	0.74	0.91	0.92	0.98
1.32	1.30	1.26	0.70	0.69	0.66	0.98	0.92	1.00
1.15	1.07	1.04	0.62	0.57	0.55	1.00	0.93	1.03
0.99	0.92	0.89	0.53	0.49	0.47	1.00	0.98	1.04
0.66	0.83	0.80	0.35	0.44	0.42	1.00	0.94	1.05
1.65	1.45	1.45	1.10	0.97	0.95	0.73	0.85	0.95
1.57	1.44	1.44	1.04	0.96	0.95	0.76	0.85	0.94
1.49	1.43	1.40	0.99	0.96	0.92	0.79	0.85	0.94
1.32	1.23	1.21	0.88	0.82	0.79	0.85	0.89	0.96
1.16	0.99	0.97	0.77	0.66	0.64	0.93	0.93	1.01
0.99	0.86	0.85	0.66	0.58	0.56	1.00	0.96	1.02
0.66	0.81	0.78	0.44	0.54	0.51	1.00	0.96	1.03
1.65	1.45	1.45	1.49	1.29	1.27	0.58	0.71	0.80
1.50	1.45	1.44	1.35	1.29	1.26	0.61	0.71	0.80
1.46	1.42	1.38	1.32	1.26	1.21	0.63	0.73	0.83
1.30	1.15	1.12	1.17	1.02	0.98	0.69	0.83	0.91
1.14	0.92	0.90	1.03	0.82	0.79	0.77	0.89	0.98
0.97	0.84	0.81	0.88	0.74	0.71	0.85	0.91	1.02
0.65	0.80	0.77	0.59	0.71	0.68	1.00	0.92	1.05

Table 4-1 Summary of results for box sections

a/b	b/t	δ/b	CRITICAL CODE	THEORY	ABAQUS	Code Error	Theory Error	ULTIMATE CODE	THEORY	ABAQUS	Code Error	Theory Error
0.5	100	0.000	73	94	98	26%	4%	143	165	180	21%	8%
0.5	100	0.025	80	95	98	18%	4%	150	166	186	19%	11%
0.5	100	0.050	90	104	112	20%	7%	157	174	183	14%	5%
0.5	100	0.10	113	189	206	45%	8%	174	235	251	31%	7%
0.5	100	0.15	148	270	292	49%	7%	195	274	276	29%	1%
0.5	100	0.200	201	310	330	39%	6%	221	282	293	25%	4%
0.5	100	0.300	453	320	346	-31%	7%	299	286	317	6%	10%
0.5	200	0.000	18	23	24	25%	3%	76	83	87	13%	5%
0.5	200	0.025	20	24	25	20%	4%	79	84	87	9%	4%
0.5	200	0.050	22	32	35	36%	7%	84	97	106	21%	8%
0.5	200	0.100	28	66	72	61%	8%	93	139	148	37%	7%
0.5	200	0.150	37	76	82	55%	7%	106	149	165	36%	10%
0.5	200	0.200	50	78	86	42%	10%	122	151	159	23%	5%
0.5	200	0.300	113	79	87	-30%	9%	174	152	164	-6%	7%

Table 4-1 Summary of results for box sections

[illegible]			normalized lamda			normalized shear stress		
CODE	THEORY	ABAQUS	CODE	THEORY	ABAQUS	CODE	THEORY	ABAQUS
1.65	1.45	1.45	2.20	1.93	1.89	0.41	0.47	0.52
1.57	1.45	1.45	2.09	1.92	1.89	0.43	0.47	0.53
1.49	1.38	1.35	1.98	1.83	1.77	0.45	0.50	0.52
1.32	1.02	1.00	1.76	1.36	1.30	0.50	0.67	0.72
1.16	0.86	0.84	1.54	1.14	1.10	0.56	0.78	0.79
0.99	0.80	0.79	1.32	1.06	1.03	0.63	0.81	0.84
0.66	0.79	0.77	0.88	1.05	1.01	0.85	0.82	0.91
1.65	1.45	1.45	4.39	3.86	3.80	0.22	0.24	0.25
1.57	1.43	1.42	4.17	3.81	3.73	0.23	0.24	0.25
1.49	1.23	1.20	3.95	3.28	3.16	0.24	0.28	0.30
1.32	0.87	0.84	3.52	2.31	2.21	0.27	0.40	0.42
1.16	0.80	0.79	3.08	2.14	2.06	0.30	0.43	0.47
0.99	0.80	0.77	2.64	2.12	2.01	0.35	0.43	0.45
0.66	0.79	0.76	1.76	2.10	2.00	0.50	0.44	0.47

Table 4-1 Summary of results for box sections

[illegible]	[illegible]	[illegible]	CRITICAL					ULTIMATE				
			CODE	THEORY	ABAQUS	Code Error	Theory Error	CODE	THEORY	ABAQUS	Code Error	Theory Error
0.25	40	0.000	449	677	697	36%	3%	299	322	347	14%	7%
0.25	40	0.025	505	678	705	28%	4%	309	322	348	11%	8%
0.25	40	0.050	550	687	742	26%	7%	319	322	349	8%	8%
0.25	40	0.100	708	822	896	21%	8%	342	327	359	5%	9%
0.25	40	0.125	925	1198	1294	29%	7%	350	334	361	3%	7%
0.25	50	0.000	300	438	446	33%	2%	255	305	341	25%	11%
0.25	50	0.025	340	430	451	25%	5%	265	305	338	22%	10%
0.25	50	0.050	358	434	479	25%	9%	275	306	336	18%	9%
0.25	50	0.100	453	590	623	27%	5%	299	316	342	13%	7%
0.25	50	0.150	592	867	948	38%	9%	325	328	355	8%	7%
0.25	66	0.000	163	244	251	35%	3%	203	264	298	32%	12%
0.25	66	0.025	181	246	254	29%	3%	212	264	296	28%	11%
0.25	66	0.125	201	260	274	27%	5%	221	268	306	28%	12%
0.25	66	0.100	255	370	403	37%	8%	243	296	326	26%	9%
0.25	66	0.125	333	574	626	47%	8%	268	317	348	23%	9%

Table 4-1 Summary of results for box sections

			normalized lambda			normalized peak stress		
CUFSM	THEORY	ABAQUS	CUFSM	THEORY	ABAQUS	CUFSM	THEORY	ABAQUS
1.65	1.35	1.35	0.88	0.72	0.71	0.85	0.92	0.99
1.56	1.35	1.34	0.83	0.72	0.70	0.88	0.92	0.99
1.49	1.34	1.31	0.80	0.71	0.69	0.91	0.92	1.00
1.31	1.23	1.19	0.70	0.65	0.63	0.98	0.93	1.03
1.15	1.01	0.99	0.62	0.54	0.52	1.00	0.96	1.03
1.65	1.35	1.35	1.08	0.89	0.89	0.73	0.87	0.97
1.55	1.36	1.34	1.01	0.90	0.88	0.76	0.87	0.97
1.51	1.36	1.30	0.99	0.90	0.85	0.79	0.87	0.96
1.34	1.16	1.14	0.88	0.77	0.75	0.85	0.90	0.98
1.17	0.96	0.93	0.77	0.64	0.61	0.93	0.94	1.01
1.65	1.35	1.35	1.46	1.20	1.18	0.58	0.75	0.85
1.57	1.34	1.34	1.39	1.19	1.17	0.61	0.76	0.85
1.49	1.31	1.29	1.32	1.16	1.13	0.63	0.77	0.87
1.32	1.10	1.06	1.17	0.97	0.93	0.69	0.85	0.93
1.16	0.88	0.85	1.03	0.78	0.75	0.77	0.90	1.00

Table 4-1 Summary of results for box sections

[illegible]	[illegible]	[illegible]	CRITICAL [illegible]	THEORY	ABAQUS	[illegible]	[illegible]	ULTIMATE [illegible]	THEORY	ABAQUS	[illegible]	[illegible]
0.25	100	0.000	77	110	112	31%	1%	143	178	194	26%	8%
0.25	100	0.025	86	109	113	24%	4%	150	178	200	25%	11%
0.25	100	0.050	95	118	128	26%	7%	157	186	195	19%	5%
0.25	100	0.10	113	207	228	50%	9%	174	247	264	34%	7%
0.25	100	0.13	148	305	329	55%	7%	195	283	286	32%	1%
0.25	200	0.000	16	27	28	43%	3%	76	89	93	19%	5%
0.25	200	0.025	22	27	29	24%	6%	79	90	94	15%	4%
0.25	200	0.050	22	37	39	43%	6%	84	103	112	25%	8%
0.25	200	0.100	28	72	81	65%	11%	93	147	157	41%	7%
0.25	200	0.125	37	84	94	61%	11%	106	160	177	40%	10%

Table 4-1 Summary of results for box sections

[illegible]			Normalized lambda			Normalized [illegible] stress		
CODE	THEORY	ABAQUS	CODE	THEORY	ABAQUS	CODE	THEORY	ABAQUS
1.65	1.35	1.35	2.13	1.78	1.77	0.41	0.51	0.55
1.56	1.36	1.34	2.02	1.79	1.76	0.43	0.51	0.57
1.49	1.30	1.26	1.92	1.72	1.65	0.45	0.53	0.56
1.36	0.98	0.94	1.76	1.30	1.24	0.50	0.71	0.75
1.19	0.81	0.79	1.54	1.07	1.03	0.56	0.81	0.82
1.65	1.35	1.35	4.68	3.60	3.54	0.22	0.25	0.27
1.41	1.35	1.33	3.99	3.60	3.48	0.23	0.26	0.27
1.40	1.15	1.14	3.95	3.08	2.99	0.24	0.29	0.32
1.24	0.83	0.79	3.52	2.20	2.08	0.27	0.42	0.45
1.09	0.77	0.73	3.08	2.04	1.93	0.30	0.46	0.51

Table 4-2 Summary of results for channel sections

[illegible]	[illegible]	[illegible]	CRITICAL			Code	Theory	[illegible]			Normalized [illegible]		
			CODE	THEORY	ABAQUS	Error	Error	CODE	THEORY	ABAQUS	CODE	[illegible]	[illegible]
1	40	0.000	49	95	97	49%	2%	5.00	3.60	3.60	1.00	0.72	0.72
1	40	0.025	55	96	98	44%	2%	4.75	3.59	3.59	0.95	0.72	0.72
1	40	0.050	61	102	105	42%	3%	4.50	3.48	3.47	0.90	0.70	0.69
1	40	0.100	77	167	178	57%	6%	4.00	2.72	2.66	0.80	0.54	0.53
1	40	0.150	101	254	260	61%	2%	3.50	2.20	2.20	0.70	0.44	0.44
1	40	0.200	137	324	339	60%	4%	3.00	1.95	1.93	0.60	0.39	0.39
1	40	0.250	197	371	401	51%	7%	2.50	1.82	1.77	0.50	0.36	0.35
1	50	0.000	32	61	61	48%	0%	5.00	3.60	3.60	1.00	0.72	0.72
1	50	0.025	35	61	62	43%	1%	4.75	3.59	3.58	0.95	0.72	0.72
1	50	0.050	39	67	68	43%	1%	4.50	3.42	3.42	0.90	0.68	0.68
1	50	0.100	49	122	126	61%	3%	4.00	2.54	2.51	0.80	0.51	0.50
1	50	0.150	64	175	183	65%	4%	3.50	2.12	2.08	0.70	0.42	0.42
1	50	0.200	88	214	229	62%	6%	3.00	1.92	1.86	0.60	0.38	0.37
1	50	0.250	126	261	273	54%	4%	2.50	1.74	1.70	0.50	0.35	0.34
1	66	0.000	18	34	35	49%	1%	5.00	3.60	3.60	1.00	0.72	0.72
1	66	0.025	20	35	35	44%	1%	4.75	3.58	3.58	0.95	0.72	0.72
1	66	0.050	22	41	41	46%	1%	4.50	3.31	3.31	0.90	0.66	0.66
1	66	0.100	28	81	84	67%	4%	4.00	2.34	2.30	0.80	0.47	0.46
1	66	0.150	36	105	111	67%	5%	3.50	2.05	2.00	0.70	0.41	0.40
1	66	0.200	49	135	138	64%	2%	3.00	1.81	1.80	0.60	0.36	0.36
1	66	0.250	71	160	173	59%	7%	2.50	1.66	1.61	0.50	0.33	0.32

Table 4-2 Summary of results for channel sections

[illegible]	b/t	R/b	CRITICAL CODE	THEORY	ABAQUS	Code Error	Theory Error	[illegible] CODE	THEORY	ABAQUS	normalized resistance CODE	THEORY	[illegible] ABAQUS
1	100	0.000	8	15	15	49%	1%	5.00	3.60	3.60	1.00	0.72	0.72
1	100	0.025	9	16	16	47%	1%	4.75	3.48	3.48	0.95	0.70	0.70
1	100	0.050	10	22	22	56%	1%	4.50	2.99	2.99	0.90	0.60	0.60
1	100	0.100	12	45	48	74%	5%	4.00	2.09	2.05	0.80	0.42	0.41
1	100	0.150	16	69	74	78%	7%	3.50	1.69	1.64	0.70	0.34	0.33
1	100	0.200	22	97	106	79%	8%	3.00	1.43	1.37	0.60	0.29	0.27
1	100	0.250	32	108	123	74%	12%	2.50	1.35	1.27	0.50	0.27	0.25
1	200	0.000	2	4	4	54%	2%	5.00	3.60	3.60	1.00	0.72	0.72
1	200	0.025	2	7	7	70%	3%	4.75	2.75	2.74	0.95	0.55	0.55
1	200	0.050	2	19	20	88%	4%	4.50	1.67	1.66	0.90	0.33	0.33
1	200	0.100	3	33	35	91%	6%	4.00	1.28	1.26	0.80	0.26	0.25
1	200	0.150	4	36	39	90%	8%	3.50	1.23	1.19	0.70	0.25	0.24
1	200	0.200	5	37	43	87%	13%	3.00	1.20	1.13	0.60	0.24	0.23
1	200	0.250	8	41	50	84%	17%	2.50	1.15	1.05	0.50	0.23	0.21

Table 4-2 Summary of results for channel sections

a/b	b/t	R/b	CRITICAL			Code	Theory	k			Normalized [illegible]		
			CODE	THEORY	ABAQUS	Error	Error	CODE	THEORY	ABAQUS	CODE	THEORY	ABAQUS
0.5	40	0.000	49	70	72	32%	3%	5.00	4.20	4.20	1.00	0.84	0.84
0.5	40	0.025	55	70	72	24%	3%	4.75	4.19	4.20	0.95	0.84	0.84
0.5	40	0.050	61	75	78	22%	4%	4.50	4.06	4.04	0.90	0.81	0.81
0.5	40	0.100	77	122	129	40%	5%	4.00	3.17	3.14	0.80	0.63	0.63
0.5	40	0.150	101	185	193	48%	4%	3.50	2.58	2.57	0.70	0.52	0.51
0.5	40	0.200	137	237	249	45%	5%	3.00	2.28	2.26	0.60	0.46	0.45
0.5	40	0.250	197	272	285	31%	5%	2.50	2.13	2.11	0.50	0.43	0.42
0.5	50	0.000	32	45	45	30%	0%	5.00	4.20	4.20	1.00	0.84	0.84
0.5	50	0.025	35	45	46	23%	1%	4.75	4.18	4.18	0.95	0.84	0.84
0.5	50	0.050	39	51	52	24%	1%	4.50	3.93	3.92	0.90	0.79	0.78
0.5	50	0.100	49	98	102	51%	3%	4.00	2.83	2.79	0.80	0.57	0.56
0.5	50	0.150	64	134	140	54%	4%	3.50	2.43	2.38	0.70	0.49	0.48
0.5	50	0.200	88	160	168	48%	5%	3.00	2.22	2.17	0.60	0.44	0.43
0.5	50	0.250	126	194	209	40%	7%	2.50	2.02	1.95	0.50	0.40	0.39
0.5	66	0.000	18	25	25	30%	1%	5.00	4.20	4.20	1.00	0.84	0.84
0.5	66	0.025	20	25	26	23%	1%	4.75	4.17	4.17	0.95	0.83	0.83
0.5	66	0.050	22	30	30	27%	1%	4.50	3.86	3.85	0.90	0.77	0.77
0.5	66	0.100	28	59	65	57%	9%	4.00	2.74	2.63	0.80	0.55	0.53
0.5	66	0.150	36	77	87	58%	11%	3.50	2.40	2.27	0.70	0.48	0.45
0.5	66	0.200	49	99	113	56%	12%	3.00	2.12	1.99	0.60	0.42	0.40
0.5	66	0.250	71	118	140	49%	16%	2.50	1.94	1.79	0.50	0.39	0.36

Table 4-2 Summary of results for channel sections

[illegible]	[illegible]	R/t	CRITICAL CODE	THEORY	ABAQUS	Code Error	Theory Error	CODE	THEORY	ABAQUS	normalized with respect to CODE	THEORY	ABAQUS
0.5	100	0.000	8	11	11	30%	1%	5.00	4.20	4.20	1.00	0.84	0.84
0.5	100	0.025	9	12	12	27%	1%	4.75	4.06	4.06	0.95	0.81	0.81
0.5	100	0.050	10	16	16	38%	-3%	4.50	3.49	3.56	0.90	0.70	0.71
0.5	100	0.100	12	33	33	62%	-2%	4.00	2.44	2.48	0.80	0.49	0.50
0.5	100	0.150	16	51	60	73%	15%	3.50	1.97	1.82	0.70	0.39	0.36
0.5	100	0.200	22	71	85	74%	16%	3.00	1.67	1.53	0.60	0.33	0.31
0.5	100	0.250	32	79	96	67%	17%	2.50	1.58	1.44	0.50	0.32	0.29
0.5	200	0.000	2	3	3	42%	2%	5.00	4.20	4.20	1.00	0.84	0.84
0.5	200	0.025	2	3	3	32%	3%	4.75	4.37	4.35	0.95	0.87	0.87
0.5	200	0.050	2	6	6	59%	4%	4.50	3.21	3.18	0.90	0.64	0.64
0.5	200	0.100	3	9	10	68%	6%	4.00	2.56	2.52	0.80	0.51	0.50
0.5	200	0.150	4	9	10	61%	8%	3.50	2.51	2.43	0.70	0.50	0.49
0.5	200	0.200	5	9	11	50%	13%	3	2.50	2.35	0.60	0.50	0.47
0.5	200	0.250	8	9	11	31%	17%	2.5	2.50	2.29	0.50	0.50	0.46

Table 4-2 Summary of results for channel sections

a/h	b/t	%	CRITICAL CODE	THEORY	ABAQUS	Code Error	Theory Error	CODE	THEORY	ABAQUS	Normalized CODE	THEORY	ABAQUS
0.25	40	0.000	30	30	31	2%	2%	1.60	1.60	1.60	0.32	0.32	0.32
0.25	40	0.025	31	30	32	3%	4%	1.58	1.59	1.57	0.32	0.32	0.31
0.25	40	0.050	32	34	37	14%	8%	1.56	1.50	1.46	0.31	0.30	0.29
0.25	40	0.100	33	64	70	52%	9%	1.52	1.10	1.06	0.30	0.22	0.21
0.25	40	0.150	35	88	102	66%	15%	1.48	0.94	0.88	0.30	0.19	0.18
0.25	40	0.200	37	105	114	67%	8%	1.44	0.86	0.83	0.29	0.17	0.17
0.25	40	0.250	39	118	123	68%	4%	1.40	0.81	0.80	0.28	0.16	0.16
0.25	50	0.000	19	19	19	0%	0%	1.60	1.60	1.60	0.32	0.32	0.32
0.25	50	0.025	20	20	20	0%	1%	1.58	1.59	1.59	0.32	0.32	0.32
0.25	50	0.050	20	23	23	13%	1%	1.56	1.46	1.46	0.31	0.29	0.29
0.25	50	0.100	21	46	48	55%	3%	1.52	1.03	1.02	0.30	0.21	0.20
0.25	50	0.150	23	59	63	64%	6%	1.48	0.91	0.89	0.30	0.18	0.18
0.25	50	0.200	24	69	76	69%	9%	1.44	0.85	0.81	0.29	0.17	0.16
0.25	50	0.250	25	83	86	71%	4%	1.40	0.77	0.76	0.28	0.15	0.15
0.25	66	0.000	11	11	11	1%	1%	1.60	1.60	1.60	0.32	0.32	0.32
0.25	66	0.025	11	11	11	1%	1%	1.58	1.58	1.58	0.32	0.32	0.32
0.25	66	0.050	11	14	16	27%	8%	1.56	1.39	1.33	0.31	0.28	0.27
0.25	66	0.100	12	29	34	65%	13%	1.52	0.97	0.91	0.30	0.19	0.18
0.25	66	0.150	13	35	41	69%	15%	1.48	0.89	0.83	0.30	0.18	0.17
0.25	66	0.200	13	43	51	74%	16%	1.44	0.80	0.74	0.29	0.16	0.15
0.25	66	0.250	14	51	65	78%	22%	1.40	0.74	0.66	0.28	0.15	0.13

Table 4-2 Summary of results for channel sections

[illegible]	[illegible]	R/t	CRITICAL CODE	THEORY	ABAQUS	Code Error	Theory Error	m CODE	THEORY	ABAQUS	Normalized [illegible] CODE	THEORY	ABAQUS
0.25	100	0.000	5	5	5	1%	1%	1.60	1.60	1.60	0.32	0.32	0.32
0.25	100	0.025	5	5	5	7%	1%	1.58	1.53	1.53	0.32	0.31	0.31
0.25	100	0.050	5	8	8	37%	-3%	1.56	1.22	1.24	0.31	0.24	0.25
0.25	100	0.100	5	16	15	65%	-2%	1.52	0.89	0.90	0.30	0.18	0.18
0.25	100	0.150	6	22	26	79%	15%	1.48	0.74	0.69	0.30	0.15	0.14
0.25	100	0.200	6	31	37	84%	16%	1.44	0.63	0.58	0.29	0.13	0.12
0.25	100	0.250	6	34	41	85%	17%	1.40	0.60	0.55	0.28	0.12	0.11
0.25	200	0.000	2	1	1	-34%	2%	1.60	1.60	1.60	0.32	0.32	0.32
0.25	200	0.025	2	2	3	14%	3%	1.52	1.22	1.22	0.30	0.24	0.24
0.25	200	0.050	2	7	8	68%	4%	1.44	0.71	0.70	0.29	0.14	0.14
0.25	200	0.100	3	11	11	73%	6%	1.28	0.59	0.58	0.26	0.12	0.12
0.25	200	0.150	4	11	12	68%	8%	1.12	0.57	0.55	0.22	0.11	0.11
0.25	200	0.200	5	12	14	60%	13%	0.96	0.56	0.53	0.19	0.11	0.11
0.25	200	0.250	8	13	16	50%	17%	0.80	0.53	0.49	0.16	0.11	0.10

REFERENCES

ABAQUS/STANDARD (Version5.5), "Manual and Examples"
Hibbit Karlsson & Sorensen, Inc.
Email : hks@hks.com

AISI (1996), "Specification for the Design of Cold-Formed Steel Structural Members", American Iron and Steel Institute, 1996 EDITION

Aluminum Association (1982), "Specifications for Aluminum Structures", AA, Washington, D.C.

ASCE Standard (1991), "Specification for the Design of Cold-Formed Stainless Steel Structural Members", ANSI/ASCE-8-90

Brush D. O., Almroth B.O. (1975), "Buckling of Bars, Plates and Shells", McGraw- Hill Inc.

Chajes A. and Winter G. (1965), "Torsional-flexural buckling of thin walled members", ASCE J. Struct Div, Vol. 91, No. ST4

Chajes A. (1976), "Principles of structural stability theory", Prentice-Hall Inc., Engleword Cliffs N.J.

Chilver A.H. (1967), "Thin-Walled Structures, Biley, New York

CSA Standard (1994), "Cold Formed Steel structural Members", CSA S136-94

Dat D.T. (1980), "The strength of cold-formed columns", Report No. 80-4, Dept. of Struct. Engr., Cornell University, Ithaca, N.Y.

DeWolf J., Pekoz T., Winter G. (1976), "Local and Overall Buckling of Cold-Formed Steel Members", ASCE J. Struct. Div., vol. 100,No ST10

DeWolf J., Pekoz T., Winter G. (1976), Closure to "Local and Overall Buckling of Cold-Formed Steel Members", ASCE J. Struct. Div., vol. 102,No ST2

Dowling P.J., Knowles P., Ownens G.W. (1988), "Structural Steel Design", The Steel Construction Institute, First published

European Convention for Constructional Steelwork (1977), "European Recommendations for the Stressed Skin Design of Steel Structures", ECCS-XVII-77-1E, March

Galambos V. (1988), "Guide to Stability Design Criteria for Metal Structures", 4th. Edition, ISBN 0-471-09737-3

Hancock G.J. (1981), "Nonlinear Analysis of Thin Sections in Compression", ASCE J. Struct. Div., Vol. 107, No ST3

ISO Technical Report (1995), Aluminum structures – Material and design – Ultimate limit state under static loading", First edition 1995-09-15

Marsh C. (1960), "Strength of Aluminum", Alcan, Canada Products Limited

Marsh C. (1969), "Single Angles in Tension and Compression" ASCE J. Struct. Div., Tech. Note, Vol. 95, No ST5

Marsh C. (1992), "Theoretical model for collapse of shear webs", Journal of Eng. Mech. Div., ASCE, 108(5), 819-832

Marsh C. (1997), "Influence of bend Radii on Local Buckling in Cold Formed Shapes", Journal of Structural Engineering Dec. 1997 Vol. 123 No 12

Marsh C. (1998), "Design Method for Buckling Failure of Plate Elements", Journal of Structural Engineering Jul.. 1998 Vol. 131 No 8

Morris L.J. (1983), "Instability and Plastic Collapse of Steel Structures", first published in Great Britain, 1983 by Granada Publishing

Narayanan R. (1985), "Steel framed structures : stability and strength", London, New York, Elsevier Applied Science Publishers

Pfluger A. (1961), "Thin-Walled Compression Members", Mitt. Inst. Statik Techn. Hochsch. Hannover

Rammerstorfer F.G. (1992), "Nonlinear analysis of shells by finite elements", Wien, New York, Springer-Verlay, 1992

Rhodes J. (1990), "Thin-walled Structures", Vol. 9 No S1-4 1990, ISSN 0263-8231

Rhodes J. (1991), "Design of Cold-formed Steel Members", Dep. Of Mech. Eng. Univ. of Strathclyde, Glasgow, U.K.

Schrefler B.A., Lewis R.W. (1987), "Microcomputers in engineering applications", Chichester, New York, John Wiley, 1987

Thomas J.R ,Hinton E. (1986), "Finite element methods for plate and shell structures", Swansea, U.K, Pineridge Press International, 1986

Timoshenko S.P., Gere J.M. (1961), "Theory of Elastic Stability", McGraw-Hill, second edition

Von Karman T., Sechler E.E., Donnell L.H. (1932), "The Strength of Thin Plates in Compression", Transactions, ASCE, vol. 54, No 2, Jan.

Wafik M. A. Ajam (1986), "Finite element study of the post-buckling behaviour of plate", Thesis (Ph.D.)- Concordia University, 1986

Walker A.C. (1975), "Design and Analysis of Cold-Formed Section", John Wiley & Sons, First publishing

Winter G. (1937), "Strength of thin steel compression flanges", Trans., ASCE, 112, 527-554

Winter G. (1970), "Commentary on the 1968 edition of the specification for the design of cold-formed steel structural members", American Iron and Steel Institute

Yu W.W. (1985), "Cold-Formed Steel Design", John Wiley and Sons Inc.